

Université du Québec
Institut National de la Recherche Scientifique
Institut Armand-Frappier

**DIINDOLYLMETHANE (DIM) AND RING-SUBSTITUTED
HALOGENATED DERIVATIVES OF DIM (RING-DIMS): THEIR ROLE IN
PROSTATE CANCER PREVENTION**

Par
HOSSAM DRAZ

Thèse présentée pour l'obtention du grade
de *Philosophiae doctor* (Ph.D.)
en Biologie

Jury d'évaluation

Président du jury et examineur interne	Prof. Yves St-Pierre INRS-Institut Armand-Frappier
Examineur externe	Prof. Diana Averill-Bates Département des sciences biologiques Université du Québec à Montréal
Examineur externe	Prof. François Yu Faculté de médecine Université de Montréal
Directeur de recherche	Prof. Thomas Sanderson INRS-Institut Armand-Frappier

ACKNOWLEDGEMENTS

It is a pleasure to express my deepest gratitude and indebtedness to those who generously devoted much effort and time in helping me to accomplish this thesis. First and foremost, I thank my academic advisor, Professor Thomas Sanderson, for his caring guidance, patience, extraordinary support, giving me intellectual freedom in my research work, supporting my attendance at various conferences, engaging me in new ideas, and demanding a high quality of work in all my endeavors. I am very proud and fortunate to be his student.

Additionally, I would like to thank my committee members Professors Yves St-Pierre, Diana Averill-Bates and François Yu for their interest in my work and for their contribution to the evaluation of my thesis. Every result described in this thesis was accomplished with the help and support of labmates, colleagues and collaborators. I would like to thank all my present and former lab members Dr. Alex Goldberg, Dr. Elyse Caron-Beaudoin, Dr. Helene Clabault, Andree-Anne Thibeault, Rachel Viau and Debbie Yancu for helping and supporting me during my research. Dr. Alex Goldberg and I worked together on several different phases of the CIHR funded ring-DIM project, and without his efforts, my job would have undoubtedly been more difficult.

I am also indebted to Professor Stephen H. Safe of Texas A&M University who deserves the credit for providing us with the synthetic ring-DIMs and for his profound reading of my three manuscripts. I am very grateful to Professor Emma Guns of the University of British Columbia who supervised the tissue microarray analyses.

I gratefully acknowledge the funding sources that made my Ph.D. work possible. I was awarded a Fondation Armand-Frappier scholarship for my first 2 years and was honored to hold a prestigious Fonds de Recherche du Québec–Santé (FRQS) doctoral scholarship for the last 3 years of my doctoral program. My profound gratitude stands toward the Canadian Institutes of Health Research (CIHR) for financing the ring-DIM project.

I would like to thank my family, especially my loving and caring wife, for always being extremely compassionate, encouraging and a driving force behind the successful

completion of my research work. She has been my inspiration and motivation for continuing to improve my scientific knowledge and move my career forward. I would like to thank my parents who raised me with a love of science and supported me in all my pursuits. I would like also to thank my sister for her support, love and encouragement.

I would like to show my gratitude to all my friends and colleagues at the INRS-IAF, especially Ahmed Fahmy, Lucas Sagrillo-Fagundes, Elham Dianati, Guillermo-Arango Duque, Ahmed Soliman, Slimane Dridi, Ghislain Paka, Akil Hammami, Monzer Khidiri, Andree-Anne Hudon Thibeault, H el ene Clabault, Marc Fraser, Mohamed Haddad, Edward Kwarting, and Mustapha Iddir for their support and providing a stimulating and fun environment during my studies.

RÉSUMÉ

Cette étude a pour objectif d'examiner les propriétés antiprolifératives d'un dérivé de légumes crucifères; le diindolylméthane (DIM), ainsi que certains de ces dérivés synthétiques (ring-DIMs) dans des cellules cancéreuses humaines de la prostate androgènes-dépendantes (AD) et androgènes-indépendants (AI). Ces cellules ont été utilisées pour étudier plusieurs mécanismes moléculaires de l'action anticancéreuse des ring-DIMs. Par ailleurs, des souris porteuses de tumeurs cancéreuses humaines de la prostate bioluminescentes ont été utilisées pour évaluer l'activité anticancéreuse de ring-DIMs *in vivo*, en utilisant une technique d'imagerie non invasive et en temps réel.

En effet, le DIM est un métabolite de l'indole-3-carbinol (I3C), un composant important des légumes crucifères de la famille des *Brassica*, tels que le brocoli et les choux de Bruxelles. Selon les études épidémiologiques, la consommation élevée de ces légumes est associée à une réduction des risques du développement de divers cancers. L'I3C et le DIM sont capables d'inhiber la croissance de diverses cellules cancéreuses *in vitro* ainsi qu'*in vivo* incluant le cancer de la prostate, le cancer le plus fréquemment diagnostiqué chez l'homme occidental. Le DIM inhibe la prolifération des cellules cancéreuses prostatiques AD (LNCaP) qui est stimulée préalablement par la dihydrotestostérone (DHT). De plus, le DIM induit l'apoptose cellulaire et inhibe la croissance des tumeurs de la prostate *in vivo*. Dans ce même contexte, nos études antérieures ont montré que le DIM et les ring-DIMs diminuent l'expression génique des récepteurs aux androgènes (AR), réduisent les taux de protéine AR et l'expression de l'antigène prostatique spécifique (PSA) médiée par l'AR. Les ring-DIMs disubstitués par des halogènes (Br₂ ou Cl₂) en positions 4- et 4'- de la molécule DIM bloquent l'accumulation de l'AR dans le noyau des cellules LNCaP stimulées par la DHT. Cependant, nos connaissances concernant la capacité du DIM et ses dérivés à affecter les mécanismes de protection cellulaire tels que l'autophagie ou le stress du réticulum endoplasmique (ER) sont faibles. Les ring-DIMs ont été décrits à agir comme des inhibiteurs de la prolifération des cellules tumorales plus puissants que DIM. En effet, ils sont efficaces contre les cellules cancéreuses de la prostate hormono-dépendantes, ainsi

qu'indépendantes. De ce fait, ils ont un potentiel supplémentaire pour le traitement du cancer de la prostate résistant au traitement par les antiandrogènes. Dans la recherche sur de nouveaux médicaments efficaces contre le cancer de la prostate et l'hyperplasie bénigne de la prostate, ces composés seraient d'excellents candidats pour des études actives sur leurs mécanismes d'action moléculaires et leurs activités biologiques *in vivo*.

Ainsi, notre hypothèse de travail est que les ring-DIMs possèdent des activités anticancéreuses prostatiques et qu'ils sont plus puissants que le DIM. Cela dans le but de développer des médicaments efficaces dans le traitement du cancer de la prostate. Le premier objectif de recherche était de déterminer les événements précoces entraînant la mort cellulaire induite par DIM et les ring-DIMs. Nous avons étudié leurs effets sur la stabilité mitochondriale, le stress du ER et l'autophagie en fonction de la concentration et le temps d'exposition. Nous avons ainsi démontré que le DIM et les ring-DIMs induisent la mort des cellules cancéreuses de la prostate LNCaP (AR-positives et AD), C4-2B (AR-positives et AI) et DU145 (AR-négatives, AI et déficientes à l'autophagie), contrairement à leur manque de toxicité chez les cellules épithéliales humaines de la prostate normales immortalisées (RWPE-1). Nous montrons également que les ring-DIMs causent la perte précoce du potentiel de la membrane mitochondriale et la diminution de la production mitochondriale d'ATP dans les cellules cancéreuses de la prostate. Nos observations mettent en évidence une perturbation de la fonction mitochondriale en tant qu'événement déterminant dans les actions cytotoxiques du DIM et tous les ring-DIMs. Cependant, le salubrinal, un inhibiteur du stress ER, inhibait seulement la mort cellulaire médiée par les 4,4'-dihaloDIMs, en revanche, le salubrinal exacerbait la toxicité des 7,7'-dihaloDIMs. En utilisant une analyse *in silico* de l'affinité par docking en 3-D, nous avons identifié la calmoduline-kinase II dépendante du Ca^{+2} (CaMKII) en tant que cible potentielle pour le ring-DIM le plus toxique, le 4,4'-dibromoDIM. Nos résultats ont montré que l'inhibiteur de CaMKII (KN93) abrogeait complètement la toxicité de ce ring-DIM, mais pas la toxicité du 7,7'-Cl₂DIM. L'implication des pores de transition de perméabilité mitochondriale dans la toxicité des ring-DIMs est suggérée par un traitement avec la cyclosporine A (inhibitrice des pores de transition de perméabilité mitochondriale), qui abrogeait la toxicité de tous les ring-DIMs, mais pas cela du DIM. L'un des principaux résultats de cette étude était que le DIM et les ring-DIMs induisaient l'autophagie dans les cellules cancéreuses de la

prostate. L'inhibition de l'autophagie avec la bafilomycine A1, la 3-méthyladénine ou par le silençage génique de *LC3B* sensibilisait les cellules LNCaP et C4-2B, mais pas les cellules DU145 déficientes en ATG5 à la mort cellulaire induite par le DIM et les ring-DIMs. Nous proposons que l'autophagie induite par le DIM et les ring-DIMs ait une fonction cytoprotectrice dans les cellules cancéreuses de la prostate.

Notre deuxième objectif de recherche était d'étudier les effets mécanistiques des ring-DIMs sur les voies de signalisation impliquées dans la mort cellulaire des cellules cancéreuses de la prostate. Nous avons trouvé que l'autophagie induite par le DIM et les ring-DIMs s'accompagnait d'une augmentation de la formation des vacuoles autophagiques et de la conversion de LC3BI en LC3BII dans les cellules cancéreuses humaines de la prostate LNCaP et C4-2B. Le DIM et les ring-DIMs induisaient également la phosphorylation de l'AMPK (protéine kinase activée par l'AMP), de l'ULK-1 (kinase d'activation de l'autophagie de type unc-51 type 1, ATG1) et de l'acétyl-CoA carboxylase (ACC). De plus, le DIM et les ring-DIMs induisaient le gène 1 des protéines astrocytaires (*AEG-1*). La régulation à la baisse d'*AEG-1* ou d'*AMPK* inhibe l'autophagie induite par le DIM et le ring-DIMs. Un prétraitement avec des siRNA d'*AEG-1* ou *AMPK* potentialisait la cytotoxicité du DIM et des ring-DIMs. Également, la régulation à la baisse d'*AEG-1* induisait la sénescence dans des cellules traitées avec des concentrations de DIM ou ring-DIMs ouvertement cytotoxiques et inhibait l'initiation de l'apoptose en réponse à ces composés. En effet, nous avons identifié un nouveau mécanisme pour l'autophagie protectrice induite par le DIM et les ring-DIMs via l'induction de l'*AEG-1* et l'activation subséquente de l'AMPK.

Notre troisième objectif de recherche était d'étudier l'effet de DIM et le ring-DIM le plus puissant (4,4'-Br₂DIM) sur le développement tumoral dans un modèle de xélogreffe murine du cancer de la prostate humaine. L'utilisation de cellules PC-3 bioluminescentes pour surveiller la croissance tumorale et les effets du traitement chimique avec les nouveaux ring-DIMs constitue l'un des principaux aspects novateurs de la présente étude. La surveillance *in vivo* en temps réel réduit le nombre d'animaux requis pour les expériences proposées, car ce n'est pas nécessaire de sacrifier les souris à des intervalles pendant la progression de la tumeur. Nous avons trouvé que l'inhibition de l'autophagie par la chloroquine (CQ) sensibilisait significativement les cellules PC-3 à la

mort en présence de concentrations du DIM ou 4,4'-Br₂DIM qui étaient sous-toxiques *in vitro*. De plus, une combinaison de DIM (10 mg/kg) et CQ (60 mg/kg), 3x par semaine, réduisait significativement la croissance des tumeurs PC-3 *in vivo* après 3 et 4 semaines de traitement. De plus, le 4,4'-Br₂DIM (10 mg/kg, 3x par semaine) inhibait significativement la croissance tumorale après 4 semaines de traitement. L'analyse de micromatrices tissulaires préparées à partir des tumeurs excisées a montré que le DIM seul ou en co-traitement avec la CQ induisait le marqueur d'apoptose TUNEL, et inhibait significativement le marqueur de prolifération cellulaire Ki67.

En conclusion, nos résultats de recherche fournissent des informations importantes sur les mécanismes d'action potentiels du DIM et les ring-DIMs qui ont des activités biologiques divergentes de DIM. Nous avons également identifié un nouveau mécanisme pour l'autophagie protectrice médiée par le DIM et les ring-DIMs via l'activation de l'AMPK et l'induction de l'AEG-1. De plus, nos découvertes pourraient faciliter le développement de nouvelles pharmacothérapies contre le cancer de la prostate qui comprennent des inhibiteurs sélectifs de l'autophagie en tant qu'adjuvants.

ENGLISH SUMMARY

The objective of this research study is to investigate the antiproliferative properties of the cruciferous vegetable-derived compound diindolylmethane (DIM), and several synthetic disubstituted halogenated DIM-derivatives (ring-DIMs) in androgen-dependent (AD) and androgen-independent (AI) human prostate cancer cells. We aimed to investigate several molecular mechanisms of anticancer action of the ring-DIMs *in vitro*. In addition, mice carrying bioluminescent human prostate cancer tumors were used to assess the anticancer activity of these compounds *in vivo*, using a non-invasive, real-time imaging technique.

DIM is formed as a metabolite of indole-3-carbinol (I3C), an important component of cruciferous vegetables of the *Brassica* family, such as broccoli and Brussels sprouts. Epidemiological studies show that high consumption of these vegetables is associated with decreased risks of various cancers. Both I3C and DIM inhibit the growth of various cancers *in vitro* and *in vivo*, including cancer of the prostate, which is the most common malignancy in Western men. DIM also inhibits dihydrotestosterone (DHT)-mediated proliferation of the AD LNCaP prostate cancer cells, induces apoptosis, and inhibits prostate tumor growth *in vivo*. Our previous studies show that DIM and ring-DIMs down-regulate androgen receptor (AR) expression; reduce AR protein levels and AR-mediated prostate specific antigen (PSA) expression. In addition, 4,4'-dihalo-substituted ring-DIMs, block accumulation of AR in the nucleus of androgen-stimulated LNCaP cells. Less is known about the ability of DIM or its derivatives to affect cell protective mechanisms such as autophagy and endoplasmic reticulum (ER) stress. Further results show that ring-DIMs are considerably more potent inhibitors of tumor cell proliferation than DIM, and are effective against hormone-dependent, as well as -independent prostate cancer cells, indicating their additional potential in the treatment of androgen-refractory prostate cancer. In the quest for novel drugs effective against prostate cancer and benign prostate hyperplasia these compounds are excellent candidates for detailed research concerning their molecular mechanisms of action and biological activity *in vivo*.

Our working hypothesis is that ring-DIMs exhibit anti-prostate cancer activities and are considerably more potent than DIM. Thus making them suitable candidates for development as drugs effective in the treatment of prostate cancer. Our first research objective was to determine the early events that result in cell death induced by DIM and ring-DIMs by determining their concentration- and time-dependent effects on mitochondrial stability, ER stress and autophagy. We demonstrated that DIM and ring-DIMs induced the death of LNCaP (AR-positives and AD), C4-2B (AR-positives and AI) and DU145 (AR-negatives, AI and autophagy deficient) prostate cancer cells, but not that of immortalized normal human prostate epithelial (RWPE-1) cells. We also showed that ring-DIMs caused the early loss of mitochondrial membrane potential (MMP) and decreased mitochondrial ATP generation in prostate cancer cells. Our evidence points at disruption of mitochondrial function as the defining event in the cytotoxic actions of all ring-DIMs. However, salubrinal, an inhibitor of ER stress, inhibited cell death mediated only by 4,4'-dihaloDIMs by contrast, it exacerbated the toxicity of the 7,7'-dihaloDIMs. Using *in silico* 3-D docking affinity analysis, we identified Ca²⁺/calmodulin-dependent kinase II (CaMKII) as a potential direct target for the most toxic ring-DIM, 4,4'-dibromoDIM. Our results showed that CaMKII inhibitor KN93 completely abrogated the toxicity of this ring-DIM, but not the toxicity of 7,7'-Cl₂DIM. Involvement of the mitochondrial permeability transition pore in the toxicity of ring-DIMs is suggested by treatment with the mitochondrial permeability transition pore-inhibitor cyclosporin A, which abrogated the toxicity of all ring-DIMs, although not that of DIM. One of the main findings of the current study was that DIM and ring-DIMs induced autophagy in prostate cancer cells. Inhibition of autophagy with bafilomycin A1, 3-methyladenine or by LC3B gene silencing sensitized LNCaP and C4-2B, but not ATG5-deficient DU145 cells to ring-DIM- and DIM-mediated cell death. We propose that autophagy induced by DIM and ring-DIMs has a cytoprotective function in prostate cancer cells.

Our second research objective was to study the mechanistic effects of ring-DIMs on signalling pathways involved in prostate cancer cell death. We found that DIM- and ring-DIM-induced autophagy was accompanied by increased autophagic vacuole formation and conversion of LC3BI to LC3BII in LNCaP and C4-2B human prostate cancer cells.

DIM and ring-DIMs also induced the phosphorylation of AMP-activated protein kinase (AMPK), ULK-1 (unc-51-like autophagy activating kinase 1; ATG1) and acetyl-CoA carboxylase (ACC). Interestingly, DIM and ring-DIMs induced the oncogenic protein astrocyte-elevated gene 1 (AEG-1). Downregulation of AEG-1 or AMPK inhibited DIM and ring-DIM-induced autophagy. Pretreatment with either AEG-1 or AMPK siRNAs potentiated the cytotoxicity of DIM and ring-DIMs. Interestingly, downregulation of AEG-1 induced senescence in cells treated with overtly cytotoxic concentrations of DIM or ring-DIMs and inhibited the onset of apoptosis in response to these compounds. Indeed, we have identified a novel mechanism for DIM- and ring-DIM-induced protective autophagy, via induction of AEG-1 and subsequent activation of AMPK.

Our third research objective was to study the effect of DIM and the most potent ring-DIM (4,4'-Br₂DIM) on tumor development in a murine xenograft model of human prostate cancer. The use of bioluminescent PC-3 cells to monitor tumor growth and the effects of chemical treatment with the new ring-DIMs is one of the novel aspects of this study. The real-time monitoring of tumor growth *in vivo* reduces the number of animals required for the proposed experiments, since they do not have to be sacrificed at intervals during tumor progression. We found that the autophagy inhibitor chloroquine (CQ) significantly sensitized PC-3 cells to death in the presence of concentrations of DIM or 4,4'-Br₂DIM that were sub-toxic *in vitro*. Moreover, a combination of DIM (10 mg/kg) and CQ (60 mg/kg), 3 x per week, significantly decreased PC-3 tumor growth *in vivo* after 3 and 4 weeks of treatment. Furthermore, 4,4'-Br₂DIM at 10 mg/kg (3 x per week) significantly inhibited tumor growth after 4 weeks of treatment. Tissues microarray analysis of excised tumors showed that DIM alone or combined with CQ induced apoptosis marker TUNEL, and significantly inhibited the cell proliferation marker Ki67.

Taken together, our research findings provide important information on the potential mechanisms of action of DIM and the ring-DIMs, which have divergent biological activities from DIM. We also identified a novel mechanism for DIM and ring-DIMs mediated protective autophagy via the activation of AMPK and induction of AEG-1. Moreover, our findings may facilitate the development of novel drug therapies against prostate cancer that include selective autophagy inhibitors as adjuvants.

TABLE OF CONTENTS

ACKNOWLEDGEMENTS.....	I
RÉSUMÉ	III
ENGLISH SUMMARY	VII
TABLE OF CONTENTS	XI
LIST OF TABLES.....	XIII
LIST OF FIGURES.....	XV
LIST OF ABBREVIATIONS	XVI
CHAPTER 1: INTRODUCTION	1
1.1 PROSTATE CANCER:	2
1.1.1 <i>Causes and development of cancer.....</i>	<i>2</i>
1.1.2 <i>Incidence and diagnosis of prostate cancer.....</i>	<i>3</i>
1.1.3 <i>Staging of prostate cancer.....</i>	<i>4</i>
1.1.4 <i>Grading of prostate cancer.....</i>	<i>5</i>
1.1.5 <i>Risk factors.....</i>	<i>6</i>
1.1.6 <i>Chemoprevention of prostate cancer.....</i>	<i>7</i>
1.1.7 <i>Hormone-dependent mechanisms of prostate cancer.....</i>	<i>8</i>
1.1.8 <i>Hormone-independent mechanisms of prostate cancer.....</i>	<i>13</i>
1.1.9 <i>Current treatments for prostate cancer.....</i>	<i>18</i>
1.1.10 <i>Causes of castration resistant prostate cancer.....</i>	<i>21</i>
1.1.11 <i>TP53 mutations and prostate cancer.....</i>	<i>21</i>
1.2 DIINDOLYLMETHANE	22
1.2.1 <i>Cruciferous vegetables and prostate cancer.....</i>	<i>23</i>
1.2.2 <i>Anti-prostate cancer activity of DIM.....</i>	<i>24</i>
1.2.3 <i>Anticancer effects of DIM in vivo.....</i>	<i>26</i>
1.2.4 <i>DIM clinical trials in treatment of prostate cancer.....</i>	<i>27</i>
1.2.5 <i>Anti-cancer properties of ring-DIMs.....</i>	<i>28</i>
1.3 AUTOPHAGY.....	29
1.3.1 <i>Types of autophagy.....</i>	<i>30</i>
1.3.2 <i>Autophagy mechanism.....</i>	<i>30</i>
1.3.3 <i>Dual Role of autophagy in cancer.....</i>	<i>32</i>
1.3.4 <i>Autophagy inhibition as an adjuvant treatment for prostate cancer.....</i>	<i>35</i>

1.3.5	<i>Regulation of autophagy by DIM in cancer cells</i>	36
1.3.6	<i>The role of AMPK in autophagy</i>	37
1.3.7	<i>AEG-1 role in cancer and autophagy</i>	38
1.4	MOLECULAR PATHWAYS OF APOPTOSIS, NECROSIS, ENDOPLASMIC RETICULUM (ER) STRESS AND SENESENCE IN CANCER.....	39
1.4.1	<i>Apoptosis</i>	39
1.4.2	<i>Necrosis and necroptosis</i>	41
1.4.3	<i>ER stress</i>	43
1.4.4	<i>Senescence</i>	46
1.5	STUDY MODELS.....	49
1.5.1	<i>Prostate cancer cell lines</i>	49
1.5.2	<i>Xenograft mouse model of prostate cancer</i>	50
1.6	HYPOTHESIS AND OBJECTIVES.....	51
1.6.1	<i>Hypothesis</i>	51
1.6.2	<i>Objectives</i>	51
1.7	PROJECT SIGNIFICANCE	52
CHAPTER 2: PUBLICATIONS		53
2.1	3,3'-DIINDOLYMETHANE (DIM) AND ITS RING-SUBSTITUTED HALOGENATED ANALOGS (RING- DIMs) INDUCE DIFFERENTIAL MECHANISMS OF SURVIVAL AND DEATH IN ANDROGEN-DEPENDENT AND –INDEPENDENT PROSTATE CANCER CELLS	54
2.2	DIINDOLYMETHANE AND ITS HALOGENATED DERIVATIVES INDUCE PROTECTIVE AUTOPHAGY IN HUMAN PROSTATE CANCER CELLS VIA INDUCTION OF THE ONCOGENIC PROTEIN AEG-1 AND ACTIVATION OF AMP-DEPENDENT KINASE (AMPK)	75
2.3	AUTOPHAGY INHIBITION IMPROVES THE CHEMOTHERAPEUTIC EFFICACY OF CRUCIFEROUS VEGETABLE-DERIVED DIINDOLYMETHANE IN A MURINE PROSTATE CANCER XENOGRAFT MODEL	90
CHAPTER 3: DISCUSSION		107
CONCLUSION AND PERSPECTIVE		119
REFERENCES		123
APPENDIX I		148
APPENDIX II		149

LIST OF TABLES

TABLE 1: TNM STAGING OF PROSTATE CANCER.....	5
TABLE 2: CHARACTERISTICS OF COMMON PROSTATE CANCER AND IMMORTALIZED CELL LINES.....	49

LIST OF FIGURES

FIGURE 1: PHASES OF CARCINOGENESIS	3
FIGURE 2: THE CLASSICAL REPRESENTATION OF THE GLEASON GRADES 1-5.....	6
FIGURE 3: STERIOGENESIS	10
FIGURE 4: AR SIGNALING PATHWAY.....	11
FIGURE 5: THE STAGES OF THE CELL CYCLE.....	14
FIGURE 6: AKT/MTOR SIGNALING PATHWAY.....	16
FIGURE 7: ARYL HYDROCARBON RECEPTOR (AHR) SIGNALING PATHWAY	18
FIGURE 8: FORMATION OF DIINDOLYLMETHANE (DIM) FROM INDOLE-3-CARBINOL (I3C).	23
FIGURE 9: CHEMICAL STRUCTURES OF RING-DIMS.....	24
FIGURE 10: AUTOPHAGY MECHANISM.....	32
FIGURE 11: DUAL ROLE OF AUTOPHAGY IN CANCER.	35
FIGURE 12: INTRINSIC AND EXTRINSIC APOPTOSIS SIGNALING PATHWAYS	41
FIGURE 13: NECROPTOSIS PATHWAY	43
FIGURE 14: ER STRESS PATHWAY	46
FIGURE 15: SENESCENCE MECHANISM.....	48
FIGURE 16: PC-3 XENOGRAFT MODEL.....	50

LIST OF ABBREVIATIONS

μ XBP-1	Unspliced form of X box-binding protein-1
3-MA	3 methyladenine
3 β HSDs	3 β -hydroxysteroid dehydrogenase
4E-BP1	4E-binding protein 1
4E-BP1	4E-binding protein 1
AD	Androgen-dependent
ADT	Androgen deprivation therapy
AEG-1	Astrocyte elevated gene-1
AhR	Aryl hydrocarbon receptor
AI	Androgen-independent
AIF	Apoptosis-inducing factor
AIP	AhR interacting protein
AJCC/UICC	American joint committee on cancer/international union against cancer
AMPK	AMP-activated protein kinase
AN	Androstenedione
AR	Androgen receptor
AREs	Androgen response elements
ARF	Alternate-reading frame protein
ARNT	AhR nuclear translocator protein
ATF4	Activating transcriptional factor 4
ATF6	Activating transcription factor 6
ATG	Autophagy-related genes
B-DIM	BioResponse DIM
<i>BECN1</i>	Beclin 1
bHLH	Basic helix-loop-helix
BLI	Bioluminescent imaging
Ca ²⁺	Calcium ion
CaMKII	Ca ²⁺ /calmodulin-dependent protein kinase
CSCs	Cancer stem cells

C-DIM	Methylene-substituted diindolylmethane
CDKs	Cyclin-dependent kinases
C-FLIP	Cellular FLICE inhibitory protein
CHOP	C/EBP homologous protein
clAP	Cellular inhibitors of apoptosis
CQ	Chloroquine
CRPC	Castration resistant prostate cancer
CsA	Cyclosporin A
ctDNA	Circulating DNA
CYP	cytochrome P450scc
CYP17	Cytochrome P450 steroid 17 α -hydroxylase/20,22-lyase
DDR	DNA damage response
DHEA	Dehydroepiandrosterone
DHT	Dihydrotestosterone
DIM	Diindolylmethane
DISC	Death-inducing signalling complex
DR4	Death receptors 4
DRE	Digital rectal examination
eIF2 α	Eukaryotic translation initiation factor 2
EGF	Epidermal growth factor
ER	Endoplasmic reticulum
ERAD	ER associated degradation
ERK	Extracellular signal-regulated kinase
EsR	Estrogen receptor
FADD	Fas-associated protein with death domain
FasL	Fas ligand
FDA	Food and drug administration
GADD34	DNA damage-inducible 34
HAHs	Halogenated aromatic hydrocarbons
HCC	Hepatocellular carcinoma
HDM2	Human double minute 2

HIF-1 α	Hypoxia-inducible factor 1-alpha
HBV	Hepatitis B virus
HSPs	Heat shock proteins
I3C	Indole-3-carbinol
IC50	Half maximal inhibitory concentration
IM-PHFA	Immortalized primary human fetal astrocyte
IRE1 α	Inositol-requiring protein-1 α
LC3	Microtubule-associated protein 1 light chain 3
LEF1	Lymphoid-enhancing factor 1
LH	Luteinizing hormone
LHRH	Luteinizing hormone-releasing hormone
MAPK	P38 mitogen-activated protein kinase
MDR1	Multidrug resistance gene 1
MLKL	Mixed lineage kinase domain like protein
MOMP	Mitochondrial outer membrane permeabilization
mPTP	Mitochondrial permeability transition pore
MRT 67307	(N-[3-[[5-Cyclopropyl-2-[[3-(4-morpholinylmethyl)phenyl]amino]-4-pyrimidinyl]amino]propyl] cyclobutanecarboxamide)
MTDH	Metadherin
mTOR	Mammalian target of rapamycin
mTORC1	mTOR complex 1
MW	Molecular weight
NF- κ B	Nuclear factor kappa-B
NRF2	Nuclear erythroid 2 p45-related factor 2
p70S6K	70S ribosomal protein S6 kinase
PAHs	Polyaromatic hydrocarbons
PDGF-D	Platelet-derived growth factor-D
PE	Phosphatidylethanolamine
PERK	Protein kinase R-like ER kinase
PIN	Prostatic intraepithelial neoplasia
PSA	Prostate specific antigen

RB	Retinoblastoma tumor suppressor protein
ring-DIMs	Ring-substituted analogs of 3,3'-diindolylmethane
RIP1	Receptor interacting protein kinase-1
ROS	Reactive oxygen species
S1P	Serine protease site-1
S2P	Proteases and metalloprotease site-2 protease
SRD5A	Steroid 5 α -reductase
sXBP-1	Spliced form of X box-binding protein-1
T-Bid	Truncated BID
TCDD	2,3,7,8-tetrachlorodibenzo- p-dioxin
TGF- β	Transforming growth factor beta 1
TIS	Therapy-induced senescence
TNM	Tumor-node-metastasis
TRADD	TNFR1-associated death domain protein
TRAF2	TNF-receptor-associated factor 2
TRAMP	Transgenic adenocarcinoma of the mouse prostate
TRUS	Trans-rectal ultrasound
TUNEL	Terminal deoxynucleotidyl transferase dUTP nick end labeling
ULK1	Uunc-51-like autophagy activating kinase 1
UPR	Unfolded protein response
XRE	Xenobiotic response elements

CHAPTER 1: INTRODUCTION

1.1 PROSTATE CANCER:

Prostate cancer is a major health problem worldwide, ranking as the most common cancer in males and the third leading cause of cancer-related deaths among American and Canadian men (Siegel et al. 2017). Estimated number of cancer related death in 2017 in the United States was 318,420. However, in 2017, 26,730 men died from prostate cancer in the United States (about 8.5% of all cancer deaths in men) (Siegel et al. 2017). Prostate cancer accounts for approximately 20% of all newly diagnosed cancer in Canadian men (21,300 diagnosed with prostate cancer out of 103,100 of all cancers). In 2017, out of 42,600 Canadian men died from cancer, 4100 men died from prostate cancer (about 10% of all cancer deaths in men)(Smith et al. 2018a).

1.1.1 Causes and development of cancer

Cancer is a complex disease with high rate of incidence and mortality, a recent report estimated that around 8 million died from cancer in 2012, which is a relatively high mortality rate compared to the mortality rates of other chronic diseases (Ferlay et al. 2015). Many causes can lead to the development of cancer. Genetic factors are one of the causes. In addition, bad dietary habit and stagnant life style may cause cancer (Anand et al. 2008). Chronic exposure to carcinogens such as toxins, and pollutants are considered as high risk factors (Cao 2015)

All types of cancer including that of the prostate develop in three main carcinogenesis phases: (a) initiation, (b) promotion and progression and finally (c) metastasis (Figure 1). Initiation of cancer is mainly caused by gene mutation after exposure to carcinogens (Berenblum 1954). Normal cells are transformed into cancer cells if there is a failure in the cellular mechanisms that either check and repair or destroy mutated cells through apoptosis (Sinicrope 2010). The initiation step is followed by promotion and progression of cancer cells. Transformed cancer cells acquire the ability to divide (uncontrolled cell proliferation) through their exposure to cancer promoters such as growth factors and hormones. Cancer promoters differ from carcinogens in the fact that they can promote cancer cell growth but cannot initiate the transformation of normal cells to cancer cells (Potter 1980). The three main carcinogenesis phases comprises

several hallmarks of cancer. Hallmarks of cancer include sustaining proliferative signaling, evading growth suppressors, resisting cell death, enabling replicative immortality, inducing angiogenesis, reprogramming of energy metabolism and activating invasion and metastasis (Hanahan and Weinberg 2011). Metastasis is the process where cancer cells migrate from their primary site to invade another organ (metastatic site) (Sethi and Kang 2011). The progression of metastatic and primary cancers are dependent on the ability of cancer cells to escape the immune system (Leber and Efferth 2009). Hence, evading immune destruction was introduced as an emerging hallmark (Hanahan and Weinberg 2011). Metastatic cancers are more aggressive and difficult to treat. The rate of mortality in cancer patient with one or more metastatic tumor are much higher than in patients without metastasis (Mehlen and Puisieux 2006).

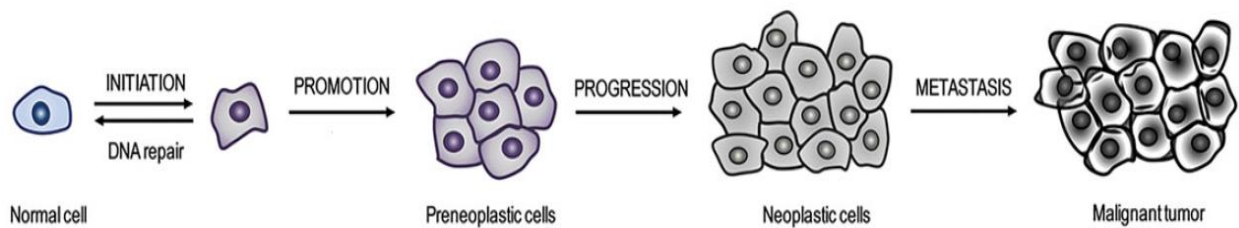


Figure 1: Phases of carcinogenesis.

Three phases of carcinogenesis include (a) initiation, (b) promotion, and progression, (c) metastasis. Adapted from (Siddiqui et al. 2015)

1.1.2 Incidence and diagnosis of prostate cancer

The incidence of certain cancers is increasing in the West, including various hormone-dependent cancers such as those of the prostate, testis and breast (Ferlay et al. 2015). Prostate cancer is expected to be the leading cancer for American and Canadian men (approximately 20% of all expected newly diagnosed male cases) (Siegel et al. 2017; Smith et al. 2018a). The burden of human suffering and cost to society are expected to increase significantly in the coming decades due to increased life-expectancy.

The age-standardized incidence of prostate cancer has not been stable over the last 30 years. Incidence of prostate cancer has peaked in 1993 and 2001. These peaks are due to the introduction of two waves of intensified screening activity using the prostate specific antigen (PSA) test. PSA, an androgen-dependent (AD) expressed protein, is used to screen for prostate cancer. Increased screening during these periods detected prevalent cancers that otherwise would not be clinically apparent until more advanced stages and temporarily increasing the incidence of prostate cancer (Leland W. K. Chung 2007). Between 1984 and 1995, the mortality rate for prostate cancer increased slowly, and then it is significantly declined from 2001 to 2009 (3.9 % per year). This decline reflects improvement in treatment strategies following the introduction of hormonal therapy (Cooperberg et al. 2003) and advances in radiation therapy (Kuban et al. 2003).

Prostate cancer is diagnosed by elevated plasma PSA levels. Prostate cancer is also diagnosed via a digital rectal examination (DRE). Diagnosis of prostate cancer is usually confirmed by a trans-rectal ultrasound (TRUS)-guided biopsy (Ukimura et al. 2015). Liquid biopsy is now introduced as non-invasive blood test that detect circulating tumor cells or circulating tumor DNA (ctDNA) that shed into blood (Hegemann et al. 2016). Recent studies showed that liquid biopsy provided potential biomarkers for prostate cancer diagnoses and may help in guiding treatment for patients with advanced prostate cancer (Pantel and Alix-Panabieres 2012; Scher et al. 2017).

1.1.3 Staging of prostate cancer

Clinical staging of prostate cancer is very important for the risk assessment of developing the disease, treatment recommendations and follow-up of disease progression. The tumor-node-metastasis (TNM) staging of malignant tumors is the most commonly used classification system that defines the cancer stages based on the following criteria: 'T' used to assess the extent of the primary tumor, 'N' describes the involvement of lymph nodes, 'M' refers to distant metastasis. The TNM staging was established by the American joint committee on cancer/international union against cancer (AJCC/UICC) (Wallace et al. 1975). The classification of prostate cancer based on TNM staging is shown in Table 1.

Table 1: TNM staging of prostate cancer.

TNM describes the tumor stage based on the size of the tumor and where it has spread, 'T' defines the extent of the primary tumor, 'N' describes the involvement of lymph nodes, and 'M' refers to distant metastatic site (Greene 2002).

The TNM staging system:	
TX	Tumor cannot be assessed
TO	No evidence of primary tumor
T1	Tumor not clinically apparent
T1a	Tumor found in resected specimen (<5%)
T1b	Tumor found in resected specimen (>5%)
T1c	Tumor found at biopsy for elevated PSA
T2	Tumor confined to prostate
T2a	Tumor involves one lobe of prostate
T2b	Tumor involves both lobes of prostate
T3	Tumor extends through the prostatic capsule
T3a	Extracapsular extension (unilateral or bilateral)
T3b	Tumor invades seminal vesicle(s)
T4	Tumor is fixed or invades adjacent structures other than seminal vesicles such as bladder
NX	Regional lymph nodes cannot be assessed
N0	No regional lymph node metastasis
N1	Metastasis in regional lymph node(s)
MX	Presence of distant metastasis cannot be assessed
M1	Distant metastasis
M1a	Distant metastasis to non-regional lymph node(s)
M1b	Distant metastasis to bone
M1c	Distant metastasis to other site(s) with or without bone metastasis

1.1.4 Grading of prostate cancer

Gleason score is the most commonly used prognostic marker for prostate cancer grading. It was introduced by Donald Gleason in 1960 (Gleason 1966). This scoring method is based on staining of tumor tissue with Haematoxylin and Eosin (H&E). The most prevalent and second most prevalent grade is assigned as the grading score. Five grades are defined based on the frequently occurring cells pattern (Harnden et al. 2007). Grade 1 represents well differentiated cells with no signs of stromal infiltration. Grade 2 signifies well differentiated cells with some evidence of stromal infiltration. Grade 3 represents moderately differentiated carcinoma, where cells had some size and shape variations. The poorly differentiated grade 4 carcinoma occurs after fusion of the gland to an anastomosing network. Grade 5 represents undifferentiated carcinoma, and is characterised by presence of clusters or sheets of cells and no evidence of gland formation (Figure 2).

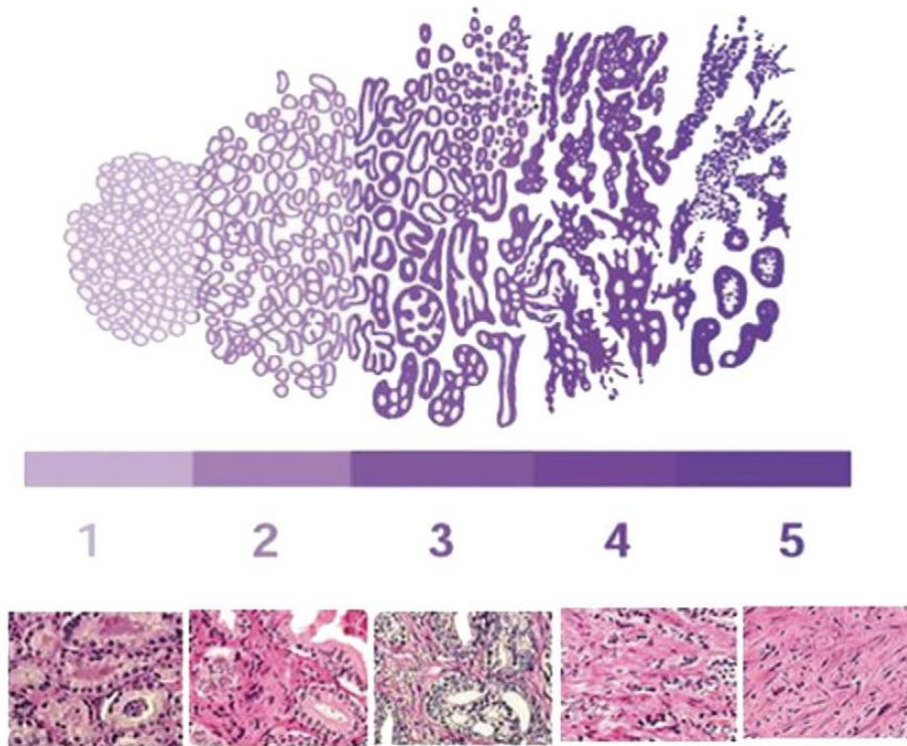


Figure 2: The classical representation of the Gleason grades 1-5.

Cells progress from grade 1 well differentiated carcinoma to grade 5 undifferentiated carcinoma (Harnden et al. 2007)

1.1.5 Risk factors

The risk of prostate cancer increases with age. Prostate cancer is rarely diagnosed in men aged below 40, with risk increasing significantly in men aged above 65 (representing approximately 85% of all cases diagnosed) (Hayat et al. 2007). Risk of prostate cancer is highly correlated with a positive family history (Zeegers et al. 2003). Race and ethnicity are also considered important risk factors for emerging prostate cancer. African-Americans having a higher incidence of prostate cancer compared to other ethnic groups (Robbins et al. 1998). Other risk factors include obesity and diet (MacInnis and English 2006; Kim and Park 2009b; Vykhovanets et al. 2011; Markozannes et al. 2016).

1.1.6 Chemoprevention of prostate cancer

Chemoprevention is the use of specific agents to block the process of tumorigenesis, thus preventing the development of invasive cancer. Cancer chemoprevention involves the chronic administration of a natural or synthetic agent to reduce or prevent the occurrence of malignancy (Steward and Brown 2013). In the past few decades, chemoprevention involving naturally occurring compounds has emerged as a promising and cost-effective approach to diminish prostate cancer incidence. Chemotherapeutic agents are designed to destroy cancer after it occurs (Aggarwal et al. 2004). However, chemopreventative agents had the advantage of inhibiting the precancerous events even before the occurrence of clinical disease (Surh 2003). Phytochemicals are plant chemicals that has chemopreventive activities (Craig 1997; Surh 2003). These phytochemicals include genistein, resveratrol, glucosinolate, indoles, lycopene, curcumin, 6-gingerol, silymarin, and catechins (Surh 2003; Baena Ruiz and Salinas Hernandez 2016). Phytochemicals are derived from natural sources, so they are generally thought to be pharmacologically safe (Aggarwal et al. 2004). However, for many natural product supplements on the market insufficient scientific data on their safety and toxicological profile exist (Pariyani et al. 2015). Moreover, many natural compounds such as capsaicin and ptaquiloside (found in chili pepper and bracken fern, respectively) are potential carcinogens and should be avoided (Bode and Dong 2015). On the other hand, most chemotherapeutic agents are known to have toxic side effects. Their toxic side effects in multiple organs and drug resistance are the major problems for successful clinical use (Sak 2012). Another advantage of chemopreventive agents that phytochemicals are naturally occurring antioxidants, whereas most chemotherapeutic agents destroy cancer cells through the production of reactive oxygen species (Somasundaram et al. 2002; Aggarwal et al. 2004).

Recently, immunotherapy has attracted a great deal of attention for cancer treatment or prevention (Umar et al. 2012; Morrison et al. 2018). A prophylactic or preventative vaccine introduces specific antigen(s) to stimulate the immune system to create antibodies selective against those antigens, which are found on the surfaces of viruses or tumour cells, thus immunizing the body against those viruses/cells, by

triggering their death. Notably, vaccines that target cancer-causing viruses, such as hepatitis B virus (HBV), have been used for hepatocellular carcinoma (HCC) prevention (Schiller and Lowy 2010). However, sipuleucel-T is the only approved autologous vaccine for prostate cancer (Mulders et al. 2015). This vaccine is based on the stimulation of the patient's T cells using autologous dendritic cells loaded with the prostate tumor antigen PA2024. Therefore, sipuleucel-T is considered to be a therapeutic autologous vaccine and not a prophylactic vaccine.

Prostate cancer, due to its high incidence and long latency, is an ideal candidate for chemoprevention as it provides a very wide window of opportunity for intervention to avert or slow tumour progression (Steward and Brown 2013). Therefore, the development of agents that offer protection against the development of this disease is highly desirable. Such chemopreventive compounds could have an important impact on disease morbidity and mortality for an important segment of the population (Powolny et al. 2011). The identification of agents and their molecular targets for prostate cancer chemoprevention is guided by data derived from a variety of sources including epidemiological, clinical and pre-clinical studies (Adhami and Mukhtar 2007). Prostate cancer develops via modifications in various molecular events, thus inhibiting only one event may not be enough to avert or delay the disease onset. Therefore, identification of chemopreventive agents that target multiple anticancer pathways is essential. Future directions for prostate cancer prevention include genetic, proteomic and immunological approaches for identifying and targeting pathways that are associated with cancer initiation and development (Umar et al. 2012; Turnbull et al. 2018).

1.1.7 Hormone-dependent mechanisms of prostate cancer

Most prostate cancers initiates with AD state and rely on cellular androgen levels. Hence, the biosynthetic pathways, which contribute to androgen production, are crucial for prostate cancer progression.

1.1.7.1 Androgen receptor signaling pathway in prostate cancer

The androgen receptor (AR) signaling pathway is triggered by binding of androgens to AR. There is a large body of evidence supporting a role for androgens in prostate

cancer development and progression (Bladou et al. 1996; Rove and Crawford 2014). Androgen production is initiated by the release of luteinizing hormone-releasing hormone (LHRH) from the hypothalamus, which stimulates the pituitary gland to secrete luteinizing hormone (LH). LH then binds to LH receptors in Leydig cells to initiate the production of androgens.

1.1.7.2 Steroidogenesis

Endocrine tissues such as the gonads and the adrenals are tissues that are able to produce active steroid hormones from cholesterol by a process known as steroidogenesis. These steroid hormones then enter the blood circulation to exert their action at sites distant from where they are produced. Steroidogenesis begins with the irreversible cleavage of a 6-carbon group from cholesterol, producing pregnenolone, catalysed by cytochrome P450_{scc} (side chain cleavage enzyme, CYP11A1). A small repertoire of cytochrome P450 and non-P450 enzymes then convert pregnenolone to other 21-carbon steroids (including glucocorticoids, and mineralocorticoids), 19-carbon steroids (androgens) and 18-carbon steroids (estrogens) (Sharifi and Auchus 2012). The transformations catalyzed by the cytochrome P450s, 5 α -reductases, and individual isoforms of 3 β -hydroxysteroid dehydrogenase (3 β HSDs) are all irreversible reactions, giving rise to the general pathways of steroidogenesis (Figure 3).

Cytochrome P450 steroid 17 α -hydroxylase/20,22-lyase (CYP17) is the key enzyme in the synthesis of 19-carbon sex steroid precursors from 21-carbon pregnanes. CYP17 is unique due to its ability to catalyze two independent reactions in the same active center, CYP17 catalyzes both the 17 α -hydroxylation of pregnenolone and progesterone and the subsequent 17,20-lyase cleavage (side chain cleavage from 17 α -hydroxypregnenolone and 17 α -hydroxyprogesterone) (Lee-Robichaud et al. 1995) to produce dehydroepiandrosterone (DHEA) and androstenedione (AN), respectively (Yamaoka et al. 2010). *CYP17A1* is expressed in testicular, adrenal and prostatic tumor tissues; the expression of *CYP17A1* in metastatic prostate cancer was 16.9-fold higher ($p = 0.0005$) than that in primary prostate tumors (Montgomery et al. 2008). Although small amounts of AN, testosterone and other 19-carbon steroid metabolites can be directly produced by the adrenal glands, most androgens in the castrated male are produced in peripheral

tissues, where 3β HSD converts DHEA to AN and androstenediol to testosterone, respectively. Testosterone is then irreversibly 5α -reduced to the higher affinity ligand DHT by steroid 5α -reductase (SRD5A) isoenzymes. Healthy prostate contains mainly SRD5A2, whereas in malignancy SRD5A1 protein becomes over-expressed. Androgens are important for the maintenance of *SRD5A* expression in healthy prostate, and anti-androgens (and possibly CYP17 inhibitors) cause downregulation of *SRD5A* expression (Nishiyama et al. 2004). *SRD5A* gene regulation is dependent on the transcription factor Sp1 (Blanchard et al. 2007).

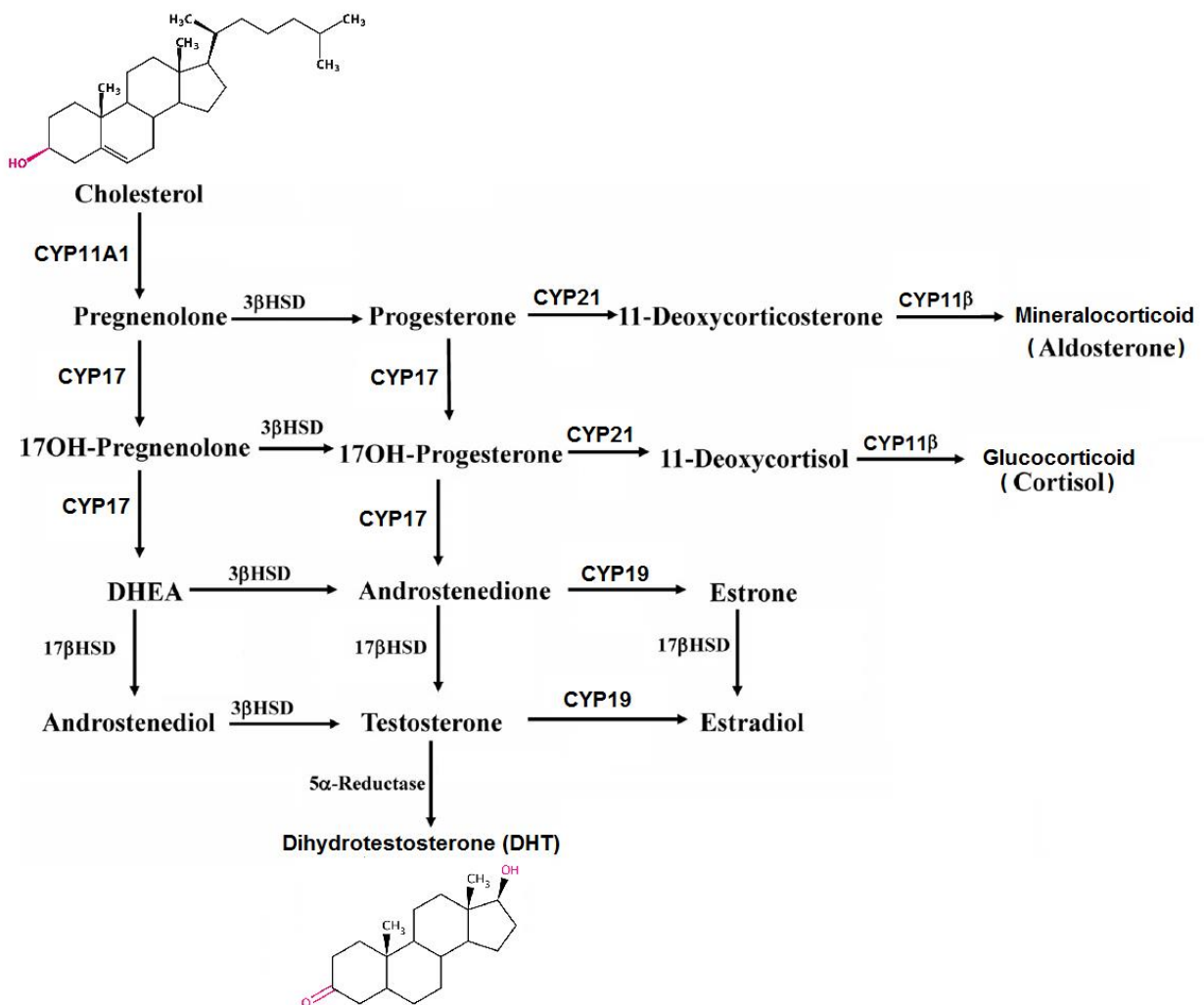


Figure 3: Steriodogenesis.

The cytochrome P450 enzyme CYP11A1 cleaves cholesterol to pregnenolone. pregnenolone is converted to other 21-carbon steroids (including glucocorticoids, and mineralocorticoids), 19-carbon steroids (androgens) and 18-carbon steroids (estrogens). Adapted from (Miller and Auchus 2011)

1.1.7.3 Activation of AR signaling

The AR is a member of the steroid–thyroid–retinoid nuclear receptor superfamily (Quigley et al. 1995). In the absence of androgens, the AR is located in the cytoplasm, in a complex with heat-shock proteins (HSPs). Androgen binding to its receptor induces conformational changes that facilitate the formation of AR homodimer complexes, which can then bind to androgen response elements (AREs) in the promoter regions of target genes (Figure 4). The activated DNA-bound AR homodimer complex recruits co-regulatory proteins, co-activators or co-repressors, to the AR complex. The co-activators/repression allow interaction of the AR complex with the general transcription machinery to stimulate or inhibit target gene transcription (McKenna et al. 1999).

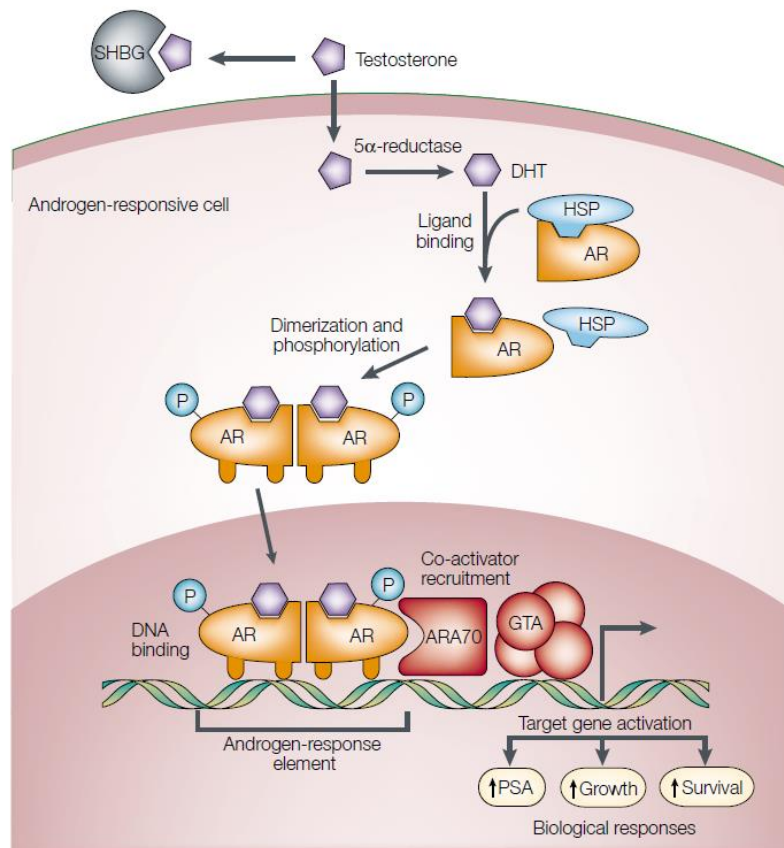


Figure 4: AR signaling pathway.

Testosterone enters prostate cells and is then converted to dihydrotestosterone (DHT) by the enzyme steroid 5 α -reductase. Binding of DHT to the AR induces receptor phosphorylation and dissociation from HSPs. The AR dimerizes then bind to androgen-response elements. Activation of target genes leads to biological responses including growth, survival (Feldman and Feldman 2001).

1.1.7.4 Activation of estrogen receptor signaling

In addition to androgens, estrogens are implicated in AD prostate tumor growth (Bosland 2000). Although considered to be growth inhibitory in normal prostate (Taplin and Ho 2001), estrogens appear to have direct proliferative effects in malignancy (Risbridger et al. 2003) and cause malignant prostate metaplasia at pharmacological doses (Levine et al. 1991). Various mechanisms have been suggested for the carcinogenic effects of endogenous estrogens in prostate, including metabolism to genotoxic 4-hydroxyestrogens (Cavalieri et al. 2002), stimulation of estrogen receptor (EsR)-mediated cell proliferation, or increased affinity of AR for estrogens (as in LNCaP cells) due to mutations in AR protein (Culig et al. 1997). EsR status also appears important as increased estrogen concentrations in aging prostate cause upregulation of EsR α (cell-proliferative) and downregulation of EsR β (anti-proliferative) (Chang and Prins 1999). Loss of EsR β occurs as prostate cancer progresses, which may be associated with increased local estrogen production (Ellem and Risbridger 2006). The key enzyme responsible for the final step in estrogen biosynthesis is aromatase (CYP19). CYP19 expression and catalytic activity has been detected in human prostate and is upregulated in benign prostate hyperplasia and prostate cancer. Importantly, in healthy prostate *CYP19* is expressed at low levels almost exclusively in stromal cells, whereas in malignancy increased epithelial expression occurs, with altered promoter usage (Ellem and Risbridger 2006). This runs remarkably parallel to what happens in hormone-dependent breast cancer, where CYP19 activity is increased in malignancy, and normal promoter usage switches from glucocorticoid-responsive I.4 to more aggressive cAMP-responsive I.3 and pII promoters (Zhou et al. 2001). However, little is known about aromatase regulation in human prostate, the signalling pathways involved, or modulation by xenobiotics. Aromatase inhibitors used clinically for the treatment of estrogen-dependent breast cancer also appear effective in the treatment of prostate cancers (Miller and Jackson 2003).

1.1.8 Hormone-independent mechanisms of prostate cancer

1.1.8.1 Cell cycle progression

The cell cycle is a complex cellular process, which controls cells growth. It relies on DNA duplication (S phase) and chromosomal separation into daughter cells (M phase). These key events are spaced by gaps of growth and reorganization (G1 and G2 phases) After M phase, cell can either enter G1 or the G0 quiescent phase (Figure 5). Cell cycle progression is regulated by cyclin-dependent kinases (CDKs) (Murray 2004). Activation of CDKs will lead to transition into the mitotic cell cycle, where association of CDKs with cyclins induces the kinases catalytic activity. Activation of CDKs is triggered by P38 mitogen-activated protein kinase (MAPK)/extracellular signal-regulated kinase (ERK)-mediated mitogenic signaling. Induction of mitogenic signaling pathways is associated with various cellular responses, such as proliferation, differentiation, survival, and transformation (McCubrey et al. 2006). Epidermal growth factor (EGF) and transforming growth factor beta 1 (TGF- β 1) induce mitogenic signaling and tumor progression through ERK pathway activation (Thakur et al. 2009; Wilson et al. 2009). Previous studies have shown that these mitogenic factors are overexpressed in prostate cancer tissues and linked to advanced malignancy (Leav et al. 1998; Cardillo et al. 2000). *IL-6* is overexpressed in prostate cancer tissues (Wegiel et al. 2008). A previous study of PC-3 xenografts treated with an anti-IL-6 antibody led to tumor suppression through inhibition of ERK phosphorylation (Steiner et al. 2003).

Cell cycle arrest occurs in response to cellular stress through activation of signal transduction pathways commonly known as checkpoints (Hartwell and Weinert 1989). The checkpoints are activated in the G1/S phase, which prevent replication of damaged DNA or in the G2/M phase to prevent damaged cells from entry to mitosis. Cell cycle checkpoints ensure the accuracy of DNA replication and division (Hartwell and Weinert 1989). Progression of cells from G2 into the M phase of the cell cycle requires activation of Cdk1/cyclin B kinase complex (Peng et al. 1997).

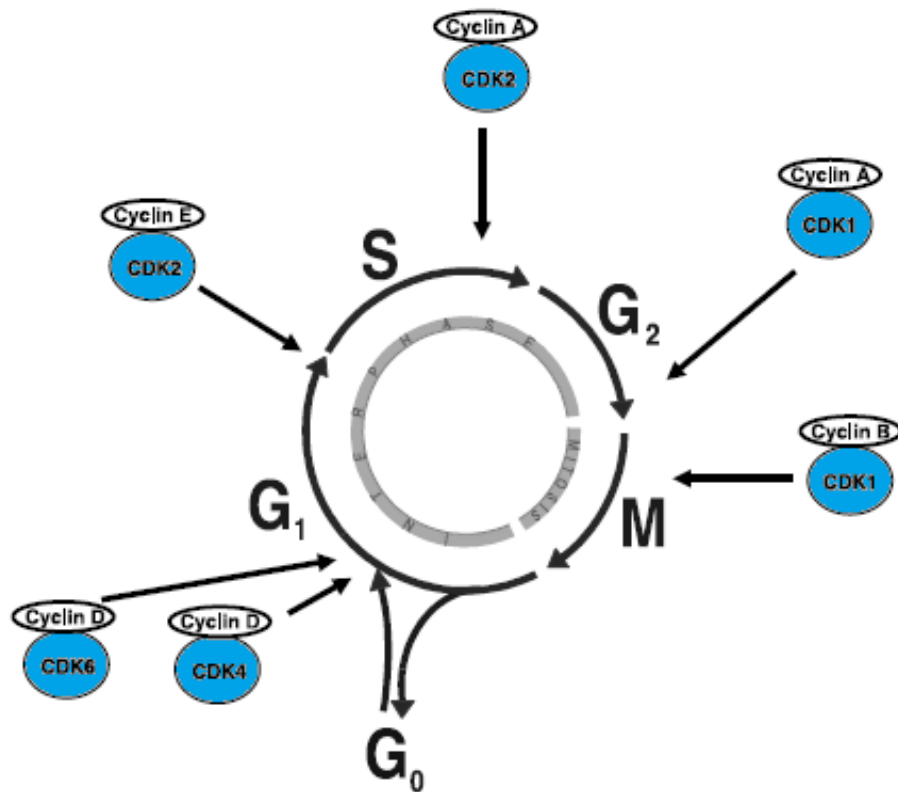


Figure 5: The stages of the cell cycle

Cell division is divided into two stages: a nuclear division stage, which is known as mitosis (M), and the interlude between two M phases, which is known as interphase. The interphase includes G₁, S and G₂ phases. DNA replication occurs in S phase. S phase is preceded by a gap called G₁ during which the cell prepares for DNA synthesis and is followed by G₂ gap during which the cell is preparing for mitosis. G₁, S, G₂ and M phases are the traditional subdivisions of cell cycle. Before commitment to DNA replication, cells in G₁ can enter a resting state called G₀. The site of activity of regulatory CDK/cyclin complexes is indicated in arrows (Vermeulen et al. 2003).

Cells can exit the cell cycle before mitogenic stimulation and enter G₀, where several gatekeepers for cell cycle transitions are activated to avoid cell cycle progression. Retinoblastoma tumor suppressor protein (RB) is one of the key gatekeepers that inhibits target genes involved in DNA replication (e.g. *cyclin A*) (Knudsen and Knudsen 2006). Cancer cells deficient in RB are resistant to cell cycle arrest mediated by CDK inhibition (Lukas et al. 1995).

1.1.8.2 PI3K/Akt/mTOR signalling pathway

The PI3K/Akt/mTOR signalling pathway is a cascade of events that plays a key role in cancer (Figure 6). It is one of the most frequently targeted pathways in all human cancers. It has been estimated that mutations in the individual components of this pathway account for as much as 30% of all known human cancers (Shaw and Cantley 2006). This complex pathway modulates AR signaling and androgen responsiveness (Liao et al. 2004; Salas et al. 2004), but is also critical for cell adhesion, growth and apoptosis (Polakis 2000). Akt activates various factors through phosphorylation, which in turn regulate four broad processes: cell-cycle progression, cell survival, cell proliferation and cell metabolism. Activation of Akt is correlated with prostate cancer progression. It has been shown that AR is upregulated by Akt in prostate cancer cells (Ha et al. 2011). The mammalian target of rapamycin (mTOR) kinase is the catalytic subunit of two complexes, mTOR complex 1 and 2 (mTORC1/2) that regulate growth and are often dysregulated in disease (Zoncu et al. 2011). The mTORC1 is the target of the well-known drug rapamycin, and includes the mTOR catalytic subunit, which phosphorylates 70S ribosomal protein S6 kinase (p70S6K) and eukaryotic translation initiation factor 4E-binding protein 1 (4E-BP1). The rapamycin-insensitive mTORC2 activates Akt by phosphorylating serine 473 (Zoncu et al. 2011). Once the PI3K/Akt/mTOR pathway is activated, it plays a crucial role in cell division and metabolism, thus influencing the metastasis, invasion and aggressiveness of cancer cells. Targeting this pathway is an important therapeutic option for better prognosis in cancer patients (Falasca et al. 2011).

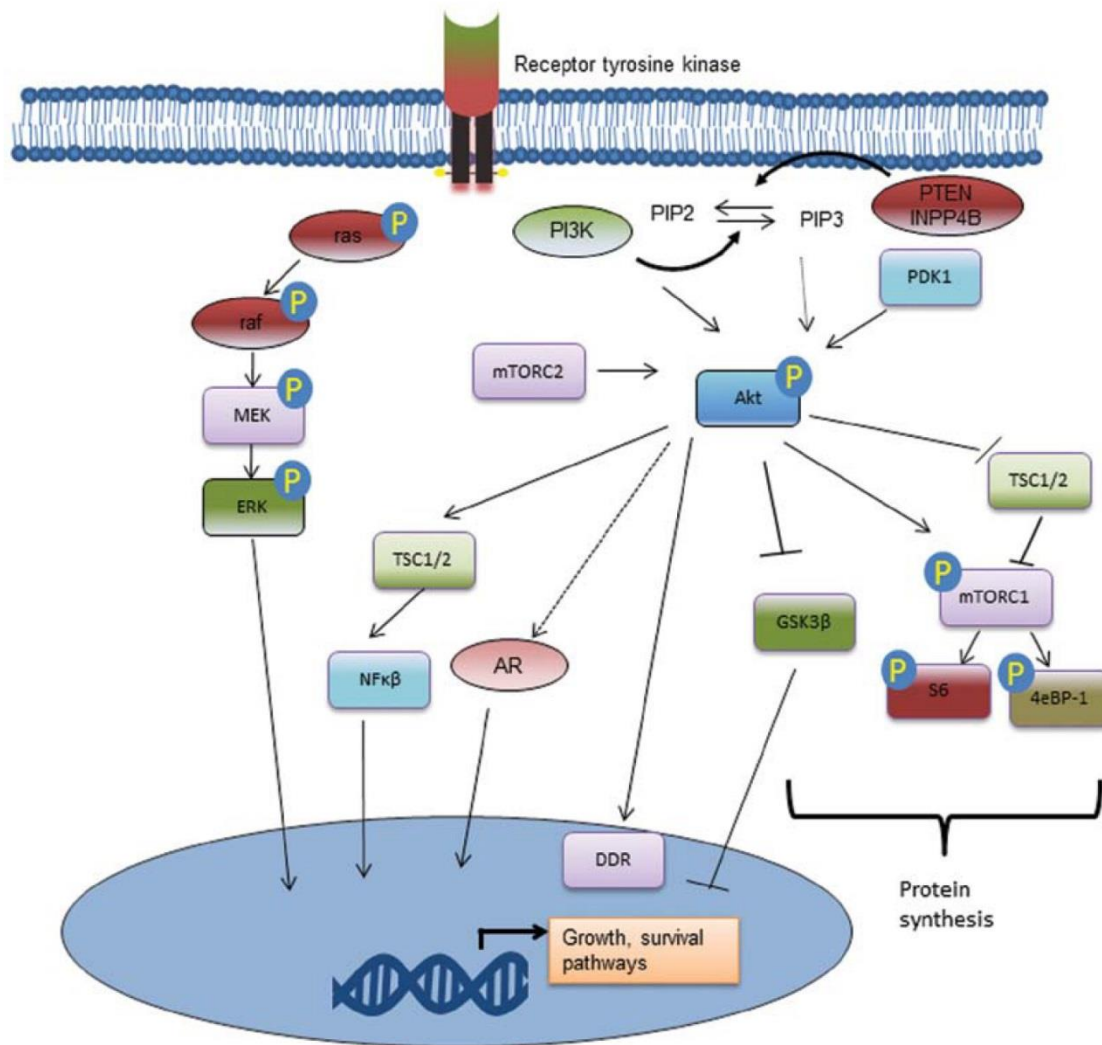


Figure 6: AKT/mTOR signaling pathway.

The PI3K/Akt pathway functions downstream of receptor tyrosine kinases (RTKs). Upon recruitment to the cell membrane, Akt is phosphorylated by phosphoinositide-dependent kinase 1 (PDK1), a reaction catalyzed by PIP3. Activated Akt is a kinase which in turn phosphorylates and activates many growth and survival pathways (Toren and Zoubeidi 2014)

1.1.8.3 Aryl hydrocarbon receptor (AhR) signaling pathway

AhR is a basic helix-loop-helix (bHLH) protein located in the cytosol. The AhR is the only ligand-activated member of the bHLH family; it is activated by the binding of a wide range of environmental hydrocarbons (Safe 2001). In the cytosol, AhR is found in a complex that consist of two molecules of heat shock protein 90 (HSP90), co-chaperone p23, immunophilin-like AhR-interacting protein (AIP) and tyrosine kinase c-Src (Perdew

and Bradfield 1996). This protein complex is designed to maintain the inactive conformation and prevent nuclear translocation. Upon binding by polycyclic aromatic hydrocarbons (PAHs) or halogenated aromatic hydrocarbons (HAHs), AhR dissociates from its chaperone proteins and translocated to the nucleus where the receptor heterodimerizes with the AhR nuclear translocator protein (ARNT) (Pollenz 1996) (Figure 7). The nuclear AhR complex interacts with xenobiotic response elements (XRE) in the promoter region of responsive genes, such as cytochrome P450 1A1 and 1B1 (*CYP1A1* and *CYP1B1*) (Bacsi et al. 1995). Although extensively studied as a key regulator of xenobiotic metabolism, AhR has been shown to influence a number of cellular processes, including differentiation, proliferation and cell cycle progression. Activation of the AhR by exogenous ligands has been reported to antagonize AR signaling. AhR ligands are a structurally diverse group of natural and synthetic compounds that elicit a broad range of biological effects. AhR ligand such as the most potent HAHs, 2,3,7,8-tetrachlorodibenzo-p-dioxin (TCDD) inhibited testosterone-dependent transcriptional activity and testosterone-regulated PSA expression in a dose dependent manner (Jana et al. 1999). TCDD blocks androgen-dependent proliferation of prostate cancer cells (Barnes-Ellerbe et al. 2004; Richmond et al. 2014). TCDD itself is carcinogenic (Enan and Matsumura 1996) and, therefore, is not suitable as anti-cancer treatment. Previous studies showed that AhR is constitutively active in AI prostate cancer (DU145 and PC-3 cells) but not in AD prostate cancer cells (LNCaP) (Richmond et al. 2014). Recently, activation of AhR using an AhR agonist in LNCaP cells promoted its invasiveness as measured by cell migration on matrigel (Ide et al. 2017).

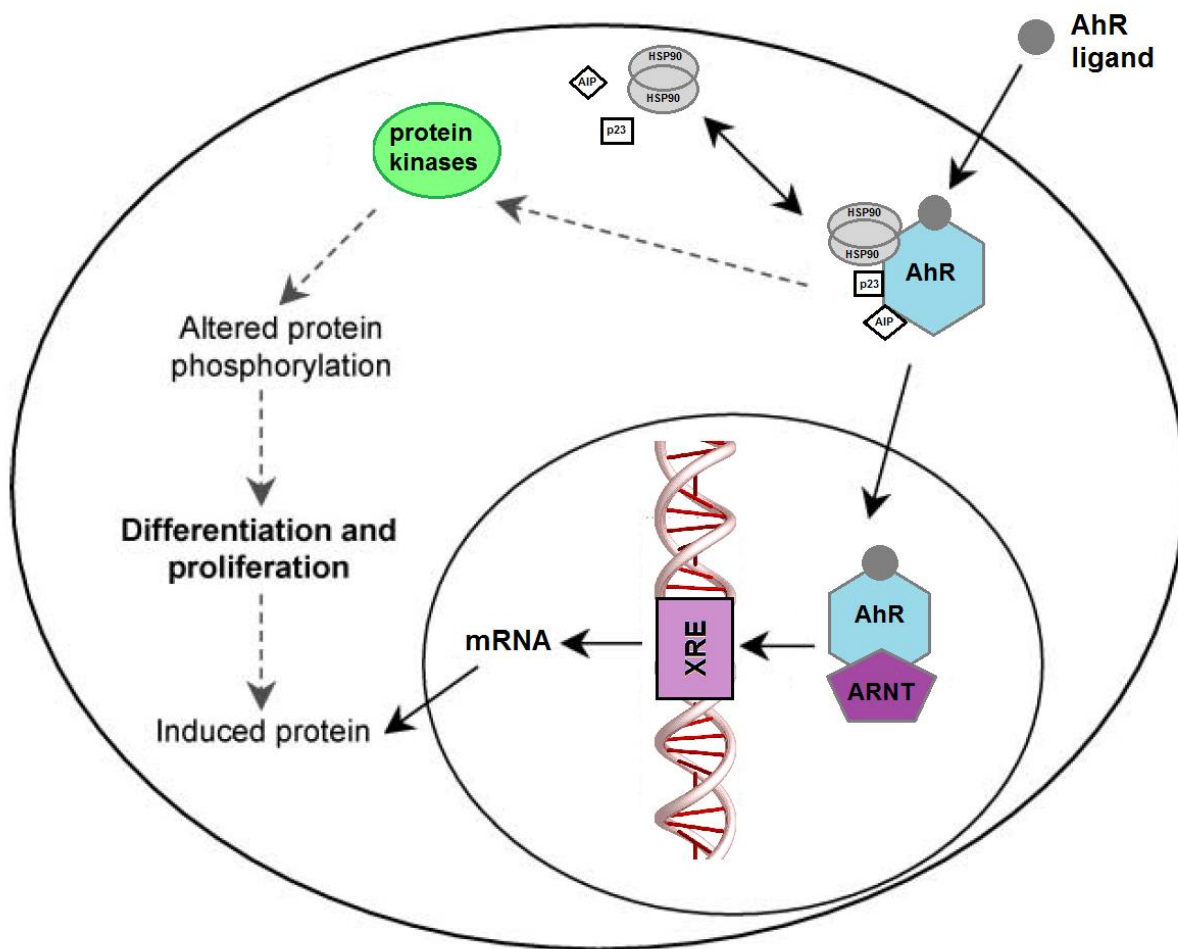


Figure 7: Aryl hydrocarbon receptor (AhR) signaling pathway

Binding of the ligand to the AhR results in the release of AhR-associated proteins and translocation of AhR to the nucleus and then dimerizes with ARNT. The AhR–ARNT complex binds the XRE promoting target gene transcription. Ligands can also exert their effects in the cytoplasm through AhR-associated protein kinases to alter the function of a variety of proteins through a cascade of protein phosphorylation (Pocar et al. 2005).

1.1.9 Current treatments for prostate cancer

Current therapies for prostate cancer include hormonal therapy, radiotherapy, surgery, chemotherapy, and immunotherapy. The most common hormonal therapies used to treat prostate cancer include chemical castration and treatment with AR antagonists, such as (hydroxy)flutamide and bicalutamide, or inhibitors of steroidogenesis. Inhibition of androgen synthesis by blocking the catalytic activity of SRD5A is another effective treatment against androgen dependent prostate tumors.

SRD5A inhibitors such as finasteride block synthesis of dihydrotestosterone (DHT), the major and most potent androgen produced by the prostate (Miyamoto et al. 2004). Finasteride and dutasteride are used clinically to inhibit SRD5A1/2 (Xu et al. 2006). Also, CYP17 inhibitors, such as abiraterone acetate, which block androgen synthesis improved overall survival in advanced prostate cancer patients (Fizazi et al. 2012).

Two phase I trials were conducted using abiraterone acetate in patients with progressive prostate cancer who were receiving androgen deprivation therapy (ADT), but had not received previous chemotherapy. In the first clinical trial, treatment with oral abiraterone acetate 250–2000 mg once daily, decreased serum testosterone levels to undetectable or near undetectable levels. Moreover, treatment with abiraterone acetate reduced PSA levels by $\geq 30\%$ in 66% of recruited patients. Levels of other components of the androgen synthesis pathway were also decreased with abiraterone acetate therapy, including androstenedione and DHEA. In the second clinical trial, treatment with abiraterone acetate 250-1000 mg daily, reduced PSA levels by $\geq 50\%$ in 55% of recruited patients; in addition, circulating cortisol and androgens levels were substantially decreased (Attard et al. 2008; Ryan et al. 2010).

Ironically, prostate cancers become apparent at an age when androgen levels in males have decreased and estrogen-to-androgen ratios have increased significantly, at least in serum (Ellem and Risbridger 2006). Estrogens play a role in prostate cancer progression, and aromatase (CYP19) inhibitors (which block estrogen synthesis) appear to offer protection (Narashimamurthy et al. 2004).

Over time, prostate cancers become refractory to hormone therapy and develop castration resistant phenotype. The poor prognosis of castration resistant prostate cancer (CRPC) has focused current research on drug therapies that delay progression to AI, or the use of cocktails of drugs with alternate targets for anticancer action (docetaxel/prednisone chemotherapy, selenium adjuvant therapy). Immunotherapy using the cancer vaccine sipuleucel-T has been approved by the US Food and Drug Administration (FDA) for the treatment of metastatic CRPC (Groves-Kirkby 2010; Drake et al. 2014; Mulders et al. 2015). Immunotherapy using immune checkpoint inhibitors has been effective in treating cancers such as metastatic melanoma (Hodi et al. 2010).

Immune checkpoint inhibitors block checkpoint proteins that prevent the immune system from attacking cancer cells. Checkpoint proteins include CTLA-4, PD-L1, (expressed on T cells), and PD-1 (expressed on tumor cells)(Venturini and Drake 2018). In recent years, immunotherapy has resulted in successful immune response to several types of tumors, such as metastatic melanoma, lung cancer and advanced renal cancer. Ipilimumab is the first antibody-based checkpoint inhibitor granted approval by FDA in 2011. Ipilimumab improved the survival of patients with metastatic melanoma (Hodi et al. 2010). However, immune checkpoint inhibitors appear to be less effective in treating prostate cancer (Goswami et al. 2016; Venturini and Drake 2018). In a recent phase 3 clinical trial, Ipilimumab (anti CTLA-4) did not improve survival of metastatic CRPC patients (Beer et al. 2017). Combination therapy is one alternative to overcome the lack of responsiveness to immune checkpoint monotherapy. Preclinical studies in mouse models of prostate cancer using immune checkpoint inhibitors combined with different cancer treatments such as surgical resection of primary tumor, cryoablation or tumor vaccines resulted in effective tumor immune response (Kwon et al. 1999; Curran and Allison 2009; Waitz et al. 2012).

A phase 3 clinical trial conducted using patients with CRPC showed that the CYP17 inhibitor abiraterone prolonged the survival time of patients by 4 months (de Bono et al. 2011). Recently, a phase 3 trial showed a prolonged survival with apalutamide (also a CYP17 inhibitor) in non-metastatic CRPC (Smith et al. 2018b). Another drug that is attracting attention for prostate cancer treatment is enzalutamide (an AR antagonist)(Nadal and Bellmunt 2016). Enzalutamide decreased the risk of metastasis and death in nonmetastatic CRPC patients (Hussain et al. 2018). A phase 3 trial conducted using 1199 men with CRPC after previous chemotherapy showed that enzalutamide prolonged the survival of metastatic CRPC patients after chemotherapy (Scher et al. 2012). Enzalutamide and abiraterone acetate have shown promising efficacies in clinical trials and the FDA has approved both drugs for treatment of CRPC. However, resistance to enzalutamide and abiraterone acetate treatment is still a challenge. Enzalutamide and abiraterone acetate resistance are associated with the presence of AR splice variants (AR-V7) (Antonarakis et al. 2014). Novel potential drugs,

such as phytochemicals, which are less toxic to healthy tissues, need to be evaluated to improve the clinical care of patients suffering from prostate cancer.

1.1.10 Causes of castration resistant prostate cancer

Various mechanisms contribute to CRPC, including (1) mutations in AR resulting in expression of constitutively active AR splice variant such as ARv7 that lacks the ligand binding domain (Germann 2002; Recouvreux et al. 2017), (2) overexpression of AR increasing its sensitivity to low androgen levels, thus impairing effectiveness of antiandrogen treatment (Linja et al. 2001), (3) induction of bypass pathways independent of AR such glucocorticoid receptor signaling (Kassi and Moutsatsou 2011), (4) increased intraprostatic androgen biosynthesis (Stanbrough et al. 2006) or (5) constitutive activation of cell proliferative pathways with gradual loss of AR (Gioeli 2010).

1.1.10.1 Cancer stem cells (CSCs) and CRPC

CSCs are a small subpopulation of cells within a tumor capable of self-renewal, tumor initiation and differentiation into various cell types that constitute the tumor (Yu et al. 2012). A great challenge for current therapies of advanced prostate cancer is the development of drug resistance. Accumulated experimental evidence has demonstrated differences in drug resistance among different clones of a tumor (Carreira et al. 2014; Tereshchenko et al. 2014; Bansal et al. 2016). Previous studies suggest that a subset of such clones represent resistant CSCs (Ojha et al. 2014; Leao et al. 2017; Howard et al. 2018). The cellular origin of CRPC is still controversial, but several studies have found CSCs in CRPC (Vander Griend et al. 2008; Qin et al. 2012). In addition, CSCs appear to contribute substantially to drug resistance in multiple cancer types including that of prostate (Ni et al. 2014). Therefore, targeting CSCs represent a potential strategy for prostate cancer treatment (Yun et al. 2016).

1.1.11 *TP53 mutations and prostate cancer*

The *TP53* gene is a tumor suppressor gene. p53 protein regulates cell division by preventing uncontrolled cell division and prevents the formation of tumor. P53 suppress tumor formation through 3 main mechanisms: cell cycle arrest, triggering apoptosis,

activation of DNA repair (Brady and Attardi 2010).The *TP53* gene is mutated in approximately 30% of prostate tumors (Ecke et al. 2007). Analysis of the genomically aberrant pathways in metastatic CRPC revealed that the frequency of TP53 mutations was significantly increased among metastatic CRPC samples (53.3%) compared to primary prostate cancer (Robinson et al. 2015). In addition, mutations in *TP53* contribute to tumor progression and drug resistance, and is often associated with increased risk of recurrence (Olivier et al. 2010). Moreover, p53 mutated proteins acquire new activities referred to as gain of function that contribute to tumor progression and increased resistance to cancer therapeutics (Santoro et al. 2014).

Mutations in *TP53* influence multiple cellular process including cell proliferation, apoptosis, autophagy, DNA damage and senescence (Aubrey et al. 2016).

P53 mutants with gain of function inhibit the formation of autophagic vesicles through repression of some key autophagy genes (*BECN1* and *ATG12*) (Cordani et al. 2016). In vitro and in vivo studies demonstrated that mutant p53 promoted cell proliferation, and inhibited apoptosis and senescence (Murphy et al. 2000; Matas et al. 2001; Lehmann et al. 2007; Duan et al. 2008). It has been shown that two *TP53* mutants (p53-223Leu and p53-274Phe) inhibit Fas expression in DU145 cells, which contributes to apoptosis resistance in prostate carcinoma cells (Gurova et al. 2003). In addition, a previous study demonstrated that targeting mutant p53 using RNA interference induced apoptosis in DU145 cells (Zhu et al. 2011).

1.2 DIINDOLYLMETHANE

Cruciferous vegetables contain large amounts of indole-3-carbinol (I3C), which in the stomach undergoes acid-catalyzed condensation reactions to produce various metabolites, of which a major condensation product is diindolylmethane (DIM) (Figure 8) (De Kruif et al. 1991b). Particularly DIM is considered to be the most abundant biologically active metabolite formed in the stomach (Reed et al. 2006). Oral administration of I3C in mice showed that I3C is not detected in plasma or tissues within 1 hour of treatment. However, DIM reached a maximum concentration in plasma after 2 hours of treatment and remained detectable as a major bioactive compound in plasma after 6 hours

(Anderton et al. 2004). In addition, a clinical study using single and multiple oral doses of I3C did not detect the pure indole in the plasma of study participants, but instead detected only DIM (Reed et al. 2006).

1.2.1 Cruciferous vegetables and prostate cancer

Epidemiological studies consistently associate vegetable and fruit consumption with reduced incidence of several types of cancer (Murillo and Mehta 2001). Previous study showed no association of vegetables and fruit consumption with the overall prostate cancer risk. However, a decreased risk of stage III or IV extra-prostatic prostate cancer was associated with consumption of cruciferous vegetables. In addition, broccoli consumption decreased the risk of both aggressive and extra-prostatic prostate cancer. Moreover, the risk of aggressive prostate cancer decreased with increasing spinach consumption. The consumption of spinach also decreased the risk of extra-prostatic disease but this observation was not statistically significant (Kirsh et al. 2007). Vegetables contain a large variety of phytochemicals purported to have many health benefits. In particular, vegetables of the *Brassica* family have been identified as important dietary protectors against cancer (Kim and Park 2009b), including hormone-dependent cancers such as that of the prostate (Cohen et al. 2000). DIM and I3C have been shown to inhibit growth of various cancer cells *in vitro* (Le et al. 2003; Goldberg et al. 2013; Ye et al. 2016; Zhang et al. 2017) and in animal models *in vivo* (Chen et al. 1998; Nachshon-Kedmi et al. 2004a).

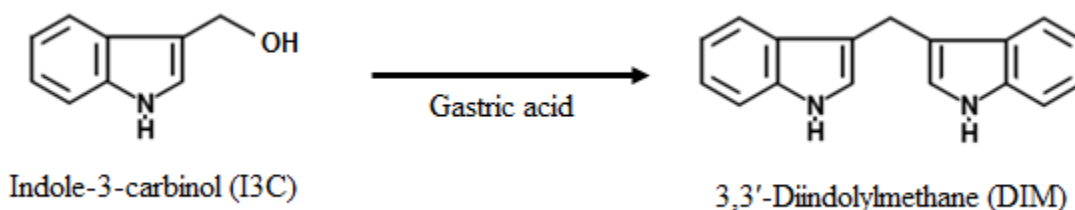


Figure 8: Formation of diindolylmethane (DIM) from indole-3-carbinol (I3C).

I3C undergoes acidic reactions in the stomach and produce DIM as a major condensation product.

There is accumulating evidence that DIM acts via hormone-dependent as well as -independent pathways (Contractor et al. 2005). This observation is crucial as most aggressive prostate cancers ($\approx 30\%$ of all cases) evolve from an AD to androgen-independent (AI) state, rendering the cancer poorly treatable by conventional medications, resulting in metastases and ultimately death of the patient (Gittes 1991). Several drugs approved by the FDA for treatment of CRPC, such as enzalutamide and abiraterone acetate (de Bono et al. 2011; Nadal and Bellmunt 2016) have improved the survival of CRPC patients. However, chemoresistance is still a challenge (Antonarakis et al. 2014; Wade and Kyprianou 2018). We have recently shown that ring-substituted analogs of DIM (ring-DIMs) (Figure 9) are potent inhibitors of the growth of LNCaP (AD) and PC-3 (AI) human prostate cancer cells (Abdelbaqi et al. 2011; Goldberg et al. 2013).

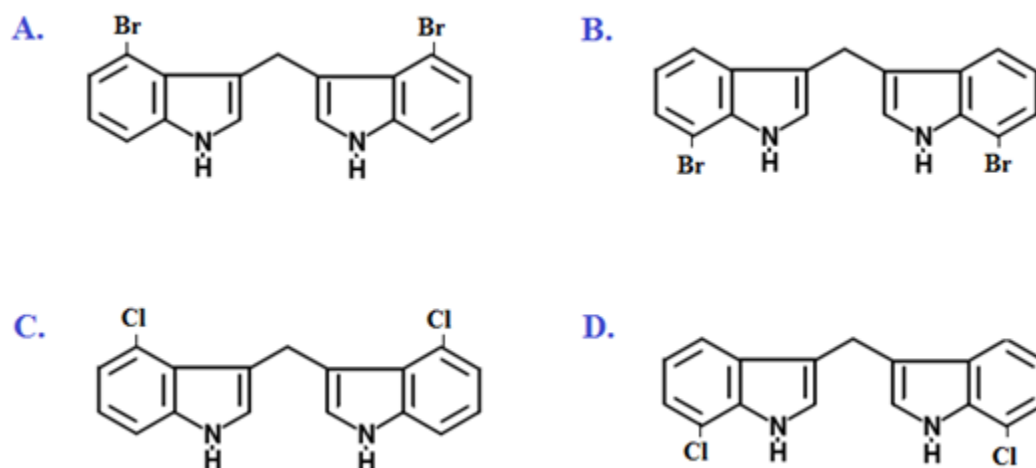


Figure 9: Chemical structures of ring-DIMs.

(A) 4,4'-Br₂DIM, (B) 7,7'-Br₂DIM, (C) 4,4'-Cl₂DIM, and (D) 7,7'-Cl₂DIM.

1.2.2 Anti-prostate cancer activity of DIM

1.2.2.1 Antiandrogenicity

DIM has been described as a relatively potent AR antagonist in LNCaP human prostate cancer cells (Le et al. 2003). In this study, DIM inhibited growth of DHT-stimulated LNCaP cells (half maximal inhibitory concentration, $IC_{50} \approx 30 \mu M$), but had no effect in AR-negative PC-3 human prostate cancer cells. It reduced DHT-induced PSA production to control levels at $50 \mu M$. In addition, DIM inhibited DHT-stimulated luciferase

activity in LNCaP cells transiently transfected with an AR-responsive reporter ($IC_{50} \approx 3 \mu M$). DIM also inhibited nuclear translocation of ligand-bound AR at concentrations $\geq 1 \mu M$. A hormone-binding assay ultimately showed that DIM displaced [3H]-DHT from AR (in pure recombinant form and in LNCaP extracts) with a relative binding affinity 3500 to 8000 times weaker than that of DHT. Nevertheless, it had an affinity close to that of bicalutamide (Le et al. 2003). Another study comparing DIM to its parent compound I3C found that I3C produced similar antiandrogenic responses in LNCaP cells, but with lesser potency (Hsu et al. 2005). In addition, 200 μM I3C downregulated AR expression, whereas 50 μM DIM did not. Recently, 10 and 25 μM BioResponse DIM (B-DIM), a DIM formulation with greater bioavailability, was reported to reduce AR protein and mRNA expression in LNCaP cells (Bhuiyan et al. 2006). More recently, 1 μM DIM inhibited androgen responsive genes (PSA, NKX3.1, and IGF-1R) in LNCaP cells (Wang et al. 2012). Above studies indicate that the antiprostata cancer activity of DIM may, at least in part, be due to antagonism and/or downregulation of AR. However, our laboratory recent studies (Abdelbaqi et al. 2011; Goldberg et al. 2014) find DIM to be less potent and act differently than described in earlier studies, which have not since been re-examined or challenged.

1.2.2.2 Induction of apoptotic and anti-proliferative signaling pathways

Apoptosis or programmed cell death plays an important role in several biological processes including a key mechanism for tumor suppression. Mutant or damaged cells could either progress into cancer cells or be eradicated via apoptosis (Delbridge et al. 2012).

Many studies have confirmed that DIM induces apoptosis in cancer cells through two main mechanisms. The first includes inhibition of the expression of anti-apoptotic proteins such as Bcl-2, Bcl-xl and cellular FLICE inhibitory protein (C-FLIP). The second mechanism involves induction of proapoptotic proteins such as Bax, Smac/DIABLO and apoptosis-inducing factor (AIF), as well as the release of cytochrome C and activation of caspase-9, caspase-8 and caspase-3 (both intrinsic and extrinsic apoptosis) (Hong et al. 2002; Nachshon-Kedmi et al. 2004b; Aggarwal and Ichikawa 2005; Pappa et al. 2006; Kim et al. 2007).

DIM also targets multiple apoptotic pathways in prostate cancer cells. DIM sensitised LNCaP and C4-2B prostate cells to apoptotic cell death induced by taxotere through repression of survivin expression, a known inhibitor of apoptosis (Rahman et al. 2009). Previous studies showed that DIM induced apoptosis in prostate cancer cells via inhibition of AKT and MAPK (Bhuiyan et al. 2006; Khwaja et al. 2009). DIM activate AMPK signaling, and induced apoptosis through downregulation of AR in LNCaP and C4-2B cells (Chen et al. 2012). DIM induced apoptosis in PC-3 and DU145 prostate through activation of MAPK pathway (Khwaja et al. 2009).

DIM decreased cell proliferation in PC-3 cells over expressing platelet-derived growth factor-D (PDGF-D) through inhibition Akt and mTOR (Kong et al. 2008). DIM interacts with this pathway by inhibiting phosphorylation of Akt, resulting in increased degradation of β -catenin (presumably due to stabilization of GSK-3 β) (Li et al. 2007). As β -catenin and p-Akt activate AR-transactivation, possibly via site-selective AR phosphorylation (Rochette-Egly 2003), inhibition of this pathway results in downregulation of AR and reduced sensitivity to androgens (Liao et al. 2004; Salas et al. 2004).

DIM anticancer activity was mediated by its inhibition of PI3K as well as Akt in cancer cells. B-DIM also suppressed mTOR in LNCaP cells (Chen et al. 2012). DIM is known to be a selective AhR receptor modulator (Yin et al. 2012). It activates AhR-controlled pathways which results in CYP1 induction and strong inhibition of estrogen receptor- α expression and estrogen signaling (Okino et al. 2009).

DIM induces G1/S cell cycle arrest in various cancer cell types, including prostate cancer cells (Chinnakannu et al. 2009). DIM induced cell cycle arrest in LNCaP and DU145 cells via induction of the cell cycle inhibitor p27 and inhibition of CDK (Vivar et al. 2009). DIM also inhibits histone deacetylase activity and induced the cell cycle inhibitor p21 in LNCaP and PC-3 prostate cancer cells (Beaver et al. 2012).

1.2.3 Anticancer effects of DIM *in vivo*

Several studies showed inhibitory effects of DIM on tumor growth *in vivo* in different types of cancer including lung (Qian et al. 2013), colon (Kim et al. 2009), breast (Chang

et al. 2005; Jin 2011), ovarian (Kandala and Srivastava 2012a; Kandala and Srivastava 2012b; Kandala et al. 2012), and nasopharyngeal carcinoma (Li et al. 2016).

In vivo studies also showed chemoprevention activity of DIM against prostate cancer (Bjeldanes et al. 1991; Chen et al. 2012; Cunningham and You 2015). DIM significantly reduced tumor growth in TRAMP mice through inhibition of cyclins, CDKs and induction of p27 and Bax expression (Cho et al. 2011). Another study on TRAMP-C mice showed the ability of DIM to inhibit tumor growth through induction of apoptosis and reduction in cell proliferation (Nachshon-Kedmi et al. 2004a). B-DIM suppresses tumor growth in C4-2B xenograft mice via down regulation of AR and activation of AMPK (Chen et al. 2012). Moreover, B-DIM blocked critical survival signaling pathways and enhanced the radiation efficacy in prostate cancer xenograft nude mice (Singh-Gupta et al. 2012). Recently, a pharmacological formulation containing DIM, cod liver oil and vitamin E showed an inhibitory effect on tumor growth of LNCaP xenograft mice model (Kiselev et al. 2014).

1.2.4 DIM clinical trials in treatment of prostate cancer

A phase I clinical trial of B-DIM, a formulated DIM with higher bioavailability, were conducted in non-metastatic CRPC patients to determine the maximum tolerated dose and pharmacokinetics of B-DIM. B-DIM maximum tolerated dose was 300 mg and 225 mg of B-DIM was recommended for phase II clinical trials (Heath et al. 2010).

Recently, a phase II clinical trial was conducted on treatment-naïve patients diagnosed with T1 or T2 prostate cancer. Patients received 225 mg B-DIM. 96% of patients received B-DIM showed nuclear exclusion of AR, while prostate biopsy samples collected before treatment showed no nuclear exclusion of AR, which confirms the anti-androgenic effect of B-DIM. These results suggests that further investigations into the therapeutic and chemopreventive effectiveness of B-DIM are warranted (Hwang et al. 2016).

A phase II clinical trial was also conducted on the new DIM formulated drug (Infemin) with higher bioavailability which comprises DIM solution in hard gelatin capsules (Paltsev et al. 2016). The clinical trial includes high-grade prostatic intraepithelial neoplasia (PIN) patients who receive either Infemin containing 900 mg DIM or placebo. The results of this

clinical trial showed 45.5 % of PIN regression in patients treated with Infemin compared to placebo with no observed PIN regression (Paltsev et al. 2016).

1.2.5 Anti-cancer properties of ring-DIMs

Previous studies reported that ring-DIMs significantly inhibited DHT-stimulated growth of LNCaP cells with IC₅₀ values between 2- and 3.5-fold lower than DIM. In this earlier study, cell growth was assessed by measuring mitochondrial reductase activity after a 96 h exposure to the ring-DIMs (Abdelbaqi et al. 2011). Recently, the inhibitory effects of ring-DIMs were confirmed on DHT-stimulated LNCaP cell proliferation in real-time using an xCELLigence label-free cell analysis system (Goldberg et al. 2014). Inhibition of AD cell proliferation by the ring-DIMs occurred rapidly, before signs of cytotoxicity with potencies differing in a structure-dependent manner. Notably, both 7,7'-Br₂- (IC₅₀=0.40±0.23 μM) and 7,7'-Cl₂DIM (IC₅₀=0.64± 0.18 μM) were most effective at inhibiting DHT-stimulated proliferation of LNCaP cells, with about 2-2.5 times greater potencies than DIM (IC₅₀=0.94±0.26 μM). 4,4'-Br₂DIM (IC₅₀=0.81±0.28 μM), but not 4,4'-Cl₂DIM (IC₅₀=1.36±0.42 μM), was still more effective than DIM, but was less potent than the 7,7'- dihaloDIMs (Goldberg et al. 2014).

Moreover, ring-DIMs induced apoptosis and necrosis in LNCaP and PC-3 prostate cancer cells. In this study, ring-DIMs were consistently more effective at killing these cells than DIM (IC₅₀ values were 23.8 μM ±0.4 in LNCaP cells and 18.3 μM±1.0 in PC-3 cells). 4,4'-Br₂DIM was the most potent inducer of LNCaP and PC-3 cell death, with IC₅₀ values of 7.5±0.1 μM and 8.9±0.3 μM, respectively, while IC₅₀ values for 4,4'-Cl₂DIM (18.1±0.3 μM and 16.0 ±1.3 μM), 7,7'-Br₂DIM (16.8±0.3 μM and 16.6±0.8 μM) (Goldberg et al. 2014). Both 4,4'- and 7,7'-Br₂DIM decreased AR levels and increased nuclear localization of AR, while 4,4'- and 7,7'-Cl₂DIM had minimal effect. Ring-DIMs also inhibited the fluorescence induced by androgens in LNCaP cells transfected with an androgen-responsive probasin promoter-GFP gene construct, with potencies up to 10-fold greater than that of DIM (Abdelbaqi et al. 2011). Moreover, ring-DIMs induced apoptosis and necrosis in LNCaP and PC-3 cells with 2-4 fold greater potency than DIM. 4,4'-Br₂DIM-induced apoptosis was caspase-3 dependent. Ring-DIMs induced the

expression of Fas, FasL, and death receptors DR4 and DR5 in LNCaP and PC-3 cells (Goldberg et al. 2014).

The differences in cytotoxic potency of DIM and ring-DIMs could be attributed, in part, to differences in intracellular concentrations attained in cell culture. Previous study by Goldberg and coworkers (Goldberg et al. 2014) showed that about 20-30 % of DIM was found in the cellular fraction of both LNCaP and PC-3 cells. Whereas exposure to 7,7'-Br₂-, 4,4'-Cl₂- or 7,7'- Cl₂DIM resulted in intracellular levels of ≥38 % (LNCaP) and ≥29 % (PC-3) of the amount of compound added to the cell culture media, cells treated with 4,4'-Br₂DIM contained 2-5 times lower intracellular levels compared to the other ring-DIMs. Moreover, in LNCaP cells, intracellular levels of 7,7'-dihaloDIMs were twice as high as that of DIM (Goldberg et al. 2014). The structure dependent differences of ring-DIMs and their mechanisms of action need to be studied in more detail to reveal their role in prostate cancer chemoprevention.

1.3 AUTOPHAGY

Stress stimuli such as starvation, hypoxia or toxic insult activate homeostatic mechanisms of acclimation, which are crucial either to tolerate cellular stress conditions or to initiate cell death mechanisms, such as apoptosis, to eliminate damaged cells (Hanahan and Weinberg 2011). Stress activates a self-digestion process called autophagy, where dysfunctional organelles and protein aggregates are sequestered in double membrane vesicles (Klionsky and Emr 2000; Mizushima et al. 2002), then transported to lysosomes for degradation and recycling to maintain cellular homeostasis (Glick et al. 2010).

Autophagy has as main function to protect cells from stress conditions, such as nutrient deprivation and cellular stress (Glick et al. 2010). Cancer is considered to be one of the leading health threats worldwide. More effective cancer therapies are needed to reduce the high risk of mortality. The higher mortality rates are attributed mainly to tumor relapse, metastasis and lack of effective treatments (Guan 2015) .

Autophagy plays an important role in tumor progression; its induction in response to stresses following chemotherapy may promote survival of cancer cells. However, excessive autophagy could activate a cell death mechanism known as cytotoxic autophagy or type II programmed cell death, which is different from type I programmed cell death (apoptosis) (Yang and Winslet 2011; White 2015). Uncontrolled growth of cancer cells is due to the inactivation of cell death pathways (e.g. apoptosis) and/or stimulation of cell survival pathways (Hanahan and Weinberg 2011; Portt et al. 2011) . Thus, the activation of cell death pathways by the autophagic machinery in cancer cells could help in controlling this disease. The role of autophagy in carcinogenesis is complex and still controversial.

1.3.1 Types of autophagy

Autophagy includes three types; macroautophagy (degradation of proteins and cellular organelles within the autophagic vacuoles after their delivery to lysosome), microautophagy (cytoplasmic degradation directly through the invagination of the lysosome without formation of autophagic vacuoles) and chaperone mediated autophagy (selective protein debasement where proteins are recognised by specific chaperons such as heat shock proteins) (Mizushima, 2007). Macroautophagy is the main and most studied autophagy pathway; this review will focus only on macroautophagy (hereafter referred to as autophagy).

1.3.2 Autophagy mechanism

Autophagy is a highly conserved, complex process controlled by a group of genes called autophagy-related genes (ATG). A key step in autophagy is the formation of autophagosome which requires the progressive modification of the autophagy regulator known as microtubule-associated protein 1 light chain 3 (LC3) (Mizushima et al. 2011).

1.3.2.1 Initiation step

There are different factors and stress stimuli that can induce autophagy. Starvation (nutrient deprivation) is one of the known autophagy inducers, which causes inhibition of the mTOR. Inhibition of mTOR activates the autophagy initiator ULK1 (unc-51-like

autophagy activating kinase 1; ATG1) and thereby autophagy (Nazio et al. 2013). Starvation also activates AMP-activated protein kinase (AMPK) as a consequence of a decreased ATP to AMP ratio. AMPK activation also induces autophagy via activation of ULK1 (Kim et al. 2011) (Figure 10).

1.3.2.2 Double membrane vesicle initiation

Inhibition of mTOR and activation of ULK1 leads to the initiation of double membrane vesicle (phagophore) formation through the activation of the nucleation complex of autophagy that includes Beclin1 and class III PI3K. The autophagy regulator LC3 is cleaved by ATG4, to produce LC3-I with a molecular weight (MW) of 18 kDa. LC3-I is localized throughout the entire cytoplasm (diffuse form)(Parzych and Klionsky 2014). Upon autophagy induction, a portion of LC3-I is coupled to phosphatidylethanolamine (PE) to form LC3-II (punctate form) with a MW of 16 kDa. This step is mediated by two autophagy regulators, ATG3 and ATG7. LC3-II forms punctate structures within the autophagosome, LC3-I to LC3-II conversion is considered as a specific and classical marker of the autophagosome formation (autophagy induction) (Tanida et al. 2004).

1.3.2.3 Double membrane elongation

Several ATGs, such as ATG5, ATG12 and ATG-16 form an elongation complex for autophagosome completion. ATG5-ATG12-ATG16 complex is essential for elongation of the double membrane vesicle and recruitment of LC3-II on the surface of the phagophore to form an autophagosome that surrounds the cargo (dysfunctional organelles and protein aggregates)(Klionsky 2010).

1.3.2.4 Fusion with lysosome and degradation of cargo

After the elongation step and completion of the autophagosome, damaged cellular organelles (mitochondria, peroxisomes, ribosomes, proteins etc.) are delivered to lysosome. Fusion between autophagosome and lysosome will lead to the formation of autolysosome and cellular degradation of cargo by the action of lysosomal enzymes (Klionsky and Emr 2000). Simple molecular components resulted from this degradation process are recycled and used by the cell (Tanida et al. 2004).

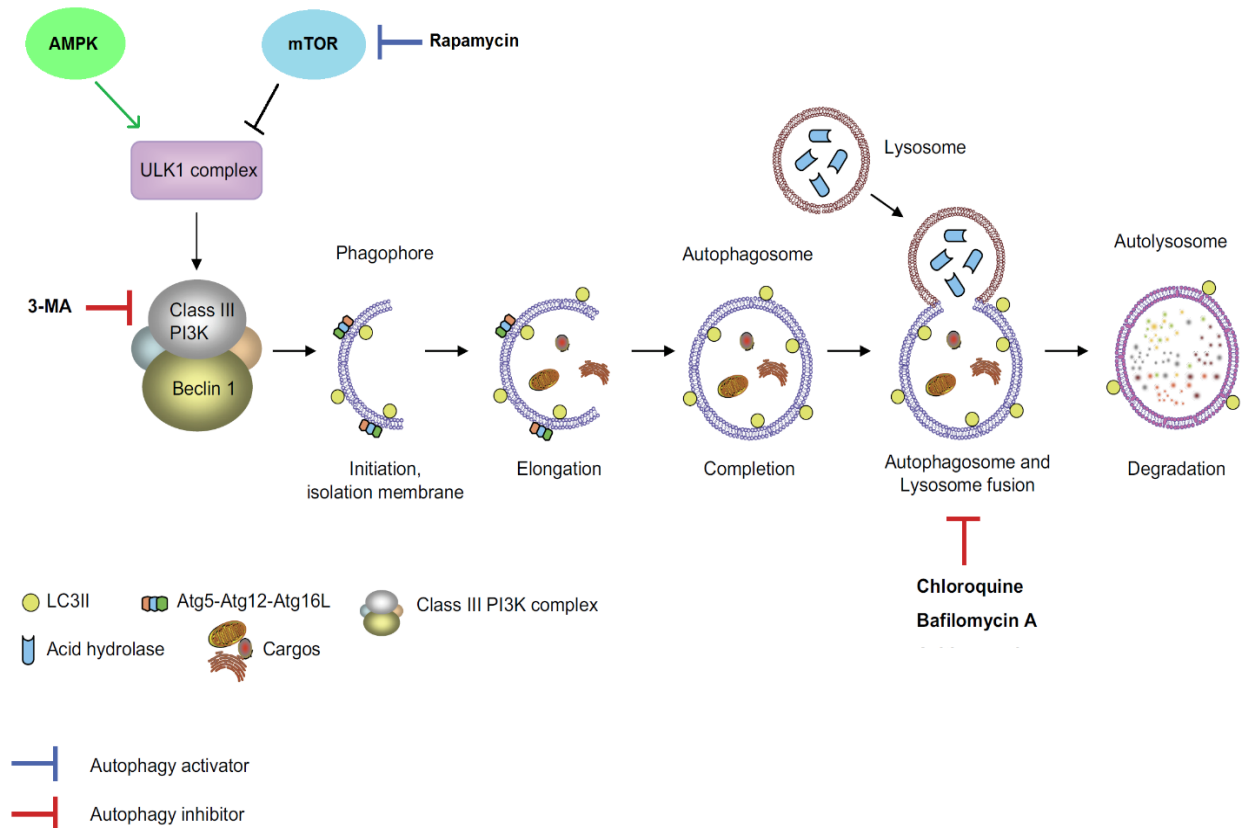


Figure 10: Autophagy mechanism.

Starvation is one of the known autophagy inducers, causing inhibition of mTOR. Starvation also activates AMPK. Inhibition of mTOR activates the autophagy initiator ULK1 which leads to initiation of phagophore formation through the activation of the nucleation complex of autophagy including Beclin1 and class III PI3K. The double membrane phagophore is then elongated to produce an autophagosome in the presence of the ATG5-ATG12 complex. This is followed by fusion of the autophagosome with a lysosome for cargo degradation. Adapted from (Nakahira and Choi 2013)

1.3.3 Dual Role of autophagy in cancer

An important question has been raised about the role of autophagy in cancer progression. Some studies have shown that autophagy acts as a mechanism of tumor suppression; in contrast, other studies have demonstrated that the autophagic machinery is utilised to enhance tumorigenesis (Figure 11).

1.3.3.1 Tumor suppressor function of autophagy

Initially, autophagy was believed to have a tumor suppressor function. This idea was concluded from the fact that the key autophagy related gene ATG6 (Beclin 1 or *BECN1*)

was deficient in approximately 60% of human cancers (Aita et al. 1999; Liang et al. 1999; Choi et al. 2013). Moreover, mutations in *BECN1* promote tumorigenesis in mice (Qu et al. 2003) (Figure 2). In addition, autophagy inhibition that results in accumulation of its substrate, P62 protein, which activates nuclear factor kappa-B (NF- κ B), induces oxidative stress and thereby promotes tumor growth (Mathew et al. 2009). In many human cancers, autophagy is inhibited as a consequence of activation the oncogenic proteins AKT and mTOR, which provide evidence of its function in tumor suppression (Qu et al. 2003).

The role of autophagy in initiation and progression of cancer is quite complex. Autophagy as a cytoprotective mechanism protects cells from the harmful effects of reactive oxygen species (ROS), such as DNA damage, and will get rid of defective mitochondria (a source of ROS production) through lysosomal degradation (Morselli et al. 2009). Oxidative stress is a metabolic process whereby oxygen free radicals accumulate in the cell (Cross et al. 1987). Normal cells need low level of ROS for survival, whereas high levels of ROS may cause DNA damage and induce lipid and protein oxidative modifications (Martinez-Cayuela 1995). Cancer cells require high levels of ROS to maintain the high cell proliferation rate. DNA damage by ROS is also important to induce DNA mutations that are essential for tumor initiation (Fruehauf and Meyskens 2007). Inhibition of autophagy during tumor initiation increases ROS accumulation and hence stimulates cancer cell proliferation (Debnath 2011).

Another form of tumor suppression is the induction of cytotoxic autophagy in cancer cells. The anticancer drug doxorubicin induces cytotoxic autophagy in breast cancer cells. The induction of cytotoxic autophagy by doxorubicin was confirmed by LC3-I to II conversion and cell death, which occurred independent of caspases activation (Akar et al. 2008). In addition, the natural product resveratrol induced autophagy and caspase independent cell death in breast cancer cells (Scarlatti et al. 2008). Moreover, the antibiotic lasalocid induced cytotoxic autophagy in PC-3 prostate cancer cells.

1.3.3.2 Autophagy and tumor promotion

Cancer cells (H1299, HCT116 and T24) expressing high levels of the oncogenic protein Ras have an evident upregulation in autophagy, in these cancer cell models (bladder, lung, colon cancers) autophagy promotes cancer cell proliferation, and

tumorigenesis (Guo et al. 2011). Autophagy may protect cancer cells from metabolic stress such as oxidative stress, hypoxia, nutrient starvation, thus preventing cancer cell death (Horbinski et al. 2010).

During cancer progression, autophagy is very crucial for the dividing cancer cells to survive in a hypoxic microenvironment. Hypoxia induces the production of ROS via hypoxia-inducible factor 1-alpha (HIF-1 α) stabilisation (Debnath 2011). Prolonged hypoxia will lead to the activation of autophagy and selective removal of damaged mitochondria from the cells (a process recently known as mitophagy)(Radogna et al. 2015). Autophagy inhibition using siRNA targeting gene expression of its main regulators such as ATG5, ATG7 or Beclin 1 induces hypoxia-dependent cell death (Karantza-Wadsworth et al. 2007). Therefore, autophagy induction protects cancer cells during cancer progression, which is in contrast to its tumor suppressor role during the early step of tumor initiation.

Autophagy inhibition with chloroquine, which prevents the late stage of autophagy induction (fusion between lysosome and autophagosome), suppresses cancer cell proliferation *in vitro* and *in vivo* (Kimura et al. 2013; Balic et al. 2014; Park et al. 2016). Moreover, knocking down ATG7 leads to the accumulation of dysfunctional mitochondria, induction of the tumor suppressor gene *TP53*, cell cycle arrest and apoptosis in non-small cell lung cancer (NSCLC) cells, which again confirms the effect of autophagy in promoting tumor growth (Guo et al. 2011). In addition, autophagy induction stimulates pancreatic cancer growth in mice through inhibition of p53 activity (Rosenfeldt et al. 2013). The oncogenic protein astrocyte elevated gene-1 (AEG-1), also known as Metadherin (MTDH) or protein LYRIC, is overexpressed in various cancers (Bhutia et al. 2010; Zou et al. 2016). AEG-1 contributes to chemoresistance in HCC cells (Yoo et al. 2010). AEG-1 induces protective autophagy via activation of AMPK in response to cellular metabolic stress (Bhutia et al. 2011). A recent study also showed that autophagy inhibition exaggerated the cytotoxic effect of NVP-BEZ235, a PI3K/mTOR dual inhibitor, in colorectal cancer cells (Yang et al. 2016).

Dual role of autophagy in cancer



Role of autophagy in tumor suppression

Mutation of Beclin 1 in vivo

↓
Inhibition of autophagy

↑ P62 accumulation
↑ Activation of NF-κB
↑ Oxidative stress

↓
DNA damage

↓
Tumor initiation

Role of autophagy in tumor promotion

Mutational activation of RAS genes in cancer cells

↓
Induction of autophagy

↓ P53
↓ Oxidative stress
↓ Mitochondrial dysfunction

↓
Tumor promotion

Figure 11: Dual role of autophagy in cancer.

Mutation of Beclin 1 (*BECN1*) leads to autophagy inhibition and DNA damage resulted from accumulation of free radicles and oxidative stress. DNA damage favors tumor initiation. On the other hand, activation of the RAS oncogene in cancer cells induces autophagy as a survival mechanism and supports tumor promotion in a low-nutrient and hypoxic conditions. Adapted from (Ziparo et al. 2013).

1.3.4 Autophagy inhibition as an adjuvant treatment for prostate cancer

Previous studies showed that inhibition of autophagy in combination with chemotherapy or hormonal therapy enhances their anti-cancer efficacy (Boutin et al. 2013; Nguyen et al. 2014). Inhibitors of autophagy include 3 methyladenine (3-MA) and

siRNA for selective inhibition of ATGs, but for clinical studies, chloroquine (CQ) and bafilomycin A1 are most commonly used (Kung 2013).

ABT-737, a small molecule inhibitor of the anti-apoptotic proteins Bcl-2, Bcl-xL and Bcl-w, induced protective autophagy in LNCaP and PC-3 prostate cancer cells. Inhibition of autophagy with CQ sensitised LNCaP and PC-3 cells to cell death mediated by ABT-737 (Saleem et al. 2012). Moreover, combination of ABT-737 with CQ significantly inhibited tumor growth of PC-3 xenografts compared to mice treatment with ABT-737 alone (Saleem et al. 2012). Inhibition of autophagy with 3-MA sensitized LNCaP, but not PC-3 prostate cancer cells to TNF-alpha-mediated apoptosis via repression of the apoptosis inhibitor c-Flip (Giampietri et al. 2012).

In addition, inhibition of autophagy using shRNA against Beclin1 or CQ-sensitized prostate cancer cells to cell death mediated by Saracatinib (tyrosine kinase inhibitor). Moreover, a combination of saracatinib and CQ inhibited tumor growth of PC-3 xenografts in mice (Wu et al. 2010). A previous study by Boutin and coworkers also showed that autophagy inhibition using selective ATG5 siRNA sensitized LNCaP cells to apoptotic cell death mediated by bicalutamide (Boutin et al. 2013). Inhibition of *AMPK* expression using selective siRNA repressed autophagy and induced cell death in LNCaP, CWR22Rv1 and PC-3 prostate cancer cells treated with enzalutamide or bicalutamide (Nguyen et al. 2014).

Previous studies showed that most prostate cancer therapeutic agents induce cytoprotective autophagy, although some prostate cancer drugs, such as atorvastatin and zoledronic acid, induce cytotoxic autophagy (Kung 2013). The induction of cytotoxic autophagy by these drugs is attributed to increased expression of ATGs and *Beclin 1* (Kung 2013).

1.3.5 Regulation of autophagy by DIM in cancer cells

A number of studies have shown effects of DIM on autophagy regulation in cancer cells but with contradictory findings. A low dose of DIM (1 μ M) protects MDA-MB-231 breast cancer cells from oxidative stress triggered by H₂O₂ through inhibition of autophagy via repression of Beclin1 (Fan et al. 2009). However, another study showed that C-DIM

(a methylene-substituted derivative of DIM) induced autophagic cell death in estrogen receptor-negative breast cancer cells (Vanderlaag et al. 2010). Moreover, DIM has been shown to induce autophagy in ovarian cancer cells (Kandala and Srivastava 2012b). Recently, DIM was shown to reduce cell viability and induce autophagy in gastric cancer cells (BGC-823 and SGC-7901) via induction of *ATG5* expression through inhibition of miRNA (miR-30e) that regulate *ATG5* gene expression (Ye et al. 2016). Interestingly, miR-30e mimic attenuated DIM mediated inhibition of BGC-823 and SGC-7901 cell viability indicating that DIM repressed gastric cancer cells viability via modulation of autophagic machinery (Ye et al. 2016).

1.3.6 The role of AMPK in autophagy

AMPK is recognized as a key sensor of cellular energy status. Both AMPK and autophagy can be stimulated under stress conditions, such as serum starvation, or glucose deprivation (Hardie 2011). AMPK is activated in response to low ATP levels and upregulates signaling pathways that restore ATP supplies including fatty acid oxidation and autophagy; AMPK also inhibits ATP-dependent processes such as lipid and protein synthesis (Meijer and Codogno 2007).

The mTOR complex 1 (mTORC1) is well recognised for its inhibitory functions in autophagy (Chang et al. 2009; Jung et al. 2010). AMPK regulation of autophagy was first shown by the fact that AMPK stimulated autophagy by inhibiting mTORC1 (Inoki et al. 2003). Recently, several studies showed that AMPK phosphorylates unc-51-like autophagy activating kinases 1 (ULK1) at multiple sites including Ser317, Ser555 to stimulate autophagy (Egan et al. 2011; Mao and Klionsky 2011). More recently, Zhang and coworkers showed that AMPK also phosphorylates BECN1 at Thr388 to stimulate autophagy (Zhang et al. 2016). However, the autophagy inhibitor, mTORC1 phosphorylates ULK1 at Ser757 to suppress autophagy through the disruption in the interaction between ULK1 and AMPK (Kim et al. 2011).

1.3.7 AEG-1 role in cancer and autophagy

AEG-1, also known as MTDH, and protein LYRIC, was initially cloned as an inducible gene in fetal astrocytes infected with human immunodeficiency virus (HIV) (Su et al. 2003). AEG-1 has emerged as key protein in cancer progression (Hu et al. 2009). Several studies showed the elevation of AEG-1 expression in different types of cancer including the prostate (Ash et al. 2008; Bhatnagar et al. 2014; Shi and Wang 2015b). AEG-1 induces cancer progression through regulation of different signaling pathways including PI3K/Akt, NF κ B, Wnt/ β -catenin, MAPK, cell proliferation, and apoptosis (Wang and Yang 2011; Shi and Wang 2015a). AEG-1 activates NF κ B through its interaction with p65 subunit of NF κ B complex (Emdad et al. 2006). Kikuno and coworkers showed that downregulation of AEG-1 induced apoptosis in LNCaP and PC-3 prostate cancer cells through upregulation of FOXO3a activity (Kikuno et al. 2007). AEG-1 activates PI3K/AKT, and its expression is being regulated by the same pathway (Lee et al. 2006). AEG-1 is induced by the *Ha-ras* oncogene, which activates the PI3K/Akt signaling pathway leading to the binding of c-Myc to *AEG-1* promoter, which subsequently activates AEG-1 expression (Lee et al. 2006). AEG-1 activates Wnt/ β -catenin pathway through upregulation of lymphoid-enhancing factor 1 (LEF1), activation of ERK42/44, and subsequent nuclear translocation of β -catenin in HCC cells (Yoo et al. 2009). AEG-1 overexpression was linked to chemoresistance and hence to the development of aggressive cancers. AEG-1 induces doxorubicin resistance by increasing the expression of multidrug resistance gene 1 (MDR1) protein and inhibiting the proteasomal degradation of MDR1 (Yoo et al. 2010). Moreover, knockdown of *AEG-1* inhibits chemoresistance in cervical cancer cells (Liu et al. 2014). Several studies showed that AEG-1 positive contribution in cancer metastasis and invasion (Lee et al. 2009; Wang et al. 2011; Sun et al. 2012b)

AEG-1 was first described as an oncogene by Emdad and coworkers (Emdad et al. 2009). This observation was based on the fact that AEG-1-expressing clones form aggressive tumors in nude mice; also AEG-1 overexpression induces oncogenic transformation and angiogenesis (Emdad et al. 2009).

In addition to its role in cancer progression, AEG-1 plays a key role in induction of protective autophagy through activation of AMPK. Induction of autophagy by AEG-1 involves reduction in ATP/AMP ratio, which results in activation of AMPK and subsequent inhibition of mTOR. Overexpression of AEG-1 and activation of AMPK/mTOR induces noncanonical protective autophagy through the elevated expression of ATG5 (Bhutia et al. 2010; Bhutia et al. 2011). Another study showed that AEG-1 overexpression was found to enhance autophagy in malignant glioma cells undergoing TGF β 1-induced endothelial-mesenchymal transition (Zou et al. 2016).

1.4 MOLECULAR PATHWAYS OF APOPTOSIS, NECROSIS, ENDOPLASMIC RETICULUM (ER) STRESS AND SENESENCE IN CANCER

A growing body of evidence indicates that cancer could develop as a consequence of a disruption in signaling pathways, such as apoptosis, necroptosis and senescence (Ouyang et al. 2012; Cerella et al. 2016). Eliminating damaged cells via cell death mechanisms such as apoptosis or necroptosis is important to avoid development of cancer (Ouyang et al. 2012). Senescence is also linked to tumor suppression through the prevention of uncontrolled cell proliferation (Cerella et al. 2016).

1.4.1 Apoptosis

Apoptosis (type I programmed cell death) plays an important role in eradicating the potentially harmful DNA-damaged cells for maintaining the genetic stability while defective apoptosis can lead to carcinogenesis (Hassan et al. 2014). Suppression of apoptosis is crucial for cancer progression and most anti-cancer drugs eradicate cancer cells predominantly by activating apoptotic pathway (Shankar and Srivastava 2004). Apoptosis is characterised by cellular morphological changes that lead to cell death. Specifically, cells undergoing apoptosis are characterised by the presence of chromatin condensation, cell shrinking, membrane blebbing, DNA fragmentation and formation of small apoptotic bodies (He et al. 2009).

Apoptosis is triggered either by external stimuli (extrinsic) where inducers of apoptosis bind cell death receptors (such as DR4, DR5, FasR) or internal stimuli (intrinsic) through the mitochondrial pathway (Adams 2003; Kroemer et al. 2007) (Figure 12). Both the intrinsic and extrinsic pathways are dependent on the activation of cysteine-dependent aspartate specific proteases (Caspases) (Logue and Martin 2008). The intrinsic pathway is triggered by intracellular death stimuli such as oxidative stress or genetic damage to activate the mitochondrial pathway through the mitochondrial outer membrane permeabilization (MOMP). MOMP will permit the release of various pro-apoptotic mitochondrial proteins such as cytochrome C, AIF, second mitochondria-derived activator of caspases (Smac/Diablo) and the serine protease HtrA2/Omi that further activate the apoptotic cascade (Coultas and Strasser 2003). Cytochrome C-release triggers the formation of the apoptosome. The apoptosome consists of cytochrome C, apoptotic peptidase activating factor 1 (apaf-1) and procaspase-9. Cytochrome C acts as a pro-apoptotic signal that activates the cleavage of procaspase-9, which in turn activates caspase-3 through cleavage of procaspase-3 to trigger apoptosis (Kroemer et al. 2007).

The extrinsic pathway is triggered by binding of ligand (FasL, TNF-alpha or TRAIL) to death receptors resulting in the formation of the death-inducing signalling complex (DISC). DISC consists of the death receptor, Fas-associated protein with death domain (FADD), and pro-caspase 8 (Lee et al. 2012a). Pro-caspase-8 is subsequently cleaved to caspase 8, which can directly activate the effector caspase-3 without any contribution from the mitochondria. However if the level of caspase-8 is insufficient to induce apoptosis, intrinsic apoptosis is activated via caspase-8-mediated cleavage of Bid through the removal of its N-terminus to form a truncated BID variant t-Bid (Ozoren and El-Deiry 2002). Bid is a pro-apoptotic proteins of the Bcl-2 family, t-Bid activates the oligopolymerisation of Bax and Bak (members of the Bcl-2 family) to promote MOMP and stimulate the release of cytochrome c. The protein t-Bid also inhibits the antiapoptotic members of the Bcl-2 family (Bcl-2 and Bcl-xL). Cytochrome C release activates the cleavage of procaspase-9, which in turn activates caspase-3 to trigger apoptosis (Sayers 2011).

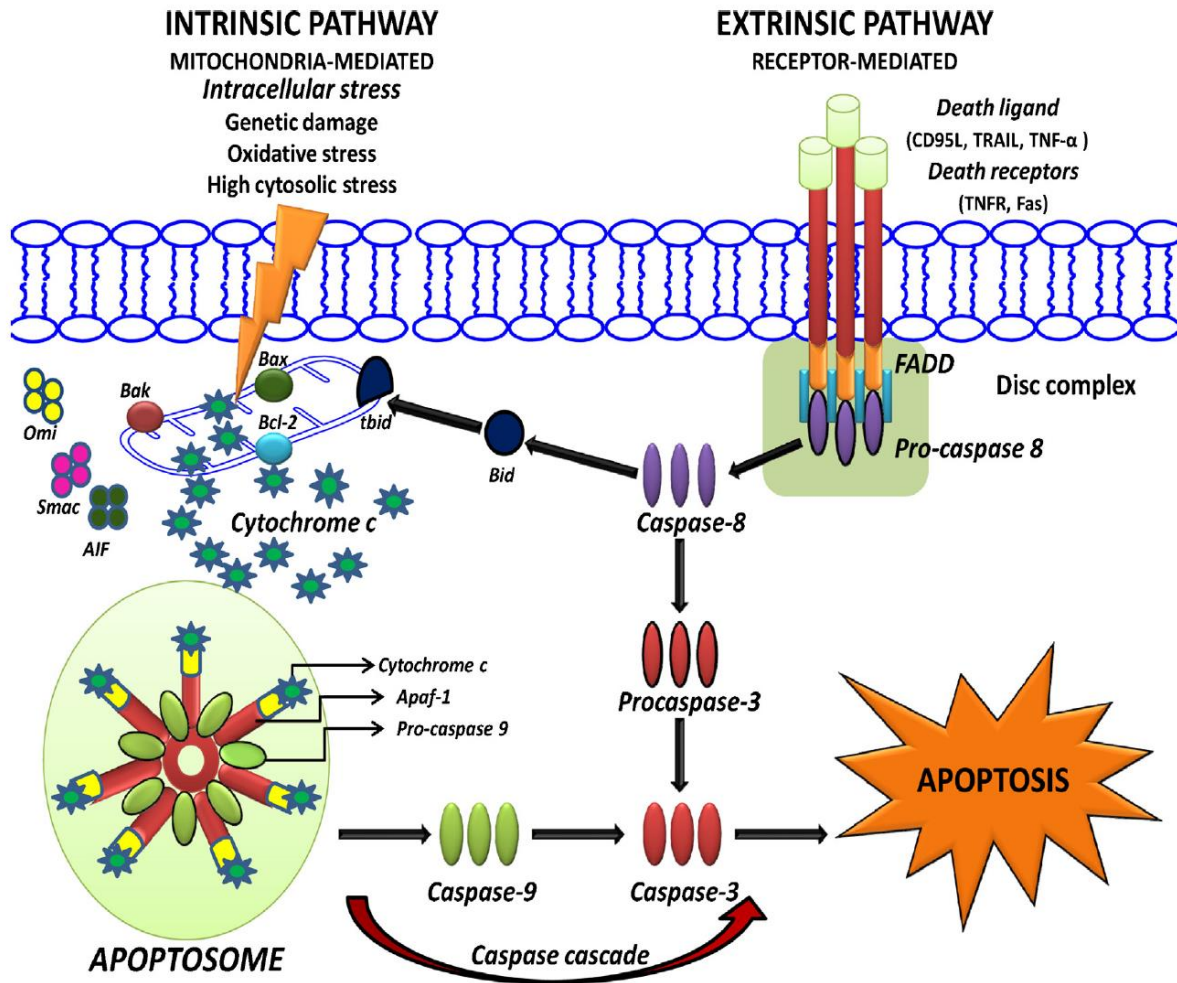


Figure 12: Intrinsic and extrinsic apoptosis signaling pathways

Apoptosis is induced through either the extrinsic or the intrinsic signalling pathways. The extrinsic pathway (receptor-mediated) involves the activation of death receptors with their ligands resulting in activation of caspase-8, and -3, which cleaves target proteins leading to apoptosis. Intrinsic (mitochondria-mediated) death stimuli, e.g. oxidative stress, or DNA-damaging reagents activate the mitochondrial pathway by inducing release of cytochrome c and formation of the apoptosome, composed of Apaf-1 and pro-caspase-9. Pro-caspase-9 is activated at the apoptosome and, in turn, activates caspase-3. Activation of caspase-8 through intrinsic apoptosis may also induce cleavage of Bid, which induces the translocation of Bax to the mitochondrial membrane and amplifies the mitochondrial apoptosis pathway (Beesoo et al. 2014).

1.4.2 Necrosis and necroptosis

Necrosis is a form of premature cell death, which is distinguished from apoptosis. Unlike apoptosis, necrosis does not activate caspases. Morphologically, necrosis is

associated with oncosis or cell swelling. Necrosis is characterised by the swelling of organelles such as mitochondria and endoplasmic reticulum, cell membrane rupture and leakage of intracellular organelles (Schweichel and Merker 1973). In contrast to apoptosis, the nucleus will remain intact. Necrotic cell death could be triggered by external stimuli such as toxins (especially heavy metals), carcinogens, or inflammation (Laster et al. 1988).

Recent studies have shown that necrosis also includes another form of programmed cell death called necroptosis, which is distinguished from type 1 (apoptosis) and type 2 (autophagy) programmed cell death. Although the same death receptor could activate both necroptosis and apoptosis, necroptosis is morphologically and functionally different from apoptosis. Necroptosis is generally activated as a backup mechanism when apoptosis is blocked due to caspase inhibition or under low levels of ATP (Skulachev 2006).

Cancer is characterized by uncontrolled proliferation of cells and resistance to apoptosis. Hence, necroptosis functions as a crucial cell death mechanism when apoptosis is blocked. Chemotherapeutic agents or inflammatory cytokines may trigger necroptosis. Necroptosis is triggered upon binding of ligand (FasL, TNF-alpha or TRAIL) to death receptors resulting in the formation of complex-I, which consists of TNFR1-associated death domain protein (TRADD), receptor-interacting protein kinase-1 (RIP1), TNF-receptor-associated factor 2 (TRAF2) and the cellular inhibitors of apoptosis (cIAP1, cIAP2) (Vercammen et al. 1998). During the process of complex-I formation, RIP1 is ubiquitinated by cIAP1/2. Autoubiquitination of cIAPs promotes RIP1 deubiquitination and its dissociation and subsequent formation of complex-II, which consists of caspase-8, FADD and RIP1 (Figure 13). When apoptotic cell death is activated, caspase-8 cleaves RIP1 and results in its activation. However, caspase inactivation results in formation of the necrosome (a complex of RIP1 and RIP3) (Holler et al. 2000). The mixed lineage kinase domain-like protein (MLKL) is an important substrate for RIP1 and is activated by RIP1. Once activated, MLKL is oligomerized and translocated from cytosol to plasma membrane causing loss of plasma membrane integrity and promotion of necroptotic cell death (Sun et al. 2012a).

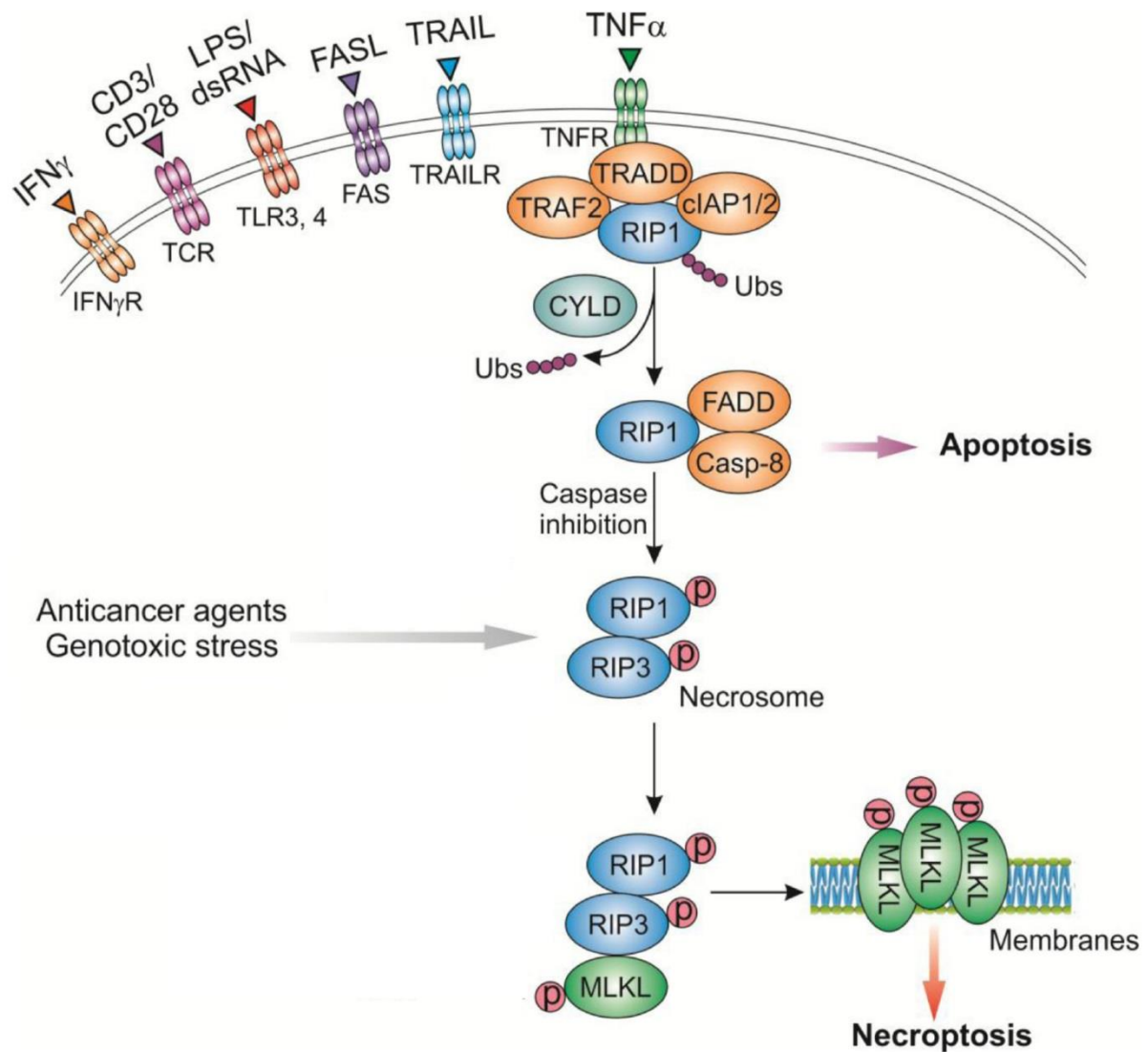


Figure 13: Necroptosis pathway

Necroptosis is initiated upon binding of TNF- α to death receptor TNFR resulting in the formation of complex-I, which consists of TNFR-associated death domain protein (TRADD), RIP1, TRAF2 and the cellular inhibitors of apoptosis (cIAP1, cIAP2); this is followed by RIP1 polyubiquitination. When apoptosis is activated, caspase-8 cleaves RIP1. However, caspase inhibition activates RIP1 and results in the formation of a necrosome (a complex of RIP1 and RIP3); this results in RIP3 auto-phosphorylation and activation, allowing RIP3 to recruit and phosphorylate MLKL. This leads to MLKL oligomerization, membrane insertion of MLKL oligomers, disruption of plasma and intracellular membrane integrity, and necroptotic cell death. Adapted from (Chen et al. 2016).

1.4.3 ER stress

ER stress is a cellular process that is triggered by a variety of conditions such as hypoxia, starvation or infections. The disruption of ER function (ER stress activation)

interferes with correct protein folding in the ER and triggers an unfolded protein response (UPR). The UPR involves the activation of three sensors that transduce signaling cascades to restore homeostasis. The UPR sensors include the inositol-requiring protein-1 α (IRE1 α), protein kinase R-like ER kinase (PERK), and activating transcription factor 6 (ATF6) (Schroder and Kaufman 2005)(Figure 14).

The UPR sensors are transmembrane proteins that binds to the chaperone GRP78/BiP in the ER lumen. Accumulation of unfolded proteins in the ER triggers the dissociation of GRP78/BiP from ER stress sensors and their activation (Ron and Walter 2007).

IRE1 α is multidomain protein that consists of kinase and an endoribonuclease. The RNase domain processes an intron from the unspliced form of X box-binding protein-1 (μ XBP-1) mRNA to allow production of the spliced XBP-1 (sXBP-1) protein (Hollien and Weissman 2006). The sXBP-1 protein is a transcription factor that regulates ER chaperones and degradation of misfolded proteins to restore protein homeostasis and promote cytoprotection (Acosta-Alvear et al. 2007).

Upon ER stress activation, GRP78 is dissociated from ATF6 luminal domain and ATF6 is translocated to the Golgi apparatus. In the Golgi compartment, ATF6 is cleaved by two groups of proteases, the serine protease site-1 (S1P) proteases and metalloprotease site-2 protease (S2P). The cleaved ATF6 then translocates into the nucleus and regulates several genes encoding ER chaperones, and ER associated degradation (ERAD)(Shen et al. 2002).

Inhibition of global protein synthesis is important during ER stress to prevent the accumulation of newly synthesised proteins within the stressed ER compartment. PERK plays a crucial role in the inhibition of protein translation through the phosphorylation of eukaryotic translation initiation factor 2 (eIF2 α). eIF2 α phosphorylation at serine 51 inhibits the activation of eIF2 α to its GTP-bound form, which is crucial for the initiation phase of polypeptide chain synthesis. On the other hand, phosphorylation of eIF2 α allows the preferential translation of selective UPR genes such as the activating transcriptional factor 4 (ATF4). ATF4 target genes include the transcriptional factor C/EBP homologous protein (CHOP), a well-known pro-apoptotic protein; as well as the growth arrest and DNA

damage-inducible 34 (GADD34)(Tabas and Ron 2011). Moreover, PERK also phosphorylates the nuclear erythroid 2 p45-related factor 2 (NRF2), which promotes expression of genes that prevent oxidative stress (Iurlaro and Munoz-Pinedo 2016). PERK promotes the expression of GADD34 and CHOP to mediate ER stress-induced apoptosis. PERK also promotes anti-oxidant responses through the activation of NRF2. Therefore, depending on the severity and duration of stress, PERK activation can lead to either cell survival or cell death.

The general outcome of ER stress activation is an return to cell homeostasis through adaptive mechanisms, such as protein folding, ERAD and inhibition of global protein synthesis. In case of excessive ER stress, cells enter apoptotic pathways when the adaptive mechanisms become overwhelmed by the unfolded protein response. This may occur in both normal cells and cancer cells. Hence, depending on the context, ER stress activation could contribute to either survival or death of cancer cells (Iurlaro and Munoz-Pinedo 2016).

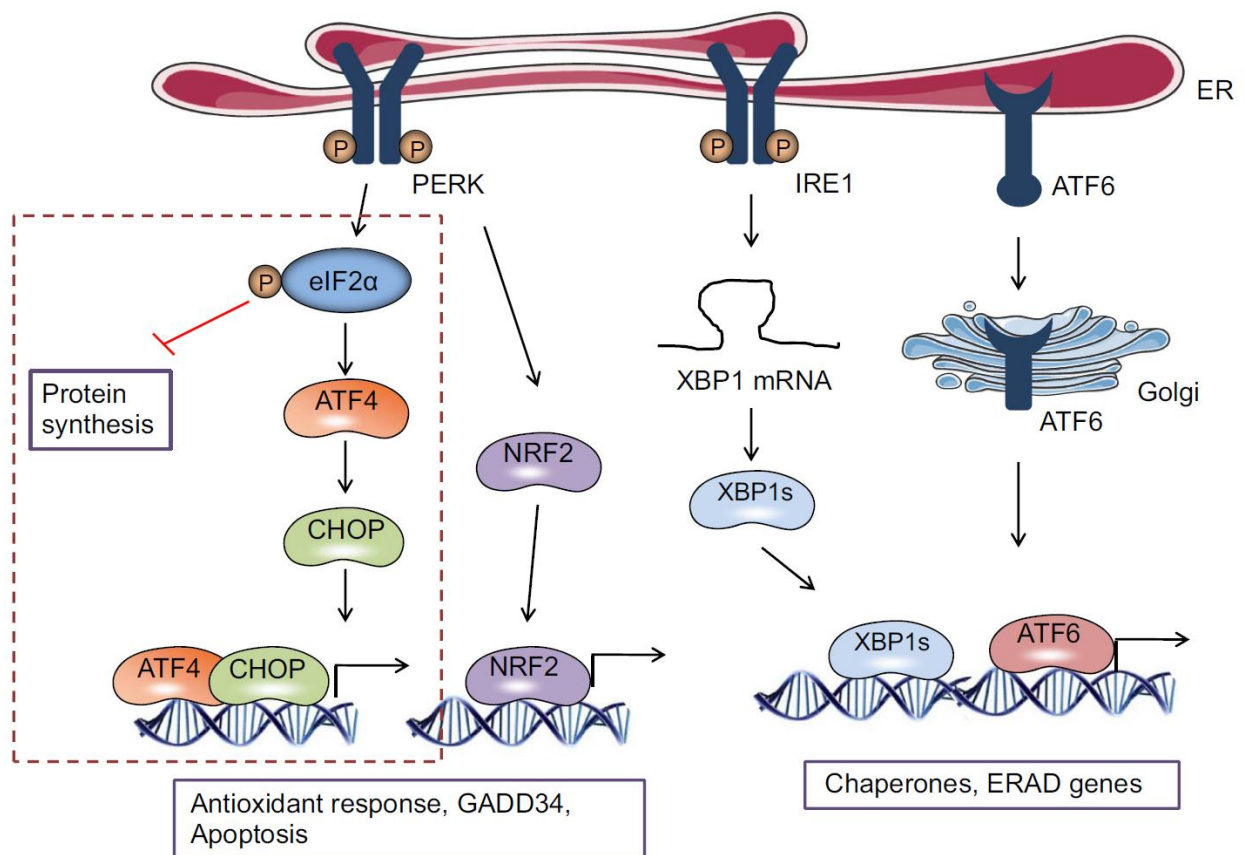


Figure 14: ER stress pathway

The three main sensors of the ER stress pathway are PERK, IRE1 and ATF6. PERK phosphorylates eIF2a attenuating the global protein synthesis, but allows the preferential translation of the transcription factors ATF4 and CHOP, which regulates the expression of genes involved in the restoration of the homeostasis and GADD34. PERK also activates the transcription factor NRF2, which induces an antioxidant responses. The second sensor, IRE1 regulates the splicing of the transcription factor XBP1, resulting in the transcription of genes involved in restoration of the ER folding capacity. ATF6 is translocated into the Golgi where it is cleaved to release the transcription factor that regulates chaperone expression and ERAD genes. Adapted from (Iurlaro and Munoz-Pinedo 2016).

1.4.4 Senescence

Cancer cells are characterised by uncontrolled cell division. In normal cells, DNA replication is monitored by cell cycle checkpoints where repair mechanisms adjust minor DNA damage. However, when repair mechanisms fail to correct DNA damage, cells may become malignant and be transformed to cancerous cells. Cells with accumulated DNA damage may undergo apoptosis or senescence (irreversible cell cycle arrest) (Schmitt 2003).

Inducers of cellular senescence include telomere shortening, DNA damage, stress stimuli and oncogene activation (Campisi and d'Adda di Fagagna 2007). RB and p53 pathways are the main effector pathways for senescence (Vicencio et al. 2008). In normal cells, the tumor suppressor gene *TP53* is degraded by the E3 ubiquitin-protein ligase, human double minute 2 (HDM2). HDM2 is negatively regulated by the alternate-reading frame protein (ARF). Cells exposed to mitogenic stress, telomere shortening or DNA damage elicit a DNA damage response (DDR) which includes the activation of ARF and subsequent p53 induction. p53 activates the cyclin dependent kinase inhibitor p21 to induce cell cycle arrest. Cellular stress or DNA damage may also activate the RB pathway through the induction of the cyclin dependent kinase inhibitor p16. RB blocks cell proliferation by repressing the family of transcription factors E2F (Vaziri and Benchimol 1999). Considering the occurrence of *TP53* mutations in cancer cells and the regulatory role of p53 in senescence, p53 is an attractive target for induction of senescence in cancer cells. Pervious work has shown that reactivation of p53 in a mouse model of liver carcinoma results in induction of senescence (Xue et al. 2007). Overexpression of the protein kinase PIM1 induces senescence in 22Rv1 human prostate cells, which express

wild-type p53 but not in DU145 cells, which express mutant p53 (Zemskova et al. 2010). Moreover, transfection of DU145 cells with wild-type p53 induced cell death through induction of senescence and apoptosis (Lehmann et al. 2007). These studies show that the induction of senescence in cancer cells is dependent on wild-type p53.

Therapy-induced senescence (TIS) has been introduced as a promising approach to improve cancer treatment (Roninson 2003). TIS represents an effective treatment strategy in immunocompetent cancer patients (Schmitt et al. 2002; Xue et al. 2007). TIS may be used as an alternative therapy in cancer cells possessing disabled apoptotic pathways (Schmitt et al. 2002).

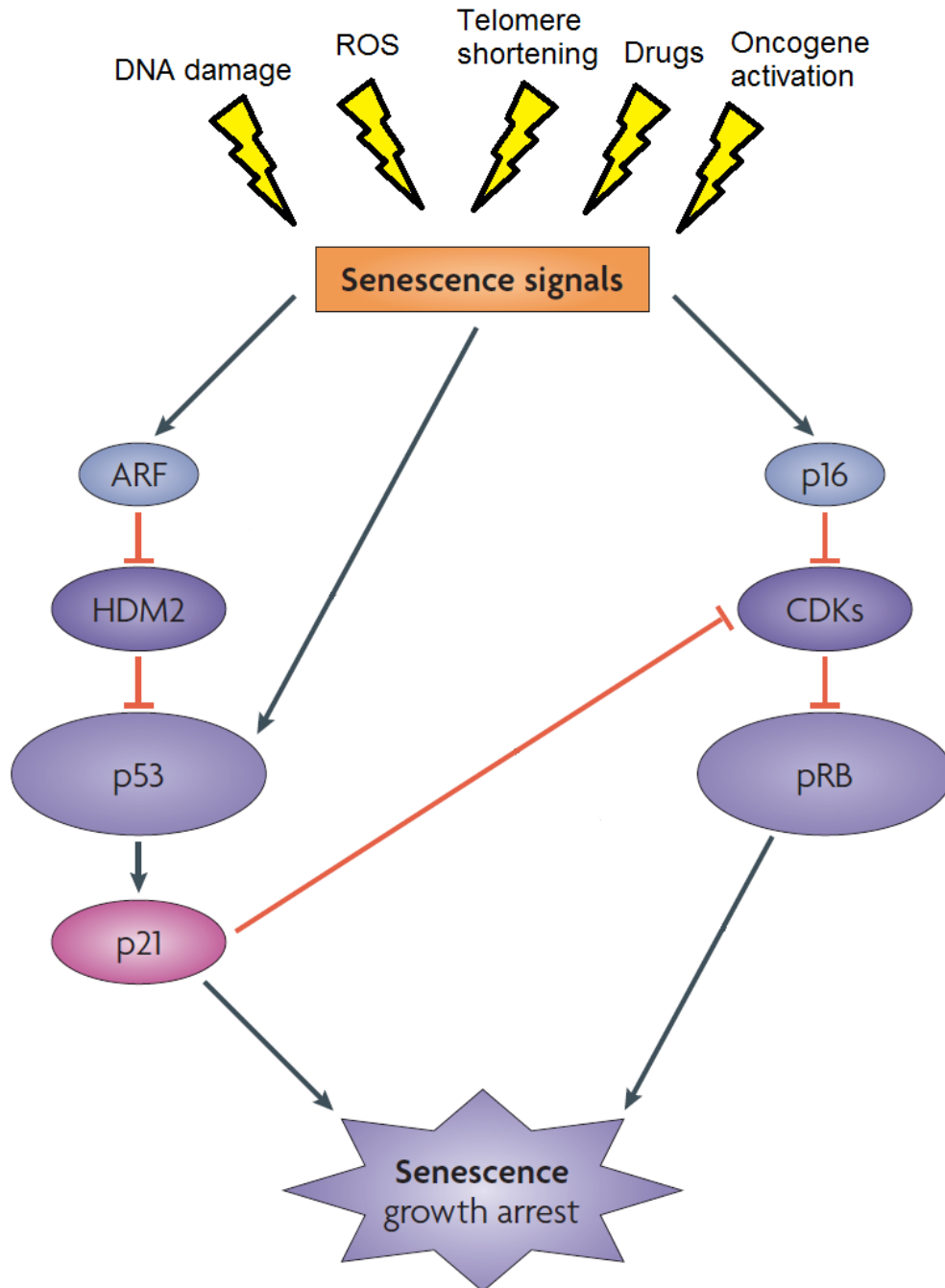


Figure 15: Senescence mechanism.

Senescence signals include those that trigger a DNA-damage response, as well as many other stresses such as ROS and chemotherapeutic drugs. Senescence signals can induce the expression of p16, which inhibits CDK that prevents pRB phosphorylation. pRB blocks cell proliferation by suppressing the activity of transcription factor E2F. Senescence signals can also induce p53, which is negatively regulated by the E3 ubiquitin-protein ligase HDM2. HDM2 is negatively regulated by the alternate-reading-frame protein (ARF). p53 triggers growth arrest by inducing the expression of the CDK inhibitor p21. Adapted from (Campisi and d'Adda di Fagagna 2007).

1.5 STUDY MODELS

1.5.1 Prostate cancer cell lines

Human prostate cancer cell lines were established from metastatic prostate tumor tissues excised from patients, whereas the immortalized RWPE-1 cell line was derived from normal human prostate epithelial tissue as shown in Table 2. The normal prostate cell line (RWPE-1) is used as a negative control. Four prostate cancer cell lines were used in our study to represent both the androgen dependent and independent prostate cells. LNCaP cells are androgen dependent prostate cancer cells, however the AR positive LNCaP-C4-2B, as well as the AR negative PC-3 and DU145 cells are all androgen independent (Russell and Kingsley 2003).

Cell line	Source	AR	Androgen sensitivity	Mutation and cells characteristics	References
LNCaP	Lymph node metastasis	+	AD	Mutated AR (cells are able to proliferate in presence of androgens)	(Horoszewicz et al. 1980; Veldscholte et al. 1990; Veldscholte et al. 1992)
LNCaP-C4-2B	Metastatic subline of LNCaP after coinoculation of LNCaP and fibroblasts in mice followed by reinoculation into castrated mice	+	AI	Mutated AR (cells are able to proliferate in absence of androgens)	(Thalmann et al. 1994; Wu et al. 1994)
PC-3	Bone metastasis	-	AI	Deletion mutation of p53 (non-functional p53)	(Kaighn et al. 1979; van Bokhoven et al. 2001)
DU145	Brain metastasis	-	AI	Mutated p53 and nonsense mutation in ATG5 (thermolabile mutant of p53 that may possess a gain of function and autophagy deficient)	(van Bokhoven et al. 2001; Sobel and Sadar 2005; Ouyang et al. 2013)
RWPE-1	Normal human prostate	+	AD	Immortalized with human papilloma virus	(Cunningham and You 2015)

Table 2: Characteristics of common prostate cancer and immortalized cell lines.

LNCaP, VCaP, LNCaP-C4-2B, PC-3, and DU145 are established from metastatic prostate tumor tissues while RWPE-1 is established from normal prostate tissue. AD, androgen dependent; AI, androgen independent. Adapted from (Russell and Kingsley 2003).

1.5.2 Xenograft mouse model of prostate cancer

In preclinical research of prostate cancer, murine xenograft models are considered important tools for understanding the development, progression and treatment of this disease (Shappell et al. 2004). We developed a xenograft model using a bioluminescent human PC-3 prostate cells, where tumor growth were monitored using IVIS bioluminescent imaging (BLI).

BLI has emerged as a sensitive tool for monitoring biological processes within living organisms (Contag et al. 1998). BLI is based on detection of light emission from cells or tissues. Bioluminescence is the biochemical generation of light photons by the oxidation of luciferin by luciferase enzymes, and this technique showed to be very beneficial in analysing, tracking of cancer cells and monitoring tumor growth in living organism (Vidal et al. 2015). BLI provides a low-cost, non-invasive, and real-time analysis of disease progress *in vivo* using bioluminescent imaging (Sato et al. 2004).

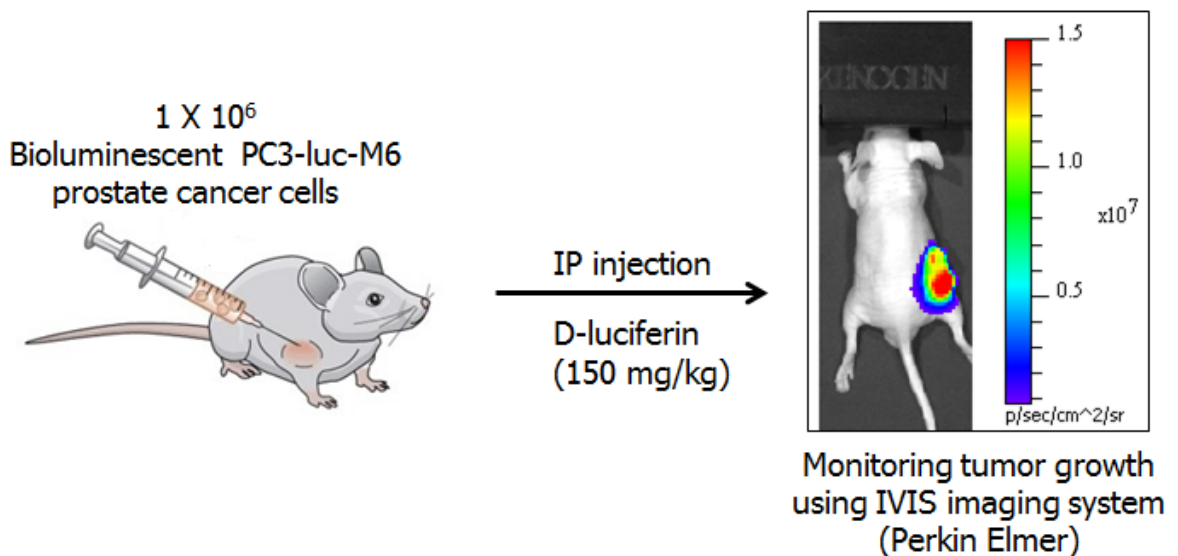


Figure 16: PC-3 xenograft model.

1×10^6 PC-3-luc-M6 cells suspended in matrigel were implanted by subcutaneous injection into male CD-1 nude mice. Mice were injected intraperitoneally with D-luciferin (150 mg/kg). Tumor growth was monitored using IVIS imaging system.

1.6 HYPOTHESIS AND OBJECTIVES

1.6.1 Hypothesis

The overall hypothesis of this thesis is that ring-DIMs exhibit anti-prostate cancer activities by selectively killing prostate cancer cells, and are considerably more potent than DIM, making them suitable candidates for development as drugs effective in the treatment of prostate cancer. Specifically, we hypothesize that DIM and ring-DIMs inhibit human prostate cancer cell growth via multiple mechanisms including apoptosis, ER stress, mitochondrial dysfunction and autophagy. In addition, we will test the hypothesis that ring-DIMs are potent chemopreventive agents *in vivo* in a mouse xenograft model of human prostate cancer.

1.6.2 Objectives

The overall objective is to investigate the anticancer properties of synthetic ring-DIMs of the cruciferous vegetable-derived compound DIM in human prostate cancer cells *in vitro* and in a mouse xenograft model of human prostate cancer.

Objective 1

Determine the early events that result in death of various types of prostate cancer cells induced by determining concentration- and time-dependent effects of ring-DIMs and DIM on mitochondrial stability, ER stress and autophagy.

Objective 2

Study the mechanistic effects of ring-DIMs on signalling pathways involved in the processes of autophagy and senescence in prostate cancer cells.

Objective 3

Study the tumor growth-inhibitory activities of ring-DIMs and the role of autophagy inhibition in their effectiveness against tumor growth in nude mice carrying PC-3 human prostate tumors.

1.7 PROJECT SIGNIFICANCE

The treatment of prostate cancer, although successful in early hormone-dependent stages, is hampered by an inability to prevent progression of the tumor to an AI stage, which is refractory to most chemotherapeutic treatments and readily metastasizes, ultimately resulting in death of the patient and to effectively kill AI tumors once established or metastasized. The natural compound DIM continues to be evaluated globally as an anticancer agent against various tumors. Our laboratory has previously identified a series of ring-substituted derivatives that are 2 to 4 times more potent than DIM *in vitro* and show remarkably rapid, structure-dependent cytotoxic effects in AD as well as AI prostate cancer cells (Goldberg et al. 2014). It is important to study these cytotoxic effects in order to improve our understanding of the mechanisms mediating the cytotoxic effects of the 4,4,'- and 7,7,'-dihalo-substituted-ring DIMs, which are distinct from those of DIM. Clearly, this class of DIM derivatives qualifies for continued investigation of its antiproliferative and cytotoxic activities selective to cancer cells of the prostate. In addition, it is important to use a preclinical experimental model of human prostate cancer to study the anti-prostate cancer effects of DIM and its synthetic derivatives *in vivo*.

The *in vivo* imaging approach used in our laboratory allows for the study of the biological effectiveness of DIM and its derivatives against human prostate cancer by using a murine xenograft model of nude mice bearing bioluminescent human prostate tumors. The results of the study of ring-substituted diindolymethanes presented in this thesis provides important information on effectiveness of these ring-DIMs against hormone-dependent as well as -independent prostate cancer *in vitro* and *in vivo*. Discovering the primary cellular targets of the ring-DIMs that are decisive in causing prostate cancer cell death will improve our fundamental understanding of the processes that are key to cancer cell survival and will uncover novel targets for anticancer agents.

CHAPTER 2: PUBLICATIONS

2.1 3,3'-Diindolylmethane (DIM) and its ring-substituted halogenated analogs (Ring-DIMs) induce differential mechanisms of survival and death in androgen-dependent and -independent prostate cancer cells

Alexander A. Goldberg^{1,2*}, Hossam Draz^{1,3,*}, Diana Montes-Grajales⁴, Jesus Olivero-Verbél⁴, Stephen H. Safe⁵ and J. Thomas Sanderson¹

¹ *INRS-Institut Armand-Frappier, Laval, Québec, Canada.*

² *Critical Care Division and Mealins-Christie laboratories, Faculty of Medicine, McGill University, Québec, Canada.*

³ *Department of Biochemistry, National Research Centre, Dokki, Cairo, Egypt.*

⁴ *Environmental and Computational Chemistry Group, University of Cartagena, Colombia.*

⁵ *Veterinary Physiology and Pharmacology, Texas A&M University, College Station, TX, United States.*

This article was published in *genes and cancer* (2015), 6: 265-280.

Author contributions:

*Hossam Draz and Dr. Alexander Goldberg contributed equally to the content and successful publication of this article.

Hossam Draz designed and performed the experiments to study the effect of DIM and ring-DIMs on cell viability of prostate cancer and normal prostate epithelial cells (Fig 1), on mitochondrial dysfunction and ER stress (Fig 2 and 3), on autophagy (Fig 6), and of the effects of Ca²⁺/calmodulin-dependent kinase II inhibitor KN93 on 4,4'-Br₂DIM-mediated cell death (Fig 7). Hossam Draz also participated in performing the statistical analyses and writing the manuscript by contributing to each of the sections as pertaining to the experiments he performed above.

Dr. Alexander Goldberg designed and performed the experiments for the effects of salubrinal and cyclosporin A on mitochondrial activity and ER stress of prostate cancer cells treated with DIM and ring-DIMs (Fig 4, 5), in addition to the supplementary Figures

S1 and S2, and participated in performing the statistical analyses and writing the manuscript.

Diana Montes-Grajales and Prof. Jesus Oliver-Verbel performed the in silico identification of potential protein targets for ring-DIMs (Table 1, Figure S3).

Prof. Stephen Safe synthesised the ring-DIMs in his laboratory at Texas A&M University and revised the manuscript.

Prof. Thomas Sanderson obtained the research funding, supervised the project and participated in writing and revising the manuscript.

3,3'-Diindolylmethane (DIM) and its ring-substituted halogenated analogs (ring-DIMs) induce differential mechanisms of survival and death in androgen-dependent and -independent prostate cancer cells

Alexander A. Goldberg^{1,2,*}, Hossam Draz^{1,3,*}, Diana Montes-Grajales⁴, Jesus Olivero-Verbél⁴, Stephen H. Safe⁵ and J. Thomas Sanderson¹

¹ INRS-Institut Armand-Frappier, Laval, Québec, Canada

² Critical Care Division and Meakins-Christie Laboratories, Faculty of Medicine, McGill University, Montreal, Quebec H3A 1A1, Canada

³ Department of Biochemistry, National Research Centre, Dokki, Cairo, Egypt

⁴ Environmental and Computational Chemistry Group, University of Cartagena, Colombia

⁵ Veterinary Physiology and Pharmacology, Texas A&M University, College Station, TX, United States

* These authors have contributed equally to this work

Correspondence to: J. Thomas Sanderson, **email:** thomas.sanderson@laf.inrs.ca

Keywords: prostate cancer, LNCaP, C42B, DU145, mitochondrial function

Received: January 29, 2015

Accepted: April 16, 2015

Published: April 26, 2015

This is an open-access article distributed under the terms of the Creative Commons Attribution License, which permits unrestricted use, distribution, and reproduction in any medium, provided the original author and source are credited.

ABSTRACT

We recently reported that novel ring-substituted analogs of 3,3'-diindolylmethane (ring-DIMs) induce apoptosis and necrosis in androgen-dependent and -independent prostate cancer cells. In this paper, we have focused on the mechanism(s) associated with ring-DIM-mediated cell death, and on identifying the specific intracellular target(s) of these compounds. The 4,4'- and 7,7'-dichloroDIMs and 4,4'- and 7,7'-dibromoDIMs induced the death of LNCaP, C42B and DU145 prostate cancer cells, but not that of immortalized normal human prostate epithelial (RWPE-1) cells. Ring-DIMs caused the early loss of mitochondrial membrane potential (MMP) and decreased mitochondrial ATP generation in prostate cancer cells. Cyclosporin A, an inhibitor of the mitochondrial permeability transition pore, inhibited ring-DIM-mediated cell death, and salubrinal, an inhibitor of ER stress, inhibited cell death mediated only by 4,4'-dihaloDIMs. We found that although salubrinal did not inhibit the onset of ER stress, it prevented 4,4'-dibromoDIM mediated loss of MMP. Salubrinal potentiated cell death in response to 7,7'-dihaloDIMs and DIM, and this effect concurred with increased loss of MMP. Using *in silico* 3-D docking affinity analysis, we identified Ca²⁺/calmodulin-dependent kinase II (CaMKII) as a potential direct target for the most toxic ring-DIM, 4,4'-dibromoDIM. An inhibitor of CaMKII, KN93, but not its inactive analog KN92, abrogated cell death mediated by 4,4'-dibromoDIM. The ring-DIMs induced ER stress and autophagy, but these processes were not necessary for ring-DIM-mediated cell death. Inhibition of autophagy with bafilomycin A1, 3-methyladenine or by LC3B gene silencing sensitized LNCaP and C42B, but not ATG5-deficient DU145 cells to ring-DIM- and DIM-mediated cell death. We propose that autophagy induced by the ring-DIMs and DIM has a cytoprotective function in prostate cancer cells.

INTRODUCTION

Prostate cancer accounts for almost one third of all cancer deaths in the United States and is the second highest cause of cancer-related death in males [1]. Most prostate tumours are initially androgen-dependent (AD). However, a large contingent will progress to an aggressive androgen-independent (AI) form, which are more drug-resistant and lead to increased morbidity and mortality among patients. Currently, prostate cancer is treated with a combination of radiotherapy, chemical castration, androgen receptor (AR) antagonists (hydroxyflutamide, bicalutamide), or inhibitors of steroidogenesis (abiraterone). Patients treated with hydroxyflutamide or bicalutamide often suffer from severe side-effects as a result of the anti-androgenic therapy [2, 3], necessitating the search for novel chemotherapeutic agents with fewer deleterious effects. Moreover, it is imperative to search for novel therapeutic targets which may aid the development of a new generation of drugs effective in the elimination of AI prostate tumours.

3,3'-Diindolylmethane (DIM) is a natural small molecule produced in the stomach after ingestion of vegetables of the *Brassica* family containing high amounts of indole-3-carbinol (I3C). I3C is converted via acid-catalyzed reactions in the stomach to various condensation products, of which DIM is considered its most biologically active metabolite [4, 5]. DIM has been studied extensively as an anticancer agent due to its ability to inhibit the growth of a multitude of cancer cell types *in vitro* and *in vivo* [6, 7] and has produced positive responses in clinical trials for the treatment of prostate cancer when applied in an absorption-enhanced formulation [8]. DIM affects a number of distinct yet overlapping pathways, leading to the inhibition of cancer cell proliferation. For example, DIM down-regulates AR transcriptional activity, thereby reducing AR-mediated gene expression [9-12]. DIM also inhibits pro-survival cell signaling pathways such as phosphatidylinositol 3-kinase (PI3K), Akt, mammalian target of rapamycin (mTOR) and c-Met, and also activates pro-apoptotic pathways such as Hippo and glycogen synthase kinase 3-beta (GSK-3 β), resulting in inhibition of cancer cell proliferation [13-19]. DIM activates the pro-apoptotic proteins Fas, FasL and death receptor 5 (DR5), leading to caspase-dependent apoptosis [7, 9, 17, 20]. DIM also increases the intracellular flux of calcium ions, resulting in the induction of endoplasmic reticulum (ER) stress genes [21-23], in addition to decreasing mitochondrial function through inhibition of ATP synthase [24-26], which in turn induces AMP-activated protein kinase-(AMPK)-dependent autophagy [27]. DIM also exerts effects on DNA methyltransferases, resulting in modified methylation patterns of genes involved in inflammation, cell signaling, cell motility and apoptosis [28]. However, the specific molecular targets that directly interact with DIM to cause ER stress, mitochondrial dysfunction, autophagy, and ultimately cell death have yet

to be discerned.

We have previously shown that several halogenated analogs of DIM, termed ring-DIMs, act as anti-androgenic compounds that inhibit AD proliferation of LNCaP human prostate cancer cells and induce apoptosis and necrosis of AD as well as AI prostate cancer cells with greater potencies than DIM [11, 17]. Cell death induced only by the most potent ring-DIM, 4,4'-Br₂DIM, was partially dependent on activation of caspase-3, which occurred concomitant with increases in Fas, FasL, DR4 and DR5 expression. The objective of the present study was to determine the early events that ultimately result in cell death induced by 4,4'- and 7,7'-dibromo- and dichloro-substituted ring-DIMs and DIM by determining their concentration- and time-dependent effects on mitochondrial stability, ER stress and autophagy. We also performed an *in silico* docking affinity analysis to identify proteins that could potentially interact with ring-DIMs and DIM.

RESULTS

Ring-DIMs kill LNCaP, C42B and DU145 prostate cancer cells, but not RWPE-1 immortalized normal prostate epithelial cells

We tested the ability of the ring-DIMs to kill prostate cancer cells that express a DHT-responsive AR (LNCaP), a constitutively active AR (C42B) and cells lacking AR (DU145). In LNCaP and C42B cells, 4,4'-Br₂DIM (IC₅₀ = 13.1 μ M, 16.7 μ M, respectively), 4,4'-Cl₂DIM (IC₅₀ = 20.2 μ M, 29.3), 7,7'-Br₂DIM (IC₅₀ = 19.5 μ M, 25.3 μ M) and 7,7'-Cl₂DIM (IC₅₀ = 15.8 μ M, 25.7 μ M) were all significantly more potent at killing cells than DIM (IC₅₀ = 23.3, 46.1 μ M), (Fig. 1A, B). The most cytotoxic ring-DIM, 4,4'-Br₂DIM, killed AR-negative DU145 cells with the same potency as C42B cells with an IC₅₀ of 20 μ M (Supplementary Fig. S1A). At concentrations that were toxic to the prostate cancer cells neither the ring-DIMs nor DIM induced cell death in RWPE-1 cells (Fig. 1C).

Mitochondrial dysfunction and ER stress are early events in ring-DIM induced cell death

To further investigate the mechanism of ring-DIM-induced toxicity, we looked at MMP, mitochondrial ATP generation and ER stress in response to ring-DIM exposure. After only 1 hour of exposure to the 4,4'-dihaloDIMs, MMP decreased by 36-40% in LNCaP and 54-60% in C42B cells, whereas MMP decreased by only 30% in LNCaP and 36% in C42B cells after a 1 hour treatment with DIM. The 7,7'-dihaloDIMs (Fig. 2A, B) decreased MMP by only 15-18% in LNCaP and 16-24% in C42B cells. The observed decreases in MMP were

Table 1: Docking affinities (kcal/mol) of DIM and its derivatives for the four isoforms of the calmodulin-dependent kinase II protein involved in mitochondrial metabolism and signaling pathways.

Short name	Pathway	PDB ID	Docking affinity (kcal/mol)				
			4,4'-dibromo DIM	4,4'-dichloro DIM	7,7'-dibromo DIM	7,7'-dichloro DIM	diindolylmethane (DIM)
CaMK-II subunit α	Signal transduction	2VZ6/Q9UQM7	-8.8±0.0	-9.0±0.0	-8.8±0.1	-8.9±0.1	-9.2±0.0
CaMK-II subunit β	Signal transduction	3BHH/Q13554	-9.5±0.0	-9.5±0.0	-9.0±0.0	-8.9±0.1	-9.1±0.0
CaMK-II subunit γ	Signal transduction	2V7O/Q13555	-8.9±0.1	-9.1±0.0	-9.1±0.7	-8.6±0.8	-9.2±0.1
CaMK-II subunit δ	Signal transduction	2WEL/Q13557	-7.4±0.0	-7.6±0.0	-7.4±0.1	-7.7±0.1	-7.5±0.0

sustained for at least 8 hours. DIM and all ring-DIMs, except 7,7'-Br₂DIM, significantly decreased mitochondrial ATP generation in both cell lines by up to 80% (Fig. 2C, D). In DU145 cells treated with 4,4'-Br₂DIM, we observed decreases in MMP by 63% and ATP generation by 45% compared to controls (Supplementary Fig. S1B, C).

Treatment of LNCaP and C42B cells with 4,4'-Br₂DIM, 7,7'-Cl₂DIM or DIM also caused a significant increase in the levels of expression of ER stress-related proteins CHOP and ATF4 and the phosphorylation of eIF2 α between 1 and 8 hours of exposure (Fig. 2E, F). These results were also observed in DU145 cells using 4,4'-Br₂DIM, which also increased ATF4 and CHOP levels after treatment for 1 to 8 hours (Supplementary Fig. S1D).

Ring-DIM-induced cell death is dependent on mitochondrial dysfunction

We next assessed whether CsA, an inhibitor of the mitochondrial permeability transition pore, could abrogate the toxicity of cells exposed to the ring-DIMs or DIM. We found that pre-treatment with 5 μ M of CsA prevented ring-DIM-mediated loss of cell viability, but did not affect DIM-induced death of LNCaP or C42B cells (Fig. 3A, B). In LNCaP and C42B cells, CsA prevented the loss of MMP caused by the 4,4'-dihaloDIMs and, to a lesser extent, DIM, but had no effect on the loss of MMP mediated by the 7,7'-dihaloDIMs (Fig. 3C, D). We confirmed that CsA also prevented 4,4'-Br₂DIM-mediated cell death and loss of MMP in AI DU145 cells (Supplementary Fig. S1E and B). However, CsA had no effect on the phosphorylation status of eIF2 α or the expression levels of CHOP and ATF4 in LNCaP or C42B cells treated with either of the three compounds (Fig. 3E-G); this was confirmed using only 4,4'-Br₂DIM in DU145 cells (Supplementary Fig. S1F). Treatment with CsA alone did not affect cell viability or eIF2 α phosphorylation in LNCaP, C42B or DU145 cells (Supplementary Fig. S2A, B); nor did it significantly affect MMP (Supplementary Fig. S2C).

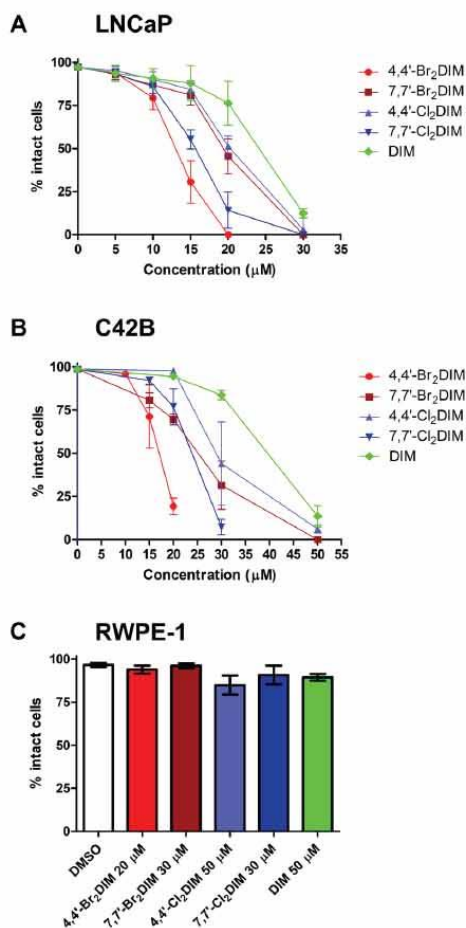


Figure 1: Ring-DIMs kill LNCaP and C42B prostate cancer cells, but not RWPE-1 immortalized normal prostate epithelial cells. The percentage of intact LNCaP (A) and C42B (B) cells that do not have fragmented nuclei, condensed chromatin or propidium iodide staining was determined after a 24 hour exposure to increasing concentrations of 4,4'-Br₂DIM, 7,7'-Br₂DIM, 4,4'-Cl₂DIM, 7,7'-Cl₂DIM or DIM. (C) Percentage of intact RWPE-1 cells after a 48 hour exposure to the ring-DIMs or DIM.

Salubrinal inhibits cell death and loss of MMP but not ER stress mediated by 4,4'-Br₂DIM

Salubrinal is an inhibitor of ER stress that blocks dephosphorylation of eIF2 α , and we investigated the effects of this compound on the cytotoxicity of the ring-DIMs and DIM. Pre-treatment of LNCaP and C42B cells with 20 μ M of salubrinal inhibited cell death caused by 4,4'-dihaloDIMs, but not 7,7'-dihaloDIMs or DIM (Fig 4A, B); in DU145 cells salubrinal pre-treatment also completely prevented 4,4'-Br₂DIM-induced cell death (Supplementary Fig. S1E).

In cells exposed to 4,4'-Br₂DIM or 4,4'-Cl₂DIM, pre-treatment with salubrinal attenuated the 4,4'-dihaloDIM-mediated decrease in MMP (Fig 4C, D) (Supplementary Fig. S1B). Salubrinal pre-treatment alone did not significantly affect MMP in LNCaP, C42B or DU145 cells (Supplementary Fig. S2C). Using the most toxic of the 4,4'-dihaloDIMs as prototype, the 4,4'-Br₂DIM-mediated increase in phosphorylation of eIF2 α was inhibited by pre-treatment with salubrinal in all three cell lines (Fig. 4E and Supplementary Fig. S1G). However, in LNCaP and C42B cells, pre-treatment with

salubrinal did not consistently abrogate the 4,4'-Br₂DIM-induced levels of CHOP or ATF4 (Fig. 4E), and in DU145 cells salubrinal only partially reduced the 4,4'-Br₂DIM-induced expression of these markers of ER stress (Supplementary Figure S1G). Salubrinal alone did not affect cell viability or eIF2 α phosphorylation in either of the three cell lines (Supplementary Figure S2A, B).

Salubrinal potentiates 7,7'-dihaloDIM- and DIM-mediated toxicity via loss of MMP

Next, we asked if salubrinal could sensitize prostate cancer cells to cell death induced by the 7,7'-dihaloDIMs and DIM. Pre-treatment of LNCaP and C42B cells with salubrinal enhanced the loss of cell viability caused by concentrations of the 7,7'-dihaloDIMs or DIM that are otherwise sub-toxic (defined as all cells being intact and not visibly Hoechst- or PI-stained) in cells that are exposed to the 7,7'-dihaloDIMs alone. Loss of viability mediated by co-treatment of LNCaP or C42B cells with salubrinal and sub-toxic concentrations of 7,7'-dihaloDIMs was attenuated by pre-treatment with CsA (Fig. 5A, B). Consistent with the lack of abrogation of the cytotoxicity

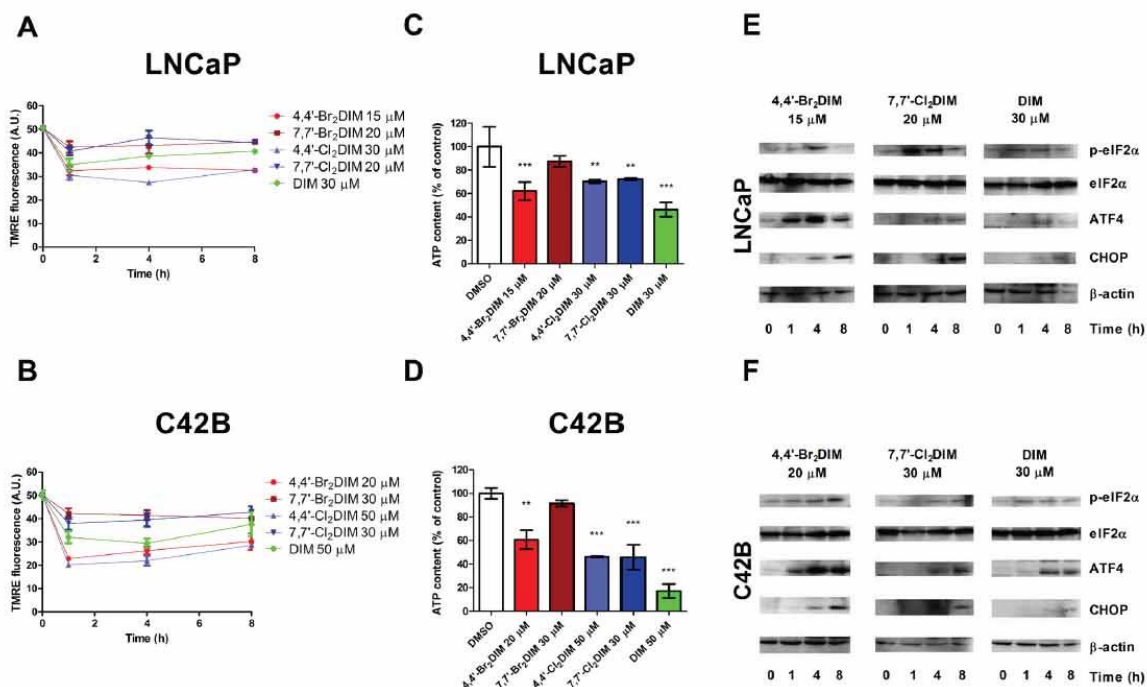


Figure 2: Mitochondrial dysfunction and ER stress are early events in ring-DIM- and DIM-mediated prostate cancer cell death. Tetramethylrhodamine ethyl ester (TMRE) fluorescence of LNCaP (A) and C42B (B) cells after 0, 1, 4, and 8 hrs of exposure to 4,4'-Br₂DIM, 7,7'-Br₂DIM, 4,4'-Cl₂DIM, 7,7'-Cl₂DIM or DIM. Relative mitochondrial ATP levels of LNCaP (C) and C42B (D) cells treated with 5 mM 2-deoxy-D-glucose after a 1 h exposure to 4,4'-Br₂DIM, 7,7'-Br₂DIM, 4,4'-Cl₂DIM, 7,7'-Cl₂DIM or DIM. Phosphorylation of eIF2 α , and levels of ER stress proteins were assayed by immunoblot of LNCaP (E) and C42B (F) cells after 0, 1, 4, and 8 hrs of exposure to 4,4'-Br₂DIM, 7,7'-Cl₂DIM or DIM.

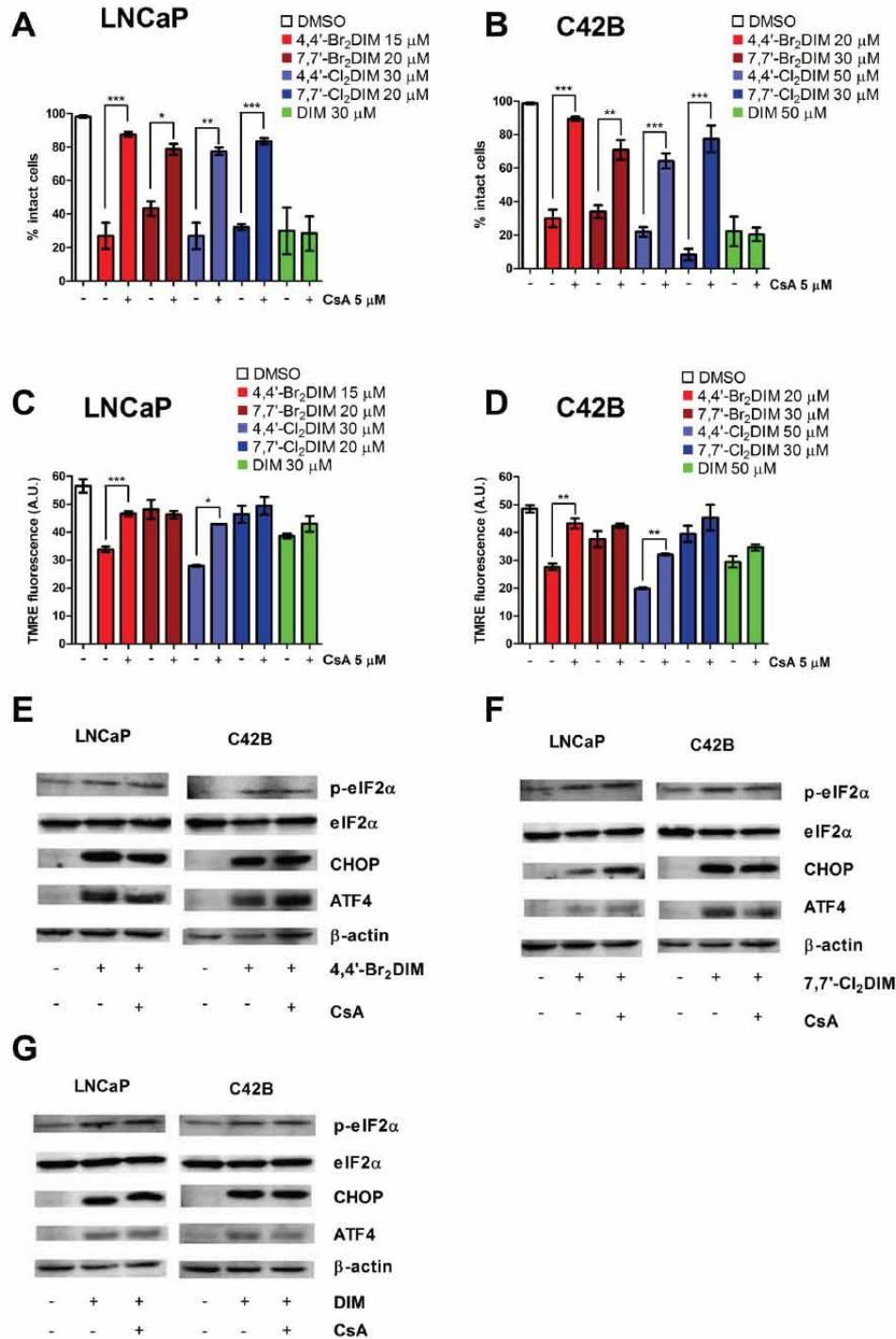


Figure 3: Ring-DIM mediated cell death is dependent on the mitochondrial permeability transition pore (mPTP). Percentage of intact LNCaP (A) and C42B (B) cells after a 24 h exposure to 4,4'-Br₂DIM, 7,7'-Br₂DIM, 4,4'-Cl₂DIM, 7,7'-Cl₂DIM, or DIM with or without a 4 h pre-treatment with cyclosporin A (CsA). TMRE fluorescence of LNCaP (C) or C42B (D) cells after a 4 h exposure to 4,4'-Br₂DIM, 7,7'-Br₂DIM, 4,4'-Cl₂DIM, 7,7'-Cl₂DIM, or DIM with or without a 4 h pre-treatment with cyclosporin A (CsA). Phosphorylation of eIF2α, and levels of ER stress proteins in LNCaP and C42B cell extracts after a 24 hour exposure to 4,4'-Br₂DIM (E), 7,7'-Cl₂DIM (F) or DIM (G) with or without a 4 hour pre-treatment with CsA.

of DIM by CsA alone (Fig 3A,B) CsA was also incapable of abrogating the cytotoxicity of DIM that was potentiated by pre-treatment with salubrinal (Fig. 5A, B)

LNCaP and C42B cells pre-treated with salubrinal and treated with either 7,7'-Br₂DIM, 7,7'-Cl₂DIM or DIM, exhibited a sharp decrease in MMP after 4 hours (Fig. 5C, D). Combined pre-treatment of cells with salubrinal and CsA partially or fully restored the loss of MMP caused by 7,7'-Cl₂DIM, 7,7'-Br₂DIM and DIM (Fig 5C, D). Neither salubrinal nor combined salubrinal and CsA pre-treatments

affected eIF2 α phosphorylation in response to sub-toxic concentrations of 7,7'-dihaloDIMs or DIM as determined in C42B cells (Fig. 5E).

Ring-DIMs and DIM induce protective autophagy in prostate cancer cells

We investigated the potential of DIM and the ring-DIMs to induce autophagy in prostate cancer cells. A dose-

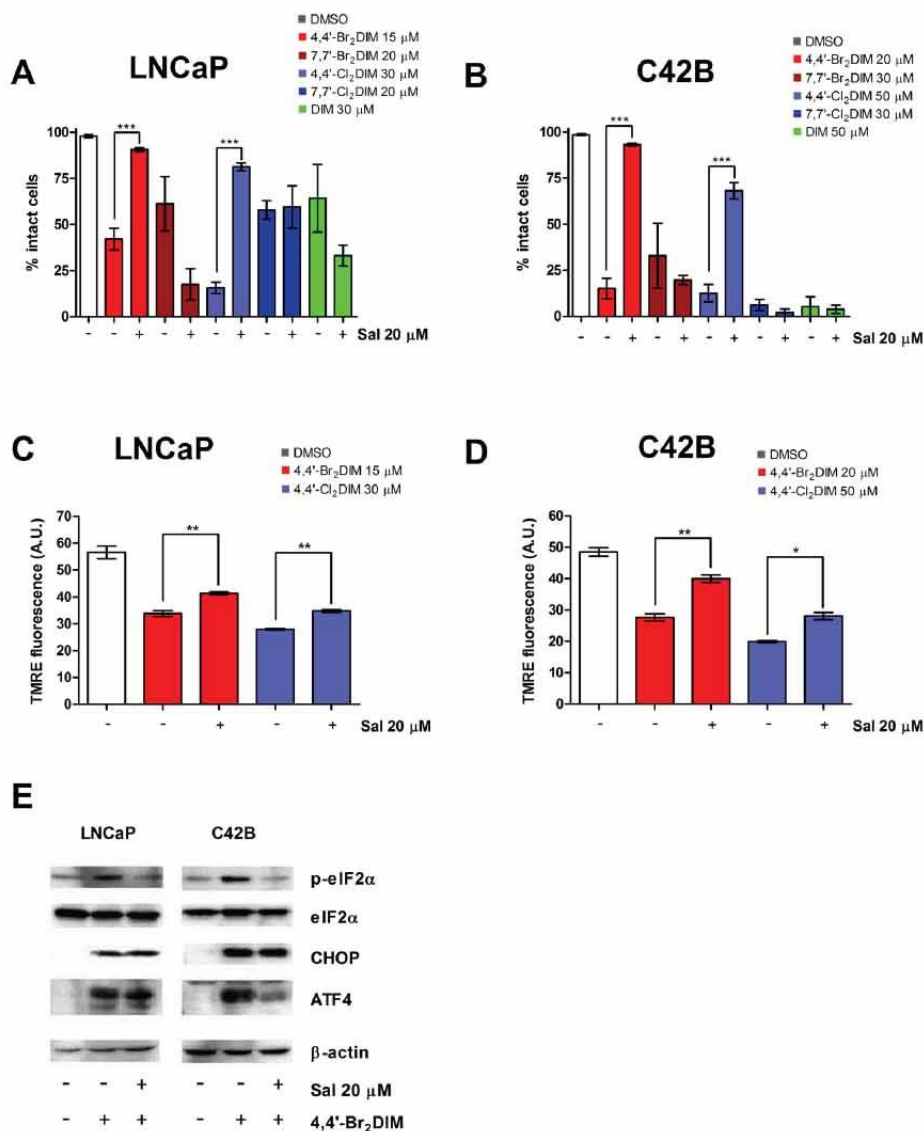


Figure 4: Salubrinal modulates mitochondrial activity in prostate cancer cells treated with 4,4'-dihaloDIMs. The percentage of intact LNCaP (A) and C42B (B) cells was calculated after a 24 hour exposure to toxic concentrations of 4,4'-Br₂DIM, 7,7'-Br₂DIM, 4,4'-Cl₂DIM, 7,7'-Cl₂DIM, DIM with or without a 4 h pre-treatment with salubrinal. TMRE fluorescence of LNCaP (C) and C42B (D) cells after a 4 hour exposure to 4,4'-Br₂DIM or 4,4'-Cl₂DIM with or without a 4 h pre-treatment with salubrinal. (E) Phosphorylation of eIF2 α , and levels of ER stress proteins after a 24 hour exposure to 4,4'-Br₂DIM with or without a 4 hour pre-treatment with salubrinal.

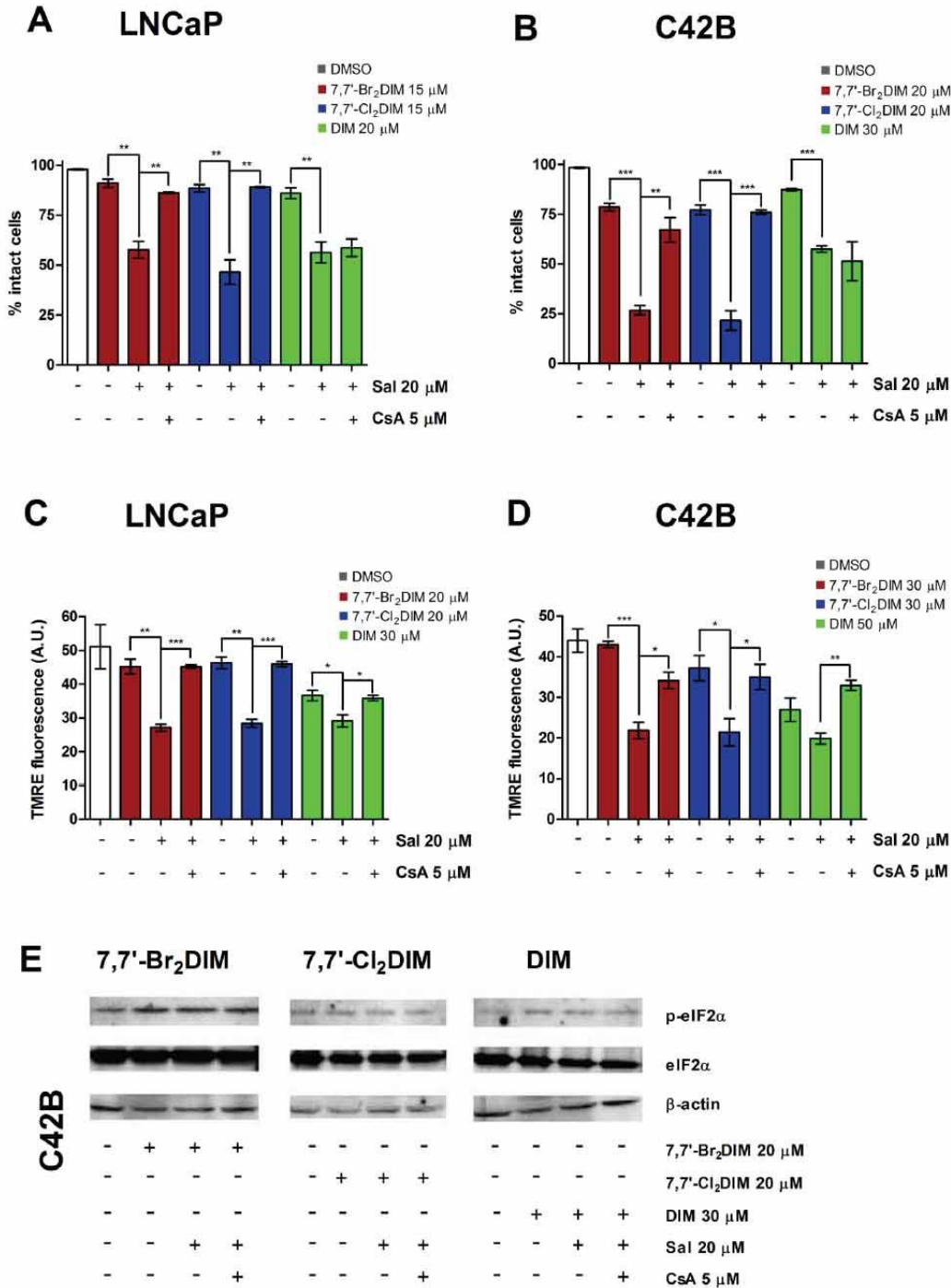


Figure 5: Cyclosporin A (CsA) abrogates salubrinal-mediated sensitization of prostate cancer cells to mitochondrial dysfunction using sub-toxic concentrations of 7,7'-dihaloDIMS or DIM. The percentage of intact LNCaP (A) and C42B (B) cells pre-treated for 4 hours with salubrinal, salubrinal and CsA, or 0.3% DMSO, followed by a 24 hour exposure to mildly toxic concentrations of 7,7'-Br₂DIM, 7,7'-Cl₂DIM or DIM. TMRE fluorescence of LNCaP (C) and C42B (D) cells pre-treated for 4 hours with salubrinal and cyclosporin A (CsA), or 0.3% DMSO followed by a 4 hour exposure to 7,7'-Br₂DIM or 7,7'-Cl₂DIM. (E) Phosphorylation of eIF2α in C42B cell extracts after a 24 hour exposure to mildly toxic concentrations of 7,7'-Br₂DIM, 7,7'-Cl₂DIM or DIM with or without a 4 hour pre-treatment with salubrinal, salubrinal and CsA, or 0.3 % DMSO.

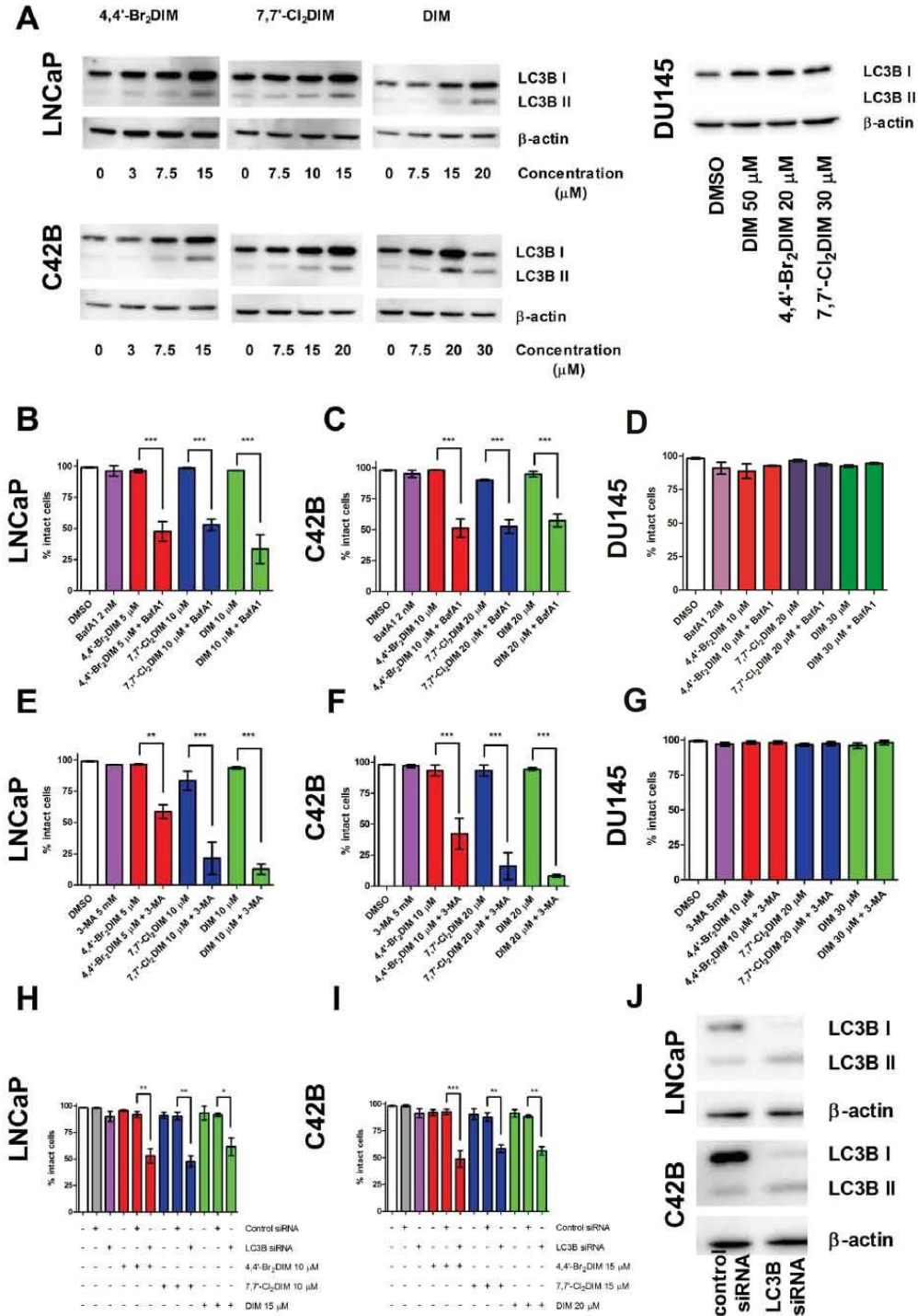


Figure 6: Ring-DIMs and DIM induce protective autophagy. (A) Levels of LC3B I and II protein in LNCaP, C42B and DU145 cells after a 24 hr exposure to 4,4'-Br₂DIM, 7,7'-Cl₂DIM or DIM. Percentage of intact LNCaP (B, E), C42B (C, F) and DU145 (D, G) cells after a 24 h exposure to 4,4'-Br₂DIM, 7,7'-Cl₂DIM or DIM with or without a 4 hour pre-treatment with bafilomycin A1 (BafA1) or 3-methyladenine (3-MA). Percentage of intact LNCaP (H) and C42B (I) cells after a 24 hour exposure to 4,4'-Br₂DIM, 7,7'-Cl₂DIM or DIM with or without a 24 hour pre-treatment with LC3B siRNA. (J) Protein levels of LC3B I and II in LNCaP and C42B cells after treatment with or without LC3B siRNA.

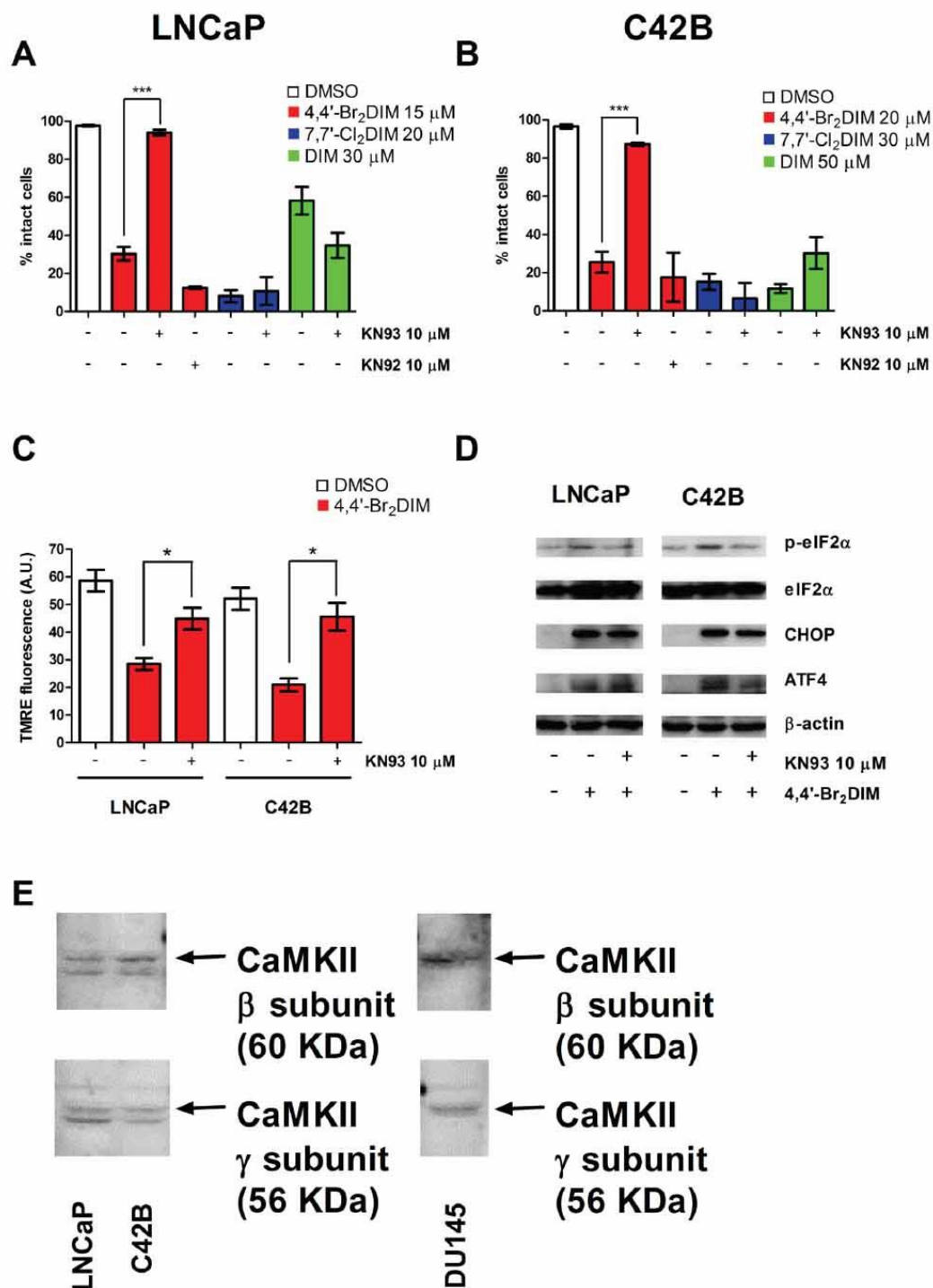


Figure 7: KN93 abrogates 4,4'-Br₂DIM mediated cell death. Percentage of intact LNCaP (A) and C42B (B) cells after a 24 hour exposure to 4,4'-Br₂DIM, 7,7'-Cl₂DIM or DIM with or without a 4 hour pre-treatment with KN92 or KN93. (C) TMRE fluorescence of LNCaP and C42B cells after a 4 hour exposure to 4,4'-Br₂DIM with or without a 4 hour pre-treatment with KN93. (D) Phosphorylation of eIF2α, and levels of ER stress proteins in LNCaP and C42B cells after a 24 hour exposure to 4,4'-Br₂DIM with or without a 4 hour pre-treatment with KN93. (E) Protein levels of Ca²⁺/calmodulin-dependent protein kinase (CaMKII) beta and gamma subunits in LNCaP, C42B and DU145 cells.

dependent increase in LC3B conversion was observed in LNCaP and C42B cells, but not in autophagy-deficient DU145 cells, exposed to sub-toxic concentrations of 4,4'-Br₂DIM, 7,7'-Cl₂DIM or DIM for 24 hours (Fig. 6A). Pre-treatment of cells with autophagy inhibitors bafilomycin A1 (Fig. 6B-D) or 3-MA (Fig. 6E-G) sensitized LNCaP and C42B cells, but not DU145 cells, to sub-toxic concentrations of 4,4'-Br₂DIM, 7,7'-Cl₂DIM or DIM. We next silenced the LC3B gene in LNCaP and C42B cells using siRNA and then exposed them to sub-toxic concentrations of 4,4'-Br₂DIM, 7,7'-Cl₂DIM or DIM. We observed significant decreases in viability of cells treated with the LC3B-selective siRNA, but not control siRNA, with each of the three compounds (Fig. 6H, I). We confirmed the effectiveness of the LC3B-selective siRNA in decreasing the expression of LC3B in LNCaP and C42B cells to almost undetectable levels relative to control siRNA (Fig. 6J).

***In silico* identification of protein targets for ring-DIMs and DIM**

To identify potential molecular targets for the ring-DIMs and DIM, we performed *in silico* 3-D affinity docking studies of 61 proteins with known 3-D crystal structures and which are involved in cell survival or death and mitochondrial function, to determine possible high-affinity interactions with the 4,4'-dihaloDIMs, 7,7'-dihaloDIMs and DIM. We identified CaMKII subunits alpha, beta and gamma, but not delta as possible high-affinity targets common to all five compounds (Table 1). Each compound had *in silico* docking affinities for each of the subunits with free energy values less than -8.5 kcal/mol, with a value lower than -8.0 kcal/mol considered a high-affinity interaction.

KN93 abrogates cell death induced by 4,4'-Br₂DIM

The involvement of the various CaMKII subunits in DIM or ring-DIM-mediated toxicity in prostate cancer cells was assessed using a selective CaMKII inhibitor, KN93. In LNCaP, C42B and DU145 cells, a 4 hour pre-treatment with KN93 resulted in a marked reduction of cell death caused by 4,4'-Br₂DIM, but not 7,7'-Cl₂DIM or DIM (Fig. 7A-B, Supplementary Fig. S1E). Additionally, KN92, an inactive derivative of KN93, did not abrogate cell death induced by 4,4'-Br₂DIM (Fig. 7A-B, Supplementary Fig. S1E). Pre-treatment with KN93 restored the loss of MMP caused by 4,4'-Br₂DIM in all three prostate cancer cell lines (Fig. 7C, Supplementary Fig. S1B). Pre-treatment of LNCaP and C42B cells with KN93 reduced 4,4'-Br₂DIM-mediated eIF2 α phosphorylation, but it did not affect 4,4'-Br₂DIM-mediated increases in CHOP and ATF4 levels (Fig. 7D).

In DU-145 cells, pre-treatment with KN93 did not alter the increases in eIF2 α phosphorylation or levels of ATF4 and CHOP caused by 4,4'-Br₂DIM (Supplementary Fig. S1H). In addition, the expression of the beta and gamma subunits of CaMKII in LNCaP C42B, and DU145 cells was confirmed (Fig. 7E). The alpha and delta subunits of CaMKII were not found (data not shown).

DISCUSSION

Ring-DIMs kill AD and AI prostate cancer cells but not non-tumourigenic RWPE-1 cells

We have previously reported that ring-DIMs and DIM induce apoptosis and necrosis in androgen receptor-positive (AR+) AD LNCaP and in androgen receptor-negative (AR-) AI PC-3 prostate cancer cells. Similar to our previous report [17], 4,4'-Br₂DIM induced cell death in AD AR+ LNCaP, AI AR+ C42B and AI AR- DU145 cells with the greatest potency of all five compounds tested. Concentrations of ring-DIMs that killed 100% of prostate cancer cells after 24 hours (20 μ M for 4,4'-Br₂DIM, 30 μ M for 7,7'-Br₂DIM, 30 μ M for 7,7'-Cl₂DIM, 50 μ M for 4,4'-Cl₂DIM and 50 μ M for DIM) were not toxic to non-tumourigenic RWPE-1 prostate epithelial cells (Fig. 1). This confirms that DIM and its 4,4'- and 7,7'- ring-substituted analogs selectively affect processes and pathways that are dysregulated in cancerous tissues, and are not toxic to normal cells.

Cell death induced by the ring-DIMs is dependent on mitochondrial dysfunction but not ER stress or autophagy

In our previous study, we hypothesized that 4,4'-Br₂DIM induces cell death by independently activating both intrinsic and extrinsic apoptosis pathways based on the observation that this derivative activated caspases-8 and -9, but did not increase Bid cleavage. We further hypothesized that ER stress plays a role in ring-DIM-induced cell death, as both 4,4'-Br₂DIM and 7,7'-Cl₂DIM induced increased expression of DR4 and DR5, and 4,4'-Br₂DIM also increased Fas receptor and Fas ligand (FasL) [17]. Here, we show that ER stress and mitochondrial dysfunction are early events in ring-DIM- and DIM-induced prostate cancer cell death. ATF4 expression was increased by 4,4'-Br₂DIM within 1 hour of exposure, while 7,7'-Cl₂DIM and DIM increased ATF4 expression after 4 hours. We observed a significant decrease in MMP in cells treated with 4,4'-dihaloDIMs and DIM, but only a slight decrease in mitochondrial activity of cells treated with 7,7'-dihaloDIMs (Fig. 2). CsA, a potent inhibitor of the mitochondrial permeability transition pore (mPTP) complex, completely abrogated

ring-DIM-induced death of LNCaP and C42B cells, but could not prevent DIM-induced cell death (Fig. 3). CsA also abrogated the toxicity of 4,4'-Br₂DIM in DU-145 cells (Supplementary Figure S1B, E). The loss of MMP was inhibited by CsA in cells treated with the ring-DIMs as well as DIM, suggesting that mitochondrial dysfunction is necessary for cell death caused by the ring-DIMs but not DIM. However, pre-treatment with CsA did not abrogate eIF2 α phosphorylation or cause a decline in the levels of ATF4 or CHOP in cells treated with either 4,4'-Br₂DIM, 7,7'-Cl₂DIM or DIM (Fig. 3E-G). Therefore, our results suggest that ring-DIM-mediated ER stress is activated in parallel, and not downstream, of mitochondrial dysfunction. It has been reported previously that eIF2 α could play a role in the survival of tumorigenic cells in response to Akt inhibition [39], and DIM has been shown to be a potent inhibitor of the Akt pathway [15, 40]. Our *in silico* data support the notion that DIM may act as a direct Akt inhibitor, as Akt showed a significant binding affinity to DIM and the ring-DIMs (Supplementary Table S1). Therefore, the observed induction of ER stress may be a pro-survival response to the mitochondrial disruption caused by the ring-DIMs and DIM, and is not necessary for ring-DIM-induced toxicity.

Although ER stress does not appear to be responsible for ring-DIM-induced cell death, we wished to confirm this using salubrinal, a compound commonly used to inhibit ER stress by blocking dephosphorylation of eIF2 α . Pre-treatment with 20 μ M of salubrinal inhibited cell death caused by 4,4'-Br₂DIM and 4,4'-Cl₂DIM in LNCaP and C42B cells, and by 4,4'-Br₂DIM in DU145 cells. In contrast, pre-treatment with salubrinal sensitized LNCaP and C42B cells to the toxicity of 7,7'-Br₂DIM, 7,7'-Cl₂DIM and DIM (Fig. 4A, B). Interestingly, the increased phosphorylation of eIF2 α mediated by 4,4'-Br₂DIM was abrogated by pre-treatment with salubrinal in all three cell lines (Fig. 4E; Supplementary Fig S1G). However, in LNCaP and C42B cells, pre-treatment with salubrinal did not consistently abrogate the 4,4'-Br₂DIM-induced levels of CHOP or ATF4 (Fig. 4E), and in DU145 cells salubrinal only partially reduced the 4,4'-Br₂DIM-induced expression of these markers of ER stress (Supplementary Fig S1G). Moreover, salubrinal alone did not affect phosphorylation of eIF2 α in all three cell lines (Fig. S2A, B), suggesting that, in prostate cancer cells, salubrinal does not directly modify the phosphorylation status of eIF2 α ; nor does it significantly inhibit the onset of ring-DIM-mediated ER stress. These

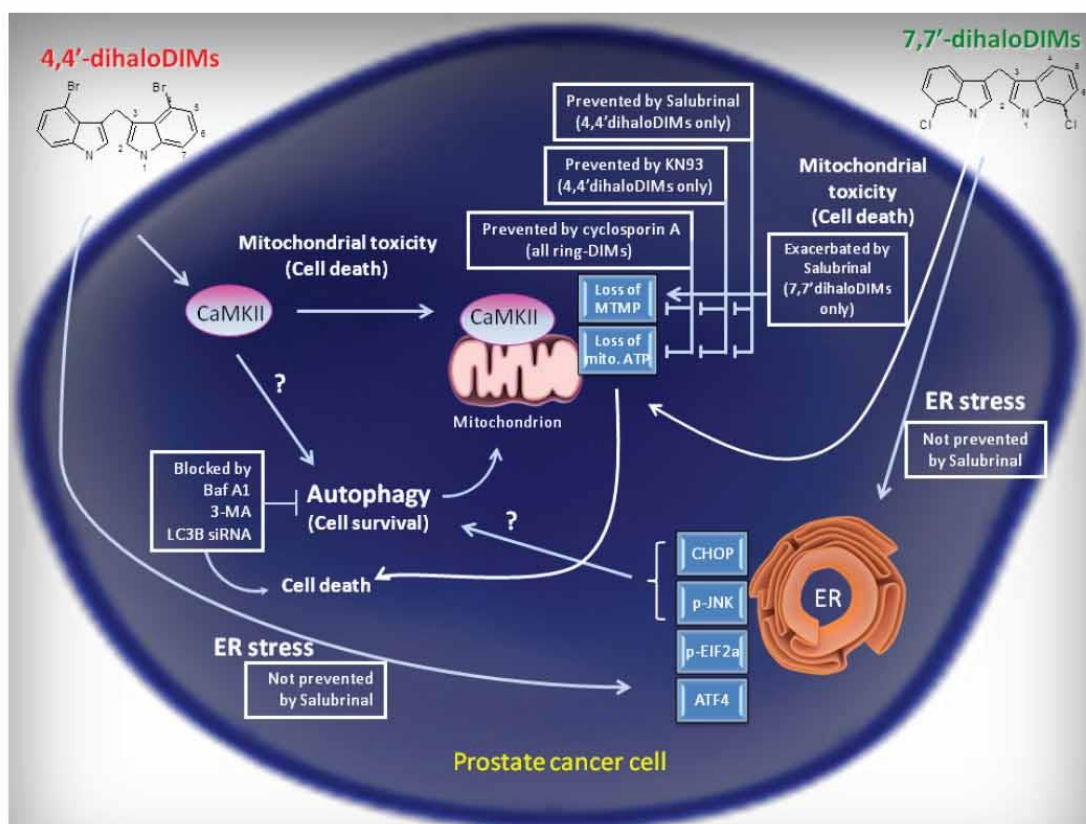


Figure 8: A schematic representation of the differential pathways activated by the 4,4'- and 7,7'-dihalogenated ring-DIMs and their role in ring-DIM-induced prostate cancer cell death.

results are consistent with two other reports showing that salubrinal did not modify the phosphorylation status of eIF2 α , and interacted directly with Bcl-2 [41, 42]. We propose that the mitochondrion is a novel target of salubrinal which differentially modulates the disruption of mitochondrial stability caused by the ring-DIMs: whereas salubrinal abrogates 4,4'-Br₂DIM-mediated loss of MMP (Fig. 4C, D), it exacerbates the loss of MMP induced by 7,7'-dihaloDIMs and DIM (Fig. 5C, D). Furthermore, it appears that salubrinal's ability to modulate the cell death caused by the ring-DIMs is dependent on the loss of MMP, as pre-treatment with CsA negated the synergistic cytotoxic effects of co-treatment with salubrinal and 7,7'-dihaloDIMs or DIM (Fig. 5A-D). Future studies will investigate the mitochondrial target(s) affected by salubrinal, and how they may be utilized to further increase the cytotoxic potency of the 7,7'-dihaloDIMs and DIM in prostate cancer cells.

DIM has been shown to induce ER stress-dependent autophagy in ovarian cancer cells, with the autophagic response being partially responsible for DIM-mediated cell death *in vitro* and *in vivo* [27]. In contrast, our studies show that DIM- and ring-DIM-mediated autophagy is cytoprotective, since pre-treatment with either bafilomycin A1, 3-MA or transcriptional silencing of LC3B sensitized both LNCaP and C42B cells to cell death induced by DIM or the ring-DIMs. However, in DU145 cells, which are autophagy-deficient due to a mutation in the *ATG5* gene leading to the premature termination of *ATG5* transcripts [43], bafilomycin A1 and 3-MA had no effect (Fig. 6). Additionally, Kandala and Srivastava [27] provided evidence that DIM mediated autophagy was dependent on CHOP signalling. However, in LNCaP, C42B and DU145 cells, ER stress was not sufficient to induce cell death in prostate cancer cells. Thus, it is possible that the onset of ER stress might also serve a cytoprotective function in prostate cancer cells by activating autophagy via CHOP signaling.

Is Ca²⁺/calmodulin-dependent protein kinase (CaMKII) involved in 4,4'-Br₂DIM-mediated mitochondrial dysfunction?

Our *in silico* docking experiments revealed CaMKII as a potential high affinity target for the ring-DIMs and DIM (Table 1). In prostate cancer cells, CaMKII activity has been implicated in cell survival and loss of androgen-dependence [44]. However, in a variety of cases, CaMKII can be pro-apoptotic and in hepatocellular carcinoma cells CaMKII is necessary for melittin-induced apoptosis [13], and CaMKII activation has been linked to sustained c-Jun N-terminal kinase and p38 mitogen-activated kinase stress signaling [13, 45, 46]. Moreover, CaMKII has been shown to play a role in the simultaneous induction of ER stress and mitochondrial dysfunction [46]. We observed

that KN93, a selective inhibitor of CaMKII, but not its inactive form KN92, prevented the death of cells treated with 4,4'-Br₂DIM, but not 7,7'-Cl₂DIM or DIM (Fig. 7A, B). In addition, KN93 abrogated the loss of MMP observed after exposure to 4,4'-Br₂DIM and decreased eIF2 α phosphorylation, but did not significantly prevent expression of ATF4 or CHOP (Fig. 7D). Thus, CaMKII activation may directly initiate the intrinsic pathway of apoptosis in prostate cancer cells, and this effect is independent of induction of ER stress. Interestingly, we found protein expression of only the beta and gamma subunits of CaMKII in the three prostate cancer cell lines tested (Fig. 7E), with both subunits exhibiting high docking affinity values for 4,4'-Br₂DIM (Table 1). The crystal structure of CaMKII-beta and the docking site of each ring-DIM and DIM are shown in Supplementary Fig. S3. C42B cells have been shown to transcriptionally express all four subunits of CaMKII (alpha, beta, gamma, delta), whereas LNCaP and DU145 cells only expressed the beta, gamma and delta transcripts [47]. Our study confirms that the CaMKII-beta and -gamma proteins are indeed produced from these transcripts, but that protein levels of the CaMKII-alpha and -delta subunits are undetectable in each of the three cell lines. These data suggest that CaMKII may be a selective upstream target of 4,4'-Br₂DIM that is responsible for the early onset of mitochondrial dysfunction and ER stress in prostate cancer cells. Although our *in silico* analysis identified a potential interaction between CaMKII and 7,7'-Cl₂DIM and between CaMKII and DIM, it appears that CaMKII activity is not necessary for 7,7'-Cl₂DIM- or DIM-mediated cell death. This differential response between the 4,4'-dihalo- and 7,7'-dihaloDIMs to inhibition of CaMKII by KN93 provides further evidence that the mechanisms of action of the ring-DIMs is highly structure-dependent. We previously showed that the 4,4'-dihaloDIMs, but not the 7,7'-dihaloDIMs induced the Fas receptor and FasL in LNCaP cells [17]; additionally, the 7,7'-dihaloDIMs were shown to be more potent inhibitors of DHT-mediated LNCaP cell proliferation than the 4,4'-dihaloDIMs [17]. In the present study we also show that the 4,4'- and 7,7'-dihaloDIMs elicit opposite responses in prostate cancer cells pre-treated with salubrinal, but that these effects are unrelated to ER stress. Moreover, pre-treatment of all three cell lines with KN93 did not prevent the increase in expression of either CHOP or ATF4, further confirming that ER stress is not a key contributor to 4,4'-Br₂DIM-mediated cell death.

CONCLUSION

We have confirmed that ring-substituted dihaloDIMs act via distinct, structure-dependent, yet overlapping mechanisms (Figure 8) to induce potent cytotoxic effects in AD and AI prostate cancer cells, but not normal prostate epithelium. We have shown that cell death mediated by

the most potent ring-DIM, 4,4'-Br₂DIM, is dependent on CaMKII activation and subsequent mitochondrial dysfunction, and that ER stress is insufficient to induce cell death in response to either the ring-DIMs or DIM. We also show that the ring-DIMs and DIM induce protective autophagy in prostate cancer cells. Future studies will concentrate on the relationship between 4,4'-Br₂DIM, CaMKII and mitochondrial dysfunction, the effectiveness of this potent anti-cancer compound in animal models of prostate cancer, and the potential for targeting the ER stress and autophagy pathways in order to increase the effectiveness of the ring-DIMs and DIM as anti-neoplastic agents.

MATERIALS AND METHODS

Cell lines and reagents

LNCaP, and DU145 human prostate cancer cells as well as RWPE-1 immortalized normal prostate epithelial cells were purchased from the American Type Culture Collection (Manassas, VA). LNCaP C4-2B (C42B) cells were purchased from the MD Anderson Cancer Center (Houston, TX). LNCaP, C42B, DU145, and RWPE-1 cells were grown in RPMI 1640 supplemented with 10% fetal bovine serum, 2 mM L-glutamine, 1% HEPES, 1% sodium-pyruvate and 10ml/L of 100x antibiotic-antimycotic solution (Sigma-Aldrich, St-Louis, MO). Cells were maintained in a humidified atmosphere (5% CO₂) at 37°C. Ring-substituted 4,4'- and 7,7'-dihaloDIMs were synthesized in our laboratories at >95% purity and were dissolved in 100% dimethyl sulfoxide (DMSO) to obtain 100 mM stock solutions. Dihydrotestosterone (DHT; Steraloids Inc., Newport, RI) was dissolved in DMSO to make a 100 mM stock solution. Cyclosporin A (CsA; Cell Signaling, Beverly, MA), salubrinal (Enzo Life Sciences, Farmingdale, NY), KN92, KN93 (Millipore, Billerica, MA) and bafilomycin A1 (Sigma Aldrich) were dissolved in DMSO as 1000-fold concentrated stock solutions. The final concentration of DMSO in culture medium was 0.1% for single exposures and not greater than 0.3% for combined exposures.

Treatment of cells with ring-DIMs, pharmacological inhibitors and siRNA

LNCaP, C42B, and DU145 cells were exposed to the ring-DIMs at the indicated final concentrations in their respective culture medium, supplemented with 2% dextran-coated charcoal-stripped FBS. DHT was added to LNCaP cells after serial dilution in DMSO to a working stock solution of 100 nM, resulting in a final DHT concentration of 0.1 nM in culture medium. CsA, KN92 and KN93, salubrinal, bafilomycin A1 were added

to cell cultures 4 hours prior to treatment with either ring-DIMs, DIM or DMSO vehicle control. 3-Methyladenine was dissolved directly in water and added freshly to the cells 4 hours prior to exposure to the diindolylmethane compounds.

For siRNA experiments, LNCaP or C42B cells were transfected with SMARTpool *ON-TARGETplus* siRNA oligonucleotide for *LC3B* (Dharmacon, USA) using lipofectamine RNAiMAX (Life Technologies, USA) in serum free Opti-MEM according to manufacturer's protocols. *ON-TARGETplus* Non-targeting Control siRNAs was used a negative control. After a 24-hour incubation, transfected cells were exposed to the ring DIMs, DIM or vehicle control for a further 24 hours.

Cell death and mitochondrial membrane potential (MMP)

For cell death measurements, LNCaP, C42B, and DU145 cells were seeded in 24-well plates in 2% stripped FBS. Cells were then treated with (LNCaP) or without (C42B, DU145) 0.1 nM DHT and several concentrations of ring-DIMs, DIM or vehicle control (DMSO). After 24 hours, Hoechst 33342 (Sigma-Aldrich) and propidium iodide (PI; Invitrogen, Carlsbad, CA) stains were both added to each well at a concentration of 1 µg/ml (in water) after which the plates were incubated for 15 minutes at 37°C. Hoechst- and PI-positive cells were then counted under a Nikon Eclipse (TE-2000U) inverted fluorescence microscope at 20x magnification using filter cubes with excitation wavelengths of 330-380 and 532-587 nm, respectively. Intact cells were counted as exhibiting neither chromatin condensation, chromatin fragmentation nor PI staining. To measure MMP, tetramethylrhodamine ethyl ester (TMRE) was added to each well at a final concentration of 50 nM for 15 minutes at 37°C. TMRE is a cell permeable, positively charged dye that accumulates in active negatively charged mitochondria. In inactive or (partially) depolarized mitochondria, membranes have decreased potential and fail to sequester TMRE. Cells were then observed under an inverted fluorescence microscope using a filter cube with an excitation wavelength of 532-587 nm. The photos of cells treated with either TMRE, Hoechst 33342 or PI were analyzed using ImageJ image processing software [29].

ATP measurements

LNCaP, C42B, and DU145 cells were seeded in 96-well plates in 2% stripped-FBS. Cells were then treated with (LNCaP) or without (C42B, DU145) 0.1 nM DHT and several concentrations of ring-DIMs, DIM or DMSO alone. A 0.5 M stock solution of 2-deoxy-D-glucose (Sigma-Aldrich) was prepared in water and added to the wells at a final concentration of 5 mM 4 hours

prior to addition of ring-DIMs, DIM or DMSO alone. Mitochondrial ATP levels were measured 1 hour later using a ViaLight Plus kit (Lonza, Basel, Switzerland). Briefly, cells were treated for 10 minutes with lysis buffer, after which a bioluminescent ATP monitoring reagent was added to each well for 2 minutes. The bioluminescent signal was measured using a SpectroMax M5 microplate reader (Molecular Devices, Sunnydale, CA).

SDS-PAGE and immunoblotting

Crude protein extracts (50 µg) were resolved by electrophoresis in 10% sodium dodecyl sulfate-polyacrylamide gels and then transferred to PVDF Immobilon-P membranes (Bio-Rad, Mississauga, ON). Blots were blocked using 5% milk powder (Selection brand, Marché Jean-Talon, Montréal, QC) and incubated with antibodies using a dilution of 1:500 for anti-β-actin, a 1:250 dilution for anti-CaMKII beta subunit and anti-CaMKII gamma subunit (Santa Cruz Biotechnology, Santa Cruz, CA), a 1:500 dilution for anti-CHOP, a 1:1000 dilution for anti-LC3B, anti-ATF4, anti-phospho eIF2α (Ser51), and a 1:10000 dilution for anti-eIF2α (Cell Signaling). Immunoreactive proteins were exposed to anti-rabbit or anti-mouse horseradish peroxidase-conjugated secondary antibodies (Millipore) that were diluted 1:5000. Antigen-antibody complexes were detected using Immobilon ECL Western Chemiluminescent HRP Substrate (Millipore) and recorded with a VersaDoc imaging system (Bio-Rad).

In Silico 3-D affinity docking analyses

The structures of DIM and the ring-DIMs were optimized in a Gaussian 09 program package (Frisch et al., 2004) by the Density Functional Theory (DFT) method at the B3LYP/6-31G level. The output file was translated to pdb and pdbqt formats using Open Babel [30] and AutoDock Tools [31], respectively. The 3-D structures of the proteins were downloaded from the Protein Data Bank (PDB) in pdb format [32]. The structure of TrailR1 was obtained from ModBase because its crystal structure was not reported in PDB. Protein structures were then prepared using Sybyl-X 2.0 (Tripos, St. Louis, MO). In this process, all ions, water molecules and other substructures were removed [33]. We also fixed all side-chains, backbones and protonation types. Once prepared, proteins underwent a two-step optimization procedure using Sybyl-X 2.0. The first step included the Powell method applying Kollman's united force field AMBER (Assisted Model Building with Energy Refinement) charges, dielectric constant 1.0, NB cutoff 8.0, maximum interactions 1000 and termination gradient 0.001 kcal/mol. The second step utilized Kollman's All Atom approach with the same parameters. The resultant structures were saved as pdb files and then

converted to pdbqt format using AutoDock Tools [31]. Kollman charges and polar hydrogen atoms were added to the 3-D structures of the proteins using the same software [34].

Docking and docking-refinement experiments were carried out through a blind docking strategy by AutoDock Vina [35] to allow inclusion of the whole protein surface and all possible binding sites. The 3-D docking grid was centered on the macromolecule [36] and coordinates were calculated with a resolution of 0.357 Å using AutoDock Tools [31]. Docking analyses were performed with the AutoDock Vina 1.1 molecular docking and virtual screening program [35] running on a Linux operating system using the following settings: energy range = 1.5, number of modes = 20 and exhaustiveness = 25. The docking models of protein/DIM and protein/ring-DIM complexes with high-affinity scores (less than -8.0 kcal/mol) were refined with repetitions of 100 runs to increase accuracy and identify alternative *in silico* binding sites for each compound.

Protein/compound complexes underwent conformational analyses to determine the contact residues and interaction type using LigandScout 3.1 software with default settings [37]. The interaction cutoff threshold of the pdb interpretation, which defines a sphere around the ligand, was set at 7.0 Å. The atoms of the protein found inside the ligand-sphere were considered to be able to interact with the ligand [38].

Statistical analyses

All experiments were performed in at least triplicate and results presented as mean ± SEM. Statistically significant differences (* P < 0.05, ** P < 0.01, *** P < 0.005) were calculated using a two-tailed Student t-test. IC₅₀ values were calculated using nonlinear curve-fit analysis. All analyses were performed using GraphPad Prism v5.03 (GraphPad Software, San Diego, CA).

REFERENCES

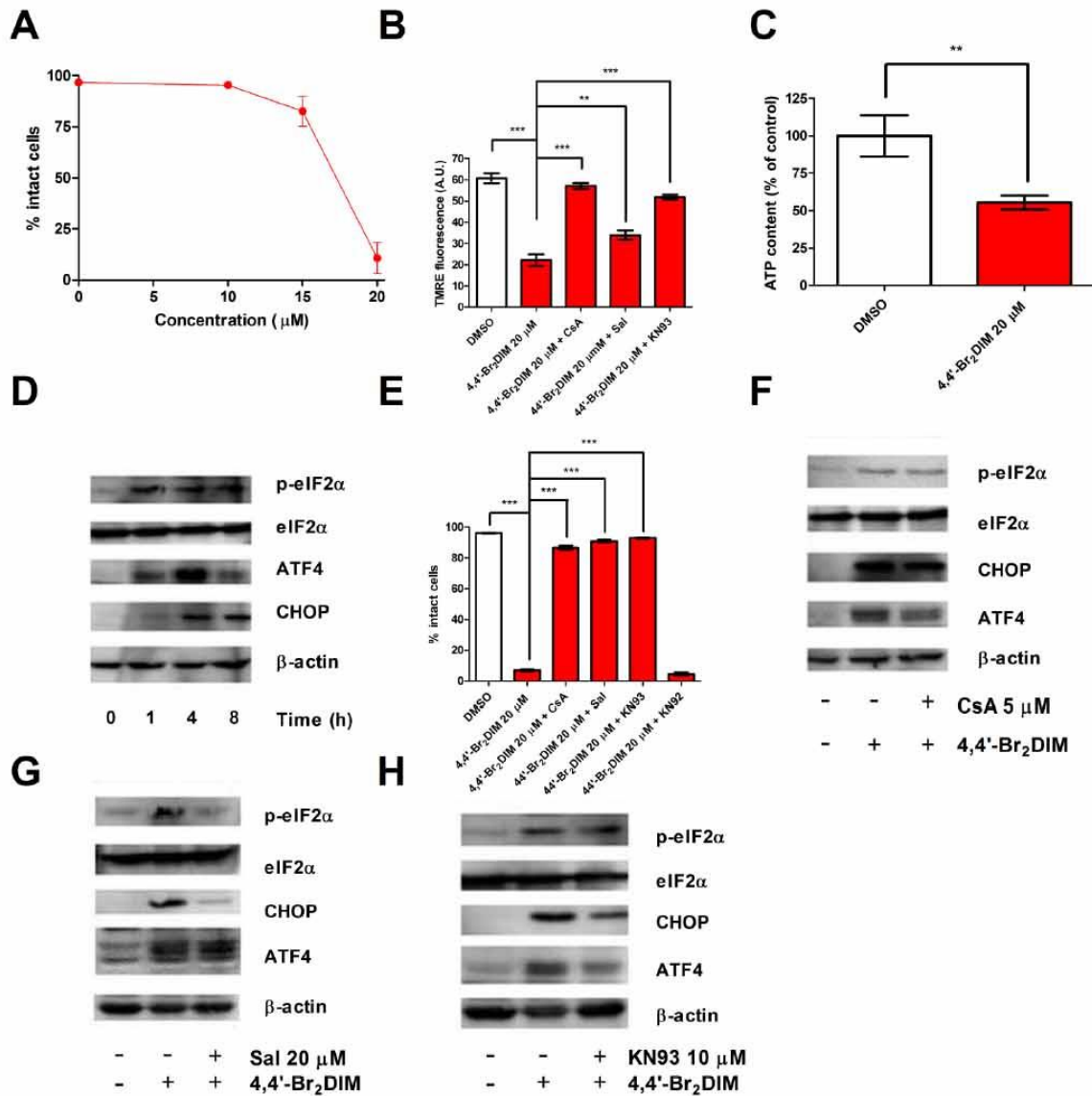
1. Siegel R, Naishadham D and Jemal A. Cancer statistics, 2013. *CA Cancer J Clin.* 2013; 63:11-30.
2. McLeod DG. Tolerability of Nonsteroidal Antiandrogens in the Treatment of Advanced Prostate Cancer. *Oncologist.* 1997; 2:18-27.
3. Wysowski DK, Freiman JP, Tourtelot JB and Horton ML, 3rd. Fatal and nonfatal hepatotoxicity associated with flutamide. *Ann Intern Med.* 1993; 118:860-864.
4. Bjeldanes LF, Kim JY, Grose KR, Bartholomew JC and Bradfield CA. Aromatic hydrocarbon responsiveness-receptor agonists generated from indole-3-carbinol in vitro and in vivo: comparisons with 2,3,7,8-tetrachlorodibenzo-p-dioxin. *Proc Natl Acad Sci U S A.* 1991; 88:9543-9547.
5. De Kruif CA, Marsman JW, Venekamp JC, Falke HE,

- Noordhoek J, Blaauboer BJ and Wortelboer HM. Structure elucidation of acid reaction products of indole-3-carbinol: detection in vivo and enzyme induction in vitro. *Chem Biol Interact.* 1991; 80:303-315.
6. Ge X, Yannai S, Rennert G, Gruener N and Fares FA. 3,3'-Diindolylmethane induces apoptosis in human cancer cells. *Biochem Biophys Res Commun.* 1996; 228:153-158.
 7. Nachshon-Kedmi M, Fares FA and Yannai S. Therapeutic activity of 3,3'-diindolylmethane on prostate cancer in an in vivo model. *Prostate.* 2004; 61:153-160.
 8. Heath EI, Heilbrun LK, Li J, Vaishampayan U, Harper F, Pemberton P and Sarkar FH. A phase I dose-escalation study of oral BR-DIM (BioResponse 3,3'- Diindolylmethane) in castrate-resistant, non-metastatic prostate cancer. *Am J Transl Res.* 2010; 2:402-411.
 9. Bhuiyan MM, Li Y, Banerjee S, Ahmed F, Wang Z, Ali S and Sarkar FH. Down-regulation of androgen receptor by 3,3'-diindolylmethane contributes to inhibition of cell proliferation and induction of apoptosis in both hormone-sensitive LNCaP and insensitive C4-2B prostate cancer cells. *Cancer Res.* 2006; 66:10064-10072.
 10. Le HT, Schaldach CM, Firestone GL and Bjeldanes LF. Plant-derived 3,3'-diindolylmethane is a strong androgen antagonist in human prostate cancer cells. *J Biol Chem.* 2003; 278:21136-21145.
 11. Abdelbaqi K, Lack N, Guns ET, Kotha L, Safe S and Sanderson JT. Antiandrogenic and growth inhibitory effects of ring-substituted analogs of 3,3'-diindolylmethane (Ring-DIMs) in hormone-responsive LNCaP human prostate cancer cells. *Prostate.* 2011; 71:1401-1412.
 12. Wang TT, Schoene NW, Milner JA and Kim YS. Broccoli-derived phytochemicals indole-3-carbinol and 3,3'-diindolylmethane exerts concentration-dependent pleiotropic effects on prostate cancer cells: comparison with other cancer preventive phytochemicals. *Mol Carcinog.* 2012; 51:244-256.
 13. Chinnakannu K, Chen D, Li Y, Wang Z, Dou QP, Reddy GP and Sarkar FH. Cell cycle-dependent effects of 3,3'-diindolylmethane on proliferation and apoptosis of prostate cancer cells. *J Cell Physiol.* 2009; 219:94-99.
 14. Gao N, Cheng S, Budhraj A, Liu EH, Chen J, Chen D, Yang Z, Luo J, Shi X and Zhang Z. 3,3'-Diindolylmethane exhibits antileukemic activity in vitro and in vivo through a Akt-dependent process. *PLoS One.* 2012; 7:e31783.
 15. Garikapaty VP, Ashok BT, Tadi K, Mittelman A and Tiwari RK. 3,3'-Diindolylmethane downregulates pro-survival pathway in hormone independent prostate cancer. *Biochem Biophys Res Commun.* 2006; 340:718-725.
 16. Kong D, Banerjee S, Huang W, Li Y, Wang Z, Kim HR and Sarkar FH. Mammalian target of rapamycin repression by 3,3'-diindolylmethane inhibits invasion and angiogenesis in platelet-derived growth factor-D-overexpressing PC3 cells. *Cancer Res.* 2008; 68:1927-1934.
 17. Goldberg AA, Titorenko VI, Beach A, Abdelbaqi K, Safe S and Sanderson JT. Ring-substituted analogs of 3,3'-diindolylmethane (DIM) induce apoptosis and necrosis in androgen-dependent and -independent prostate cancer cells. *Invest New Drugs.* 2013.
 18. Li Y, Wang Z, Kong D, Murthy S, Dou QP, Sheng S, Reddy GP and Sarkar FH. Regulation of FOXO3a/beta-catenin/GSK-3beta signaling by 3,3'-diindolylmethane contributes to inhibition of cell proliferation and induction of apoptosis in prostate cancer cells. *J Biol Chem.* 2007; 282:21542-21550.
 19. Li XJ, Park ES, Park MH and Kim SM. 3,3'-Diindolylmethane suppresses the growth of gastric cancer cells via activation of the Hippo signaling pathway. *Oncol Rep.* 2013; 30:2419-2426.
 20. Nachshon-Kedmi M, Yannai S, Haj A and Fares FA. Indole-3-carbinol and 3,3'-diindolylmethane induce apoptosis in human prostate cancer cells. *Food Chem Toxicol.* 2003; 41:745-752.
 21. Abdelrahim M, Newman K, Vanderlaag K, Samudio I and Safe S. 3,3'-diindolylmethane (DIM) and its derivatives induce apoptosis in pancreatic cancer cells through endoplasmic reticulum stress-dependent upregulation of DR5. *Carcinogenesis.* 2006; 27:717-728.
 22. Savino JA, 3rd, Evans JF, Rabinowitz D, Auburn KJ and Carter TH. Multiple, disparate roles for calcium signaling in apoptosis of human prostate and cervical cancer cells exposed to diindolylmethane. *Mol Cancer Ther.* 2006; 5:556-563.
 23. Sun S, Han J, Ralph WM, Jr., Chandrasekaran A, Liu K, Auburn KJ and Carter TH. Endoplasmic reticulum stress as a correlate of cytotoxicity in human tumor cells exposed to diindolylmethane in vitro. *Cell Stress Chaperones.* 2004; 9:76-87.
 24. Gong Y, Sohn H, Xue L, Firestone GL and Bjeldanes LF. 3,3'-Diindolylmethane is a novel mitochondrial H(+)-ATP synthase inhibitor that can induce p21(Cip1/Waf1) expression by induction of oxidative stress in human breast cancer cells. *Cancer Res.* 2006; 66:4880-4887.
 25. Riby JE, Firestone GL and Bjeldanes LF. 3,3'-diindolylmethane reduces levels of HIF-1alpha and HIF-1 activity in hypoxic cultured human cancer cells. *Biochem Pharmacol.* 2008; 75:1858-1867.
 26. Roy A, Ganguly A, BoseDasgupta S, Das BB, Pal C, Jaisankar P and Majumder HK. Mitochondria-dependent reactive oxygen species-mediated programmed cell death induced by 3,3'-diindolylmethane through inhibition of F0F1-ATP synthase in unicellular protozoan parasite *Leishmania donovani*. *Mol Pharmacol.* 2008; 74:1292-1307.
 27. Kandala PK and Srivastava SK. Regulation of macroautophagy in ovarian cancer cells in vitro and in vivo by controlling glucose regulatory protein 78 and AMPK. *Oncotarget.* 2012; 3:435-449.
 28. Wong CP, Hsu A, Buchanan A, Palomera-Sanchez Z, Beaver

- LM, Houseman EA, Williams DE, Dashwood RH and Ho E. Effects of sulforaphane and 3,3'-diindolylmethane on genome-wide promoter methylation in normal prostate epithelial cells and prostate cancer cells. *PLoS One*. 2014; 9:e86787.
29. Schneider CA, Rasband WS and Eliceiri KW. NIH Image to ImageJ: 25 years of image analysis. *Nat Methods*. 2012; 9:671-675.
 30. Guha R, Howard MT, Hutchison GR, Murray-Rust P, Rzepa H, Steinbeck C, Wegner J and Willighagen EL. The Blue Obelisk-interoperability in chemical informatics. *J Chem Inf Model*. 2006; 46:991-998.
 31. Morris GM, Huey R, Lindstrom W, Sanner MF, Belew RK, Goodsell DS and Olson AJ. AutoDock4 and AutoDockTools4: Automated docking with selective receptor flexibility. *J Comput Chem*. 2009; 30:2785-2791.
 32. Berman HM, Westbrook J, Feng Z, Gilliland G, Bhat TN, Weissig H, Shindyalov IN and Bourne PE. The Protein Data Bank. *Nucleic Acids Res*. 2000; 28:235-242.
 33. Hetenyi C and van der Spoel D. Efficient docking of peptides to proteins without prior knowledge of the binding site. *Protein Sci*. 2002; 11:1729-1737.
 34. Lim SV, Rahman MB and Tejo BA. Structure-based and ligand-based virtual screening of novel methyltransferase inhibitors of the dengue virus. *BMC Bioinformatics*. 2011; 12 Suppl 13:S24.
 35. Trott O and Olson AJ. AutoDock Vina: improving the speed and accuracy of docking with a new scoring function, efficient optimization, and multithreading. *J Comput Chem*. 2010; 31:455-461.
 36. Ranjan N, Andreasen KF, Kumar S, Hyde-Volpe D and Arya DP. Aminoglycoside binding to *Oxytricha nova* telomeric DNA. *Biochemistry*. 2010; 49:9891-9903.
 37. Wolber G and Langer T. LigandScout: 3-D pharmacophores derived from protein-bound ligands and their use as virtual screening filters. *J Chem Inf Model*. 2005; 45:160-169.
 38. Durdagi S, Duff HJ and Noskov SY. Combined receptor and ligand-based approach to the universal pharmacophore model development for studies of drug blockade to the hERG1 pore domain. *J Chem Inf Model*. 2011; 51:463-474.
 39. Mounir Z, Krishnamoorthy JL, Wang S, Papadopoulou B, Campbell S, Muller WJ, Hatzoglou M and Koromilas AE. Akt determines cell fate through inhibition of the PERK-eIF2alpha phosphorylation pathway. *Sci Signal*. 2011; 4:ra62.
 40. Rahman KW and Sarkar FH. Inhibition of nuclear translocation of nuclear factor- κ B contributes to 3,3'-diindolylmethane-induced apoptosis in breast cancer cells. *Cancer Res*. 2005; 65:364-371.
 41. Huang X, Chen Y, Zhang H, Ma Q, Zhang YW and Xu H. Salubrinal attenuates beta-amyloid-induced neuronal death and microglial activation by inhibition of the NF- κ B pathway. *Neurobiol Aging*. 2012; 33:1007 e1009-1017.
 42. Kessel D. Protection of Bcl-2 by salubrinal. *Biochem Biophys Res Commun*. 2006; 346:1320-1323.
 43. Ouyang DY, Xu LH, He XH, Zhang YT, Zeng LH, Cai JY and Ren S. Autophagy is differentially induced in prostate cancer LNCaP, DU145 and PC-3 cells via distinct splicing profiles of ATG5. *Autophagy*. 2013; 9:20-32.
 44. Rokhlin OW, Taghiyev AF, Bayer KU, Bumcrot D, Koteliansk VE, Glover RA and Cohen MB. Calcium/calmodulin-dependent kinase II plays an important role in prostate cancer cell survival. *Cancer Biol Ther*. 2007; 6:732-742.
 45. Liu Y and Templeton DM. Initiation of caspase-independent death in mouse mesangial cells by Cd2+: involvement of p38 kinase and CaMK-II. *J Cell Physiol*. 2008; 217:307-318.
 46. Timmins JM, Ozcan L, Seimon TA, Li G, Malagelada C, Backs J, Backs T, Bassel-Duby R, Olson EN, Anderson ME and Tabas I. Calcium/calmodulin-dependent protein kinase II links ER stress with Fas and mitochondrial apoptosis pathways. *J Clin Invest*. 2009; 119:2925-2941.
 47. Mamaeva OA, Kim J, Feng G and McDonald JM. Calcium/calmodulin-dependent kinase II regulates notch-1 signaling in prostate cancer cells. *J Cell Biochem*. 2009; 106:25-32.

3,3'-Diindolylmethane (DIM) and its ring-substituted halogenated analogs (ring-DIMs) induce differential mechanisms of survival and death in androgen-dependent and -independent prostate cancer cells

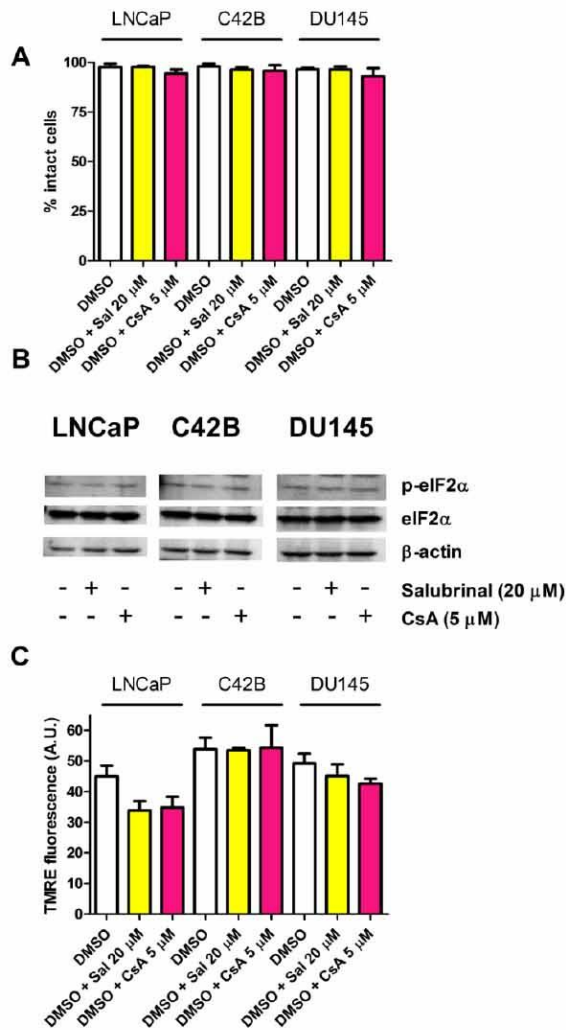
Supplementary Material



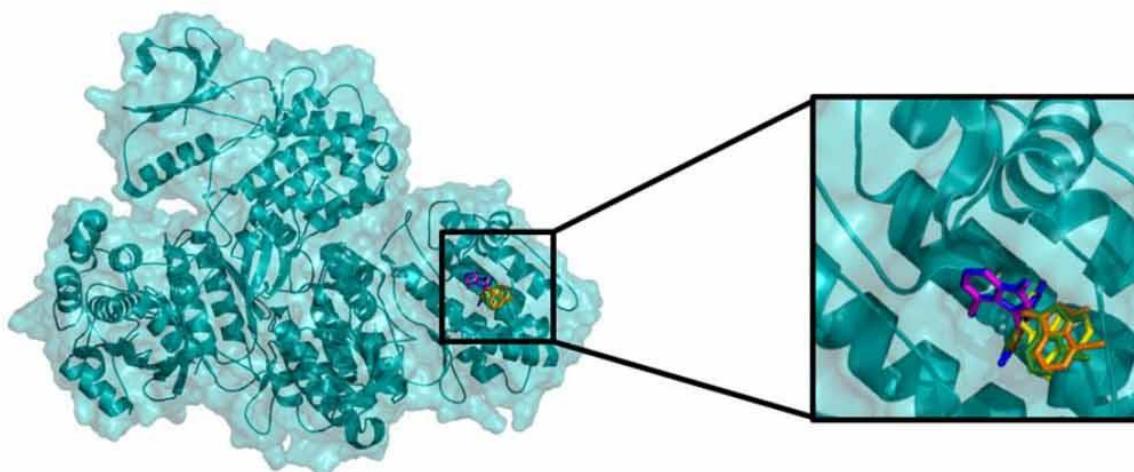
Supplementary Figure S1: Effects of 4,4'-Br₂DIM on the AI prostate cancer cell line DU145.

(A) Percentage of intact DU145 cells treated with increasing concentrations (5-20 μM) of 4,4'-Br₂DIM. (B) TMRE fluorescence of DU145 cells after a 4 hour exposure to 4,4'-Br₂DIM with or

without a 4 hour pre-treatment with either CsA, Sal or KN93. (C) Relative mitochondrial ATP levels of DU145 cells treated with 5 mM 2-deoxy-D-glucose after a 4 hour exposure to 4,4'-Br₂DIM with or without a 4 hour pre-treatment with either CsA, Sal or KN93. (D) Phosphorylation of eIF2 α , and levels of ER stress proteins were assayed by immunoblot of DU145 cells after 0, 1, 4 and 8 hours of exposure to 4,4'-Br₂DIM. (E) Percentage of intact DU145 cells after a 24 hour exposure to 4,4'-Br₂DIM, with or without a 4 hour pre-treatment with either CsA, Sal, KN92 or KN93. Phosphorylation of eIF2 α , and levels of ER stress proteins were assayed by immunoblot of DU145 cells after 24 hrs of exposure to 4,4'-Br₂DIM with or without a 4 h pre-treatment with either CsA (F), Sal (G) or KN93 (H).



Supplementary Figure S2: Neither salubrinal nor CsA alone influences eIF2 α phosphorylation. (A) Percentage of intact LNCaP, C42B, or DU145 cells exposed to either salubrinal or CsA for 24 hours. (B) Phosphorylation of eIF2 α in LNCaP, C42B, and DU145 cells exposed to salubrinal or CsA for 24 hours. (C) TMRE fluorescence of LNCaP, C42B or DU145 cells exposed to salubrinal or CsA for 24 hours.



Supplementary Figure S3: Three-dimensional view of the docking between CaMK-II subunit beta (protein database: 3BHH) and diindolylmethane (DIM; yellow), and its derivatives 4,4'-dibromoDIM (blue); 4,4'-dichloroDIM (magenta); 7,7'-dibromoDIM (orange) and 7,7'-dichloroDIM (green).

2.2 Diindolylmethane and its halogenated derivatives induce protective autophagy in human prostate cancer cells via induction of the oncogenic protein AEG-1 and activation of AMP-dependent kinase (AMPK)

Hossam Draz^{1,2}, Alexander A. Goldberg^{1,3}, Vladimir I. Titorenko⁴, Emma Guns⁵ Stephen H. Safe⁶ and J. Thomas Sanderson^{1,*}

¹ INRS-Institut Armand-Frappier, Laval, QC, Canada.

² Department of Biochemistry, National Research Centre, Dokki, Cairo, Egypt.

³ Critical Care Division and Meakins-Christie Laboratories, Faculty of Medicine, McGill University, Montréal, QC, Canada

⁴ Department of Biology, Concordia University, Montréal, QC, Canada.

⁵ The Prostate Centre, University of British Columbia, Vancouver, BC, Canada.

⁶ Veterinary Physiology and Pharmacology, Texas A&M University, College Station, TX, United States.

This article was published in *cellular signaling* (2017), 40:172-182.

Author contributions:

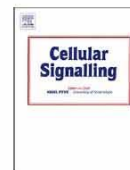
Hossam Draz designed and performed the experiments, the statistical analyses and wrote the manuscript.

Dr. Alexander Goldberg conducted the electron microscopy experiments in prostate cancer cells.

Professors Vladimir Titorenko and Emma Guns were involved in revising the scientific content of the manuscript.

Prof. Stephen Safe provided us with ring-DIMs synthesised in his laboratory at Texas A&M University and participated in revising the manuscript.

Prof. Thomas Sanderson obtained the research funding, supervised the project and participated in writing and revising the manuscript.



Diindolylmethane and its halogenated derivatives induce protective autophagy in human prostate cancer cells via induction of the oncogenic protein AEG-1 and activation of AMP-activated protein kinase (AMPK)



Hossam Draz^{a,b}, Alexander A. Goldberg^{a,c}, Vladimir I. Titorenko^d, Emma S. Tomlinson^e, Stephen H. Safe^f, J. Thomas Sanderson^{a,*}

^a INRS-Institut Armand-Frappier, Laval, QC, Canada

^b Department of Biochemistry, National Research Centre, Dokki, Cairo, Egypt

^c Critical Care Division and Meakins-Christie Laboratories, Faculty of Medicine, McGill University, Montréal, QC, Canada

^d Department of Biology, Concordia University, Montréal, QC, Canada

^e The Prostate Centre, University of British Columbia, Vancouver, BC, Canada

^f Veterinary Physiology and Pharmacology, Texas A & M University, College Station, TX, United States

ARTICLE INFO

Keywords:

Prostate cancer
LNCaP
C42B
Autophagy
AMPK
AEG-1

ABSTRACT

3,3'-Diindolylmethane (DIM) and its synthetic halogenated derivatives 4,4'-Br₂- and 7,7'-Cl₂DIM (ring-DIMs) have recently been shown to induce protective autophagy in human prostate cancer cells. The mechanisms by which DIM and ring-DIMs induce autophagy have not been elucidated. As DIM is a mitochondrial ATP-synthase inhibitor, we hypothesized that DIM and ring-DIMs induce autophagy via alteration of intracellular AMP/ATP ratios and activation of AMP-activated protein kinase (AMPK) signaling in prostate cancer cells. We found that DIM and ring-DIMs induced autophagy was accompanied by increased autophagic vacuole formation and conversion of LC3BI to LC3BII in LNCaP and C42B human prostate cancer cells. DIM and ring-DIMs also induced AMPK, ULK-1 (unc-51-like autophagy activating kinase 1; Atg1) and acetyl-CoA carboxylase (ACC) phosphorylation in a time-dependent manner. DIM and the ring-DIMs time-dependently induced the oncogenic protein astrocyte-elevated gene 1 (AEG-1) in LNCaP and C42B cells. Downregulation of AEG-1 or AMPK inhibited DIM- and ring-DIM-induced autophagy. Pretreatment with ULK1 inhibitor MRT 67307 or siRNAs targeting either AEG-1 or AMPK potentiated the cytotoxicity of DIM and ring-DIMs. Interestingly, downregulation of AEG-1 induced senescence in cells treated with overtly cytotoxic concentrations of DIM or ring-DIMs and inhibited the onset of apoptosis in response to these compounds. In summary, we have identified a novel mechanism for DIM- and ring-DIM-induced protective autophagy, via induction of AEG-1 and subsequent activation of AMPK. Our findings could facilitate the development of novel drug therapies for prostate cancer that include selective autophagy inhibitors as adjuvants.

1. Introduction

Prostate cancer is a major health problem worldwide, ranking as the second most common cancer in males [1] and the third leading cause of cancer-related deaths among American and Canadian men [2]. Treatment with drugs targeting androgen receptor (AR) signaling is the main therapy for early-stage androgen-dependent (AD) prostate cancer [3]. Unfortunately, many patients with AD prostate cancer will progress to an androgen-independent (AI) phenotype, which is harder to treat and often fatal [4,5]. Diindolylmethane (DIM) is a promising anticancer agent derived from the ingestion of *Brassica* plants (cabbage, broccoli,

etc.) [6]. We have shown that several di-halogenated analogs of DIM (ring-DIMs) have anti-androgenic effects in human AD LNCaP prostate cancer cells [7] and induce apoptosis and necrosis in LNCaP and human AI PC-3 prostate cancer cells with greater potencies than DIM [8]. More recently, we have shown that DIM and ring-DIMs induce ER stress, mitochondrial dysfunction, and autophagy in prostate cancer cells [9]. Autophagy is a self-digestion process activated by cellular stress, in which dysfunctional organelles and protein aggregates are sequestered in double-membraned vesicles [10], and then transported to lysosomes for proteolytic degradation and recycling to maintain cellular homeostasis [11].

* Corresponding author at: INRS-Institut Armand-Frappier, 531 boulevard des Prairies, Laval, QC H7V 1B7, Canada.
E-mail address: thomas.sanderson@iaf.inrs.ca (J.T. Sanderson).

<http://dx.doi.org/10.1016/j.cellsig.2017.09.006>

Received 8 May 2017; Received in revised form 21 August 2017; Accepted 14 September 2017
Available online 18 September 2017

0898-6568/© 2017 Elsevier Inc. All rights reserved.

Autophagy plays an important role in cancer cell progression; its induction in response to stresses following chemotherapy may promote cancer cell survival. However, excessive autophagy could activate a cell death mechanism known as cytotoxic autophagy, which is different from programmed cell death (apoptosis) [12,13]. Uncontrolled growth of cancer cells is facilitated by the inactivation of cell death pathways, such as apoptosis, and stimulation of cell survival pathways [14]. Thus, the dysregulation of autophagic machinery in cancer cells, leading to imbalances in the activation of cell death- or survival-related pathways, may have a critical influence on either tumor progression or regression. Various Atg (autophagy-related) proteins are involved in the initiation and regulation of autophagy [15]. The conversion of LC3B (Atg3) from its diffuse LC3BI form to the punctuated LC3BII, which associates with the autophagosome [16], is used as a classic marker of autophagy. AMP-activated protein kinase (AMPK) regulates autophagy via phosphorylation of the autophagy-initiating protein ULK1 (Atg1) [17]. The oncogenic protein, astrocyte elevated gene-1 (AEG-1), also known as metadherin (MTDH) or protein LYRIC, is overexpressed in various cancer including that of the prostate [18,19], where it acts as a mediator of AMPK activity and autophagy in response to cellular metabolic stress [20,21]. AEG-1 contributes to chemoresistance in hepatocellular carcinoma (HCC) cells [22] and promotes hepato-carcinogenesis through inhibition of senescence in transgenic mice that overexpress hepatocyte-specific AEG-1 [23].

Although DIM is known to be a mitochondrial ATP synthase inhibitor [24] that alters AMP/ATP ratios leading to activation of AMPK [25], the exact mechanism(s) of DIM-induced protective autophagy has not been elucidated. Previous studies have shown that AEG-1 induces protective autophagy via activation of AMPK [21]. Therefore, we wished to determine the possible involvement of AEG-1 in AMPK activation as well as DIM- and ring-DIM-mediated induction of autophagy.

2. Materials and methods

2.1. Cell culture and treatment

LNCAp AR-positive and AD human prostate cancer cells were purchased from the American Type Culture Collection (Manassas, VA); LNCAp C4-2B (C42B) AR-positive and AI human prostate cancer cells were purchased from the MD Anderson Cancer Centre (Houston, TX). LNCAp and C42B prostate cancer cells were cultured in RPMI 1640 medium supplemented with 10% FBS, and 1% penicillin/streptomycin (Life Technologies, Gaithersburg, MD) at 37 °C and 5% CO₂. Ring-DIMs were synthesized in our laboratories as previously described [8].

For cell treatments, LNCAp and C42B were seeded in 24-well CellBind culture plates (Corning Inc., Corning, NY) at a density of 1.5×10^5 cells/well in RPMI 1640 supplemented with 2% dextran-coated charcoal-stripped FBS (Hyclone, Logan, UT); LNCAp cell medium was supplemented with 0.1 nM dihydrotestosterone (DHT; Steraloids Inc., Newport, RI). Cells were then treated with either DIM, ring-DIMs, or DMSO vehicle control (0.1% or 0.2% in the case of co-exposures). The ULK1 inhibitor MRT 67307 (Sigma-Aldrich, St-Louis, MO) was added to cell cultures 4 h prior to treatment.

2.2. Cell death assay

For cell death measurements, LNCAp and C42B cells were treated with DIM, ring-DIMs, or vehicle control (DMSO). After 24 h of exposure, Hoechst 33342 (Sigma-Aldrich) and propidium iodide (PI; Invitrogen, Carlsbad, CA) stains were both added to each well at a concentration of 1 µg/ml for 15 min at 37 °C to detect apoptotic and necrotic (or late-apoptotic) cell death, respectively. Hoechst- and PI-positive cells were counted under a Nikon Eclipse (TE-2000U) inverted fluorescence microscope at 20 × magnification using filter cubes with excitation wavelengths of 330–380 and 532–587 nm, respectively.

Intact (viable) cells were counted as exhibiting neither Hoechst (chromatin condensation/fragmentation) nor PI (cell membrane disintegration) staining. Subtoxic concentrations used for cell death analysis were as follows: 10 µM for DIM, 5 µM for both 4,4'-Br₂DIM and 7,7'-Cl₂DIM in LNCAp cells; then 20 µM for DIM, 10 µM for both 4,4'-Br₂DIM and 7,7'-Cl₂DIM in C42B cells. On the other hand, toxic concentrations used for cell death analysis were as follows: 20 µM for DIM, 15 µM for both 4,4'-Br₂DIM and 7,7'-Cl₂DIM in LNCAp cells; then, 30 µM for DIM, 15 µM for 4,4'-Br₂DIM and 20 µM 7,7'-Cl₂DIM in C42B cells. At least 100 cells per treatment were examined.

2.3. Cell proliferation assay

The effect of AEG-1 siRNA on cell proliferation of LNCAp and C42B cells treated with DIM was determined using a WST-1 kit (Roche, Basel, Switzerland), which measures mitochondrial reductase activity of viable cells. LNCAp and primary C42B cells were plated in 96-well CellBind plates (Corning Inc.) at a density of 1×10^3 cells/well in their appropriate culture medium for 24 h. Cells were then incubated with WST-1 substrate for 2 h and the formation of formazan was then measured using the absorbance at 440 nm with SpectraMax M5 spectrophotometer (Molecular Devices, Sunnyvale, California).

2.4. Autophagic vacuole detection

Autophagic vacuoles were measured using a Cyto-ID Autophagy detection kit (Enzo Life Sciences, Farmingdale, NY) according to the manufacturer's protocol. Cells were cultured in 24 well plates and treated with DIM or ring-DIMs for 24 h. Cells were washed with 1 × assay buffer, then stained with CYTO-ID green detection reagent. Plates were protected from light and incubated for 30 min at 37 °C.

Cells were counterstained with Hoechst 33342 and the number of autophagic vacuoles per cell was counted in vehicle control (DMSO), DIM- and ring-DIM-treated cells under a Nikon Eclipse inverted fluorescence microscope. At least 50 cells per treatment were counted.

2.5. Gene silencing with small interfering RNA (siRNA)

LNCAp and C42B cells underwent reverse transfection with SMARTpool siRNA oligonucleotides (a mixture of 4 siRNA; Dharmacon, Lafayette, CO) targeting either AMPK or AEG-1 gene expression. Lipofectamine RNAiMAX reagent (Life Technologies) was used for the reverse transfection of cells in serum free Opti-MEM medium (Life Technologies) according to the manufacturer's protocol.

2.6. Immunoblotting

Cells were treated with DIM, ring-DIMs, or DMSO in 6-well CellBind culture plates (Corning Inc.) at a density of 7.5×10^5 cells/well. Cells were harvested using RIPA buffer (Pierce Biotechnologies, Rockford, IL) containing protease inhibitor cocktail and Halt phosphatase inhibitor (ThermoFisher, Waltham, MA). Protein concentrations were measured in cell lysates using a Pierce BCA protein assay kit (ThermoFisher). Twenty-five microgram aliquots of protein underwent electrophoresis on 10% sodium dodecyl sulfate-polyacrylamide gels and were then transferred to polyvinylidene difluoride (PVDF) membranes using a Trans-Blot Turbo Transfer System (Bio-Rad, Mississauga, ON). Rabbit primary antibodies for phospho-AMPK (T172), AMPK (23A3), phospho-acetyl-CoA carboxylase (pACC) (S79), ACC (C83B10), phospho-ULK1 (D1H4) and mouse primary antibodies for AEG-1 (2F11C3) and β-actin (8H10D10) were purchased from Cell Signaling Technology (Danvers, MA). LC3B (L7543) rabbit primary antibody was purchased from Sigma-Aldrich. PVDF membranes were incubated with 1:1000 dilutions of the primary antibodies overnight (4 °C) in a shaking rotator. Membranes were washed three times with PBS and then incubated with a 1:5000 dilution of either goat anti-rabbit or goat anti-mouse

horseradish peroxidase-conjugated secondary antibodies (Millipore, Billerica, MA) for 1 h at room temperature. Washing steps were repeated before adding clarity Western ECL substrate (Bio-Rad) for 5 min, after which the membranes were digitally photographed using a ChemiDoc MP Gel Doc system (Bio-Rad).

2.7. Senescence assay

LNCaP and C42B cells were cultured in their respective media in 6-well CellBind culture plates (Corning Inc.) at a density of 7.5×10^5 cells/well. After treatment with DIM or ring-DIMs, senescent cells were detected using a Senescence β -galactosidase staining kit (Cell Signaling) according to the manufacturer's instructions. Cells were cultured in 6-well plates and treated with DIM or ring-DIMs for 24 h. Cells were washed with $1 \times$ PBS, then fixed with $1 \times$ Fixative Solution. Cells were then washed with $1 \times$ PBS and stained with β -galactosidase staining solution. Plates were incubated at 37°C overnight in a non-humidified incubator. Cells positive for β -galactosidase activity were counted by light microscopy under $100 \times$ magnification in at least triplicate using different cell passages for each treatment. At least 50 cells per treatment were counted.

2.8. Electron microscope analysis

C42B cells were cultured in RPMI medium supplemented with 2% dextran-coated charcoal-stripped FBS and seeded in 6-well CellBind culture plates (Corning Inc.) at a density 7.5×10^5 cells/well. Cells were treated with DIM or ring-DIMs for 8 h and then fixed using 2.5% glutaraldehyde in 0.1 M phosphate buffer at pH 7.2 for 15 min. Cells were scraped with a rubber policeman, transferred to 1.5 ml tubes and centrifuged for 3 min at 1200 rpm. The cells were washed 3 times for 15 min with 3% sucrose in 0.1 M cacodylate buffer. Cells were fixed with freshly prepared 1.3% (w/v) osmium tetroxide in collidine buffer for 1–2 h. Fixed cells were dehydrated by successive passage through 25, 50, 75, 95 and 100% solutions of acetone in water (15–30 min each), then embedded in SPURR resin mixtures (Mecalab, Montreal, QC). The block containing fixed cells were cut and encapsulated in mold filled with SPURR resin. Ultrathin sections were prepared with an ultramicrotome (LKB, Sollentuna, Sweden) and placed onto copper grids. After staining with uranyl acetate and lead citrate, sections were examined using a Hitachi H-7100 transmission electron microscope.

2.9. Statistical analyses

All experiments were performed at least 3 times independently using different cell passages. Treatments were performed in at least triplicate per experiment. Data are presented as mean \pm SEM. Statistically significant differences ($P < 0.05$) between groups were determined using a one-way analysis of variance (ANOVA) followed by Dunnett's post-hoc test to correct for multiple comparisons to vehicle control. All data were analyzed using GraphPad Prism (version 5.01, GraphPad Software, San Diego, CA).

3. Results

3.1. DIM and ring-DIMs induce the formation of autophagic vacuoles in prostate cancer cells

An 8-h treatment of androgen-sensitive LNCaP and androgen-insensitive C42B cells with DIM, 4,4'-Br₂DIM and 7,7'-Cl₂DIM significantly increased the formation of autophagic vacuoles (Fig. 1A–D). The concentrations used in these experiments were based on our previous studies on DIM- and ring-DIM-mediated induction of protective autophagy in the same prostate cancer cells [8,9]. We also confirmed the formation of autophagosomes by transmission electron microscopy after exposure of C42B cells to DIM and the ring-DIMs for 8 h (Fig. 1E).

3.2. DIM and ring-DIMs induce autophagy via activation of AMPK signaling

To investigate the mechanism of DIM- and ring-DIM-mediated autophagy, we determined their effects on AMPK signaling. DIM and ring-DIMs significantly increased the conversion of LC3BI to LC3BII (LC3BII/I ratio) in LNCaP and C42B cells (Figs. 2A, B, S2B, S3B). In LNCaP cells, a time-dependent increase of AMPK phosphorylation by 4,4'-Br₂DIM was observed, whereas DIM significantly induced phosphorylation of AMPK only after treatment for 1 and 4 h, with levels decreasing after 8 h of exposure; however, 7,7'-Cl₂DIM treatment didn't change the levels of AMPK phosphorylation (Figs. 2A, S2A). DIM and ring-DIMs significantly and time dependently increased AMPK phosphorylation in C42B cells at all time-points (Figs. 2B, S3A). Activation of AMPK signaling was confirmed in both cell lines by assessing the phosphorylation of its substrate acetyl-CoA carboxylase, ACC (Figs. 2A, B, S2A, S3A). Next, we assessed whether the stimulation of AMPK activity resulted in an increased autophagic response by activating the autophagy initiator ULK1. We found that DIM and the ring-DIMs increased ULK1 phosphorylation time-dependently in both LNCaP and C42B cells (Figs. 2A, B, S2B, S3B). Pretreatment of cells with an ULK1 inhibitor (MRT67307, 10 μM) significantly sensitized LNCaP and C42B cells to cell death in the presence of sub-toxic concentrations of DIM or ring-DIMs (Fig. 2C, D).

To confirm the role of AMPK signaling in the autophagy induced by DIM and the ring-DIMs, siRNA was used to inhibit AMPK gene expression. The increased conversion of LC3BI to LC3BII (LC3BII/I ratio) after a 24-h exposure of LNCaP to DIM or ring-DIMs and C42B cells to ring-DIMs was inhibited when cells were pretreated with AMPK-selective siRNA, while pretreatment of C42B cells exposed to DIM with AMPK siRNA didn't affect LC3BII/I ratio (Fig. 3A, B, C, D). The siRNA-mediated inhibition of AMPK expression sensitized LNCaP and C42B cells to the cytotoxicity of normally sub-toxic concentrations of DIM and ring-DIMs (Fig. 3E, F).

3.3. DIM and ring-DIMs promote autophagy via induction of AEG-1

Since AEG-1 is an upstream regulator of AMPK [20,21], we therefore investigated the effect of DIM and ring-DIMs on induction of AEG-1 and AMPK-mediated autophagy. DIM induced AEG-1 expression in a time-dependent manner in both LNCaP and C42B cells (Fig. 4A, B, C, D). 4,4'-Br₂DIM, and 7,7'-Cl₂DIM time dependently increased AEG-1 levels in LNCaP and C42B cells after a 1- and 4-h exposure, an effect that was no longer seen after 8 h. (Fig. 4A, B, C, D). Pretreatment of LNCaP and C42B cells with AEG-1-selective siRNA inhibited DIM- and ring-DIM-mediated LC3BI-to-LC3BII conversion (Fig. 5A, B, C, D) and sensitized LNCaP and C42B cells to the cytotoxicity of normally sub-toxic concentrations of DIM or ring-DIMs (Fig. 5E, F). To know whether AEG-1 acts upstream or downstream of AMPK, ACC phosphorylation (a substrate uniquely phosphorylated by AMPK) was measured in LNCaP and C42B cells exposed to DIM or ring-DIMs in the presence or absence of pretreatment with AEG-1 siRNA. Our results showed that inhibition of AEG-1 using selective siRNA reduced AMPK activation based on the phosphorylation of ACC (Fig. 5A, B, C, D), which indicates that AEG-1 is an upstream regulator of AMPK.

3.4. Downregulation of AEG-1 induces senescence in LNCaP and C42B cells

To further explore the role of AEG-1 in DIM- and ring-DIM-mediated cytotoxicity, we assessed the effect of AEG-1 downregulation in LNCaP and C42B cells on their response to cytotoxic concentrations of DIM and ring-DIMs. Interestingly, siRNA-mediated silencing of AEG-1 expression protected LNCaP and C42B cells against the toxicity of DIM and ring-DIMs (Fig. 6A, B). AEG-1 may affect multiple pathways related to cancer progression; hence, we investigated the effect of AEG-1 downregulation on cellular senescence. Pretreatment with AEG-1-selective siRNA promoted senescence as indicated by increased β -galactosidase

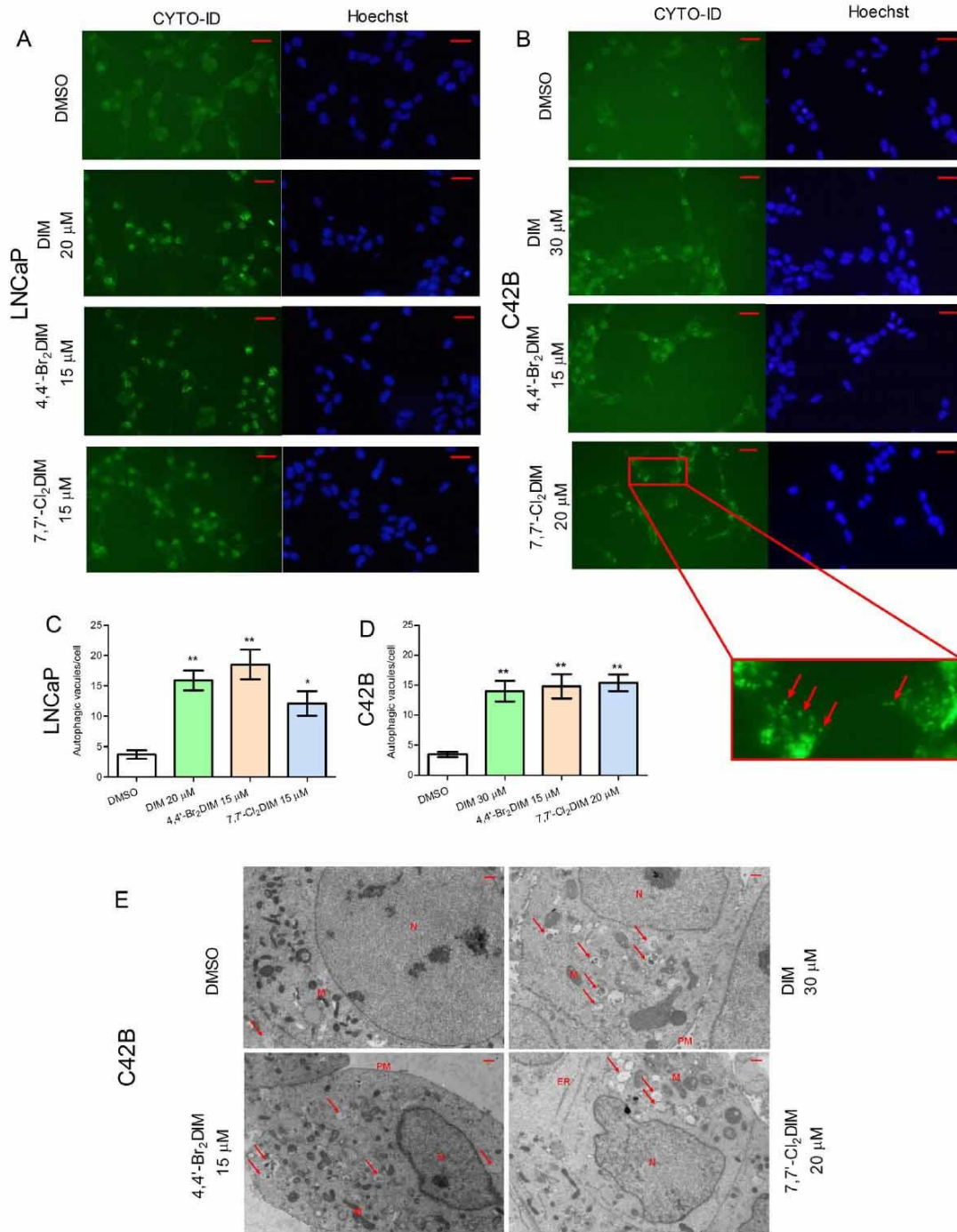


Fig. 1. DIM, 4,4'-Br₂DIM and 7,7'-Cl₂DIM induce autophagic vacuole formation in LNCaP (A) and C42B (B) cells after an 8-h exposure. Autophagic vacuoles were detected using a Cyto-ID autophagy detection kit and nuclei were counterstained with Hoechst 33342 as described in **Materials and methods**. LNCaP cells were treated with 20 μ M DIM, 15 μ M 4,4'-Br₂DIM or 15 μ M 7,7'-Cl₂DIM, whereas C42B cells were treated with 30 μ M DIM, 15 μ M 4,4'-Br₂DIM or 20 μ M 7,7'-Cl₂DIM. Red arrows indicate representative examples of autophagic vacuoles stained with Cyto-ID. Scale bar = 50 μ m. Fluorescence images are representative of three independent experiments. Number of autophagic vacuoles counted per cell in LNCaP (C) and C42B (D) cells are presented as means \pm SEM of three independent experiments, each performed in triplicate. Statistically significant difference (* P < 0.05, ** P < 0.01) were determined by one-way ANOVA and a Dunnett posthoc test to correct for multiple comparisons to control. Transmission electron microscopic images of C42B cells treated with DIM, 4,4'-Br₂DIM or 7,7'-Cl₂DIM (E) for 8 h. Red arrows indicate autophagic vacuoles. Scale bar = 500 nm. ER = endoplasmic reticulum, M = mitochondria, PM = plasma membrane, N = nucleus.

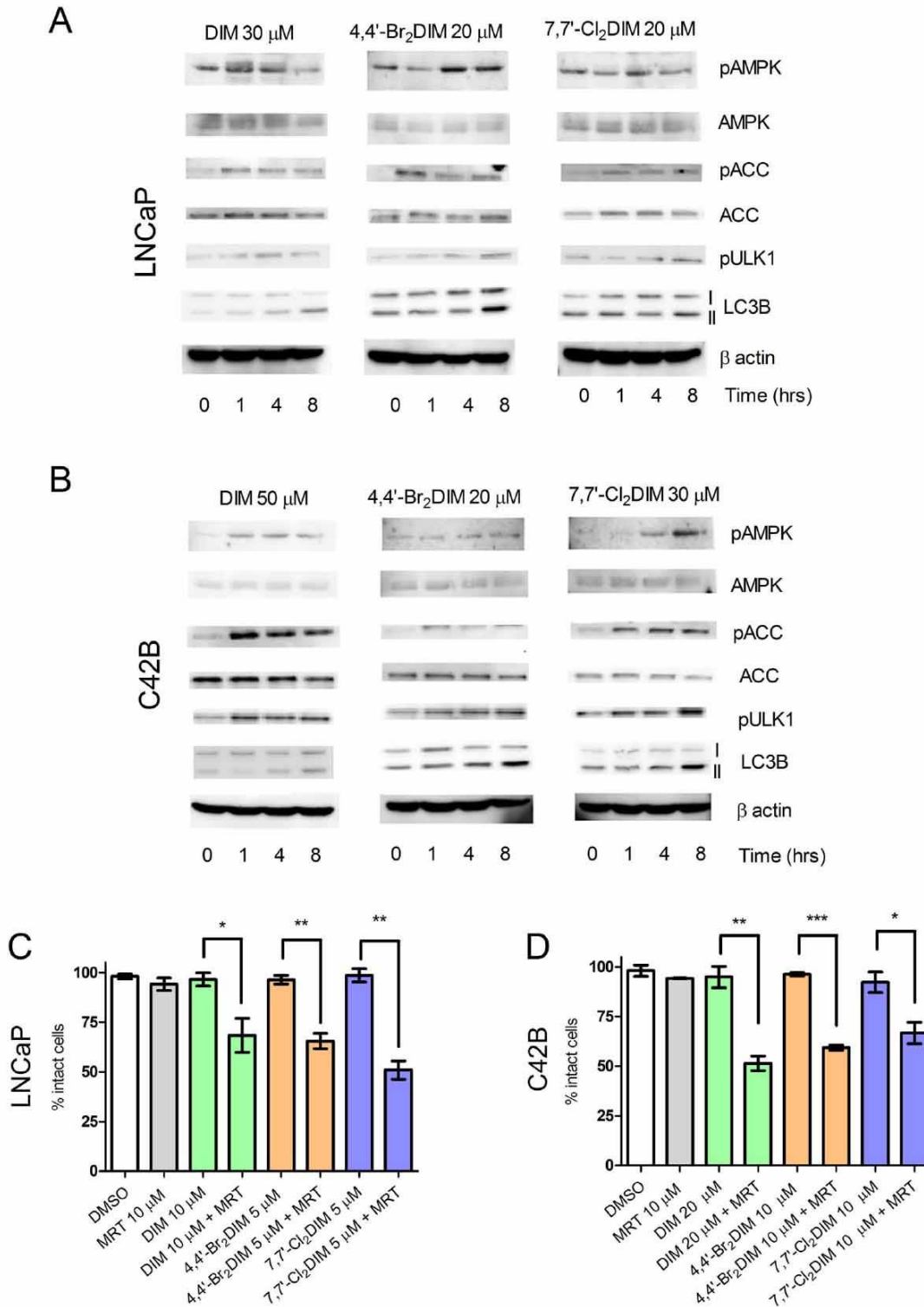


Fig. 2. DIM and ring-DIMs induce phosphorylation of AMPK, ACC, ULK1 and the conversion of LC3BI to II in LNCaP (A) and C42B (B) cells. LNCaP cells were exposed for 0, 1, 4, 8 h to 30 μM DIM, 20 μM 4,4'-Br₂DIM or 20 μM 7,7'-Cl₂DIM whereas C42B cells were exposed to concentrations of 50 μM DIM, 20 μM 4,4'-Br₂DIM or 30 μM 7,7'-Cl₂DIM. Each gel is representative of three independent experiments. Percentage of intact LNCaP (C) and C42B (D) cells treated with DIM or ring-DIMs for 24 h with or without a 4-h pretreatment with ULK-1 inhibitor MRT 67307. Percentages are presented as means ± SEM of three independent experiments. Statistically significant difference (**P* < 0.05, ***P* < 0.01, ****P* < 0.001) were determined by one-way ANOVA and a Dunnett posthoc test to correct for multiple comparisons to control.

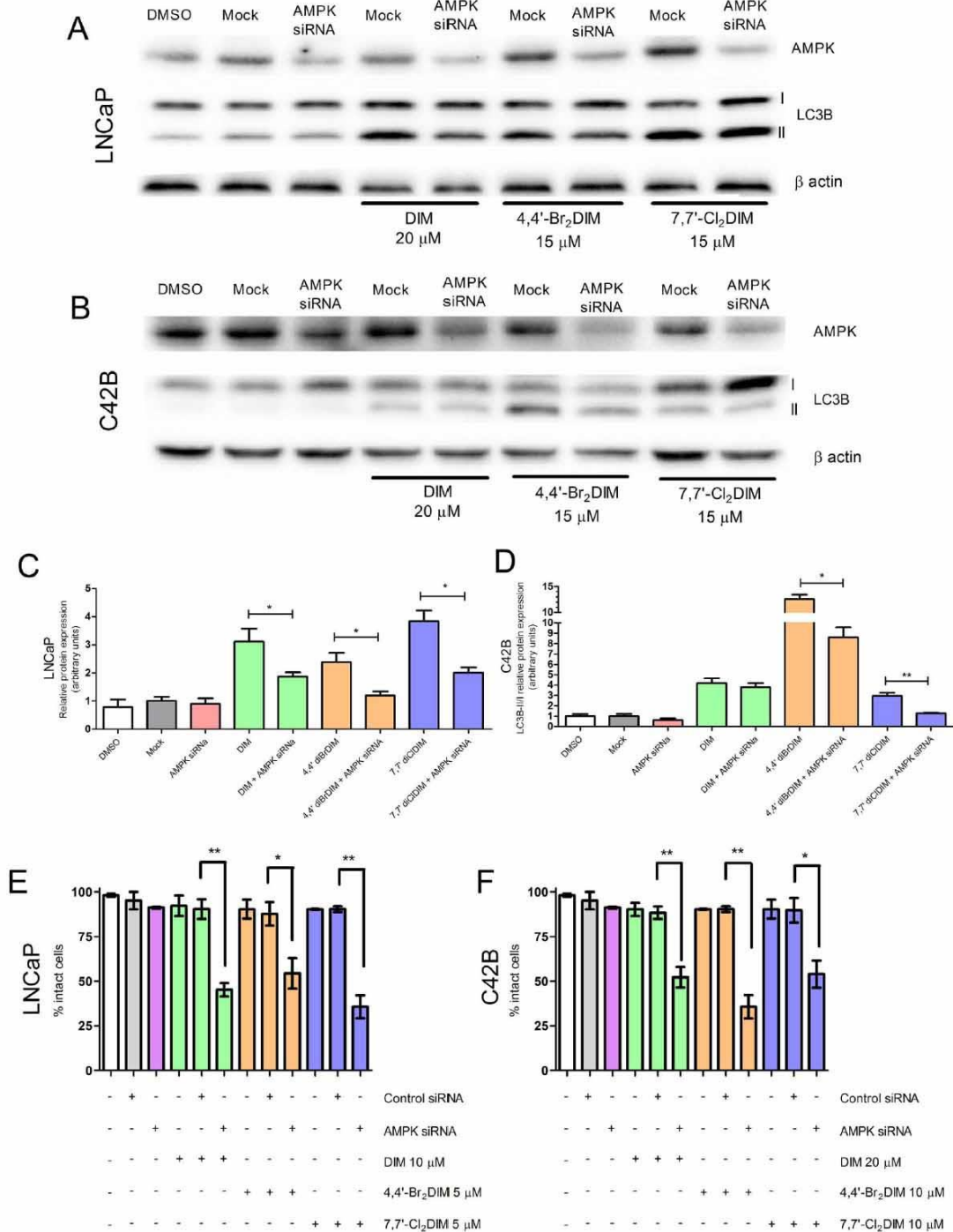


Fig. 3. DIM and ring-DIMs mediated autophagy is dependent on AMPK. Levels of AMPK and LC3B/I/II in LNCaP (A, C) and C42B (B, D) cells exposed to DIM, or ring-DIMs for 24 h with or without a 24-h pretreatment with AMPK siRNA. LNCaP and C42B cells were treated with 20 μ M DIM, 15 μ M 4,4'-Br₂DIM or 15 μ M 7,7'-Cl₂DIM. Each gel is representative of three independent experiments. Percentage of intact LNCaP (E) and C42B (F) cells treated with DIM or ring-DIMs for 24 h with or without a 24-h pretreatment with AMPK siRNA. Results are representative of three independent experiments and shown as mean \pm SEM. Statistically significant difference (* P < 0.05, ** P < 0.01) were determined by one-way ANOVA and a Dunnett posthoc test to correct for multiple comparisons to control.

activity in LNCaP (Fig. 6C, E) and C42B (Fig. 6D, F) cells treated with toxic concentrations of DIM and ring-DIMs. Induction of senescence was also confirmed by investing the effect of AEG-1 siRNA on cell

proliferation of LNCaP and C42B cells treated with DIM. Our results showed a significant inhibition of cell proliferation in LNCaP and C42B cells pretreated with AEG-1 siRNA and then treated with DIM compared

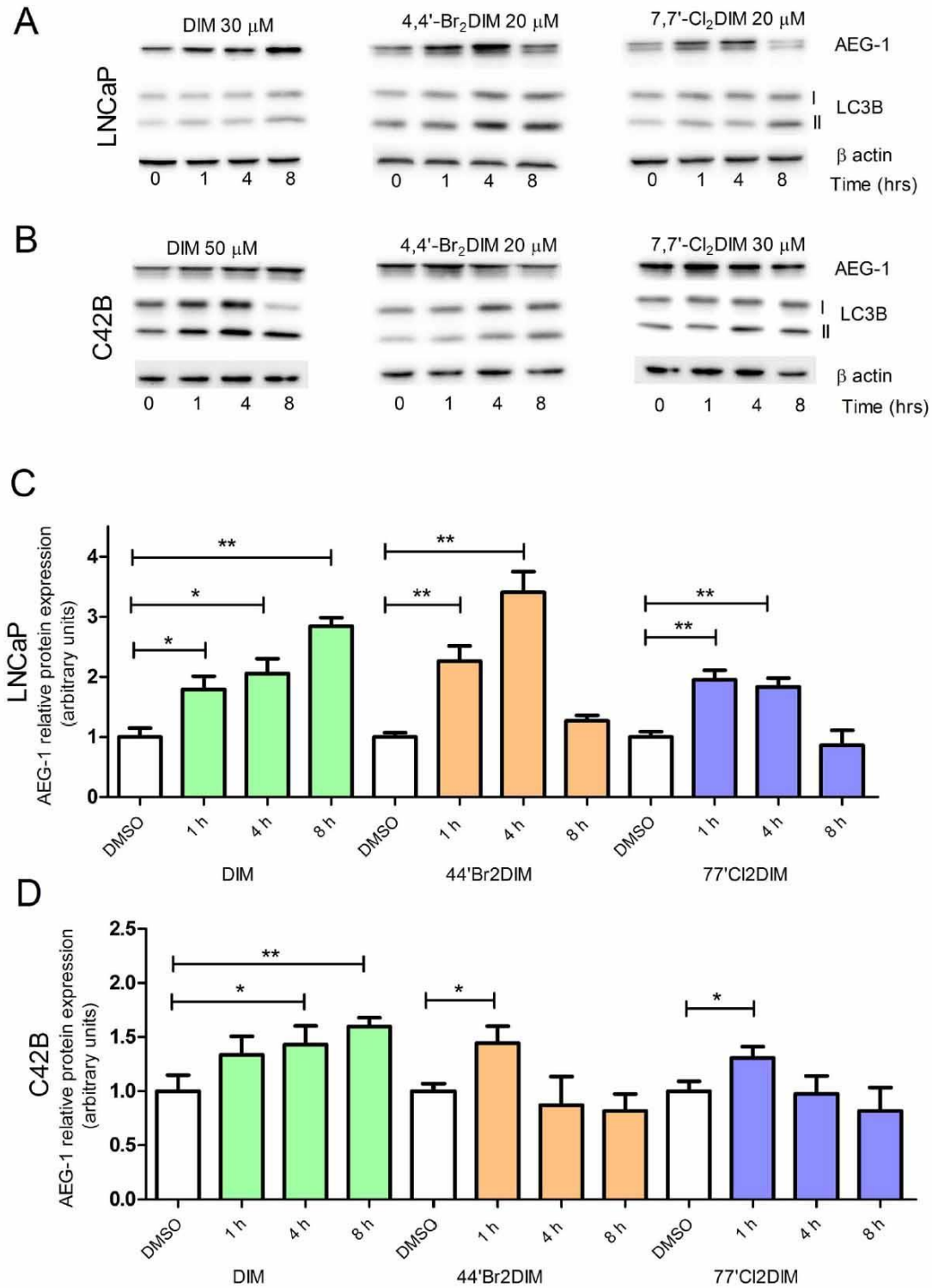


Fig. 4. DIM and ring-DIMs induce AEG-1 in LNCaP and C42B cells. AEG-1 and LC3B I/II levels in LNCaP (A, C) and C42B (B, D) cells treated for 24 h with DIM, 4,4'-Br₂DIM or 7,7'-Cl₂DIM. LNCaP cells were treated with 30 μ M DIM, 20 μ M 4,4'-Br₂DIM or 20 μ M 7,7'-Cl₂DIM, whereas C42B cells were treated with 50 μ M DIM, 20 μ M 4,4'-Br₂DIM or 30 μ M 7,7'-Cl₂DIM. Statistically significant difference (* P < 0.05, ** P < 0.01) were determined by one-way ANOVA and a Dunnett posthoc test to correct for multiple comparisons to control.

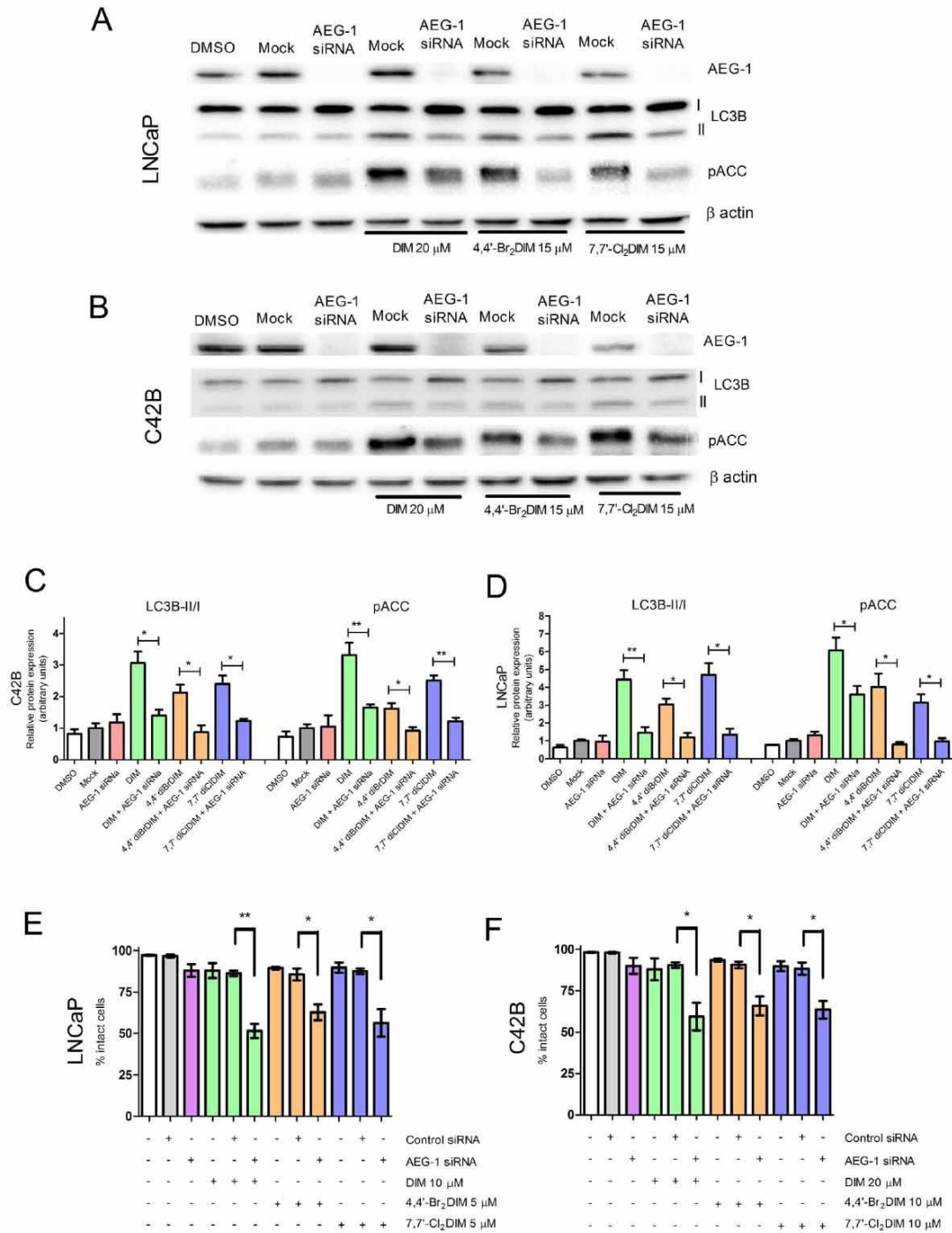


Fig. 5. DIM- and ring-DIM-mediated autophagy is dependent on AEG-1. Levels of AEG-1, phospho-ACC, and LC3B/I/II in LNCaP (A, C) and C42B (B, D) cells exposed to DIM, 4,4'-Br₂DIM or 7,7'-Cl₂DIM for 24 h with or without a 24-h pretreatment with AEG-1 siRNA. LNCaP and C42B cells were treated with 20 μ M DIM, 15 μ M 4,4'-Br₂DIM or 15 μ M 7,7'-Cl₂DIM. Each gel is representative of three independent experiments. Percentage of intact LNCaP (E) and C42B (F) cells after a 24-h exposure to DIM, 4,4'-Br₂DIM or 7,7'-Cl₂DIM with or without a 24-h pretreatment with AEG-1 siRNA. Percentages are presented as means \pm SEM of three independent experiments. Statistically significant difference (* P < 0.05, ** P < 0.01) were determined by one-way ANOVA and a Dunnett posthoc test to correct for multiple comparisons to control.

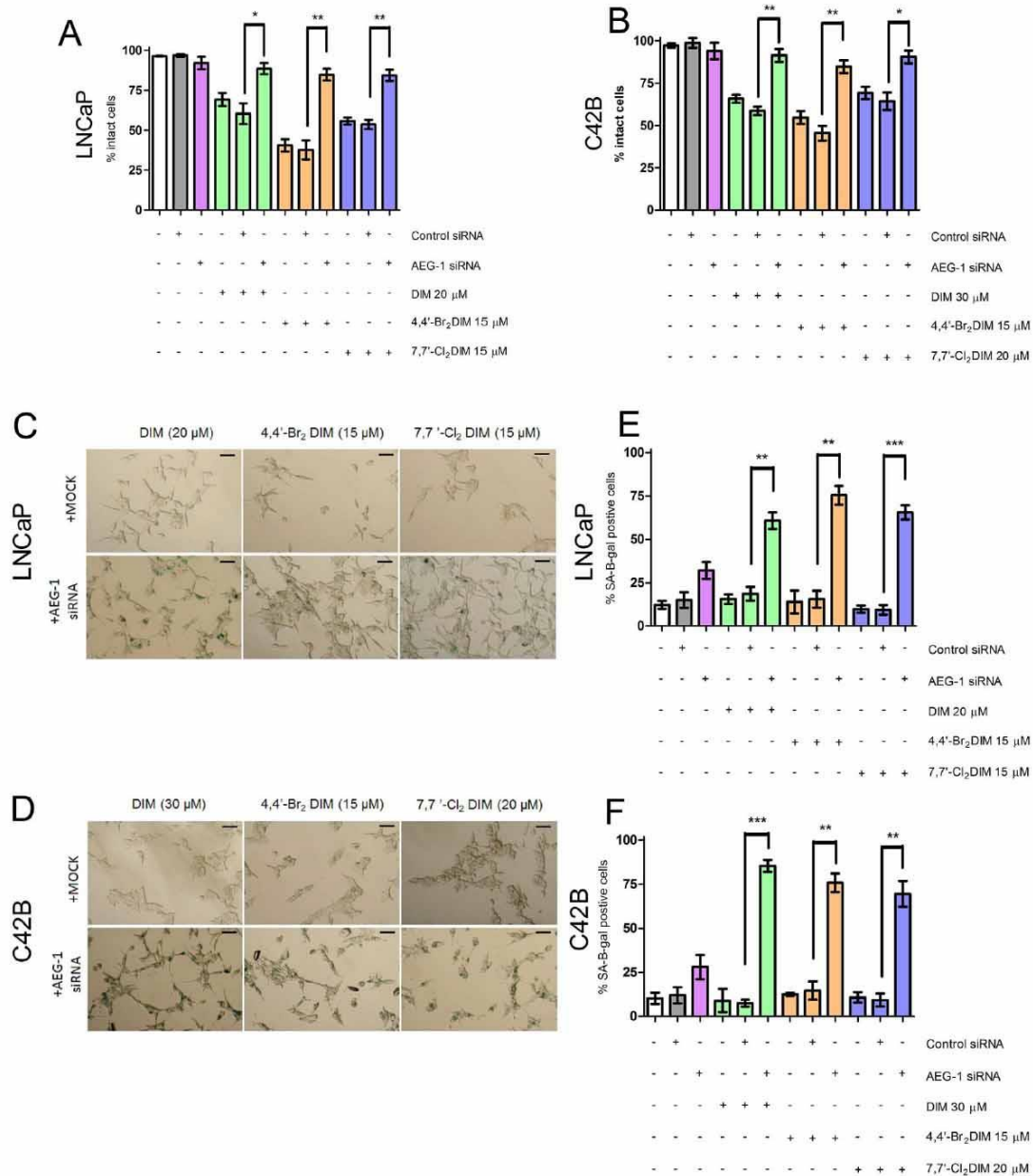


Fig. 6. Percentage of intact LNCaP (A) and C42B (B) cells exposed to DIM, 4,4'-Br₂DIM or 7,7'-Cl₂DIM for 24 h with or without a 24-h pretreatment with AEG-1 siRNA. Senescence in LNCaP (C) and C42B (D) cells after a 24 h exposure to DIM, 4,4'-Br₂DIM and 7,7'-Cl₂DIM with or without a 24 h pretreatment with AEG-1 siRNA. LNCaP cells were treated with 20 μ M DIM, 15 μ M 4,4'-Br₂DIM or 15 μ M 7,7'-Cl₂DIM, whereas C42B cells were treated with 30 μ M DIM, 15 μ M 4,4'-Br₂DIM or 20 μ M 7,7'-Cl₂DIM. Senescence was measured using a senescence β -galactosidase staining kit as described in materials and methods. Images are representative of three independent experiments. Scale bar = 50 μ m. Percentage of β -galactosidase-positive LNCaP (E) and C42B (F) cells treated as described above. Percentages are presented as means \pm SEM of three independent experiments. Statistically significant difference (* P < 0.05, ** P < 0.01, *** P < 0.001) were determined by one-way ANOVA and a Dunnett posthoc test to correct for multiple comparisons to control.

to DMSO control cells (Fig. S1A, B).

4. Discussion

Our current findings demonstrate that DIM and ring-DIMs activate the AMPK signaling in LNCaP and C42B cells by increasing AMPK-, ACC-(a substrate uniquely phosphorylated by AMPK) and ULK1 phosphorylation in a time-dependent manner (Fig. 2). Chen and coworkers previously reported that a formulated DIM (B-DIM), which has

increased bioavailability in vivo, can activate AMPK signaling as early as 3 h after exposure [25]. DIM has also been shown to activate AMPK signaling in ovarian cancer cells, and that this activation was required for induction of autophagy by DIM [26]. In our study, inhibition of AMPK expression using siRNA inhibited DIM- and ring-DIM-mediated conversion of LC3BI-to-LC3BII, indicating that the induction of autophagy by each of these compounds is dependent on AMPK activation (Fig. 3). We found that the autophagy induced by DIM and ring-DIMs is cytoprotective in nature, since inhibition of either AMPK or ULK1

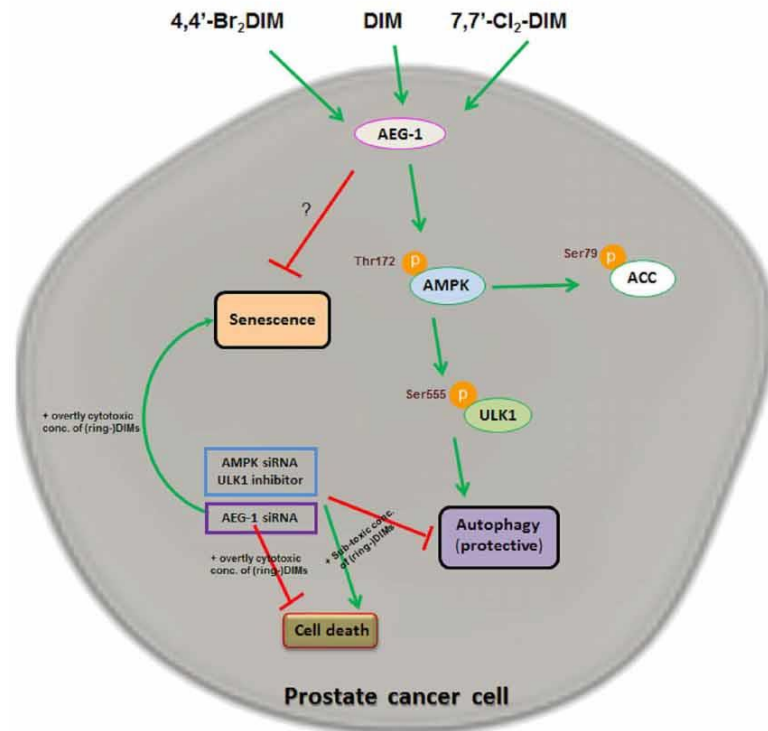


Fig. 7. A schematic representation of the proposed mechanism of DIM-, 4,4'-Br₂DIM- and 7,7'-Cl₂DIM- mediated induction of protective autophagy in human prostate cancer cells.

expression sensitized LNCaP and C42B cells, which underwent significant cell death in the presence of normally sub-toxic concentrations of DIM or ring-DIMs. The results confirm our earlier observations that pre-treatment of prostate cancer cells with the autophagy inhibitors bafilomycin A1 or 3-methyladenine also sensitized the cells to sub-toxic concentrations of DIM and ring-DIMs, suggesting a protective role of the autophagic response to DIM and ring-DIMs [9]. Our previous study showed a concentration-dependent induction of autophagy after a 24-h exposure to DIM or ring-DIMs [9]. Results in Fig. 1 show that formation of autophagic vacuoles in LNCaP and C42B cells are observed after an 8-h exposure to DIM and ring-DIMs. In vivo studies to assess co-treatment of natural compound like DIM with autophagy inhibitors in various (prostate) cancer models would determine the potential to increase anticancer efficacy of such combined therapies.

AEG-1 is overexpressed in various tumors including the prostate [20,27] and contributes to chemoresistance in hepatocellular carcinoma (HCC) cells by increasing the expression of multi-drug resistance 1 (MDR1) gene [22], and knockdown of AEG-1 inhibits chemoresistance in cervical cancer cells [28]. Our present study reveals a novel mechanism of action for DIM- and ring-DIM-induced autophagy in human prostate cancer cells, which occurs via induction of AEG-1. We have shown that DIM and ring-DIMs increase AEG-1 protein levels time-dependently in both LNCaP and C42B cells (Fig. 4) and that the resultant induction of autophagy is dependent on AEG-1 (Fig. 5). Inhibition of AEG-1 using siRNA repressed AMPK activation, indicating that AEG-1 is an upstream regulator of AMPK in prostate cancer cells. In line with our results, AEG-1 has been previously shown to induce protective autophagy via activation of AMPK in response to cellular metabolic stress in immortalized primary human fetal astrocytes (IM-PHFA) and in a human malignant glioma cell line (T98G) [20,21]. In addition, AEG-1 overexpression was found to enhance autophagy in malignant glioma cells undergoing TGFβ1-induced endothelial-mesenchymal transition [27]. Kikuno and coworkers showed that down-regulation of AEG-1 induced apoptosis in LNCaP and PC-3 prostate

cancer cells through upregulation of FOXO3a activity [29]. As another example, the natural product cryptotanshinone (derived from *Salvia miltiorrhiza*) was found to exert antitumor activity via inhibition of AEG-1 in hypoxic AI PC-3 prostate cancer cells [30]. Indeed, our current findings show that AEG-1 silencing sensitizes LNCaP and C42B cells to cell death mediated by sub-toxic concentrations of DIM and ring-DIMs. Thus, the induction of AEG-1 would appear to be a cell protection mechanism against the cellular stress and cytotoxicity caused in response to DIM and ring-DIMs in prostate cancer cells.

DIM targets multiple pathways associated with cancer progression in vitro and in vivo [31–33], and our findings provide further insight into the complexity of the mechanisms of anticancer action of DIM, as well as more potent synthetic DIM derivatives in prostate cancer cells. Charcoal-stripped serum (CSS) was used instead of fetal bovine serum (FBS) to minimize the level of androgens and other hormones to which the cells would be exposed [34]. The CSS culture medium of LNCaP cells was supplemented with 0.1 nM DHT to stimulate their androgen-dependent growth in a defined manner. The AD LNCaP and AI C42B prostate cancer cells had similar patterns of autophagy induction, activation of AMPK and AEG-1 induction, upon treatment with DIM and ring-DIMs indicating a negligible effect of androgen signaling on the observed mechanisms. Interestingly we observed a protective effect after siRNA-mediated downregulation of AEG-1 against overtly cytotoxic concentrations of DIM or ring-DIMs in both LNCaP and C42B cells, which is contrast to our observed sensitization at subtoxic concentrations. Moreover, this protective effect of AEG-1 silencing was accompanied by induction of senescence in LNCaP and C42B cells treated with toxic concentration of DIM or ring-DIMs (Fig. 6). Previous studies have shown that overexpression of AEG-1 inhibits senescence in hepatocytes isolated from transgenic mice by inhibiting the DNA damage response [23]. Senescent cells undergo irreversible proliferative arrest, which may inhibit tumor progression [30,35,36]. Accumulating evidence suggests that therapies directed at inducing senescence may improve cancer treatment outcomes [36–39]. Our study reveals that DIM- and

ring-DIM-mediated induction of senescence and/or apoptosis is dependent on AEG-1, and induction of AEG-1 may be a key molecular switch that regulates the fate of prostate cancer cells either to undergo apoptosis or senescence (Fig. 7). More studies are needed to assess the mechanism(s) of inhibition of senescence by AEG-1 and to determine the potential benefits of agents that induce senescence in treatment prostate cancer.

5. Conclusion

We have identified a novel mechanism of DIM- and ring-DIM-induced protective autophagy, which is due to induction of AEG-1 and subsequent activation of AMPK. Our results suggest that development of novel drug therapies against prostate cancer could include selective autophagy inhibitors as adjuvants. Moreover, targeting DIM- and ring-DIM-mediated induction of AEG-1 and subsequent induction of senescence may be an effective novel therapy for treating prostate cancer.

Supplementary data to this article can be found online at <http://dx.doi.org/10.1016/j.cellsig.2017.09.006>.

Acknowledgments

This work was funded by an operating grant from the Canadian Institutes of Health Research (CIHR grant no. MOP-115019) to JTS, EG and SS. HD received a scholarship from the *Fonds de Recherche du Québec - Santé* (FRQS). All authors declare to have no conflicts of interest.

References

- J. Ferlay, I. Soerjomataram, R. Dikshit, S. Eser, C. Mathers, M. Rebelo, D.M. Parkin, D. Forman, F. Bray, Cancer incidence and mortality worldwide: sources, methods and major patterns in GLOBOCAN 2012, *Int. J. Cancer* 136 (5) (2015) E359–86.
- R.L. Siegel, K.D. Miller, A. Jemal, Cancer statistics, 2016, *CA Cancer J. Clin.* 66 (1) (2016) 7–30.
- D.K. Wysocki, J.P. Freiman, J.B. Tourtelot, M.L. Horton 3rd, Fatal and nonfatal hepatotoxicity associated with flutamide, *Ann. Intern. Med.* 118 (11) (1993) 860–864.
- D.G. McLeod, Tolerability of nonsteroidal antiandrogens in the treatment of advanced prostate cancer, *Oncologist* 2 (1) (1997) 18–27.
- D.G. McLeod, E.D. Crawford, E.P. DeAntoni, Combined androgen blockade: the gold standard for metastatic prostate cancer, *Eur. Urol.* 32 (Suppl. 3) (1997) 70–77.
- L.F. Bjeldanes, J.Y. Kim, K.R. Grose, J.C. Bartholomew, C.A. Bradfield, Aromatic hydrocarbon responsiveness-receptor agonists generated from indole-3-carbinol in vitro and in vivo: comparisons with 2,3,7,8-tetrachlorodibenzo-p-dioxin, *Proc. Natl. Acad. Sci. U. S. A.* 88 (21) (1991) 9543–9547.
- K. Abdelbaqi, N. Lack, E.T. Guns, L. Kotha, S. Safe, J.T. Sanderson, Antiandrogenic and growth inhibitory effects of ring-substituted analogs of 3,3'-diindolylmethane (ring-DIMs) in hormone-responsive LNCaP human prostate cancer cells, *Prostate* 71 (13) (2011) 1401–1412.
- A.A. Goldberg, V.I. Titorenko, A. Beach, K. Abdelbaqi, S. Safe, J.T. Sanderson, Ring-substituted analogs of 3,3'-diindolylmethane (DIM) induce apoptosis and necrosis in androgen-dependent and -independent prostate cancer cells, *Investig. New Drugs* 32 (1) (2014) 25–36.
- A.A. Goldberg, H. Draz, D. Montes-Grajales, J. Olivero-Verbel, S.H. Safe, J.T. Sanderson, 3,3'-Diindolylmethane (DIM) and its ring-substituted halogenated analogs (ring-DIMs) induce differential mechanisms of survival and death in androgen-dependent and -independent prostate cancer cells, *Genes Cancer* 6 (5–6) (2015) 265–280.
- C.W. Wang, D.J. Klionsky, The molecular mechanism of autophagy, *Mol. Med.* 9 (3–4) (2003) 65–76.
- D. Glöck, S. Barth, K.F. Macleod, Autophagy: cellular and molecular mechanisms, *J. Pathol.* 221 (1) (2010) 3–12.
- E. White, The role for autophagy in cancer, *J. Clin. Invest.* 125 (1) (2015) 42–46.
- S.Y. Yang, M.C. Winslet, Dual role of autophagy in colon cancer cell survival, *Ann. Surg. Oncol.* 18 (Suppl. 3) (2011) S239.
- C.B. Blackadar, Historical review of the causes of cancer, *World J Clin Oncol.* 7 (1) (2016) 54–86.
- N. Mizushima, T. Yoshimori, Y. Ohsumi, The role of Atg proteins in autophagosome formation, *Annu. Rev. Cell Dev. Biol.* 27 (2011) 107–132.
- T.E. Hansen, T. Johansen, Following autophagy step by step, *BMC Biol.* 9 (2011) 39.
- J. Kim, M. Kundu, B. Viollet, K.L. Guan, AMPK and mTOR regulate autophagy through direct phosphorylation of Ulk1, *Nat. Cell Biol.* 13 (2) (2011) 132–141.
- G. Hu, Y. Wei, Y. Kang, The multifaceted role of MTDH/AEG-1 in cancer progression, *Clin. Cancer Res.* 15 (18) (2009) 5615–5620.
- X. Shi, X. Wang, The role of MTDH/AEG-1 in the progression of cancer, *Int. J. Clin. Exp. Med.* 8 (4) (2015) 4795–4807.
- S.K. Bhutia, T.P. Kegelman, S.K. Das, B. Azab, Z.Z. Su, S.G. Lee, D. Sarkar, P.B. Fisher, Astrocyte elevated gene-1 induces protective autophagy, *Proc. Natl. Acad. Sci. U. S. A.* 107 (51) (2010) 22243–22248.
- S.K. Bhutia, T.P. Kegelman, S.K. Das, B. Azab, Z.Z. Su, S.G. Lee, D. Sarkar, P.B. Fisher, Astrocyte elevated gene-1 activates AMPK in response to cellular metabolic stress and promotes protective autophagy, *Autophagy* 7 (5) (2011) 547–548.
- B.K. Yoo, D. Chen, Z.Z. Su, R. Gredler, J. Yoo, K. Shah, P.B. Fisher, D. Sarkar, Molecular mechanism of chemoresistance by astrocyte elevated gene-1, *Cancer Res.* 70 (8) (2010) 3249–3258.
- J. Srivastava, A. Siddiq, L. Emdad, P.K. Santhekadur, D. Chen, R. Gredler, X.N. Shen, C.L. Robertson, C.I. Dumur, P.B. Hylemon, N.D. Mukhopadhyay, D. Bhore, K. Shah, R. Ahmad, S. Ghashuddin, J. Stafflinger, M.A. Subler, J.J. Windle, P.B. Fisher, D. Sarkar, Astrocyte elevated gene-1 promotes hepatocarcinogenesis: novel insights from a mouse model, *Hepatology* 56 (5) (2012) 1782–1791.
- Y. Gong, H. Sohn, L. Xue, G.L. Firestone, L.F. Bjeldanes, 3,3'-Diindolylmethane is a novel mitochondrial H(+)-ATP synthase inhibitor that can induce p21(Cip1/Waf1) expression by induction of oxidative stress in human breast cancer cells, *Cancer Res.* 66 (9) (2006) 4880–4887.
- D. Chen, S. Banerjee, Q.C. Cui, D. Kong, F.H. Sarkar, Q.P. Dou, Activation of AMP-activated protein kinase by 3,3'-diindolylmethane (DIM) is associated with human prostate cancer cell death in vitro and in vivo, *PLoS One* 7 (10) (2012) e47186.
- P.K. Kandala, S.K. Srivastava, Regulation of macroautophagy in ovarian cancer cells in vitro and in vivo by controlling glucose regulatory protein 78 and AMPK, *Oncotarget* 3 (4) (2012) 435–449.
- M. Zou, W. Zhu, L. Wang, L. Shi, R. Gao, Y. Ou, X. Chen, Z. Wang, A. Jiang, K. Liu, M. Xiao, P. Ni, D. Wu, W. He, G. Sun, P. Li, S. Zhai, X. Wang, G. Hu, AEG-1/MTDH-activated autophagy enhances human malignant glioma susceptibility to TGF-beta1-triggered epithelial-mesenchymal transition, *Oncotarget* 7 (11) (2016) 13122–13138.
- X. Liu, D. Wang, H. Liu, Y. Feng, T. Zhu, L. Zhang, B. Zhu, Y. Zhang, Knockdown of astrocyte elevated gene-1 (AEG-1) in cervical cancer cells decreases their invasiveness, epithelial to mesenchymal transition, and chemoresistance, *Cell Cycle* 13 (11) (2014) 1702–1707.
- N. Kikuno, H. Shiina, S. Urakami, K. Kawamoto, H. Hirata, Y. Tanaka, R.F. Place, D. Pookot, S. Majid, M. Igawa, R. Dahiya, Knockdown of astrocyte-elevated gene-1 inhibits prostate cancer progression through upregulation of FOXO3a activity, *Oncogene* 26 (55) (2007) 7647–7655.
- H.J. Lee, D.B. Jung, E.J. Sohn, H.H. Kim, M.N. Park, J.H. Lew, S.G. Lee, B. Kim, S.H. Kim, Inhibition of hypoxia inducible factor alpha and astrocyte-elevated gene-1 mediates cryptotanshinone exerted antitumor activity in hypoxic PC-3 cells, *Evidence-based Complementary and Alternative Medicine: eCAM* 2012 (2012) 390957.
- X. Ge, S. Yannai, G. Rennert, N. Gruener, F.A. Fares, 3,3'-Diindolylmethane induces apoptosis in human cancer cells, *Biochem. Biophys. Res. Commun.* 228 (1) (1996) 153–158.
- M. Nachshon-Kedmi, F.A. Fares, S. Yannai, Therapeutic activity of 3,3'-diindolylmethane on prostate cancer in an in vivo model, *Prostate* 61 (2) (2004) 153–160.
- M. Nachshon-Kedmi, S. Yannai, F.A. Fares, Induction of apoptosis in human prostate cancer cell line, PC3, by 3,3'-diindolylmethane through the mitochondrial pathway, *Br. J. Cancer* 91 (7) (2004) 1358–1363.
- J.P. Sedelaar, J.T. Isaacs, Tissue culture media supplemented with 10% fetal calf serum contains a castrate level of testosterone, *Prostate* 69 (16) (2009) 1724–1729.
- G.P. Dimri, What has senescence got to do with cancer? *Cancer Cell* 7 (6) (2005) 505–512.
- M. Lee, J.S. Lee, Exploiting tumor cell senescence in anticancer therapy, *BMB Rep.* 47 (2) (2014) 51–59.
- J.A. Ewald, J.A. Desotelle, G. Wilding, D.F. Jarrard, Therapy-induced senescence in cancer, *J. Natl. Cancer Inst.* 102 (20) (2010) 1536–1546.
- A. Gbadulinova, M. Pastorek, P. Filipcik, P. Radvak, L. Casaderova, B. Vojtesek, S. Pastorekova, Cancer-associated S100P protein binds and inactivates p53, permits therapy-induced senescence and supports chemoresistance, *Oncotarget* 7 (16) (2016) 22508–22522.
- J. Tato-Costa, S. Casimiro, T. Pacheco, R. Pires, A. Fernandes, I. Alho, P. Pereira, P. Costa, H.B. Castelo, J. Ferreira, L. Costa, Therapy-induced cellular senescence induces epithelial-to-mesenchymal transition and increases invasiveness in rectal cancer, *Clin. Colorectal Cancer* 15 (2) (2016) (170-178 e3).

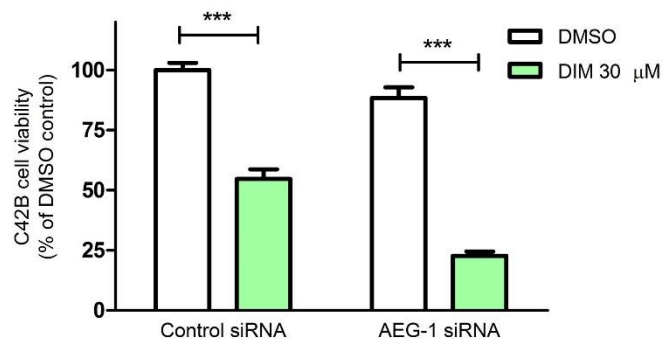
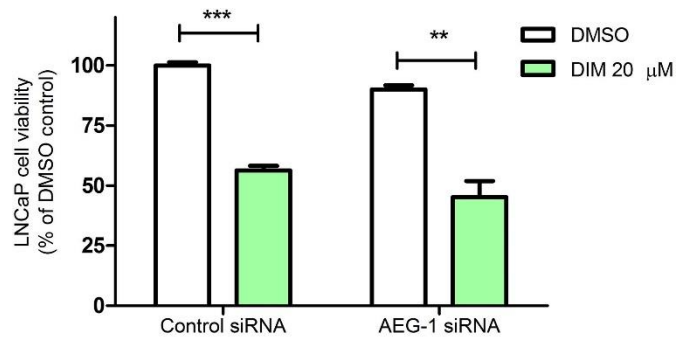


Fig. S1. Cell proliferation of LNCaP (A) and C42B (B) cells exposed to DIM with or without a 24-h pretreatment with AEG-1 siRNA.

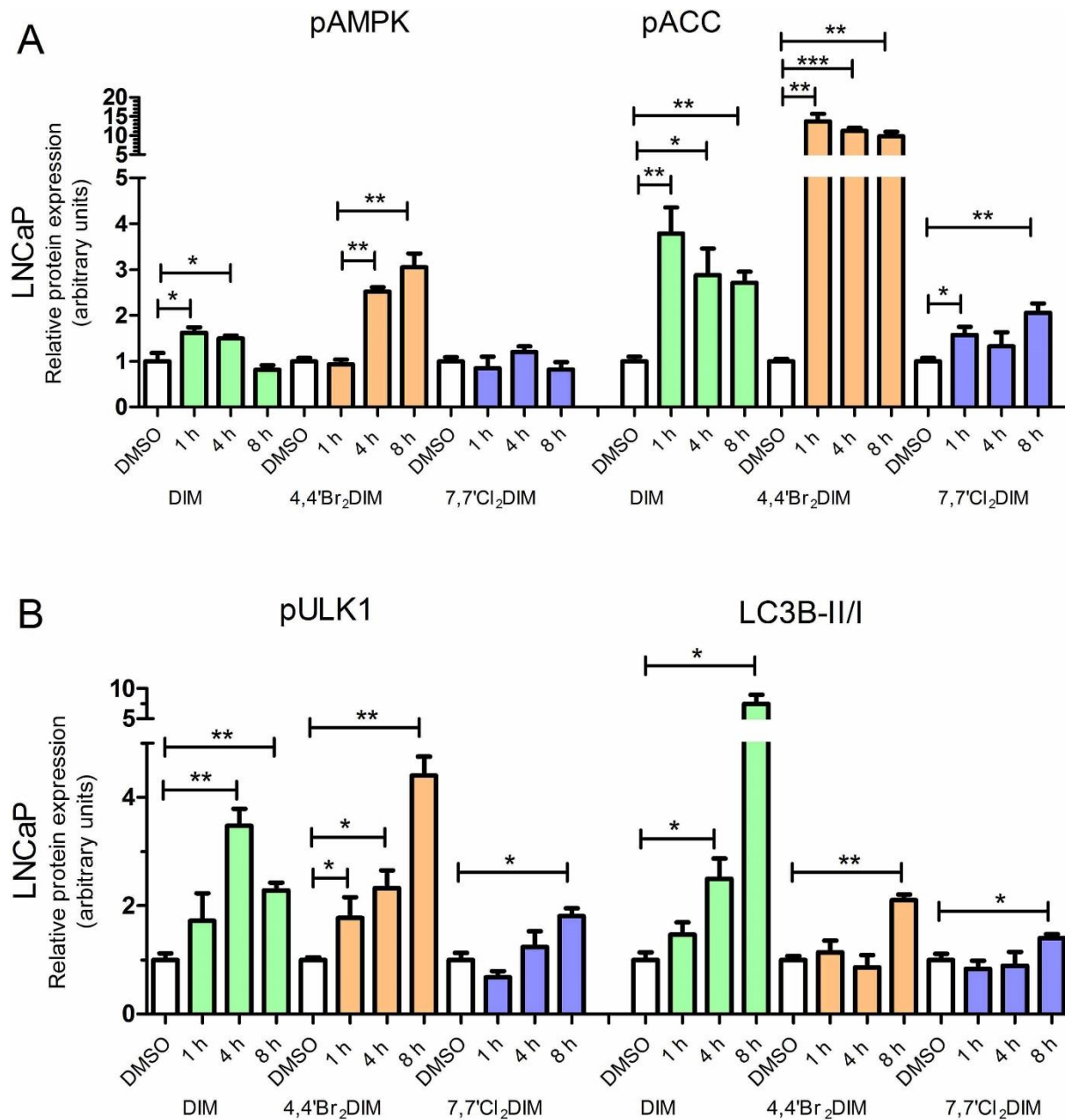


Fig. S2. Protein levels of pAMPK, pACC, ULK1, LC3BI and LC3BII (expressed as LC3BII/I ratio) in LNCaP cells after a 0, 1, 4, 8 h of exposure to DIM, 4,4'-Br₂DIM or 7,7'-Cl₂DIM. Quantification of protein bands densitometry was carried out using ImageJ 1.6 software (Wayne Rasband, NIH).

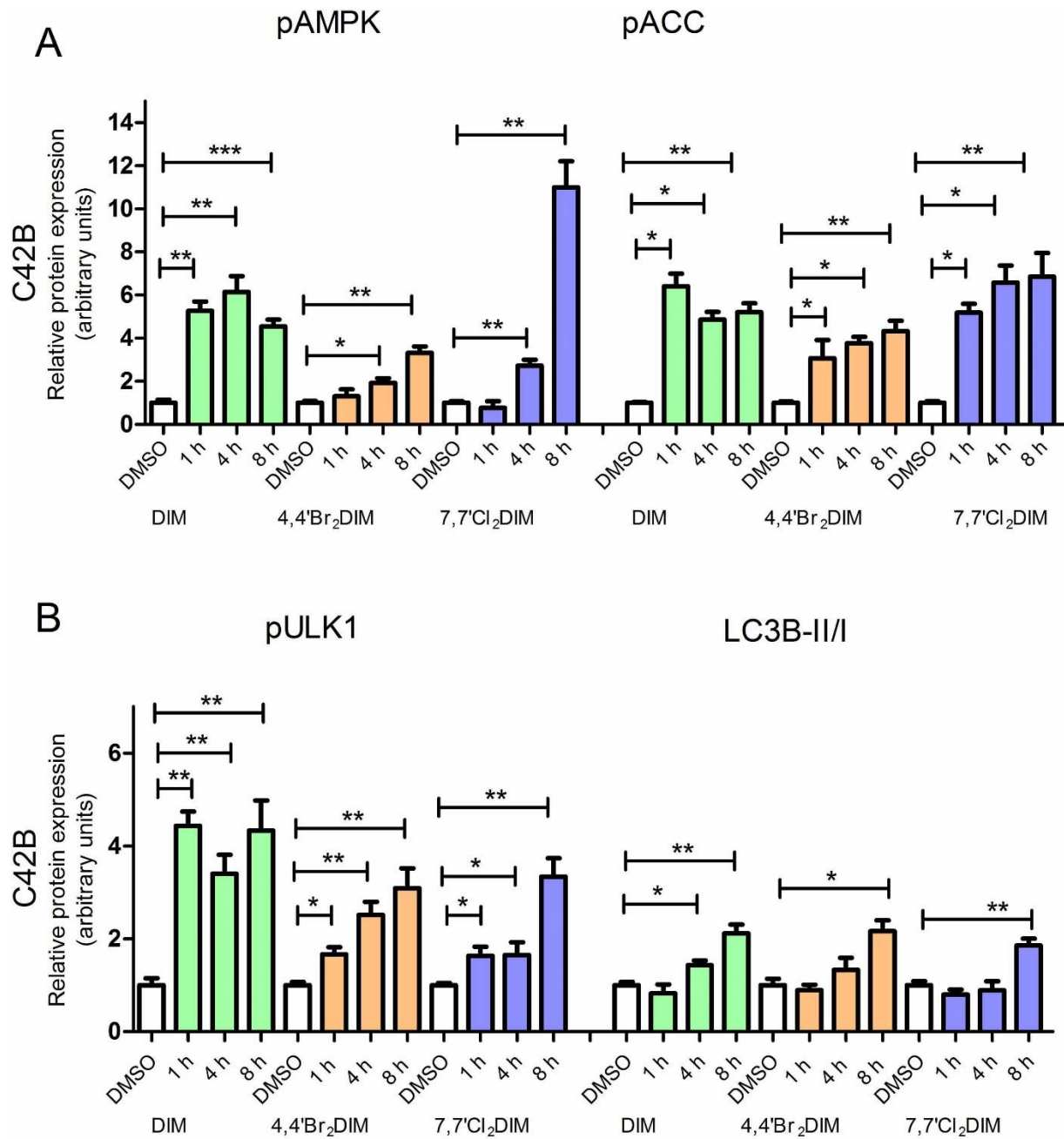


Fig. S3. Protein levels of pAMPK, pACC, ULK1 LC3BI and LC3BII (expressed as LC3BII/I ratio) in C42B cells after 0, 1, 4, 8 h of exposure to DIM, 4,4'-Br₂DIM or 7,7'-Cl₂DIM. Quantification of protein bands densitometry was carried out using ImageJ 1.6 software (Wayne Rasband, NIH)

2.3 Autophagy inhibition improves the chemotherapeutic efficacy of cruciferous vegetable-derived diindolymethane in a murine prostate cancer xenograft model

Hossam Draz^{1,2}, Alexander A. Goldberg¹, Emma S. Tomlinson Guns³, Ladan Fazli³, Stephen Safe⁴ and J. Thomas Sanderson^{1,*}

¹ *INRS-Institut Armand-Frappier, Laval, QC, Canada.*

² *Department of Biochemistry, National Research Centre, Dokki, Cairo, Egypt.*

³ *Vancouver Prostate Centre, University of British Columbia, Vancouver, BC, Canada.*

⁴ *Veterinary Physiology and Pharmacology, Texas A&M University, College Station, TX, United States.*

This article was published in *Invest New Drugs*. 2018; 36(4):718-725. doi: 10.1007/s10637-018-0595-8.

Author contributions:

Hossam Draz designed and performed the experiments, statistical analyses and wrote the manuscript.

Dr. Alexander Goldberg participated in performing the experiment to assess the effect of autophagy inhibition on DIM cytotoxicity in prostate cancer cells *in vitro* (Figure 1) and revised the manuscript.

Prof. Emma Guns coordinated and supervised the tissue microarray (TMA) analyses, which were conducted by Dr. Ladan Fazli at the Vancouver Prostate Centre.

Prof. Stephen Safe provided us with ring-DIMs synthesised in his laboratory at Texas A&M University.

Prof. Thomas Sanderson obtained the research funding, supervised the project and participated in writing and revising the manuscript.

Summary

Prostate cancer is the second leading cause of cancer-related deaths in men in North America and there is an urgent need for development of more effective therapeutic treatments against this disease. We have recently shown that diindolylmethane (DIM) and several of its halogenated derivatives (ring-DIMs) induce death and protective autophagy in human prostate cancer cells. However, the *in vivo* efficacy of ring-DIMs and the use of autophagy inhibitors as adjuvant therapy have not yet been studied *in vivo*. The objective of this study was to determine these effects on tumor growth in nude CD-1 mice bearing bioluminescent androgen-independent PC-3 human prostate cancer cells. We found that chloroquine (CQ) significantly sensitized PC-3 cells to death in the presence of sub-toxic concentrations of DIM or 4,4'-Br₂DIM *in vitro*. Moreover, a combination of DIM (10 mg/kg) and CQ (60 mg/kg), 3 x per week, significantly decreased PC-3 tumor growth *in vivo* after 3 and 4 weeks of treatment. Furthermore, 4,4'-Br₂DIM at 10 mg/kg (3 x per week) significantly inhibited tumour growth after 4 weeks of treatment. Tissues microarray analysis showed that DIM alone or combined with CQ induced apoptosis marker TUNEL; the combination also significantly inhibited the cell proliferation marker Ki67. In conclusion, we have confirmed that DIM and 4,4'-Br₂DIM are effective agents against prostate cancer *in vivo* and shown that inhibition of autophagy with CQ enhances the anticancer efficacy of DIM. Our results suggest that including selective autophagy inhibitors as adjuvants may improve the efficacy of existing and novel drug therapies against prostate cancer.

Key words Prostate cancer, PC-3, CD-1 nude mice, autophagy, diindolylmethane, ring-DIMs.

Introduction

Prostate cancer is the most common malignancy in males and the second most frequent cause of cancer-related death in North America (Siegel et al. 2016). Therefore, there is an urgent need to explore novel targets and therapies in the fight against prostate cancer. Epidemiological studies support the notion that dietary intake of cruciferous vegetables such as broccoli may reduce the risk of cancer including that of the prostate (Kim and Park 2009a). One of the active ingredients in cruciferous vegetable is indole-3-carbinol (I3C), which upon digestion is converted to 3,3'-diindolylmethane (DIM) by the action of gastric acid (De Kruif et al. 1991a).

DIM has pluripotent anticancer properties. Previous studies have indicated that DIM blocks multiple pro-oncogenic molecular pathways in tumors derived from multiple organs and tissues (Fares et al. 2010; Banerjee et al. 2011) and DIM also inhibits growth of various cancer cells *in vitro* (Le et al. 2003; Goldberg et al. 2014; Zhang et al. 2017). Growing evidence supports the efficacy of DIM as a chemopreventive and chemotherapeutic agent against prostate cancer *in vivo* (Cho et al. 2011; Singh-Gupta et al. 2012; Wu et al. 2013a). DIM inhibits prostate cancer growth in TRAMP mice through inhibition of cyclin-dependent kinases and induction of p27 (cyclin-dependent kinase inhibitor 1B) and Bax (Bcl-2-associated X protein) expression (Cho et al. 2011). A formulated form of DIM with greater bioavailability (B-DIM) blocked critical survival signaling pathways and enhanced the efficacy of radiation treatment in a murine prostate cancer xenograft model (Singh-Gupta et al. 2012). Another study in TRAMP mice showed that DIM induced apoptosis and inhibited cell proliferation in the prostate (Wu et al. 2013a).

Uncontrolled proliferation of cancer cells is due to the inhibition of cell death pathways such as apoptosis and stimulation of cell survival pathways such as ER stress or autophagy (Yang and Winslet 2011; White 2015; Blackadar 2016). Several reports show that dysregulation of autophagy signaling in cancer cells may have a critical influence on either tumor progression or regression (Chen et al. 2010; Yang and Winslet 2011; Lorin et al. 2013; White 2015; Zhou et al. 2016; Levy et al. 2017).

Our previous studies have shown that DIM and several halogenated derivatives (ring-DIMs) induce cell death, mitochondrial dysfunction, ER stress and protective autophagy in prostate cancer cells *in vitro* (Goldberg et al. 2014; Goldberg et al. 2015). We also found that chemical inhibition of autophagy sensitizes prostate cancer cells to DIM- and ring-DIM-induced death (Goldberg et al. 2015; Draz et al. 2017). However, the *in vivo* effects of ring-DIMs (among which 4,4'-Br₂DIM appeared to be the most potent *in vitro* inhibitor of prostate cancer cell growth) and the use of autophagy inhibitors as adjuvant therapy with DIM on prostate tumor growth have not yet been studied. Therefore, the objective of this study was to determine the anticancer efficacy of 4,4'-Br₂DIM as well as the effect of autophagy inhibition by chloroquine (CQ) on the anticancer efficacy of DIM in a murine xenograft model of human prostate cancer.

Materials and methods

Cell culture and treatment

PC-3 human prostate cancer cells were purchased from the American type culture collection (Manassas, VA). Bioluminescent PC-3M-luc-C6 cells were purchased from Caliper-Life Sciences (Hopkinton, MA). PC-3 and PC-3M-luc-C6 cells were cultured in a 1:1 mixture of DMEM and Ham's F12 nutrient mixture supplemented with 10 % fetal bovine serum (FBS), 1% penicillin/streptomycin (Life Technologies, Gaithersburg, MD) at 37°C in an atmosphere containing 5% CO₂. 4,4'-Br₂DIM was synthesized at Texas A&M University with a purity > 95%.

For treatments, PC-3 cells were seeded in 24-well CellBind culture plates (Corning Inc., Corning, NY) at a density of 1.5 x 10⁵ cells/well in DMEM and Ham's F12 nutrient mixture supplemented with 10 % FBS. Cells were then treated with either DIM, 4,4'-Br₂DIM, or DMSO vehicle control (0.1% or 0.2% in the case of co-exposures). CQ (Sigma-Aldrich, St-Louis, MO) was added to cell cultures 4 h prior to treatment with the DIM compounds.

Cell death assay

After a 24-h exposure of PC-3 cells to either DIM or 4,4'-Br₂DIM, Hoechst 33342 (Sigma-Aldrich) and propidium iodide (PI; Invitrogen, Carlsbad, CA) stains were both added to each well at a concentration of 1 µg/ml for 15 min at 37°C to detect apoptotic and necrotic (or late-apoptotic) cell death, respectively. Hoechst- and PI-positive cells were counted under a Nikon Eclipse (TE-2000U) inverted fluorescence microscope at 20x magnification using filter cubes with excitation

wavelengths of 330-380 and 532-587 nm, respectively. Intact (viable) cells were counted as exhibiting neither Hoechst- (chromatin condensation/fragmentation) nor PI (cell membrane disintegration) staining.

Nude mice, treatment and imaging

CD-1 male nude mice (Charles River laboratories, Montreal, QC) were housed in a 12-h light/dark cycle at 21°C. The experimental procedures were performed according to the guidelines of our animal care facility (Centre National de Biologie Expérimentale, CNBE) and approved by the CNBE Ethics Committee. Mice (7 weeks old) were injected subcutaneously into the dorsal flank with 1×10^6 PC-3M-luc-C6 cells suspended in 1:1 PBS/matrigel (Corning Inc.). Tumor growth was monitored weekly by *in vivo* bioluminescent imaging for 5 weeks. Mice were injected intraperitoneally with 150 mg/kg D-luciferin (Caliper-Life Sciences) followed 15 min later by scanning for 20 second under isoflurane anesthesia in an IVIS 100 imager (Caliper-Life Sciences). Mice were divided into seven groups based on treatment (6-8 mice per group). Seven days after injection of PC-3M-luc-C6 cells tumors were established (visibly present) and treatments were initiated (experimental week 1). Treatments were given three times a week for 4 weeks. DIM (10 mg/kg) and 4,4'-Br₂DIM (1 and 10 mg/kg) were dissolved in corn oil (Sigma-Aldrich) and administrated orally using disposable animal feeding needles (Sigma), CQ was injected intraperitoneally (60 mg/kg). For mice treated with the DIM and CQ combination, CQ was administered 30 min after DIM. Vehicle control (corn oil) was administrated orally. After 4 weeks of treatment (experimental week 5), tumor tissues were excised from the mice and fixed overnight in 10% neutral buffered formalin.

Tumor tissue processing

Tissues were subsequently processed manually as follows: rinsing with PBS for 1 h followed by 2 changes of 70% alcohol for 2 h each, then with 80% alcohol for 1 h, twice with 95% alcohol for 1 h each, 2 changes of absolute alcohol for 1 h each, 2 changes of xylene for 1 h each and finally 2 changes of paraffin wax for 1 h each. Tissues were embedded in paraffin blocks using disposable base molds and embedding rings (ThermoFisher, Waltham, MA).

Tissue microarrays (TMA)

Hemotoxylin- and eosin-stained tissue sections were prepared from each block. The slides were reviewed by a pathologist (The Prostate Centre, Vancouver, BC) blinded to the treatment

groups of study to mark the viable area of each tumor. A TMA was created by taking multiple 1 mm cores from matching marked areas of each paraffin block using a semi-automated tissue microarrayer (TMArrayer, Pathology Devices, Westminster, MD) with Leica M50 stereo microscope (Leica Microsystems, Concord, ON, Canada). Immunohistochemical staining was conducted by a Discover XT autostainer (Ventana Medical System, Tuscan, AZ) using an enzyme-labeled biotin streptavidin system and solvent resistant DAB Map kit for the following antibodies: Ki-67 (ThermoFisher), caspase 3 (Cell Signaling, Danvers, MA), TUNEL (Roche, Basel, Switzerland), LC3B (Abcam, Toronto, ON), p62/SQSTM1 (Cell Signaling) .

All stained slides were imaged digitally using a SL801 autoloader and SCN400 scanning system (Leica Microsystems) at a magnification equivalent to 40 x. The images were subsequently stored in the SlidePath digital imaging hub (Leica Microsystems) of the Vancouver Prostate Centre. Entire-slides were scored using the Aperio positive pixel count algorithm (Leica Microsystems).

Statistical analyses.

Data are presented as mean \pm SEM. Statistically significant differences ($p < 0.05$) among treatment groups were determined using one-way analysis of variance (ANOVA) followed by Dunnett's posthoc test for multiple comparisons to control. All data were analyzed using GraphPad Prism (version 5.01, GraphPad Software, San Diego, CA).

Results

Autophagy inhibition enhances the cytotoxicity of DIM and 4,4'-Br₂DIM in PC-3 prostate cancer cells

We assessed whether pretreatment of PC-3 cells with the autophagy inhibitor CQ (40 μ M) affected the cytotoxicity of DIM or 4,4'-Br₂DIM and found that CQ significantly sensitized PC-3 cells to death in the presence of sub-toxic concentrations of DIM (10 μ M) or 4,4'-Br₂DIM (5 μ M) (Figure 1).

A combination of DIM and autophagy inhibitor CQ synergistically inhibits PC-3 tumor growth in nude CD-1 mice

The effects of DIM alone or in combination with CQ were evaluated *in vivo* in nude mice bearing PC-3 tumors. We found that treatment with either DIM or CQ alone significantly inhibited

tumor growth on experimental week 5 (after 4 weeks of treatment) compared to control mice. Interestingly, a combined treatment with DIM and CQ resulted in a more pronounced reduction of tumor growth after 3 and 4 weeks of treatment with tumor sizes being smaller than their established size on week 1 when treatment was initiated (Figure 2A, B).

4,4'-Br₂DIM inhibits PC-3 tumor growth in nude CD-1 mice

We further explored the effects of 4,4'-Br₂DIM, the ring-DIM that was more potent than DIM or other dihalo-DIMs in our previous *in vitro* studies (Goldberg et al. 2014; Goldberg et al. 2015), on PC-3 tumor growth in our xenograft model. 4,4'-Br₂DIM (10 mg/kg, 3 x per week) significantly inhibited tumour growth after 4 weeks of treatment whereas at a dose of 1 mg/kg (3 x per week) it had no effect (Figure 3A, B).

Tissue microarrays

To investigate the mechanism of DIM- and 4,4'-Br₂DIM-mediated inhibition of prostate cancer growth, we determined their effects on several protein markers of cell proliferation, apoptosis, necrosis and autophagy using TMA analysis. DIM and a combination of DIM and CQ significantly induced DNA fragmentation as determined by TUNEL assay in PC-3 tumors excised from nude CD-1 mice (Figure 4H and 5A). The combined treatment also significantly inhibited expression of Ki67 (Figure 4 D and 5 A). The combination of DIM with CQ also tended to increase necrosis and caspase-3 levels but these incremental changes were not statistically significant (Figure 5 A). Autophagy markers LC3-B and P62 were not statistically different for any of the treatments groups relative to vehicle control (Figure 5A). Although 4,4'-Br₂DIM dose-dependently induced necrosis, its variable response did not result in a statistically significant difference from control (Figure 5B).

Discussion

In this study, we have demonstrated for the first time that autophagy inhibition enhances the anticancer activity of DIM on prostate tumor growth in CD-1 mice bearing subcutaneous PC-3 tumors. A combination of the autophagy inhibitor CQ and DIM significantly reduced tumor growth further than DIM alone, resulting in tumor sizes at week 4 and 5 (after 3 and 4 weeks of treatment) that were even smaller than those initially established 1 week after injection of the tumor cells (Figure 2). *In vitro*, we have shown that CQ significantly sensitizes PC-3 cells to DIM and

4,4'-Br₂DIM-induced death in presence of sub-toxic concentration of these compounds (Figure 1). These results are consistent with our previous *in vitro* findings that pretreatment of LNCaP and C4-2B human prostate cancer cells with the autophagy inhibitors bafilomycin A1 or 3-methyladenine sensitized both cell lines to sub-toxic concentrations of DIM and several ring-DIMs, including 4,4'-Br₂DIM, suggesting a protective role of autophagy in response to DIM and the ring-DIMs (Goldberg et al. 2015). We have shown that treatment with DIM reduces prostate tumor growth compared to vehicle control in mice carrying PC-3 cell tumors, which is consistent with previous studies showing that DIM significantly inhibited prostate tumor growth in a TRAMP-C mouse model (Nachshon-Kedmi et al. 2004a; Cho et al. 2011; Wu et al. 2013a), and in SCID mice carrying C4-2B cell tumors (Chen et al. 2012).

Autophagy, as a cellular catabolic degradation mechanism in response to metabolic stress (Parzych and Klionsky 2014; Levy et al. 2017), has been extensively studied for its role as a survival mechanism in various cancers *in vivo* and *in vitro* (Chen and Karantza-Wadsworth 2009; Muilenburg et al. 2014; Zheng et al. 2015; Zhou et al. 2016). Treatment of advanced prostate cancer with current approaches, such as androgen ablation therapy, is usually accompanied by resistance to the treatment, which often results in a fatal outcome (Chen et al. 2008). Hence, there is an urgent need to develop new strategies for treatment of prostate cancer and autophagy inhibition as an adjuvant therapy has been suggested as one alternative approach to improving treatment (Lorin et al. 2013). Consistent with our results with DIM and CQ (Figure 2), inhibition of autophagy enhanced the chemotherapeutic effect of sulforaphane, another compound derived from cruciferous vegetables, in a TRAMP prostate cancer mouse model (Vyas et al. 2013). Treatment of prostate cancer with a combination of sulforaphane and CQ was accompanied by induction of apoptosis, reduction of cell proliferation and suppression of epithelial-to-mesenchymal transition (Vyas et al. 2013). These findings are in agreement with the results of our TMA analyses, which show that a combination of DIM and CQ significantly reduces tumor growth via inhibition of Ki67 expression and induction of DNA fragmentation as determined by TUNEL assay (Fig 4, 5). Our study is the first to show that 4,4'-Br₂DIM inhibits prostate tumor growth (Fig 3). These results are in line with the *in vitro* effects of 4,4'-Br₂DIM, which kills both androgen-dependent (LNCaP) and androgen-independent (C4-2B and PC-3) prostate cancer cells (Goldberg et al. 2014; Goldberg et al. 2015). Our TMA results demonstrated that there is a trend towards induction of necrosis by 4,4'-Br₂DIM, but this did not reach statistical significance due to small

number of mice used in the study . Also, the weaker response of certain TMA markers may have been caused by the fact that only viable tumor tissues were analysed (to avoid excessive non-specific background staining), thus excluding most necrotic and apoptotic cells. The results of our present study complements our previous findings *in vitro* which showed that 4,4'-Br₂DIM induced apoptosis and necrosis in prostate cancer cells (Goldberg et al. 2014; Goldberg et al. 2015).

Conclusion

We have determined that DIM and 4,4'-Br₂DIM are effective at reducing tumor growth in a murine xenograft model using androgen-independent PC-3 human prostate cancer cells. We have shown that a combination of DIM and the autophagy inhibitor CQ enhanced the antitumor efficacy of DIM. Our results suggest that the use of autophagy inhibitors as adjuvants in the treatment of prostate cancer may increase the effectiveness of current and future drug therapies against prostate cancer.

Funding

This work was supported by an operating grant from the Canadian Institutes of Health Research (CIHR grant no. MOP-115019) to Thomas Sanderson and Emma Guns. Hossam Draz received a scholarship from the *Fonds de Recherche du Québec - Santé* (FRQS).

Compliance with ethical standards

Conflict of interest

Hossam Draz, Alexander Goldberg, Emma Guns, Ladan Fazli, Stephen Safe and Thomas Sanderson each declare to have no conflicts of interest.

Ethical approval

All applicable international, national and institutional guidelines for the care and use of animals were followed. All procedures performed in studies involving animals were in accordance with the ethical standards of the *Centre National de Biologie Expérimentale* where the studies were conducted. This article does not contain any studies with human participants performed by any of the authors.

References

1. Siegel RL, Miller KD, Jemal A (2016) Cancer statistics, 2016. *CA Cancer J Clin* 66 (1):7-30. doi:10.3322/caac.21332
2. Kim MK, Park JH (2009) Conference on "Multidisciplinary approaches to nutritional problems". Symposium on "Nutrition and health". Cruciferous vegetable intake and the risk of human cancer: epidemiological evidence. *Proc Nutr Soc* 68 (1):103-110. doi:10.1017/S0029665108008884
3. De Kruif CA, Marsman JW, Venekamp JC, Falke HE, Noordhoek J, Blaauboer BJ, Wortelboer HM (1991) Structure elucidation of acid reaction products of indole-3-carbinol: detection *in vivo* and enzyme induction *in vitro*. *Chem Biol Interact* 80 (3):303-315
4. Banerjee S, Kong D, Wang Z, Bao B, Hillman GG, Sarkar FH (2011) Attenuation of multi-targeted proliferation-linked signaling by 3,3'-diindolylmethane (DIM): from bench to clinic. *Mutat Res* 728 (1-2):47-66. doi:10.1016/j.mrrev.2011.06.001
5. Fares F, Azzam N, Appel B, Fares B, Stein A (2010) The potential efficacy of 3,3'-diindolylmethane in prevention of prostate cancer development. *Eur J Cancer Prev* 19 (3):199-203. doi:10.1097/CEJ.0b013e328333fbce
6. Goldberg AA, Titorenko VI, Beach A, Abdelbaqi K, Safe S, Sanderson JT (2014) Ring-substituted analogs of 3,3'-diindolylmethane (DIM) induce apoptosis and necrosis in androgen-dependent and -independent prostate cancer cells. *Investigational new drugs* 32 (1):25-36. doi:10.1007/s10637-013-9979-y
7. Le HT, Schaldach CM, Firestone GL, Bjeldanes LF (2003) Plant-derived 3,3'-Diindolylmethane is a strong androgen antagonist in human prostate cancer cells. *J Biol Chem* 278 (23):21136-21145. doi:10.1074/jbc.M300588200
8. Zhang X, Sukamporn P, Zhang S, Min KW, Baek SJ (2017) 3,3'-diindolylmethane downregulates cyclin D1 through triggering endoplasmic reticulum stress in colorectal cancer cells. *Oncol Rep* 38 (1):569-574. doi:10.3892/or.2017.5693

9. Cho HJ, Park SY, Kim EJ, Kim JK, Park JH (2011) 3,3'-Diindolylmethane inhibits prostate cancer development in the transgenic adenocarcinoma mouse prostate model. *Mol Carcinog* 50 (2):100-112. doi:10.1002/mc.20698
10. Singh-Gupta V, Banerjee S, Yunker CK, Rakowski JT, Joiner MC, Konski AA, Sarkar FH, Hillman GG (2012) B-DIM impairs radiation-induced survival pathways independently of androgen receptor expression and augments radiation efficacy in prostate cancer. *Cancer Lett* 318 (1):86-92. doi:10.1016/j.canlet.2011.12.006
11. Wu TY, Khor TO, Su ZY, Saw CL, Shu L, Cheung KL, Huang Y, Yu S, Kong AN (2013) Epigenetic modifications of Nrf2 by 3,3'-diindolylmethane *in vitro* in TRAMP C1 cell line and *in vivo* TRAMP prostate tumors. *AAPS J* 15 (3):864-874. doi:10.1208/s12248-013-9493-3
12. Blackadar CB (2016) Historical review of the causes of cancer. *World J Clin Oncol* 7 (1):54-86. doi:10.5306/wjco.v7.i1.54
13. White E (2015) The role for autophagy in cancer. *J Clin Invest* 125 (1):42-46. doi:73941 [pii] 10.1172/JCI73941
14. Yang SY, Winslet MC (2011) Dual role of autophagy in colon cancer cell survival. *Ann Surg Oncol* 18 Suppl 3:S239. doi:10.1245/s10434-011-1789-x
15. Chen S, Rehman SK, Zhang W, Wen A, Yao L, Zhang J (2010) Autophagy is a therapeutic target in anticancer drug resistance. *Biochim Biophys Acta* 1806 (2):220-229. doi:10.1016/j.bbcan.2010.07.003
16. Levy JMM, Towers CG, Thorburn A (2017) Targeting autophagy in cancer. *Nat Rev Cancer* 17 (9):528-542. doi:10.1038/nrc.2017.53
17. Lorin S, Hamai A, Mehrpour M, Codogno P (2013) Autophagy regulation and its role in cancer. *Semin Cancer Biol* 23 (5):361-379. doi:10.1016/j.semcancer.2013.06.007
18. Zhou H, Yuan M, Yu Q, Zhou X, Min W, Gao D (2016) Autophagy regulation and its role in gastric cancer and colorectal cancer. *Cancer Biomark* 17 (1):1-10. doi:10.3233/CBM-160613
19. Goldberg AA, Draz H, Montes-Grajales D, Olivero-Verbel J, Safe SH, Sanderson JT (2015) 3,3'-Diindolylmethane (DIM) and its ring-substituted halogenated analogs (ring-DIMs) induce

differential mechanisms of survival and death in androgen-dependent and -independent prostate cancer cells. *Genes Cancer* 6 (5-6):265-280

20. Draz H, Goldberg AA, Titorenko VI, Tomlinson Guns ES, Safe SH, Sanderson JT (2017) Diindolylmethane and its halogenated derivatives induce protective autophagy in human prostate cancer cells via induction of the oncogenic protein AEG-1 and activation of AMP-activated protein kinase (AMPK). *Cell Signal* 40:172-182. doi:10.1016/j.cellsig.2017.09.006
21. Nachshon-Kedmi M, Fares FA, Yannai S (2004) Therapeutic activity of 3,3'-diindolylmethane on prostate cancer in an *in vivo* model. *Prostate* 61 (2):153-160. doi:10.1002/pros.20092
22. Chen D, Banerjee S, Cui QC, Kong D, Sarkar FH, Dou QP (2012) Activation of AMP-activated protein kinase by 3,3'-Diindolylmethane (DIM) is associated with human prostate cancer cell death *in vitro* and *in vivo*. *PLoS One* 7 (10):e47186. doi:10.1371/journal.pone.0047186
23. Parzych KR, Klionsky DJ (2014) An overview of autophagy: morphology, mechanism, and regulation. *Antioxid Redox Signal* 20 (3):460-473. doi:10.1089/ars.2013.5371
24. Chen N, Karantza-Wadsworth V (2009) Role and regulation of autophagy in cancer. *Biochim Biophys Acta* 1793 (9):1516-1523. doi:10.1016/j.bbamcr.2008.12.013
25. Muilenburg D, Parsons C, Coates J, Virudachalam S, Bold RJ (2014) Role of autophagy in apoptotic regulation by Akt in pancreatic cancer. *Anticancer Res* 34 (2):631-637
26. Zheng N, Zhang P, Huang H, Liu W, Hayashi T, Zang L, Zhang Y, Liu L, Xia M, Tashiro S, Onodera S, Ikejima T (2015) ERalpha down-regulation plays a key role in silibinin-induced autophagy and apoptosis in human breast cancer MCF-7 cells. *J Pharmacol Sci* 128 (3):97-107. doi:10.1016/j.jphs.2015.05.001
27. Chen Y, Sawyers CL, Scher HI (2008) Targeting the androgen receptor pathway in prostate cancer. *Current opinion in pharmacology* 8 (4):440-448. doi:10.1016/j.coph.2008.07.005
28. Vyas AR, Hahm ER, Arlotti JA, Watkins S, Stolz DB, Desai D, Amin S, Singh SV (2013) Chemoprevention of prostate cancer by d,l-sulforaphane is augmented by pharmacological inhibition of autophagy. *Cancer Res* 73 (19):5985-5995. doi:10.1158/0008-5472.CAN-13-0755

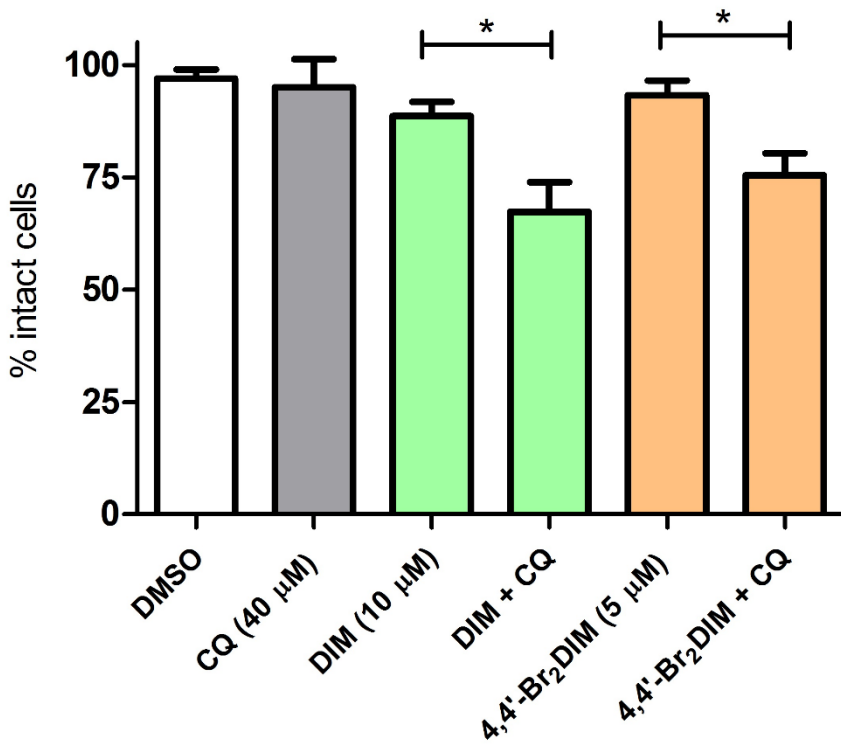


Figure 1

Inhibition of autophagy sensitizes PC-3 cells to cell death induced by DIM and 4,4'-Br₂DIM. The percentage of intact PC-3 cells treated with DIM (10 μ M) or 4,4'-Br₂DIM (5 μ M) for 24-h with or without a 4-h pretreatment with autophagy inhibitor chloroquine (CQ) are presented as means \pm SEM of three independent experiments. Statistically significant differences between treatments and control are indicated as: *P<0.05 (one-way ANOVA and Dunnett's posthoc test).

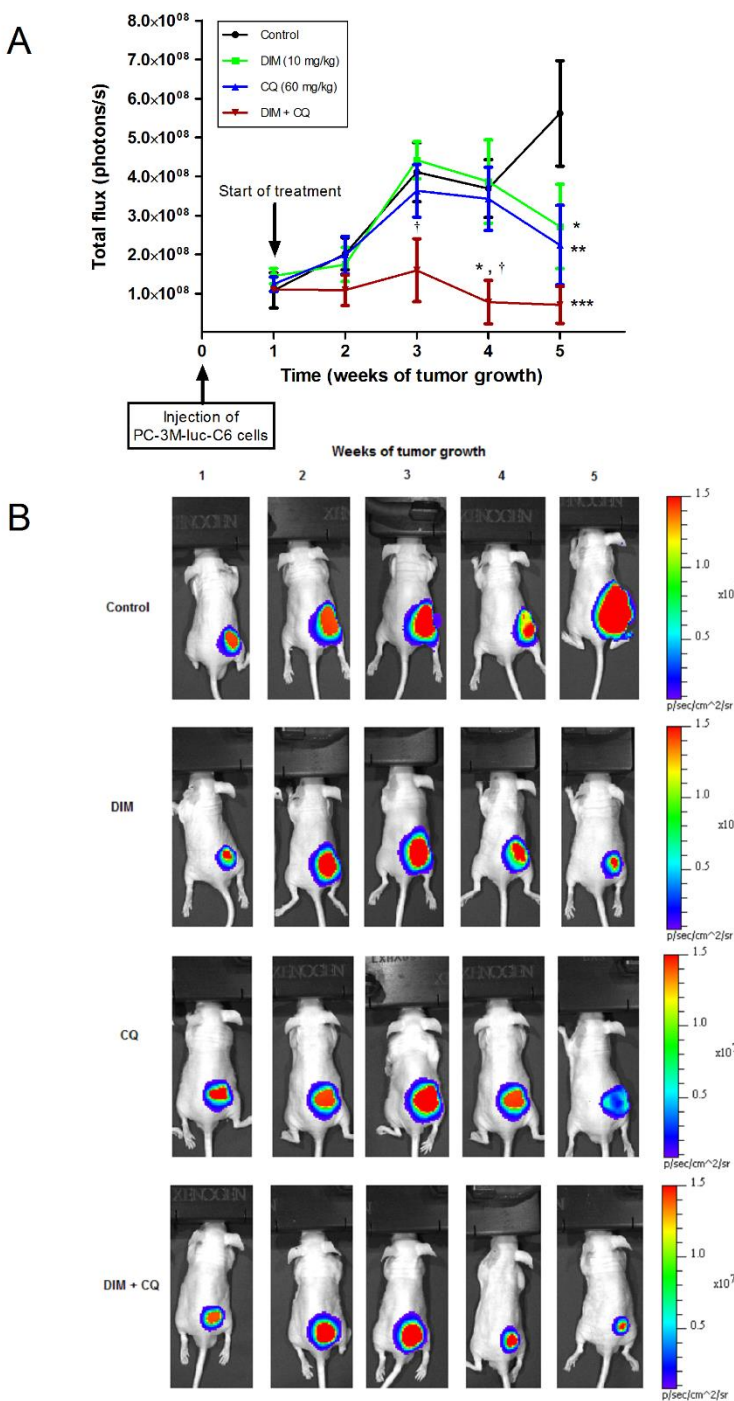


Figure 2

(A) DIM and a combination of DIM and the autophagy inhibitor chloroquine (CQ) decrease tumor growth of bioluminescent PC-3M-luc-C6 cells in nude CD-1 mice. Cells (1×10^6) were injected subcutaneously into CD-1 nude mice ($n = 6-8$) followed after 1 week by treatment (3 x per week) with either DIM (10 mg/kg), CQ (60 mg/kg), DIM + CQ or vehicle control. (B) Tumor growth was monitored weekly for 5 weeks after tumor cell injection using an IVIS imager. Note that weeks 2 to 5 on the x-axis (A) and above the images (B) represent 1 to 4 weeks of treatment. Significant

differences in bioluminescence (mean \pm SEM) between treatments and vehicle control are indicated as: * $P < 0.05$, ** $P < 0.01$, *** $P < 0.001$. Significant differences in bioluminescence (mean \pm SEM) between treatments and DIM group are indicated as: † $P < 0.05$ (two-way ANOVA and Bonferroni posthoc test).

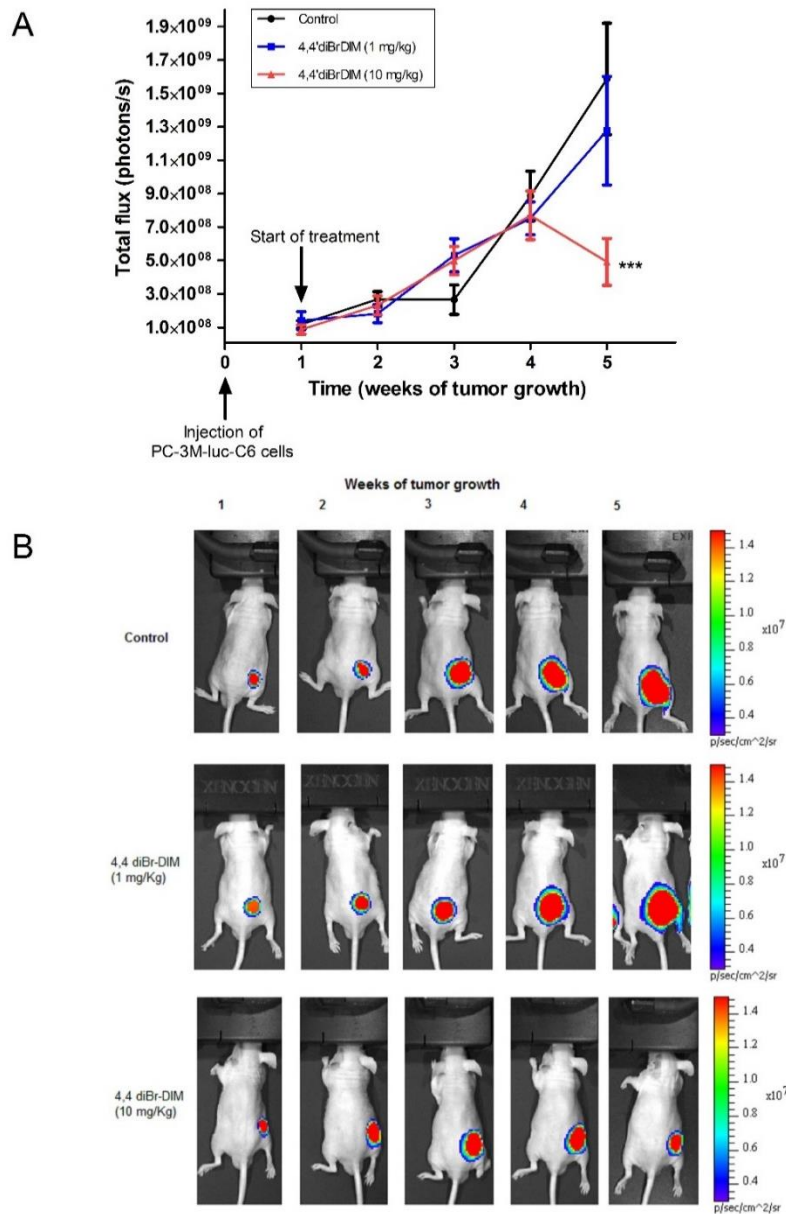


Figure 3

(A) 4,4'-Br₂DIM inhibits tumor growth of bioluminescent PC-3M-luc-C6 cells in nude CD-1 mice. Cells (1×10^6) were injected subcutaneously into CD-1 nude mice ($n = 6-8$) followed after 1 week by treatment (3 x per week) with either 4,4'-Br₂DIM (1 and 10 mg/kg) or vehicle control. (B) Tumor growth was monitored weekly for 5 weeks after tumor cell injection using an IVIS imager. Note that weeks 2 to 5 on the x-axis (A) and above the images (B) represent 1 to 4 weeks of

treatment. A significant difference in bioluminescence (mean \pm SEM) between treatment and vehicle control is indicated as: *** $P < 0.001$ (one-way ANOVA and Dunnett's posthoc test).

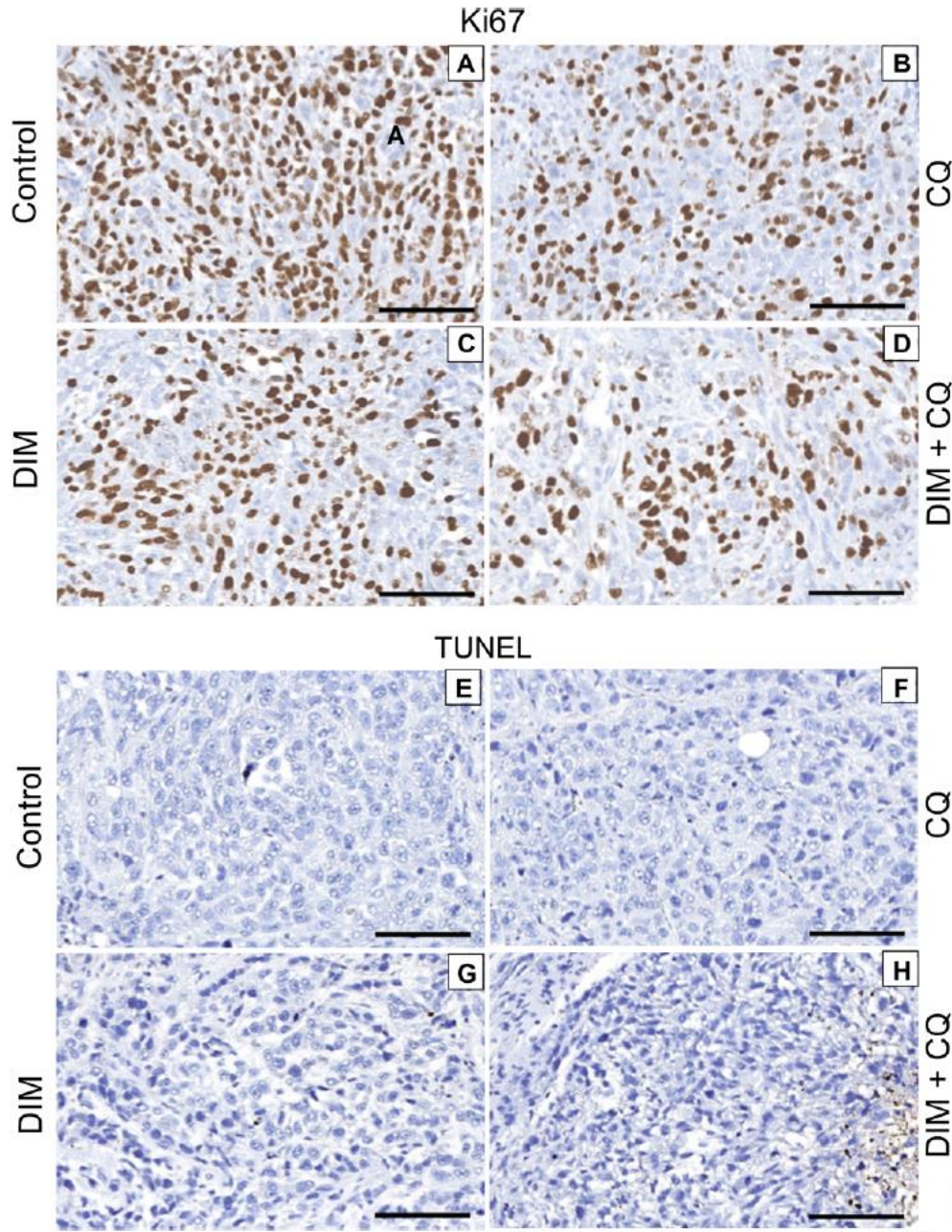


Figure 4

Representative immunohistochemical stains of Ki67 (A-D) and TUNEL (E-H) on tissue microarrays prepared from PC-3 tumors excised on week 5 from CD-1 nude mice treated 3 x per week with either 10 mg/kg DIM (C, G), 60 mg/kg CQ (B, F), a combination of DIM + CQ (D, H) or vehicle control (A, E). For ki67, (A) represent a strong, and (B, C, D) moderate staining; for TUNEL, (E) represent a weak, (F) moderate, and (G, H) strong staining. Scale bar = 100 μ m.

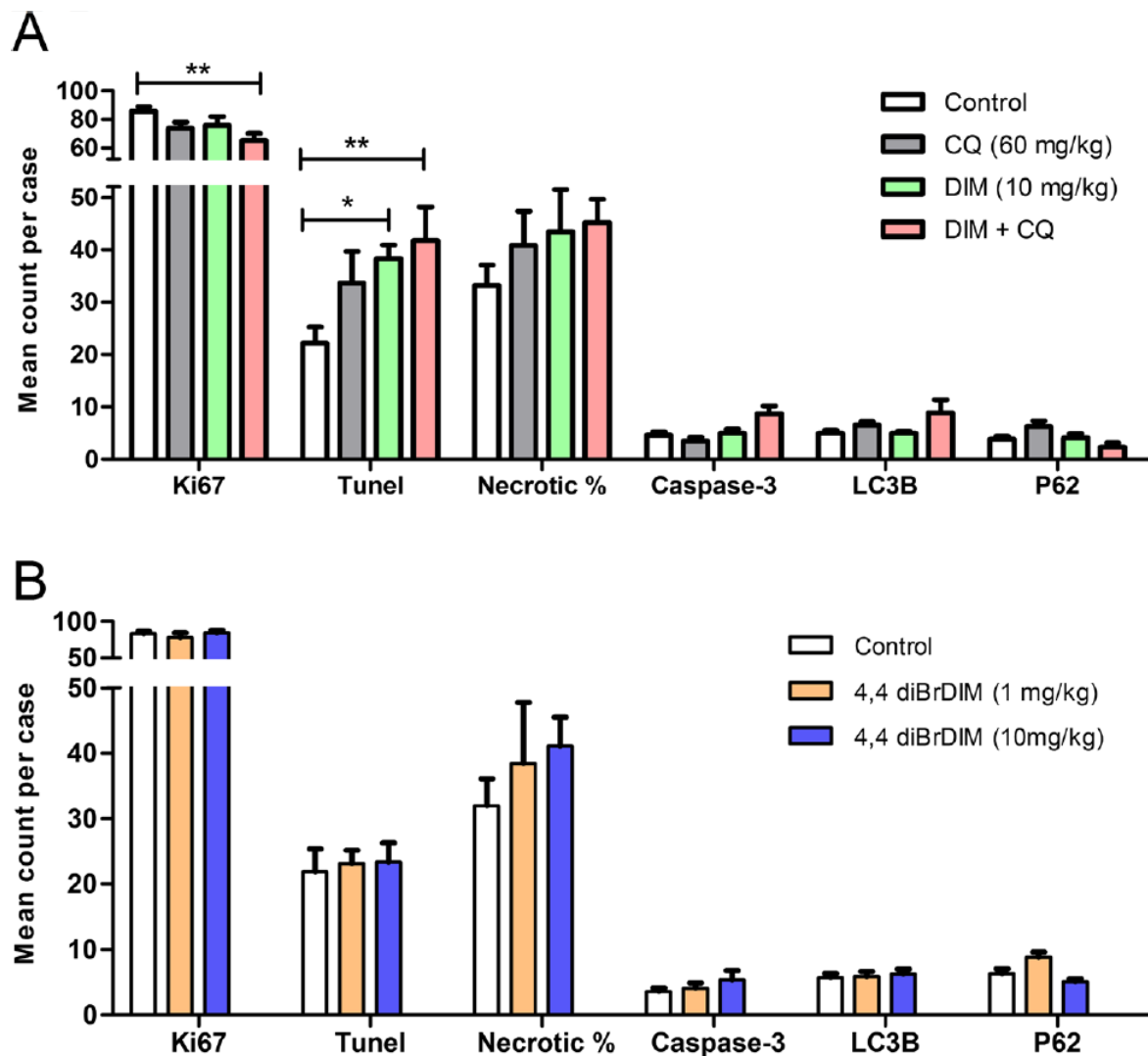


Figure 5

Average counts per case of Ki67, TUNEL, necrotic %, caspase-3, LC3B and P62 in PC-3 tumors excised on week 5 from CD-1 nude mice treated 3 x per week with (A) DIM (10 mg/kg), CQ (60 mg/Kg), DIM +CQ or vehicle control, and (B) with 4,4'-Br₂DIM (1 and 10 mg/kg) or vehicle control. Counts are presented as mean ± SEM of 5 or 6 animals per treatment group. Statistically significant differences between treatments and vehicle control are indicated as: *P< 0.05, **P<0.01 (one-way ANOVA and Dunnett's posthoc test).

CHAPTER 3: DISCUSSION

Prostate cancer is the most common malignancy and the third-leading cause of cancer-related deaths in American and Canadian men (Siegel et al. 2017). Recent advancements in prostate cancer therapies have improved the survival rate of patients with the disease. However, development of novel prostate cancer therapeutics is urgently needed. Several epidemiological and experimental studies indicate that DIM can reduce the risk of developing prostate cancer and play a beneficial role by inhibiting cancer progression (Le et al. 2003; Kim and Park 2009b; Cho et al. 2011). DIM targets multiple pathways associated with cancer progression *in vitro* and *in vivo* (Ge et al. 1996; Nachshon-Kedmi et al. 2004a; Nachshon-Kedmi et al. 2004b). Moreover, we have recently introduced a series of ring-substituted derivatives of DIM, ring-DIMs as novel inhibitors of AD prostate cancer cell proliferation. These derivatives also act as selective inducers of apoptosis in AD and AI prostate cancer cell lines as they do not kill normal prostate epithelial cells (Abdelbaqi et al. 2011; Goldberg et al. 2014). The mechanisms of action of ring-DIMs are not fully understood, but appear to be multifaceted. Thus, identifying the signaling pathway(s) targeted by ring-DIMs will help towards the development of novel drug therapies for prostate cancer, regardless of hormone-dependency.

DIM and ring-DIMs induce death of cancerous but not of immortalized normal human prostate epithelial cells

The primary step of this thesis was to assess the effect of DIM and ring-DIMs on cell viability of human prostate cancer cells and normal prostate epithelial cells. A 24-h exposure to ring-DIMs (4,4'-Br₂DIM, 4,4'-Cl₂DIM, 7,7'-Br₂DIM and 7,7'-Cl₂DIM) induces cell death with lower IC₅₀ than DIM in both LNCaP and C4-2B cells. 4,4'-Br₂DIM and 7,7'-Cl₂DIM were more potent ring-DIM at killing cells compared to DIM. In LNCaP prostate cancer cells, 4,4'-Br₂DIM and 7,7'-Cl₂DIM were ≈1.5 times, while 4,4'-Cl₂DIM and 7,7'-Br₂DIM were ≈1.2 times more potent at inducing cell death than DIM. In C4-2B prostate cancer cells, 4,4'-Br₂DIM and 7,7'-Cl₂DIM were ≈2.5 times, while 4,4'-Cl₂DIM and 7,7'-Br₂DIM were ≈1.5 times more potent at inducing cell death than DIM (Figure 1 in article #1, chapter 2, section 2.1) (Goldberg et al. 2015). Consistent with a previous report from our laboratory (Goldberg et al. 2014), a 48-h exposure to 4,4'-Br₂DIM and 7,7'-Cl₂DIM induced cell death in LNCaP, and PC-3 cells with greater potency than DIM or other tested

ring-DIMs. Moreover, our results are also in line with a previous study that demonstrated a growth inhibitory effects of DIM and ring-DIMs in LNCaP cells (Abdelbaqi et al. 2011). The results presented (see chapter 2, section 2.1) in this thesis demonstrated that the concentrations of DIM and ring-DIMs that killed LNCaP and C4-2B prostate cancer cells were not toxic to the immortalized normal prostate epithelial cells (RWPE-1) (Figure 1 in article #1, chapter 2, section 2.1) (Goldberg et al. 2015). This remarkable observation suggests that DIM and ring-DIMs can be used as safe anti-cancer agents that specifically target cancer cells over healthy cells. In agreement with our results, previous studies have shown that DIM is not toxic to normal cells including non-tumorigenic MCF10A breast epithelial cells (Rahman and Sarkar 2005; Nicastro et al. 2013) and normal human foreskin keratinocytes (Chen et al. 2001). In addition, a recent clinical study showed that B-DIM has an antiandrogenic effect with minimal toxicity (Hwang et al. 2016). Together, these findings confirm that DIM and ring-DIMs selectively target pathways that are dysregulated in cancer cells without affecting normal cells.

ER stress and mitochondrial dysfunction are early events in DIM and ring-DIM-mediated prostate cancer cell death

A previous study from our laboratory has shown that the most potent ring-DIM (4,4'-Br₂DIM) induces cell death by independently activating both intrinsic and extrinsic apoptosis pathways based on the observation that 4,4'-Br₂DIM activates caspase-8 and caspase-9 (Goldberg et al. 2014). In the present study (see chapter 2, section 2.1), we hypothesize that ring-DIM-mediated cell death is dependent on the intrinsic mitochondrial apoptosis pathway. We further propose that ER stress plays a role in ring-DIM-induced cell death. Indeed, both 4,4'-Br₂DIM and 7,7'-Cl₂DIM induce the expression of DR4 and DR5. Additionally, 4,4'-Br₂DIM increases the expression of Fas ligand (FasL) and Fas receptor (Goldberg et al. 2014). Moreover, a previous study also showed that DIM induced ER stress in pancreatic cancer cells and significantly increased ER stress markers such as ATF6, CHOP, leading to CHOP-dependent increase of DR5 and activation of caspase-8 (Abdelrahim et al. 2006). The results presented (see chapter 2, section 2.1) in this thesis demonstrate that ER stress and mitochondrial dysfunction are early events in ring-DIM- and DIM-induced prostate cancer cell death (Figure 2 in article # 1, chapter 2, section 2.1) (Goldberg et al. 2015). ATF4 and CHOP (markers of

ER stress activation) expression is increased by 4,4'-Br₂DIM, 7,7'-Cl₂DIM and DIM (Goldberg et al. 2015). In LNCaP and C4-2B cells, 4,4'-Br₂DIM increased ATF4 after 1 hr of exposure, while both DIM and 7,7'-Cl₂DIM increased ATF4 4 hr post exposure. A significant decrease in mitochondrial membrane potential (MMP) was observed in cells treated with 4,4'-dihaloDIMs and DIM after 1 hr of exposure, but only a slight decrease in mitochondrial activity was observed in cells treated with 7,7'-dihaloDIMs. All ring-DIMs except 7,7'-Br₂DIM significantly decreased mitochondrial ATP levels in both cell lines (Figure 2 in article #1, chapter 2, section 2.1) (Goldberg et al. 2015). These results demonstrated that halogen-substituted ring-DIMs act via structure dependent mechanisms.

We next used cyclosporin A (CsA), a potent inhibitor of the mitochondrial permeability transition pore (mPTP) complex, to examine the effect of DIM and ring-DIM-mediated induction of mitochondrial dysfunction on their cytotoxicity in prostate cancer cells. We showed that pretreatment with 5 μM CsA prevented ring-DIM-induced death in LNCaP and C4-2B cells, but could not prevent DIM-induced cell death, suggesting that mitochondrial dysfunction is essential for cell death triggered by the ring-DIMs but not DIM (Figure 3 in article #1, chapter 2, section 2.1) (Goldberg et al. 2015). CsA inhibited the MMP loss in cells treated with 4,4'-dihaloDIMs or DIM, but did not prevent the loss of MMP by 7,7'-dihaloDIMs. DIM, 4,4'-dihaloDIMs and 7,7'-dihaloDIMs appear to have divergent structure-activity relationships that mediate the reduction in MMP through different molecular target(s). Then, we explored the possible link between mitochondrial dysfunction and increased ER stress in prostate cancer cells by DIM and its derivatives. Pre-treatment with CsA did not affect either eIF2α phosphorylation or ATF4 and CHOP expression levels in LNCaP or C4-2B cells treated with either 4,4'-Br₂DIM, 7,7'-Cl₂DIM or DIM (Figure 3 in article # 1, chapter 2, section 2.1) (Goldberg et al. 2015). Hence, our results suggest that ring-DIM-mediated ER stress is activated in parallel, and not downstream, of mitochondrial dysfunction. A previous study showed that eIF2α may play a role in the survival of tumorigenic cells in response to Akt inhibition (Mounir et al. 2011). DIM is a potent inhibitor of the Akt pathway (Rahman and Sarkar 2005; Garikapaty et al. 2006) and our *in silico* data support the notion that DIM may act as a direct Akt inhibitor, as DIM and the ring-DIMs showed a significant binding affinity for Akt (Supplementary

Table S1 in article #1, chapter 2, section 2.1) (Goldberg et al. 2015). Therefore, we suggest that the observed induction of ER stress may be a pro-survival response to the mitochondrial disruption caused by the ring-DIMs and DIM, and is not essential for ring-DIM-induced toxicity.

We confirmed the pro-survival effect of ER stress using the ER stress inhibitor salubrinal. Pretreatment with 20 μ M salubrinal sensitized LNCaP and C4-2B to the toxicity of 7,7'-dihaloDIM and DIM (Figure 5 in article #1, chapter 2, section 2.1). In contrast, pretreatment with salubrinal inhibited cell death caused by 4,4'-dihaloDIMs in LNCaP and C4-2B cells (Figure 4 in article #1, chapter 2, section 2.1). These results confirm that ring-DIMs act through different, structure-dependent mechanisms to kill prostate cancer cells. We further tested the effect of a combination treatment of 4,4'-dihaloDIM and 7,7'-dihaloDIM in LNCaP and C4-2B cells. We found that the toxicity of 4,4'-Br₂DIM was potentiated in the presence of non-cytotoxic concentrations of 7,7'-Cl₂DIM (Appendix I). Pretreatment with salubrinal abrogated the increased phosphorylation of eIF2 α mediated by 4,4'-Br₂DIM in LNCaP and C4-2B cells (Figure 4 in article #1, chapter 2, section 2.1) (Goldberg et al. 2015). However, pretreatment with salubrinal did not abrogate the increase in CHOP and ATF4 expression mediated by 4,4'-Br₂DIM in LNCaP and C4-2B cells. Treatment of prostate cancer cells with salubrinal alone did not affect the phosphorylation status of eIF2 α . Our results demonstrate that salubrinal does not directly modify the phosphorylation status of eIF2 α , nor does it significantly inhibit the onset of ring-DIM-mediated ER stress. These results are consistent with previous reports showing that salubrinal did not modify the phosphorylation status of eIF2 α and interacted directly with Bcl-2 (Kessel 2006; Huang et al. 2012).

Previous studies demonstrated that accumulation of misfolded protein in the ER may trigger the production of ROS and the release of calcium from the ER lumen (Wang et al. 2017). Increased calcium in the cytosol is known to induce mitochondrial dysfunction and provides an explanation for the link between ER stress and mitochondrial dysfunction observed in different cellular models (Abdelrahim et al. 2006). Hence, we assessed whether salubrinal, as an ER stress inhibitor, could potentiate or attenuate DIM- and ring-DIM-mediated toxicity through the loss of MMP. Indeed, our results showed that pretreatment with salubrinal attenuated the 4,4'-dihaloDIM-mediated loss of MMP. This

suggests that the loss of MMP mediated by 4,4'-dihaloDIM is dependent on induction of ER stress. On the other hand, pretreatment with salubrinal potentiated 7,7'-dihaloDIM- and DIM-mediated toxicity through the loss of MMP. Moreover, cell death after a co-treatment of prostate cancer cells with salubrinal and either 7,7'-dihaloDIM or DIM was attenuated by CsA (Figure 5 in article #1, chapter 2, section 2.1) (Goldberg et al. 2015). These results suggest that inhibition of ER stress potentiates 7,7'-dihaloDIM and DIM-mediated MMP loss which in turn is attenuated in presence of the mPTP inhibitor CsA. The observed difference in cellular response to either DIM, the 7,7'-dihaloDIMs or the 4,4'-dihaloDIM indicate that there are important differences in their structure-activity relationships.

Ca²⁺/calmodulin-dependent protein kinase (CaMKII) is involved in 4,4'-Br₂DIM-mediated mitochondrial dysfunction

To further explore the mechanism of action of DIM and ring-DIMs in prostate cancer cells, we examined the possible involvement of CaMKII as a potential target for DIM and ring-DIMs based on our *in silico* docking experiments (Table 1 in article # 1) (Goldberg et al. 2015). We observed that KN93, the selective inhibitor of CaMKII, but not its inactive form KN92, prevented cell death mediated by 4,4'-Br₂DIM, but not 7,7'-Cl₂DIM or DIM (Figure 7 in article #1, chapter 2, section 2.1) (Goldberg et al. 2015). In contrast to our findings, previous studies have suggested an involvement of CaMKII activity in the survival of prostate cancer cells (Rokhlin et al. 2007). This was challenged by other studies where CaMKII was identified as a pro-apoptotic signal; CaMKII is essential for melittin-induced apoptosis in HCC cells (Chinnakannu et al. 2009) and CaMKII activation has been linked to induction of stress signaling pathways through c-Jun N-terminal kinase and p38 mitogen-activated kinase (Liu and Templeton 2008; Chinnakannu et al. 2009; Timmins et al. 2009). Moreover, CaMKII has been shown to play a role in the simultaneous induction of ER stress and mitochondrial dysfunction (Timmins et al. 2009). In addition, our study showed that KN93 abrogated the loss of MMP observed after exposure to 4,4'-Br₂DIM and decreased eIF2 α phosphorylation, but did not significantly prevent the expression of ATF4 or CHOP (Figure 7D in article # 1, chapter 2, section 2.1). Thus, CaMKII activation may directly initiate the intrinsic pathway of apoptosis in prostate cancer cells, and this effect may be independent of the induction of ER stress. These data

suggest that CaMKII may be a selective upstream target of 4,4'-Br₂DIM that is responsible for the early onset of mitochondrial dysfunction in prostate cancer cells.

Our *in silico* data showed a potential interaction between CaMKII and both DIM and 7,7'-Cl₂DIM, while our *in vitro* results demonstrated that CaMKII activity is not required for either DIM or 7,7'-Cl₂DIM toxicity in prostate cancer cells. This difference in cytotoxic response to the 4,4'-dihalo- and 7,7'-dihaloDIMs after inhibition of CaMKII by KN93 provides a further evidence that the mechanisms of action of the ring-DIMs are highly structure-dependent. In agreement, a previous study showed that the 4,4'-dihaloDIMs, but not the 7,7'-dihaloDIMs, induced the Fas receptor and FasL in LNCaP cells (Goldberg et al. 2013). Additionally, the 7,7'-dihaloDIMs were shown to be more potent inhibitors of DHT-mediated LNCaP cell proliferation than the 4,4'-dihalo-DIMs (Goldberg et al. 2013). In the present study we also show that the 4,4'- and 7,7'-dihaloDIMs elicit opposite responses in prostate cancer cells pre-treated with salubrinal, but these effects are unrelated to ER stress. Moreover, the pretreatment of all three cell lines with KN93 did not prevent the increase in expression of either CHOP or ATF4, further confirming that ER stress is not a key contributor to 4,4'-Br₂DIM-mediated cell death (Figure 7 in article #1, chapter 2, section 2.1) (Goldberg et al. 2015).

Induction of protective autophagy by DIM and ring-DIMs

Autophagy is a cellular catabolic pathway that eradicates damaged cellular organelles, proteins and other macromolecules through lysosomal degradation (Glick et al. 2010). Recent studies have shown that autophagy plays a key role in cancer and is either involved in cell apoptosis (cytotoxic autophagy) or cell protection (protective autophagy) (White 2015). Treatment of advanced prostate cancer with current approaches, such as androgen ablation therapy, is often accompanied by resistance to the treatment, which usually result in a fatal outcome (Chen et al. 2008). Hence, there is an urgent need to develop new strategies for treatment of prostate cancer that may include autophagy inhibition, an adjuvant therapy, as one alternative approach to improve treatment (Lorin et al. 2013).

Our study showed that DIM and ring-DIMs induced the classical marker of autophagy (LC3B I- to- II conversion) in LNCaP and C4-2B cells. However, in the

autophagy deficient DU145 cells, DIM and ring DIMs had no effect (Figure 6 in article #1, chapter 2, section 2.1) (Goldberg et al. 2015). This DIM- and ring-DIM-mediated autophagy was shown to be cytoprotective, since pre-treatment with either bafilomycin A1, 3-MA or transcriptional silencing of LC3B sensitized both LNCaP, C4-2B, but not DU145 cells, to cell death induced by DIM or the ring-DIMs. Also, the autophagy inhibitor CQ, an FDA approved drug for the treatment of malaria, significantly sensitized PC-3 cells to death in the presence of sub-toxic concentrations of DIM or 4,4'-Br₂DIM (Figure 1 in article #3, chapter 2, section 2.3)(Draz et al. 2018).

A few studies have shown a regulatory effect of DIM on autophagy in cancer cells, but those studies reported contradictory findings. In contrast to our results, they observed that a low dose of DIM (1 μ M) protected MDA-MB-231 breast cancer cells from H₂O₂-induced oxidative stress through inhibition of autophagy via repression of beclin1 (Fan et al. 2009). However, a previous study showed that a methylene-substituted derivative of DIM induced autophagic cell death in estrogen receptor-negative breast cancer cells (Vanderlaag et al. 2010). Moreover, DIM has been shown to induce ER stress-dependent autophagy in ovarian cancer cells (Kandala and Srivastava 2012b). Recently, DIM was shown to reduce cell viability and induce autophagy in gastric cancer cells (BGC-823 and SGC-7901) via induction of ATG5 expression (Ye et al. 2016). In order to investigate the possible induction of autophagy by DIM and ring-DIMs in prostate cancer cells at earlier time points, we examined their effect on the formation of autophagic vacuoles in prostate cancer cells after 8 h of treatment. Indeed our results showed that an 8-hr treatment of LNCaP and C4-2B with DIM or ring-DIMs increases the number of autophagic vacuoles (Figure 1 in article #2, chapter 2, section 2.2) (Draz et al. 2017). We also confirmed that the formation of autophagic vacuoles increased in C4-2B cells treated with DIM and ring-DIMs for 8 hr, using transmission electron microscopy (Figure 1 in article #2) (Draz et al. 2017).

DIM and ring-DIMs induce protective autophagy through induction of AEG-1 and activation of AMPK

To examine the mechanism(s) of DIM- and ring-DIM-mediated autophagy, we determined their effects on AMPK signaling, which is a known mediator of autophagy (Hardie 2011). Our study confirms the induction of cytoprotective autophagy since

inhibition of the autophagy initiator, unc-51-like autophagy activating kinase 1 (ULK1) using the kinase inhibitor MRT 67307 (N-[3-[[5-Cyclopropyl-2-[[3-(4-morpholinylmethyl)phenyl]amino]-4-pyrimidinyl]amino]propyl] cyclobutanecarboxamide) sensitized LNCaP and C4-2B cells to cell death induced by DIM or ring-DIMs (Figure 2 in article #2) (Draz et al. 2017). We investigated the mechanism of DIM and ring-DIM-mediated autophagy in prostate cancer cells by examining their effects on AMPK signaling. We demonstrated that DIM and ring-DIMs time-dependently augmented the conversion LC3BI to LC3BII as well as AMPK and acetyl-CoA carboxylase (ACC) phosphorylation (ACC being a substrate uniquely phosphorylated by AMPK) in LNCaP and C4-2B cells (Figure 2 in article #2, chapter 2, section 2.2) (Draz et al. 2017). We also show that AMPK activation is accompanied by a time-dependent activation of ULK1 (Draz et al. 2017). Indeed, inhibition of AMPK using selective siRNA inhibited autophagy through the suppression of LC3BI-to-LC3BII conversion in LNCaP cells (Figure 3 in article #2) (Draz et al. 2017).

Astrocyte elevated gene-1 (AEG-1), an oncoprotein, has been associated with cancer progression in various types of human cancers including that of the prostate (Hu et al. 2009; Shi and Wang 2015b). Previous studies have shown that AEG-1 induces protective autophagy in immortalized primary human fetal astrocyte (IM-PHFA) cells through the activation of AMPK (Bhutia et al. 2011). In our study, we examined the role of AEG-1 in DIM- and ring-DIM-mediated autophagy. In LNCaP and C4-2B cells exposed to DIM and ring-DIMs, AEG-1 protein levels were time-dependently increased (Figure 4 in article #2), and DIM-mediated autophagy was dependent on AEG-1 (Figure 5 in article #2, chapter 2, section 2.2) (Draz et al. 2017).

Selective inhibition of *AEG-1* with siRNA reduced AMPK activation, indicating that AEG-1 is an upstream regulator of AMPK (Draz et al. 2017). This findings is consistent with a previous study showing that protective autophagy in IM-PHFA is initiated by induction of AEG-1 followed by the activation of AMPK (Bhutia et al. 2011). Our study also showed that *AEG-1* inhibition sensitizes prostate cancer cells to death mediated by otherwise sub-toxic concentrations of DIM and ring-DIMs (Figure 5 in article #2, chapter 2, section 2.2) (Draz et al. 2017). From our results, it is apparent that AEG-1 is induced

in prostate cancer cells in response to DIM and ring-DIMs as a protective mechanism against the cellular stress and cytotoxicity induced by these compounds.

Interestingly, we observed a protective effect after siRNA-mediated downregulation of *AEG-1* against overtly cytotoxic concentrations of DIM or ring-DIMs in both LNCaP and C4-2B cells, which is contrast to our observed sensitization at sub-toxic concentrations. Moreover, this protective effect of *AEG-1* silencing was accompanied by induction of senescence in LNCaP and C4-2B cells treated with toxic concentration of DIM or ring-DIMs (Figure 6 in article # 2, chapter 2, section 2.2). Previous studies have shown that overexpression of *AEG-1* inhibits senescence in hepatocytes isolated from transgenic mice by inhibiting the DNA damage response (Srivastava et al. 2012). Senescent cells undergo irreversible proliferative arrest, which may inhibit tumor progression (Dimri 2005; Lee et al. 2012b; Lee and Lee 2014). Accumulating evidence suggests that therapies directed at inducing senescence may improve cancer treatment outcomes (Ewald et al. 2010; Lee and Lee 2014; Gibadulinova et al. 2016; Tato-Costa et al. 2016).

Autophagy inhibition enhances the chemopreventive effects of diindolylmethane in human prostate cancer xenograft

In our human prostate cancer xenograft model, an AI PC-3 cells were chosen because they are easier to grow in nude mice than AD LNCaP cells (Wu et al. 2013b). This was an important consideration as we had access to only limited quantities of 4,4'-Br₂DIM for animal studies. Our preliminary results demonstrated that PC-3 cells can form visible tumors monitored by IVIS imager after 1 week of injection. While, LNCaP cells do not form visible tumors until after 7 weeks of injection; in addition, only a fraction of all animals develop tumors (data not shown). Our xenograft study shows that treatment with either DIM or CQ alone significantly inhibits tumor growth on experimental week 5 (after 4 weeks of treatment) compared to control mice (Draz et al. 2018). These results are consistent with previous studies showing that DIM significantly inhibited prostate tumor growth in a TRAMP-C mouse model (Nachshon-Kedmi et al. 2004a; Cho et al. 2011; Wu et al. 2013a), and in SCID mice carrying C4-2B cell tumors (Chen et al. 2012).

Interestingly, a combined treatment with DIM and CQ resulted in a more pronounced reduction of tumor growth after 3 and 4 weeks of treatment with tumor sizes being smaller than their established size on week 1 when treatment was initiated (Figure 2 in article 3)

(Draz et al. 2018). These results are in line with the *in vitro* inhibition of autophagy with CQ which significantly sensitized PC-3 cells to DIM- and 4,4'-Br₂DIM-induced death in the presence of sub-toxic concentrations of these compounds (Figure 1 in article #3, chapter 2, section 2.3) (Draz et al. 2018). Consistent with our *in vivo* results for DIM and CQ (Figure 2 in article #3) (Draz et al. 2018), inhibition of autophagy enhanced the chemotherapeutic effect of sulforaphane, another compound derived from cruciferous vegetables, in a TRAMP prostate cancer mouse model (Vyas et al. 2013). These results are also consistent with our previous *in vitro* findings that pretreatment of LNCaP and C4-2B human prostate cancer cells with several autophagy inhibitors including bafilomycin A1, 3-MA and MRT 67307 sensitized both cell lines to sub-toxic concentrations of DIM and several ring-DIMs, including 4,4'-Br₂DIM. These findings suggest a cytoprotective role of the autophagic response to DIM and the ring-DIMs (Goldberg et al. 2014; Draz et al. 2017).

Treatment of prostate cancer with a combination of sulforaphane and CQ has been reported to be accompanied by induction of apoptosis, reduction of cell proliferation and suppression of epithelial-to-mesenchymal transition (Vyas et al. 2013). These findings are in agreement with the results of our tissue microarray analysis (TMA) analyses, which show that a combination of DIM and CQ significantly reduces tumor growth via inhibition of Ki67 expression and induction of DNA fragmentation as determined by TUNEL assay (Figure 4 and 5 in article #3, chapter 2, section 2.3) (Draz et al. 2018). The combination of DIM and CQ also tended to increase necrosis and caspase-3 levels but these incremental changes were not statistically significant (Figure 5A in article #3, chapter 2, section 2.3) (Draz et al. 2018). Autophagy markers LC3B and P62 were not statistically different for any of the treatments groups relative to vehicle control (Figure 5A in article #3, chapter 2, section 2.3)(Draz et al. 2018). We observed a trend towards induction of P62 and LC3B by the autophagy inhibitor CQ, but this did not reach statistical significance. Interestingly, our study is the first to show that 4,4'-Br₂DIM inhibits prostate tumor growth (Figure 3, in article #3, chapter 2, section 2.3) (Draz et al. 2018). These results are in line with the *in vitro* effects of 4,4'-Br₂DIM, which kills both AD (LNCaP) and AI (C4-2B and PC-3) prostate cancer cells (Goldberg et al. 2014; Goldberg et al. 2015). Our TMA results demonstrate that there is a trend towards induction of necrosis by 4,4'-

Br₂DIM (Draz et al. 2018). Also, the weaker response of certain TMA markers may have been caused by the fact that only viable tumor tissues were analysed (to avoid excessive non-specific background staining), thus excluding many necrotic and apoptotic cells (Lahat et al. 2010). The results of our present study complements our previous findings *in vitro*, which showed that 4,4'-Br₂DIM induced apoptosis and necrosis in prostate cancer cells (Goldberg et al. 2014; Goldberg et al. 2015). There are several limitations to consider in our *in vivo* study. First, the lack of statistical significance for autophagy markers meant we could not confirm the inhibition of autophagy by CQ in our *in vivo* model. Second, we could not rule out the possible alteration of other mechanisms (e.g. inhibition of toll-like receptor-9 and NF-κB) by CQ. In addition, we were not able to confirm our *in vitro* results with 4,4'-Br₂DIM in our *in vivo* model due to the lack of statistical significance for its effects on apoptotic, necrotic and autophagic markers in the PC-3 xenograft model. Although our model was very sensitive for the detection of bioluminescent tumors at the primary site of injection, the primary tumor could mask any weaker bioluminescent signals indicating the presence of small metastatic tumors, although it is not known within which time frame the development of metastasis would occur. We suggest increasing animal numbers in future *in vivo* experiments with DIM and ring-DIMs and to include both viable and non-viable excised tumour tissues for TMA analysis to improve statistical power.

CONCLUSION AND PERSPECTIVE

Prostate cancer is considered to be the most common cancer in males and the third leading cause of cancer-related deaths among American and Canadian men. Treatment of hormone responsive prostate cancer is manageable with current anticancer therapeutics. However, treatment of CRPC is still a challenge. The natural product DIM has been shown to inhibit growth of various cancers including that of the prostate. We previously showed that novel ring-substituted analogs of DIM induce apoptosis and necrosis in AD and AI prostate cancer cells.

Our results show that ring-DIMs are more potent inducers of death of prostate cancer cells than DIM. We also show that ring-DIMs act via distinct, structure-dependent mechanisms to induce pro-apoptotic and pro-necrotic effects in LNCaP, C4-2B, PC-3 and DU145 prostate cancer cells while they are non-toxic to normal epithelial prostate cells. This observation suggest that ring-DIMs may be used as safe therapies to specifically target cancer cells. Our study has also shown that 4,4'-Br₂DIM is the most potent and efficacious inducer of prostate cancer cell death. We confirmed that ring-DIMs act via distinct, structure-dependent, yet overlapping mechanisms (Figure 8 in article #1, chapter 2, section 2.1) (Goldberg et al. 2015) to induce potent cytotoxic effects in AD and AI prostate cancer cells, but not normal prostate epithelium. We have shown that cell death mediated by the most potent ring-DIM, 4,4'-Br₂DIM, is dependent on CaMKII activation and subsequent mitochondrial dysfunction, and that ER stress is insufficient to induce cell death in response to either the ring-DIMs or DIM. We also concluded that the ring-DIMs and DIM induce protective autophagy in prostate cancer cells, which is confirmed using several autophagy inhibitors (Bafilomycin A1, 3-MA, LC3B siRNA), however they have no effect on the autophagy deficient DU145 cells.

We have identified a novel mechanism of DIM- and ring-DIM-induced protective autophagy, which is mediated by induction of AEG-1 and subsequent activation of AMPK. Our results also suggest that selective autophagy inhibitors may be effective as adjuvant therapies in novel drug therapies against prostate cancer. Moreover, DIM-mediated induction of AEG-1 and induction of senescence as a consequence of AEG-1 downregulation may be novel mechanistic targets effective in treating prostate cancer. Ring-DIM-mediated induction of senescence and/or apoptosis is dependent on AEG-1, and this thesis demonstrates that induction of AEG-1 acts as a key molecular switch that

regulates the fate of prostate cancer cells by triggering either apoptosis or senescence (Figure 7 in article #2) (Draz et al. 2017).

We have revealed that DIM and 4,4'-Br₂DIM are effective at reducing tumor growth in a murine xenograft model using AI PC-3 human prostate cancer cells. Moreover, we have shown that a combination of DIM and the autophagy inhibitor CQ enhanced the antitumor efficacy of DIM. Our results suggest that the use of autophagy inhibitors as adjuvants in the treatment of prostate cancer may increase the effectiveness of current and future drug therapies against prostate cancer. Our *in vivo* xenograft prostate cancer model using bioluminescent PC-3 cells provides an accurate and non-invasive method to determine the anticancer efficacies of DIM, CQ or ring-DIMs in short-term treatment regimes. This model did not account for long-term treatment efficacy. After prolonged exposure to several treatment regimens for prostate cancer a resistance may develop (Antonarakis et al. 2014) and this could also possibly happen with DIM or the ring-DIMs.

In our study, we have shown that DIM and ring-DIMs induce mitochondrial dysfunction and protective autophagy, hence it would be interesting to examine the role of mitophagy in the mechanism of prostate tumor cell death. Mitophagy is defined as a selective degradation of mitochondria through the autophagy machinery (Ashrafi and Schwarz 2013). The selectivity depends on autophagy receptors which bind the dysfunctional organelle to the autophagosomal membrane leading to their engulfment by the autophagosome (Svenning and Johansen 2013). We further showed that autophagy inhibition enhanced the anticancer efficacy of DIM in prostate cancer xenograft model, while the potential of targeting mitophagy specifically as opposed to autophagy in general as a therapeutic strategy remains to be explored. Moreover, previous studies showed that activation of CaMKII in response to increased cytosolic Ca⁺² induces autophagy (Hawley et al. 2005; Woods et al. 2005), so it would be interesting to address the relationship between 4,4'-Br₂DIM, CaMKII modulation and autophagy in general as well as mitophagy. Future research is needed to explore the potential of targeting autophagy pathways in order to increase the effectiveness of the ring-DIMs as anti-neoplastic agents in prostate cancer xenograft mice model.

Clinical trials for either DIM or CQ (autophagy inhibitor) show promising results for cancer treatment. The formulated form of DIM with higher bioavailability, B-DIM, showed an antiandrogenic effect on phase II clinical trial (Hwang et al. 2016). Recent clinical trial have introduced chloroquine as a novel anticancer drug (Sotelo et al. 2006; Chude and Amaravadi 2017). Clinical trials to evaluate the anticancer effectiveness of the combination of DIM and CQ should be conducted.

AEG-1 is a key protein in DIM- and ring-DIM-mediated autophagy and cell death. The relationship between DIM-mediated induction of AEG-1 and senescence should be studied to explore the mechanism that induce senescence and the possible application of senescence induction in anticancer therapies. Novel therapies for prostate cancer that are more selective and effective may be developed by examining the effects of AEG-1 inhibition using an AEG-1-based DNA vaccine (Zhang et al. 2015) using murine prostate cancer xenograft models that are treated with DIM or ring-DIMs.

REFERENCES

- Abdelbaqi K, Lack N, Guns ET, Kotha L, Safe S, Sanderson JT. 2011. Antiandrogenic and growth inhibitory effects of ring-substituted analogs of 3,3'-diindolylmethane (ring-DIMs) in hormone-responsive LNCaP human prostate cancer cells. *Prostate* **71**(13): 1401-1412.
- Abdelrahim M, Newman K, Vanderlaag K, Samudio I, Safe S. 2006. 3,3'-diindolylmethane (DIM) and its derivatives induce apoptosis in pancreatic cancer cells through endoplasmic reticulum stress-dependent upregulation of DR5. *Carcinogenesis* **27**(4): 717-728.
- Acosta-Alvear D, Zhou Y, Blais A, Tsikitis M, Lents NH, Arias C, Lennon CJ, Kluger Y, Dynlacht BD. 2007. XBP1 controls diverse cell type- and condition-specific transcriptional regulatory networks. *Mol Cell* **27**(1): 53-66.
- Adams JM. 2003. Ways of dying: multiple pathways to apoptosis. *Genes Dev* **17**(20): 2481-2495.
- Adhami VM, Mukhtar H. 2007. Anti-oxidants from green tea and pomegranate for chemoprevention of prostate cancer. *Mol Biotechnol* **37**(1): 52-57.
- Aggarwal BB, Ichikawa H. 2005. Molecular targets and anticancer potential of indole-3-carbinol and its derivatives. *Cell Cycle* **4**(9): 1201-1215.
- Aggarwal BB, Takada Y, Oommen OV. 2004. From chemoprevention to chemotherapy: common targets and common goals. *Expert Opin Investig Drugs* **13**(10): 1327-1338.
- Aita VM, Liang XH, Murty VV, Pincus DL, Yu W, Cayanis E, Kalachikov S, Gilliam TC, Levine B. 1999. Cloning and genomic organization of beclin 1, a candidate tumor suppressor gene on chromosome 17q21. *Genomics* **59**(1): 59-65.
- Akar U, Chaves-Reyez A, Barria M, Tari A, Sanguino A, Kondo Y, Kondo S, Arun B, Lopez-Berestein G, Ozpolat B. 2008. Silencing of Bcl-2 expression by small interfering RNA induces autophagic cell death in MCF-7 breast cancer cells. *Autophagy* **4**(5): 669-679.
- Anand P, Kunnumakkara AB, Sundaram C, Harikumar KB, Tharakan ST, Lai OS, Sung B, Aggarwal BB. 2008. Cancer is a preventable disease that requires major lifestyle changes. *Pharm Res* **25**(9): 2097-2116.
- Anderton MJ, Manson MM, Verschoyle RD, Gescher A, Lamb JH, Farmer PB, Steward WP, Williams ML. 2004. Pharmacokinetics and tissue disposition of indole-3-carbinol and its acid condensation products after oral administration to mice. *Clin Cancer Res* **10**(15): 5233-5241.
- Antonarakis ES, Lu C, Wang H, Luber B, Nakazawa M, Roeser JC, Chen Y, Mohammad TA, Chen Y, Fedor HL et al. 2014. AR-V7 and resistance to enzalutamide and abiraterone in prostate cancer. *N Engl J Med* **371**(11): 1028-1038.
- Ash SC, Yang DQ, Britt DE. 2008. LYRIC/AEG-1 overexpression modulates BCCIPalpha protein levels in prostate tumor cells. *Biochem Biophys Res Commun* **371**(2): 333-338.
- Ashrafi G, Schwarz TL. 2013. The pathways of mitophagy for quality control and clearance of mitochondria. *Cell Death Differ* **20**(1): 31-42.

- Attard G, Reid AH, Yap TA, Raynaud F, Dowsett M, Settatree S, Barrett M, Parker C, Martins V, Folkard E et al. 2008. Phase I clinical trial of a selective inhibitor of CYP17, abiraterone acetate, confirms that castration-resistant prostate cancer commonly remains hormone driven. *J Clin Oncol* **26**(28): 4563-4571.
- Aubrey BJ, Strasser A, Kelly GL. 2016. Tumor-Suppressor Functions of the TP53 Pathway. *Cold Spring Harb Perspect Med* **6**(5).
- Bacsi SG, Reisz-Porszasz S, Hankinson O. 1995. Orientation of the heterodimeric aryl hydrocarbon (dioxin) receptor complex on its asymmetric DNA recognition sequence. *Mol Pharmacol* **47**(3): 432-438.
- Baena Ruiz R, Salinas Hernandez P. 2016. Cancer chemoprevention by dietary phytochemicals: Epidemiological evidence. *Maturitas* **94**: 13-19.
- Balic A, Sorensen MD, Trabulo SM, Sainz B, Jr., Cioffi M, Vieira CR, Miranda-Lorenzo I, Hidalgo M, Kleeff J, Erkan M et al. 2014. Chloroquine targets pancreatic cancer stem cells via inhibition of CXCR4 and hedgehog signaling. *Mol Cancer Ther* **13**(7): 1758-1771.
- Banerjee S, Kong D, Wang Z, Bao B, Hillman GG, Sarkar FH. 2011. Attenuation of multi-targeted proliferation-linked signaling by 3,3'-diindolylmethane (DIM): from bench to clinic. *Mutat Res* **728**(1-2): 47-66.
- Bansal N, Bartucci M, Yusuff S, Davis S, Flaherty K, Huselid E, Patrizii M, Jones D, Cao L, Sydorenko N et al. 2016. BMI-1 Targeting Interferes with Patient-Derived Tumor-Initiating Cell Survival and Tumor Growth in Prostate Cancer. *Clin Cancer Res* **22**(24): 6176-6191.
- Barnes-Ellerbe S, Knudsen KE, Puga A. 2004. 2,3,7,8-Tetrachlorodibenzo-p-dioxin blocks androgen-dependent cell proliferation of LNCaP cells through modulation of pRB phosphorylation. *Mol Pharmacol* **66**(3): 502-511.
- Beaver LM, Yu TW, Sokolowski EI, Williams DE, Dashwood RH, Ho E. 2012. 3,3'-Diindolylmethane, but not indole-3-carbinol, inhibits histone deacetylase activity in prostate cancer cells. *Toxicol Appl Pharmacol* **263**(3): 345-351.
- Beer TM, Kwon ED, Drake CG, Fizazi K, Logothetis C, Gravis G, Ganju V, Polikoff J, Saad F, Humanski P et al. 2017. Randomized, Double-Blind, Phase III Trial of Ipilimumab Versus Placebo in Asymptomatic or Minimally Symptomatic Patients With Metastatic Chemotherapy-Naive Castration-Resistant Prostate Cancer. *J Clin Oncol* **35**(1): 40-47.
- Beesoo R, Neergheen-Bhujun V, Bhagooli R, Bahorun T. 2014. Apoptosis inducing lead compounds isolated from marine organisms of potential relevance in cancer treatment. *Mutat Res* **768**: 84-97.
- Berenblum I. 1954. A speculative review; the probable nature of promoting action and its significance in the understanding of the mechanism of carcinogenesis. *Cancer Res* **14**(7): 471-477.
- Bhatnagar A, Wang Y, Mease RC, Gabrielson M, Sysa P, Minn I, Green G, Simmons B, Gabrielson K, Sarkar S et al. 2014. AEG-1 promoter-mediated imaging of prostate cancer. *Cancer Res* **74**(20): 5772-5781.

- Bhuiyan MM, Li Y, Banerjee S, Ahmed F, Wang Z, Ali S, Sarkar FH. 2006. Down-regulation of androgen receptor by 3,3'-diindolylmethane contributes to inhibition of cell proliferation and induction of apoptosis in both hormone-sensitive LNCaP and insensitive C4-2B prostate cancer cells. *Cancer Res* **66**(20): 10064-10072.
- Bhutia SK, Kegelman TP, Das SK, Azab B, Su ZZ, Lee SG, Sarkar D, Fisher PB. 2010. Astrocyte elevated gene-1 induces protective autophagy. *Proc Natl Acad Sci U S A* **107**(51): 22243-22248.
- . 2011. Astrocyte elevated gene-1 activates AMPK in response to cellular metabolic stress and promotes protective autophagy. *Autophagy* **7**(5): 547-548.
- Bjeldanes LF, Kim JY, Grose KR, Bartholomew JC, Bradfield CA. 1991. Aromatic hydrocarbon responsiveness-receptor agonists generated from indole-3-carbinol in vitro and in vivo: comparisons with 2,3,7,8-tetrachlorodibenzo-p-dioxin. *Proc Natl Acad Sci U S A* **88**(21): 9543-9547.
- Blackadar CB. 2016. Historical review of the causes of cancer. *World J Clin Oncol* **7**(1): 54-86.
- Bladou F, Vessella RL, Buhler KR, Ellis WJ, True LD, Lange PH. 1996. Cell proliferation and apoptosis during prostatic tumor xenograft involution and regrowth after castration. *Int J Cancer* **67**(6): 785-790.
- Blanchard Y, Seenundun S, Robaire B. 2007. The promoter of the rat 5alpha-reductase type 1 gene is bidirectional and Sp1-dependent. *Mol Cell Endocrinol* **264**(1-2): 171-183.
- Bode AM, Dong Z. 2015. Toxic phytochemicals and their potential risks for human cancer. *Cancer Prev Res (Phila)* **8**(1): 1-8.
- Bosland MC. 2000. The role of steroid hormones in prostate carcinogenesis. *J Natl Cancer Inst Monogr*(27): 39-66.
- Boutin B, Tajeddine N, Vandersmissen P, Zanou N, Van Schoor M, Mondin L, Courtoy PJ, Tombal B, Gailly P. 2013. Androgen deprivation and androgen receptor competition by bicalutamide induce autophagy of hormone-resistant prostate cancer cells and confer resistance to apoptosis. *Prostate* **73**(10): 1090-1102.
- Brady CA, Attardi LD. 2010. p53 at a glance. *J Cell Sci* **123**(Pt 15): 2527-2532.
- Campisi J, d'Adda di Fagagna F. 2007. Cellular senescence: when bad things happen to good cells. *Nat Rev Mol Cell Biol* **8**(9): 729-740.
- Cao Y. 2015. Environmental pollution and DNA methylation: carcinogenesis, clinical significance, and practical applications. *Front Med* **9**(3): 261-274.
- Cardillo MR, Petrangeli E, Perracchio L, Salvatori L, Ravenna L, Di Silverio F. 2000. Transforming growth factor-beta expression in prostate neoplasia. *Anal Quant Cytol Histol* **22**(1): 1-10.
- Carreira S, Romanel A, Goodall J, Grist E, Ferraldeschi R, Miranda S, Prandi D, Lorente D, Frenel JS, Pezaro C et al. 2014. Tumor clone dynamics in lethal prostate cancer. *Sci Transl Med* **6**(254): 254ra125.
- Cavaliere EL, Devanesan P, Bosland MC, Badawi AF, Rogan EG. 2002. Catechol estrogen metabolites and conjugates in different regions of the prostate of Noble rats treated with 4-

- hydroxyestradiol: implications for estrogen-induced initiation of prostate cancer. *Carcinogenesis* **23**(2): 329-333.
- Cerella C, Grandjettette C, Dicato M, Diederich M. 2016. Roles of Apoptosis and Cellular Senescence in Cancer and Aging. *Curr Drug Targets* **17**(4): 405-415.
- Chang WY, Prins GS. 1999. Estrogen receptor-beta: implications for the prostate gland. *Prostate* **40**(2): 115-124.
- Chang X, Tou JC, Hong C, Kim HA, Riby JE, Firestone GL, Bjeldanes LF. 2005. 3,3'-Diindolylmethane inhibits angiogenesis and the growth of transplantable human breast carcinoma in athymic mice. *Carcinogenesis* **26**(4): 771-778.
- Chang YY, Juhasz G, Goraksha-Hicks P, Arsham AM, Mallin DR, Muller LK, Neufeld TP. 2009. Nutrient-dependent regulation of autophagy through the target of rapamycin pathway. *Biochem Soc Trans* **37**(Pt 1): 232-236.
- Chen D, Banerjee S, Cui QC, Kong D, Sarkar FH, Dou QP. 2012. Activation of AMP-activated protein kinase by 3,3'-Diindolylmethane (DIM) is associated with human prostate cancer cell death in vitro and in vivo. *PLoS One* **7**(10): e47186.
- Chen D, Yu J, Zhang L. 2016. Necroptosis: an alternative cell death program defending against cancer. *Biochim Biophys Acta* **1865**(2): 228-236.
- Chen DZ, Qi M, Auburn KJ, Carter TH. 2001. Indole-3-carbinol and diindolylmethane induce apoptosis of human cervical cancer cells and in murine HPV16-transgenic preneoplastic cervical epithelium. *J Nutr* **131**(12): 3294-3302.
- Chen I, McDougal A, Wang F, Safe S. 1998. Aryl hydrocarbon receptor-mediated antiestrogenic and antitumorigenic activity of diindolylmethane. *Carcinogenesis* **19**: 1631-1639.
- Chen N, Karantza-Wadsworth V. 2009. Role and regulation of autophagy in cancer. *Biochim Biophys Acta* **1793**(9): 1516-1523.
- Chen S, Rehman SK, Zhang W, Wen A, Yao L, Zhang J. 2010. Autophagy is a therapeutic target in anticancer drug resistance. *Biochim Biophys Acta* **1806**(2): 220-229.
- Chen Y, Sawyers CL, Scher HI. 2008. Targeting the androgen receptor pathway in prostate cancer. *Curr Opin Pharmacol* **8**(4): 440-448.
- Chinnakannu K, Chen D, Li Y, Wang Z, Dou QP, Reddy GP, Sarkar FH. 2009. Cell cycle-dependent effects of 3,3'-diindolylmethane on proliferation and apoptosis of prostate cancer cells. *J Cell Physiol* **219**(1): 94-99.
- Cho HJ, Park SY, Kim EJ, Kim JK, Park JH. 2011. 3,3'-Diindolylmethane inhibits prostate cancer development in the transgenic adenocarcinoma mouse prostate model. *Mol Carcinog* **50**(2): 100-112.
- Choi AM, Ryter SW, Levine B. 2013. Autophagy in human health and disease. *N Engl J Med* **368**(19): 1845-1846.
- Chude CI, Amaravadi RK. 2017. Targeting Autophagy in Cancer: Update on Clinical Trials and Novel Inhibitors. *Int J Mol Sci* **18**(6).
- Cohen JH, Kristal AR, Stanford JL. 2000. Fruit and vegetable intakes and prostate cancer risk. *J Natl Cancer Inst* **92**(1): 61-68.

- Contag PR, Olomu IN, Stevenson DK, Contag CH. 1998. Bioluminescent indicators in living mammals. *Nat Med* **4**(2): 245-247.
- Contractor R, Samudio IJ, Estrov Z, Harris D, McCubrey JA, Safe SH, Andreeff M, Konopleva M. 2005. A novel ring-substituted diindolylmethane, 1,1-bis[3'-(5-methoxyindolyl)]-1-(p-t-butylphenyl) methane, inhibits extracellular signal-regulated kinase activation and induces apoptosis in acute myelogenous leukemia. *Cancer Res* **65**(7): 2890-2898.
- Cooperberg MR, Grossfeld GD, Lubeck DP, Carroll PR. 2003. National practice patterns and time trends in androgen ablation for localized prostate cancer. *J Natl Cancer Inst* **95**(13): 981-989.
- Cordani M, Oppici E, Dando I, Butturini E, Dalla Pozza E, Nadal-Serrano M, Oliver J, Roca P, Mariotto S, Cellini B et al. 2016. Mutant p53 proteins counteract autophagic mechanism sensitizing cancer cells to mTOR inhibition. *Mol Oncol* **10**(7): 1008-1029.
- Coultas L, Strasser A. 2003. The role of the Bcl-2 protein family in cancer. *Semin Cancer Biol* **13**(2): 115-123.
- Craig WJ. 1997. Phytochemicals: guardians of our health. *J Am Diet Assoc* **97**(10 Suppl 2): S199-204.
- Cross CE, Halliwell B, Borish ET, Pryor WA, Ames BN, Saul RL, McCord JM, Harman D. 1987. Oxygen radicals and human disease. *Ann Intern Med* **107**(4): 526-545.
- Culig Z, Hobisch A, Hittmair A, Cronauer MV, Radmayr C, Bartsch G, Klocker H. 1997. Androgen receptor gene mutations in prostate cancer. Implications for disease progression and therapy. *Drugs Aging* **10**(1): 50-58.
- Cunningham D, You Z. 2015. In vitro and in vivo model systems used in prostate cancer research. *J Biol Methods* **2**(1).
- Curran MA, Allison JP. 2009. Tumor vaccines expressing flt3 ligand synergize with ctla-4 blockade to reject preimplanted tumors. *Cancer Res* **69**(19): 7747-7755.
- de Bono JS, Logothetis CJ, Molina A, Fizazi K, North S, Chu L, Chi KN, Jones RJ, Goodman OB, Jr., Saad F et al. 2011. Abiraterone and increased survival in metastatic prostate cancer. *N Engl J Med* **364**(21): 1995-2005.
- De Kruif CA, Marsman JW, Venekamp JC, Falke HE, Noordhoek J, Blaauboer BJ, Wortelboer HM. 1991a. Structure elucidation of acid reaction products of indole-3-carbinol: detection in vivo and enzyme induction in vitro. *Chem Biol Interact* **80**(3): 303-315.
- De Kruif CA, Marsman JW, Venekamp JC, Falke HE, Noordhoek J, Blaauboer BJ, Wortelboer HM. 1991b. Structure elucidation of acid reaction products of indole-3-carbinol: detection in vivo and enzyme induction in vitro. *Chem Biol Interact* **80**: 303-315.
- Debnath J. 2011. The multifaceted roles of autophagy in tumors-implications for breast cancer. *J Mammary Gland Biol Neoplasia* **16**(3): 173-187.
- Delbridge AR, Valente LJ, Strasser A. 2012. The role of the apoptotic machinery in tumor suppression. *Cold Spring Harb Perspect Biol* **4**(11).
- Dimri GP. 2005. What has senescence got to do with cancer? *Cancer Cell* **7**(6): 505-512.

- Drake CG, Sharma P, Gerritsen W. 2014. Metastatic castration-resistant prostate cancer: new therapies, novel combination strategies and implications for immunotherapy. *Oncogene* **33**(43): 5053-5064.
- Draz H, Goldberg AA, Titorenko VI, Tomlinson Guns ES, Safe SH, Sanderson JT. 2017. Diindolylmethane and its halogenated derivatives induce protective autophagy in human prostate cancer cells via induction of the oncogenic protein AEG-1 and activation of AMP-activated protein kinase (AMPK). *Cell Signal* **40**: 172-182.
- Draz H, Goldberg AA, Tomlinson Guns ES, Fazli L, Safe S, Sanderson JT. 2018. Autophagy inhibition improves the chemotherapeutic efficacy of cruciferous vegetable-derived diindolylmethane in a murine prostate cancer xenograft model. *Invest New Drugs* **36**(4): 718-725.
- Duan W, Gao L, Jin D, Otterson GA, Villalona-Calero MA. 2008. Lung specific expression of a human mutant p53 affects cell proliferation in transgenic mice. *Transgenic Res* **17**(3): 355-366.
- Ecke TH, Schlechte HH, Hubsch A, Lenk SV, Schiemenz K, Rudolph BD, Miller K. 2007. TP53 mutation in prostate needle biopsies--comparison with patients follow-up. *Anticancer Res* **27**(6B): 4143-4148.
- Egan DF, Shackelford DB, Mihaylova MM, Gelino S, Kohnz RA, Mair W, Vasquez DS, Joshi A, Gwinn DM, Taylor R et al. 2011. Phosphorylation of ULK1 (hATG1) by AMP-activated protein kinase connects energy sensing to mitophagy. *Science* **331**(6016): 456-461.
- Ellem SJ, Risbridger GP. 2006. Aromatase and prostate cancer. *Minerva Endocrinol* **31**(1): 1-12.
- Emdad L, Lee SG, Su ZZ, Jeon HY, Boukerche H, Sarkar D, Fisher PB. 2009. Astrocyte elevated gene-1 (AEG-1) functions as an oncogene and regulates angiogenesis. *Proc Natl Acad Sci U S A* **106**(50): 21300-21305.
- Emdad L, Sarkar D, Su ZZ, Randolph A, Boukerche H, Valerie K, Fisher PB. 2006. Activation of the nuclear factor kappaB pathway by astrocyte elevated gene-1: implications for tumor progression and metastasis. *Cancer Res* **66**(3): 1509-1516.
- Enan E, Matsumura F. 1996. Identification of c-Src as the integral component of the cytosolic Ah receptor complex, transducing the signal of 2,3,7,8-tetrachlorodibenzo-p-dioxin (TCDD) through the protein phosphorylation pathway. *Biochem Pharmacol* **52**(10): 1599-1612.
- Ewald JA, Desotelle JA, Wilding G, Jarrard DF. 2010. Therapy-induced senescence in cancer. *J Natl Cancer Inst* **102**(20): 1536-1546.
- Falasca M, Selvaggi F, Buus R, Sulpizio S, Edling CE. 2011. Targeting phosphoinositide 3-kinase pathways in pancreatic cancer--from molecular signalling to clinical trials. *Anticancer Agents Med Chem* **11**(5): 455-463.
- Fan S, Meng Q, Saha T, Sarkar FH, Rosen EM. 2009. Low concentrations of diindolylmethane, a metabolite of indole-3-carbinol, protect against oxidative stress in a BRCA1-dependent manner. *Cancer Res* **69**(15): 6083-6091.
- Fares F, Azzam N, Appel B, Fares B, Stein A. 2010. The potential efficacy of 3,3'-diindolylmethane in prevention of prostate cancer development. *Eur J Cancer Prev* **19**(3): 199-203.

- Feldman BJ, Feldman D. 2001. The development of androgen-independent prostate cancer. *Nat Rev Cancer* **1**(1): 34-45.
- Ferlay J, Soerjomataram I, Dikshit R, Eser S, Mathers C, Rebelo M, Parkin DM, Forman D, Bray F. 2015. Cancer incidence and mortality worldwide: sources, methods and major patterns in GLOBOCAN 2012. *Int J Cancer* **136**(5): E359-386.
- Fizazi K, Scher HI, Molina A, Logothetis CJ, Chi KN, Jones RJ, Staffurth JN, North S, Vogelzang NJ, Saad F et al. 2012. Abiraterone acetate for treatment of metastatic castration-resistant prostate cancer: final overall survival analysis of the COU-AA-301 randomised, double-blind, placebo-controlled phase 3 study. *Lancet Oncol* **13**(10): 983-992.
- Fruehauf JP, Meyskens FL, Jr. 2007. Reactive oxygen species: a breath of life or death? *Clin Cancer Res* **13**(3): 789-794.
- Garikapaty VP, Ashok BT, Tadi K, Mittelman A, Tiwari RK. 2006. 3,3'-Diindolylmethane downregulates pro-survival pathway in hormone independent prostate cancer. *Biochem Biophys Res Commun* **340**(2): 718-725.
- Ge X, Yannai S, Rennert G, Gruener N, Fares FA. 1996. 3,3'-Diindolylmethane induces apoptosis in human cancer cells. *Biochem Biophys Res Commun* **228**(1): 153-158.
- Gelmann EP. 2002. Molecular biology of the androgen receptor. *J Clin Oncol* **20**(13): 3001-3015.
- Giampietri C, Petrunaro S, Padula F, D'Alessio A, Marini ES, Facchiano A, Filippini A, Ziparo E. 2012. Autophagy modulators sensitize prostate epithelial cancer cell lines to TNF-alpha-dependent apoptosis. *Apoptosis* **17**(11): 1210-1222.
- Gibadulinova A, Pastorek M, Filipcik P, Radvak P, Csaderova L, Vojtesek B, Pastorekova S. 2016. Cancer-associated S100P protein binds and inactivates p53, permits therapy-induced senescence and supports chemoresistance. *Oncotarget* **7**(16): 22508-22522.
- Gioeli DG. 2010. The promise of novel androgen receptor antagonists. *Cell Cycle* **9**(3): 440-441.
- Gittes RF. 1991. Carcinoma of the prostate. *N Engl J Med* **324**(4): 236-245.
- Gleason DF. 1966. Classification of prostatic carcinomas. *Cancer Chemother Rep* **50**(3): 125-128.
- Glick D, Barth S, Macleod KF. 2010. Autophagy: cellular and molecular mechanisms. *J Pathol* **221**(1): 3-12.
- Goldberg AA, Draz H, Montes-Grajales D, Olivero-Verbel J, Safe SH, Sanderson JT. 2015. 3,3'-Diindolylmethane (DIM) and its ring-substituted halogenated analogs (ring-DIMs) induce differential mechanisms of survival and death in androgen-dependent and -independent prostate cancer cells. *Genes Cancer* **6**(5-6): 265-280.
- Goldberg AA, Titorenko VI, Beach A, Abdelbaqi K, Safe S, Sanderson JT. 2013. Ring-substituted analogs of 3,3'-diindolylmethane (DIM) induce apoptosis and necrosis in androgen-dependent and -independent prostate cancer cells. *Invest New Drugs*.
- . 2014. Ring-substituted analogs of 3,3'-diindolylmethane (DIM) induce apoptosis and necrosis in androgen-dependent and -independent prostate cancer cells. *Invest New Drugs* **32**(1): 25-36.
- Goswami S, Aparicio A, Subudhi SK. 2016. Immune Checkpoint Therapies in Prostate Cancer. *Cancer J* **22**(2): 117-120.

- Greene FL. 2002. AJCC cancer staging manual. *New York; London: Springer, 6th edition.*
- Groves-Kirkby N. 2010. Prostate cancer. Immunotherapy and combined chemotherapy for castration-resistant and metastatic disease. *Nat Rev Urol* **7**(9): 472.
- Guan X. 2015. Cancer metastases: challenges and opportunities. *Acta Pharm Sin B* **5**(5): 402-418.
- Guo JY, Chen HY, Mathew R, Fan J, Strohecker AM, Karsli-Uzunbas G, Kamphorst JJ, Chen G, Lemons JM, Karantza V et al. 2011. Activated Ras requires autophagy to maintain oxidative metabolism and tumorigenesis. *Genes Dev* **25**(5): 460-470.
- Gurova KV, Rokhlin OW, Budanov AV, Burdelya LG, Chumakov PM, Cohen MB, Gudkov AV. 2003. Cooperation of two mutant p53 alleles contributes to Fas resistance of prostate carcinoma cells. *Cancer Res* **63**(11): 2905-2912.
- Ha S, Ruoff R, Kahoud N, Franke TF, Logan SK. 2011. Androgen receptor levels are upregulated by Akt in prostate cancer. *Endocr Relat Cancer* **18**(2): 245-255.
- Hanahan D, Weinberg RA. 2011. Hallmarks of cancer: the next generation. *Cell* **144**(5): 646-674.
- Hardie DG. 2011. AMPK and autophagy get connected. *EMBO J* **30**(4): 634-635.
- Harnden P, Shelley MD, Coles B, Staffurth J, Mason MD. 2007. Should the Gleason grading system for prostate cancer be modified to account for high-grade tertiary components? A systematic review and meta-analysis. *Lancet Oncol* **8**(5): 411-419.
- Hartwell LH, Weinert TA. 1989. Checkpoints: controls that ensure the order of cell cycle events. *Science* **246**(4930): 629-634.
- Hassan M, Watari H, AbuAlmaaty A, Ohba Y, Sakuragi N. 2014. Apoptosis and molecular targeting therapy in cancer. *Biomed Res Int* **2014**: 150845.
- Hawley SA, Pan DA, Mustard KJ, Ross L, Bain J, Edelman AM, Frenguelli BG, Hardie DG. 2005. Calmodulin-dependent protein kinase kinase-beta is an alternative upstream kinase for AMP-activated protein kinase. *Cell Metab* **2**(1): 9-19.
- Hayat MJ, Howlader N, Reichman ME, Edwards BK. 2007. Cancer statistics, trends, and multiple primary cancer analyses from the Surveillance, Epidemiology, and End Results (SEER) Program. *Oncologist* **12**(1): 20-37.
- He B, Lu N, Zhou Z. 2009. Cellular and nuclear degradation during apoptosis. *Curr Opin Cell Biol* **21**(6): 900-912.
- Heath EI, Heilbrun LK, Li J, Vaishampayan U, Harper F, Pemberton P, Sarkar FH. 2010. A phase I dose-escalation study of oral BR-DIM (BioResponse 3,3'-Diindolylmethane) in castrate-resistant, non-metastatic prostate cancer. *Am J Transl Res* **2**(4): 402-411.
- Hegemann M, Stenzl A, Bedke J, Chi KN, Black PC, Todenhofer T. 2016. Liquid biopsy: ready to guide therapy in advanced prostate cancer? *BJU Int* **118**(6): 855-863.
- Hodi FS, O'Day SJ, McDermott DF, Weber RW, Sosman JA, Haanen JB, Gonzalez R, Robert C, Schadendorf D, Hassel JC et al. 2010. Improved survival with ipilimumab in patients with metastatic melanoma. *N Engl J Med* **363**(8): 711-723.

- Holler N, Zaru R, Micheau O, Thome M, Attinger A, Valitutti S, Bodmer JL, Schneider P, Seed B, Tschopp J. 2000. Fas triggers an alternative, caspase-8-independent cell death pathway using the kinase RIP as effector molecule. *Nat Immunol* **1**(6): 489-495.
- Hollien J, Weissman JS. 2006. Decay of endoplasmic reticulum-localized mRNAs during the unfolded protein response. *Science* **313**(5783): 104-107.
- Hong C, Kim HA, Firestone GL, Bjeldanes LF. 2002. 3,3'-Diindolylmethane (DIM) induces a G(1) cell cycle arrest in human breast cancer cells that is accompanied by Sp1-mediated activation of p21(WAF1/CIP1) expression. *Carcinogenesis* **23**(8): 1297-1305.
- Horbinski C, Mojesky C, Kyprianou N. 2010. Live free or die: tales of homeless (cells) in cancer. *Am J Pathol* **177**(3): 1044-1052.
- Horoszewicz JS, Leong SS, Chu TM, Wajsman ZL, Friedman M, Papsidero L, Kim U, Chai LS, Kakati S, Arya SK et al. 1980. The LNCaP cell line--a new model for studies on human prostatic carcinoma. *Prog Clin Biol Res* **37**: 115-132.
- Howard N, Clementino M, Kim D, Wang L, Verma A, Shi X, Zhang Z, DiPaola RS. 2018. New developments in mechanisms of prostate cancer progression. *Semin Cancer Biol*.
- Hsu JC, Zhang J, Dev A, Wing A, Bjeldanes LF, Firestone GL. 2005. Indole-3-carbinol inhibition of androgen receptor expression and downregulation of androgen responsiveness in human prostate cancer cells. *Carcinogenesis* **26**(11): 1896-1904.
- Hu G, Wei Y, Kang Y. 2009. The multifaceted role of MTDH/AEG-1 in cancer progression. *Clin Cancer Res* **15**(18): 5615-5620.
- Huang X, Chen Y, Zhang H, Ma Q, Zhang YW, Xu H. 2012. Salubrinal attenuates beta-amyloid-induced neuronal death and microglial activation by inhibition of the NF-kappaB pathway. *Neurobiol Aging* **33**(5): 1007 e1009-1017.
- Hussain M, Fizazi K, Saad F, Rathenborg P, Shore N, Ferreira U, Ivashchenko P, Demirhan E, Modelska K, Phung et al. 2018. Enzalutamide in Men with Nonmetastatic, Castration-Resistant Prostate Cancer. *N Engl J Med* **378**(26): 2465-2474.
- Hwang C, Sethi S, Heilbrun LK, Gupta NS, Chitale DA, Sakr WA, Menon M, Peabody JO, Smith DW, Sarkar FH et al. 2016. Anti-androgenic activity of absorption-enhanced 3, 3'-diindolylmethane in prostatectomy patients. *Am J Transl Res* **8**(1): 166-176.
- Ide H, Lu Y, Yu J, Noguchi T, Kanayama M, Muto S, Yamaguchi R, Kawato S, Horie S. 2017. Aryl hydrocarbon receptor signaling involved in the invasiveness of LNCaP cells. *Hum Cell* **30**(2): 133-139.
- Inoki K, Zhu T, Guan KL. 2003. TSC2 mediates cellular energy response to control cell growth and survival. *Cell* **115**(5): 577-590.
- Iurlaro R, Munoz-Pinedo C. 2016. Cell death induced by endoplasmic reticulum stress. *FEBS J* **283**(14): 2640-2652.
- Jana NR, Sarkar S, Ishizuka M, Yonemoto J, Tohyama C, Sone H. 1999. Cross-talk between 2,3,7,8-tetrachlorodibenzo-p-dioxin and testosterone signal transduction pathways in LNCaP prostate cancer cells. *Biochem Biophys Res Commun* **256**(3): 462-468.

- Jin Y. 2011. 3,3'-Diindolylmethane inhibits breast cancer cell growth via miR-21-mediated Cdc25A degradation. *Mol Cell Biochem* **358**(1-2): 345-354.
- Jung CH, Ro SH, Cao J, Otto NM, Kim DH. 2010. mTOR regulation of autophagy. *FEBS Lett* **584**(7): 1287-1295.
- Kaighn ME, Narayan KS, Ohnuki Y, Lechner JF, Jones LW. 1979. Establishment and characterization of a human prostatic carcinoma cell line (PC-3). *Invest Urol* **17**(1): 16-23.
- Kandala PK, Srivastava SK. 2012a. Diindolylmethane-mediated Gli1 protein suppression induces anoikis in ovarian cancer cells in vitro and blocks tumor formation ability in vivo. *J Biol Chem* **287**(34): 28745-28754.
- 2012b. Regulation of macroautophagy in ovarian cancer cells in vitro and in vivo by controlling glucose regulatory protein 78 and AMPK. *Oncotarget* **3**(4): 435-449.
- Kandala PK, Wright SE, Srivastava SK. 2012. Blocking epidermal growth factor receptor activation by 3,3'-diindolylmethane suppresses ovarian tumor growth in vitro and in vivo. *J Pharmacol Exp Ther* **341**(1): 24-32.
- Karantza-Wadsworth V, Patel S, Kravchuk O, Chen G, Mathew R, Jin S, White E. 2007. Autophagy mitigates metabolic stress and genome damage in mammary tumorigenesis. *Genes Dev* **21**(13): 1621-1635.
- Kassi E, Moutsatsou P. 2011. Glucocorticoid receptor signaling and prostate cancer. *Cancer Lett* **302**(1): 1-10.
- Kessel D. 2006. Protection of Bcl-2 by salubrinal. *Biochem Biophys Res Commun* **346**(4): 1320-1323.
- Khwaja FS, Wynne S, Posey I, Djakiew D. 2009. 3,3'-diindolylmethane induction of p75^{NTR}-dependent cell death via the p38 mitogen-activated protein kinase pathway in prostate cancer cells. *Cancer Prev Res (Phila)* **2**(6): 566-571.
- Kikuno N, Shiina H, Urakami S, Kawamoto K, Hirata H, Tanaka Y, Place RF, Pookot D, Majid S, Igawa M et al. 2007. Knockdown of astrocyte-elevated gene-1 inhibits prostate cancer progression through upregulation of FOXO3a activity. *Oncogene* **26**(55): 7647-7655.
- Kim EJ, Park SY, Shin HK, Kwon DY, Surh YJ, Park JH. 2007. Activation of caspase-8 contributes to 3,3'-Diindolylmethane-induced apoptosis in colon cancer cells. *J Nutr* **137**(1): 31-36.
- Kim J, Kundu M, Viollet B, Guan KL. 2011. AMPK and mTOR regulate autophagy through direct phosphorylation of Ulk1. *Nat Cell Biol* **13**(2): 132-141.
- Kim MK, Park JH. 2009a. Conference on "Multidisciplinary approaches to nutritional problems". Symposium on "Nutrition and health". Cruciferous vegetable intake and the risk of human cancer: epidemiological evidence. *Proc Nutr Soc* **68**(1): 103-110.
- 2009b. Cruciferous vegetable intake and the risk of human cancer: epidemiological evidence. *Proc Nutr Soc* **68**(1): 103-110.
- Kim YH, Kwon HS, Kim DH, Shin EK, Kang YH, Park JH, Shin HK, Kim JK. 2009. 3,3'-diindolylmethane attenuates colonic inflammation and tumorigenesis in mice. *Inflamm Bowel Dis* **15**(8): 1164-1173.

- Kimura T, Takabatake Y, Takahashi A, Isaka Y. 2013. Chloroquine in cancer therapy: a double-edged sword of autophagy. *Cancer Res* **73**(1): 3-7.
- Kirsh VA, Peters U, Mayne ST, Subar AF, Chatterjee N, Johnson CC, Hayes RB, Prostate LC, Ovarian Cancer Screening T. 2007. Prospective study of fruit and vegetable intake and risk of prostate cancer. *J Natl Cancer Inst* **99**(15): 1200-1209.
- Kiselev VI, Drukh VM, Muiyzhnek EL, Kuznetsov IN, Pchelintseva OI, Paltsev MA. 2014. Preclinical antitumor activity of the diindolylmethane formulation in xenograft mouse model of prostate cancer. *Exp Oncol* **36**(2): 90-93.
- Klionsky DJ. 2010. The molecular machinery of autophagy and its role in physiology and disease. *Semin Cell Dev Biol* **21**(7): 663.
- Klionsky DJ, Emr SD. 2000. Autophagy as a regulated pathway of cellular degradation. *Science* **290**(5497): 1717-1721.
- Knudsen ES, Knudsen KE. 2006. Retinoblastoma tumor suppressor: where cancer meets the cell cycle. *Exp Biol Med (Maywood)* **231**(7): 1271-1281.
- Kong D, Banerjee S, Huang W, Li Y, Wang Z, Kim HR, Sarkar FH. 2008. Mammalian target of rapamycin repression by 3,3'-diindolylmethane inhibits invasion and angiogenesis in platelet-derived growth factor-D-overexpressing PC3 cells. *Cancer Res* **68**(6): 1927-1934.
- Kroemer G, Galluzzi L, Brenner C. 2007. Mitochondrial membrane permeabilization in cell death. *Physiol Rev* **87**(1): 99-163.
- Kuban DA, Thames HD, Levy LB, Horwitz EM, Kupelian PA, Martinez AA, Michalski JM, Pisansky TM, Sandler HM, Shipley WU et al. 2003. Long-term multi-institutional analysis of stage T1-T2 prostate cancer treated with radiotherapy in the PSA era. *Int J Radiat Oncol Biol Phys* **57**(4): 915-928.
- Kung HCN, G.; Yang, J.C.; Evans, C.P.; Bold, R.J.; Chuang, F. 2013. Autophagy and Prostate Cancer Therapeutics. In: *Tindall, DJ, editor Prostate Cancer Springer; New York* **16**: 497-518.
- Kwon ED, Foster BA, Hurwitz AA, Madias C, Allison JP, Greenberg NM, Burg MB. 1999. Elimination of residual metastatic prostate cancer after surgery and adjunctive cytotoxic T lymphocyte-associated antigen 4 (CTLA-4) blockade immunotherapy. *Proc Natl Acad Sci U S A* **96**(26): 15074-15079.
- Lahat G, Tuvin D, Wei C, Wang WL, Pollock RE, Anaya DA, Bekele BN, Corely L, Lazar AJ, Pisters PW et al. 2010. Molecular prognosticators of complex karyotype soft tissue sarcoma outcome: a tissue microarray-based study. *Ann Oncol* **21**(5): 1112-1120.
- Laster SM, Wood JG, Gooding LR. 1988. Tumor necrosis factor can induce both apoptic and necrotic forms of cell lysis. *J Immunol* **141**(8): 2629-2634.
- Le HT, Schaldach CM, Firestone GL, Bjeldanes LF. 2003. Plant-derived 3,3'-diindolylmethane is a strong androgen antagonist in human prostate cancer cells. *J Biol Chem* **278**(23): 21136-21145.
- Leao R, Domingos C, Figueiredo A, Hamilton R, Tabori U, Castelo-Branco P. 2017. Cancer Stem Cells in Prostate Cancer: Implications for Targeted Therapy. *Urol Int* **99**(2): 125-136.

- Leav I, McNeal JE, Ziar J, Alroy J. 1998. The localization of transforming growth factor alpha and epidermal growth factor receptor in stromal and epithelial compartments of developing human prostate and hyperplastic, dysplastic, and carcinomatous lesions. *Hum Pathol* **29**(7): 668-675.
- Leber MF, Efferth T. 2009. Molecular principles of cancer invasion and metastasis (review). *Int J Oncol* **34**(4): 881-895.
- Lee-Robichaud P, Wright JN, Akhtar ME, Akhtar M. 1995. Modulation of the activity of human 17 alpha-hydroxylase-17,20-lyase (CYP17) by cytochrome b5: endocrinological and mechanistic implications. *Biochem J* **308** (Pt 3): 901-908.
- Lee EW, Seo J, Jeong M, Lee S, Song J. 2012a. The roles of FADD in extrinsic apoptosis and necroptosis. *BMB Rep* **45**(9): 496-508.
- Lee HJ, Jung DB, Sohn EJ, Kim HH, Park MN, Lew JH, Lee SG, Kim B, Kim SH. 2012b. Inhibition of Hypoxia Inducible Factor Alpha and Astrocyte-Elevated Gene-1 Mediates Cryptotanshinone Exerted Antitumor Activity in Hypoxic PC-3 Cells. *Evid Based Complement Alternat Med* **2012**: 390957.
- Lee M, Lee JS. 2014. Exploiting tumor cell senescence in anticancer therapy. *BMB Rep* **47**(2): 51-59.
- Lee SG, Jeon HY, Su ZZ, Richards JE, Vozhilla N, Sarkar D, Van Maerken T, Fisher PB. 2009. Astrocyte elevated gene-1 contributes to the pathogenesis of neuroblastoma. *Oncogene* **28**(26): 2476-2484.
- Lee SG, Su ZZ, Emdad L, Sarkar D, Fisher PB. 2006. Astrocyte elevated gene-1 (AEG-1) is a target gene of oncogenic Ha-ras requiring phosphatidylinositol 3-kinase and c-Myc. *Proc Natl Acad Sci U S A* **103**(46): 17390-17395.
- Lehmann BD, McCubrey JA, Jefferson HS, Paine MS, Chappell WH, Terrian DM. 2007. A dominant role for p53-dependent cellular senescence in radiosensitization of human prostate cancer cells. *Cell Cycle* **6**(5): 595-605.
- Leland W. K. Chung WBI, and Jonathan W. Simons. 2007. *Prostate Cancer: Biology, Genetics, and the New Therapeutics*. Springer, New York.
- Levine AC, Kirschenbaum A, Droller M, Gabilove JL. 1991. Effect of the addition of estrogen to medical castration on prostatic size, symptoms, histology and serum prostate specific antigen in 4 men with benign prostatic hypertrophy. *J Urol* **146**(3): 790-793.
- Levy JMM, Towers CG, Thorburn A. 2017. Targeting autophagy in cancer. *Nat Rev Cancer* **17**(9): 528-542.
- Li F, Chen C, Chen SM, Xiao BK, Tao ZZ. 2016. ERK signaling mediates long-term low concentration 3,3'-diindolylmethane inhibited nasopharyngeal carcinoma growth and metastasis: An in vitro and in vivo study. *Oncol Rep* **35**(2): 955-961.
- Li Y, Wang Z, Kong D, Murthy S, Dou QP, Sheng S, Reddy GP, Sarkar FH. 2007. Regulation of FOXO3a/beta-catenin/GSK-3beta signaling by 3,3'-diindolylmethane contributes to inhibition of cell proliferation and induction of apoptosis in prostate cancer cells. *J Biol Chem* **282**(29): 21542-21550.

- Liang XH, Jackson S, Seaman M, Brown K, Kempkes B, Hibshoosh H, Levine B. 1999. Induction of autophagy and inhibition of tumorigenesis by beclin 1. *Nature* **402**(6762): 672-676.
- Liao X, Thrasher JB, Holzbeierlein J, Stanley S, Li B. 2004. Glycogen synthase kinase-3beta activity is required for androgen-stimulated gene expression in prostate cancer. *Endocrinology* **145**(6): 2941-2949.
- Linja MJ, Savinainen KJ, Saramaki OR, Tammela TL, Vessella RL, Visakorpi T. 2001. Amplification and overexpression of androgen receptor gene in hormone-refractory prostate cancer. *Cancer Res* **61**(9): 3550-3555.
- Liu X, Wang D, Liu H, Feng Y, Zhu T, Zhang L, Zhu B, Zhang Y. 2014. Knockdown of astrocyte elevated gene-1 (AEG-1) in cervical cancer cells decreases their invasiveness, epithelial to mesenchymal transition, and chemoresistance. *Cell Cycle* **13**(11): 1702-1707.
- Liu Y, Templeton DM. 2008. Initiation of caspase-independent death in mouse mesangial cells by Cd2+: involvement of p38 kinase and CaMK-II. *J Cell Physiol* **217**(2): 307-318.
- Logue SE, Martin SJ. 2008. Caspase activation cascades in apoptosis. *Biochem Soc Trans* **36**(Pt 1): 1-9.
- Lorin S, Hamai A, Mehrpour M, Codogno P. 2013. Autophagy regulation and its role in cancer. *Semin Cancer Biol* **23**(5): 361-379.
- Lukas J, Bartkova J, Rohde M, Strauss M, Bartek J. 1995. Cyclin D1 is dispensable for G1 control in retinoblastoma gene-deficient cells independently of cdk4 activity. *Mol Cell Biol* **15**(5): 2600-2611.
- MacInnis RJ, English DR. 2006. Body size and composition and prostate cancer risk: systematic review and meta-regression analysis. *Cancer Causes Control* **17**(8): 989-1003.
- Mao K, Klionsky DJ. 2011. AMPK activates autophagy by phosphorylating ULK1. *Circ Res* **108**(7): 787-788.
- Markozannes G, Tzoulaki I, Karli D, Evangelou E, Ntzani E, Gunter MJ, Norat T, Ioannidis JP, Tsilidis KK. 2016. Diet, body size, physical activity and risk of prostate cancer: An umbrella review of the evidence. *Eur J Cancer* **69**: 61-69.
- Martinez-Cayuela M. 1995. Oxygen free radicals and human disease. *Biochimie* **77**(3): 147-161.
- Matas D, Sigal A, Stambolsky P, Milyavsky M, Weisz L, Schwartz D, Goldfinger N, Rotter V. 2001. Integrity of the N-terminal transcription domain of p53 is required for mutant p53 interference with drug-induced apoptosis. *EMBO J* **20**(15): 4163-4172.
- Mathew R, Karp CM, Beaudoin B, Vuong N, Chen G, Chen HY, Bray K, Reddy A, Bhanot G, Gelinis C et al. 2009. Autophagy suppresses tumorigenesis through elimination of p62. *Cell* **137**(6): 1062-1075.
- McCubrey JA, Lahair MM, Franklin RA. 2006. Reactive oxygen species-induced activation of the MAP kinase signaling pathways. *Antioxid Redox Signal* **8**(9-10): 1775-1789.
- McKenna NJ, Lanz RB, O'Malley BW. 1999. Nuclear receptor coregulators: cellular and molecular biology. *Endocr Rev* **20**(3): 321-344.
- Mehlen P, Puisieux A. 2006. Metastasis: a question of life or death. *Nat Rev Cancer* **6**(6): 449-458.

- Meijer AJ, Codogno P. 2007. AMP-activated protein kinase and autophagy. *Autophagy* **3**(3): 238-240.
- Miller WL, Auchus RJ. 2011. The molecular biology, biochemistry, and physiology of human steroidogenesis and its disorders. *Endocr Rev* **32**(1): 81-151.
- Miller WR, Jackson J. 2003. The therapeutic potential of aromatase inhibitors. *Expert Opin Investig Drugs* **12**(3): 337-351.
- Miyamoto H, Messing EM, Chang C. 2004. Androgen deprivation therapy for prostate cancer: current status and future prospects. *Prostate* **61**(4): 332-353.
- Mizushima N, Ohsumi Y, Yoshimori T. 2002. Autophagosome formation in mammalian cells. *Cell Struct Funct* **27**(6): 421-429.
- Mizushima N, Yoshimori T, Ohsumi Y. 2011. The role of Atg proteins in autophagosome formation. *Annu Rev Cell Dev Biol* **27**: 107-132.
- Montgomery RB, Mostaghel EA, Vessella R, Hess DL, Kalhorn TF, Higano CS, True LD, Nelson PS. 2008. Maintenance of intratumoral androgens in metastatic prostate cancer: a mechanism for castration-resistant tumor growth. *Cancer Res* **68**(11): 4447-4454.
- Morrison AH, Byrne KT, Vonderheide RH. 2018. Immunotherapy and Prevention of Pancreatic Cancer. *Trends Cancer* **4**(6): 418-428.
- Morselli E, Galluzzi L, Kepp O, Vicencio JM, Criollo A, Maiuri MC, Kroemer G. 2009. Anti- and pro-tumor functions of autophagy. *Biochim Biophys Acta* **1793**(9): 1524-1532.
- Mounir Z, Krishnamoorthy JL, Wang S, Papadopoulou B, Campbell S, Muller WJ, Hatzoglou M, Koromilas AE. 2011. Akt determines cell fate through inhibition of the PERK-eIF2alpha phosphorylation pathway. *Sci Signal* **4**(192): ra62.
- Muilenburg D, Parsons C, Coates J, Virudachalam S, Bold RJ. 2014. Role of autophagy in apoptotic regulation by Akt in pancreatic cancer. *Anticancer Res* **34**(2): 631-637.
- Mulders PF, De Santis M, Powles T, Fizazi K. 2015. Targeted treatment of metastatic castration-resistant prostate cancer with sipuleucel-T immunotherapy. *Cancer Immunol Immunother* **64**(6): 655-663.
- Murillo G, Mehta RG. 2001. Cruciferous vegetables and cancer prevention. *Nutr Cancer* **41**(1-2): 17-28.
- Murphy KL, Dennis AP, Rosen JM. 2000. A gain of function p53 mutant promotes both genomic instability and cell survival in a novel p53-null mammary epithelial cell model. *FASEB J* **14**(14): 2291-2302.
- Murray AW. 2004. Recycling the cell cycle: cyclins revisited. *Cell* **116**(2): 221-234.
- Nachshon-Kedmi M, Fares FA, Yannai S. 2004a. Therapeutic activity of 3,3'-diindolylmethane on prostate cancer in an in vivo model. *Prostate* **61**(2): 153-160.
- Nachshon-Kedmi M, Yannai S, Fares FA. 2004b. Induction of apoptosis in human prostate cancer cell line, PC3, by 3,3'-diindolylmethane through the mitochondrial pathway. *Br J Cancer* **91**(7): 1358-1363.

- Nadal R, Bellmunt J. 2016. The evolving role of enzalutamide on the treatment of prostate cancer. *Future Oncol* **12**(5): 607-616.
- Nakahira K, Choi AM. 2013. Autophagy: a potential therapeutic target in lung diseases. *Am J Physiol Lung Cell Mol Physiol* **305**(2): L93-107.
- Narashimamurthy J, Rao AR, Sastry GN. 2004. Aromatase inhibitors: a new paradigm in breast cancer treatment. *Curr Med Chem Anticancer Agents* **4**(6): 523-534.
- Nazio F, Strappazon F, Antonioli M, Bielli P, Cianfanelli V, Bordi M, Gretzmeier C, Dengjel J, Piacentini M, Fimia GM et al. 2013. mTOR inhibits autophagy by controlling ULK1 ubiquitylation, self-association and function through AMBRA1 and TRAF6. *Nat Cell Biol* **15**(4): 406-416.
- Nguyen HG, Yang JC, Kung HJ, Shi XB, Tilki D, Lara PN, Jr., DeVere White RW, Gao AC, Evans CP. 2014. Targeting autophagy overcomes Enzalutamide resistance in castration-resistant prostate cancer cells and improves therapeutic response in a xenograft model. *Oncogene* **33**(36): 4521-4530.
- Ni J, Cozzi P, Hao J, Duan W, Graham P, Kearsley J, Li Y. 2014. Cancer stem cells in prostate cancer chemoresistance. *Curr Cancer Drug Targets* **14**(3): 225-240.
- Nicastro HL, Firestone GL, Bjeldanes LF. 2013. 3,3'-diindolylmethane rapidly and selectively inhibits hepatocyte growth factor/c-Met signaling in breast cancer cells. *J Nutr Biochem* **24**(11): 1882-1888.
- Nishiyama T, Hashimoto Y, Takahashi K. 2004. The influence of androgen deprivation therapy on dihydrotestosterone levels in the prostatic tissue of patients with prostate cancer. *Clin Cancer Res* **10**(21): 7121-7126.
- Ojha R, Jha V, Singh SK, Bhattacharyya S. 2014. Autophagy inhibition suppresses the tumorigenic potential of cancer stem cell enriched side population in bladder cancer. *Biochim Biophys Acta* **1842**(11): 2073-2086.
- Okino ST, Pookot D, Basak S, Dahiya R. 2009. Toxic and chemopreventive ligands preferentially activate distinct aryl hydrocarbon receptor pathways: implications for cancer prevention. *Cancer Prev Res (Phila)* **2**(3): 251-256.
- Olivier M, Hollstein M, Hainaut P. 2010. TP53 mutations in human cancers: origins, consequences, and clinical use. *Cold Spring Harb Perspect Biol* **2**(1): a001008.
- Ouyang DY, Xu LH, He XH, Zhang YT, Zeng LH, Cai JY, Ren S. 2013. Autophagy is differentially induced in prostate cancer LNCaP, DU145 and PC-3 cells via distinct splicing profiles of ATG5. *Autophagy* **9**(1): 20-32.
- Ouyang L, Shi Z, Zhao S, Wang FT, Zhou TT, Liu B, Bao JK. 2012. Programmed cell death pathways in cancer: a review of apoptosis, autophagy and programmed necrosis. *Cell Prolif* **45**(6): 487-498.
- Ozoren N, El-Deiry WS. 2002. Defining characteristics of Types I and II apoptotic cells in response to TRAIL. *Neoplasia* **4**(6): 551-557.
- Paltsev M, Kiselev V, Drukh V, Muiyzhnek E, Kuznetsov I, Andrianova E, Baranovskiy P. 2016. First results of the double-blind randomized placebo-controlled multicenter clinical trial of

- DIM-based therapy designed as personalized approach to reverse prostatic intraepithelial neoplasia (PIN). *EPMA J* **7**: 5.
- Pantel K, Alix-Panabieres C. 2012. The potential of circulating tumor cells as a liquid biopsy to guide therapy in prostate cancer. *Cancer Discov* **2**(11): 974-975.
- Pappa G, Lichtenberg M, Iori R, Barillari J, Bartsch H, Gerhauser C. 2006. Comparison of growth inhibition profiles and mechanisms of apoptosis induction in human colon cancer cell lines by isothiocyanates and indoles from Brassicaceae. *Mutat Res* **599**(1-2): 76-87.
- Pariyani R, Ismail IS, Azam AA, Abas F, Shaari K, Sulaiman MR. 2015. Phytochemical Screening and Acute Oral Toxicity Study of Java Tea Leaf Extracts. *Biomed Res Int* **2015**: 742420.
- Park EJ, Min KJ, Choi KS, Kubatka P, Kruzliak P, Kim DE, Kwon TK. 2016. Chloroquine enhances TRAIL-mediated apoptosis through up-regulation of DR5 by stabilization of mRNA and protein in cancer cells. *Sci Rep* **6**: 22921.
- Parzych KR, Klionsky DJ. 2014. An overview of autophagy: morphology, mechanism, and regulation. *Antioxid Redox Signal* **20**(3): 460-473.
- Peng CY, Graves PR, Thoma RS, Wu Z, Shaw AS, Piwnica-Worms H. 1997. Mitotic and G2 checkpoint control: regulation of 14-3-3 protein binding by phosphorylation of Cdc25C on serine-216. *Science* **277**(5331): 1501-1505.
- Perdew GH, Bradfield CA. 1996. Mapping the 90 kDa heat shock protein binding region of the Ah receptor. *Biochem Mol Biol Int* **39**(3): 589-593.
- Pocar P, Fischer B, Klonisch T, Hombach-Klonisch S. 2005. Molecular interactions of the aryl hydrocarbon receptor and its biological and toxicological relevance for reproduction. *Reproduction* **129**(4): 379-389.
- Polakis P. 2000. Wnt signaling and cancer. *Genes Dev* **14**(15): 1837-1851.
- Pollenz RS. 1996. The aryl-hydrocarbon receptor, but not the aryl-hydrocarbon receptor nuclear translocator protein, is rapidly depleted in hepatic and nonhepatic culture cells exposed to 2,3,7,8-tetrachlorodibenzo-p-dioxin. *Mol Pharmacol* **49**(3): 391-398.
- Portt L, Norman G, Clapp C, Greenwood M, Greenwood MT. 2011. Anti-apoptosis and cell survival: a review. *Biochim Biophys Acta* **1813**(1): 238-259.
- Potter VR. 1980. Initiation and promotion in cancer formation: the importance of studies on intercellular communication. *Yale J Biol Med* **53**(5): 367-384.
- Powolny AA, Bommareddy A, Hahm ER, Normolle DP, Beumer JH, Nelson JB, Singh SV. 2011. Chemopreventative potential of the cruciferous vegetable constituent phenethyl isothiocyanate in a mouse model of prostate cancer. *J Natl Cancer Inst* **103**(7): 571-584.
- Qian X, Song JM, Melkamu T, Upadhyaya P, Kassie F. 2013. Chemoprevention of lung tumorigenesis by intranasally administered diindolylmethane in A/J mice. *Carcinogenesis* **34**(4): 841-849.
- Qin J, Liu X, Laffin B, Chen X, Choy G, Jeter CR, Calhoun-Davis T, Li H, Palapattu GS, Pang S et al. 2012. The PSA(-/lo) prostate cancer cell population harbors self-renewing long-term tumor-propagating cells that resist castration. *Cell Stem Cell* **10**(5): 556-569.

- Qu X, Yu J, Bhagat G, Furuya N, Hibshoosh H, Troxel A, Rosen J, Eskelinen EL, Mizushima N, Ohsumi Y et al. 2003. Promotion of tumorigenesis by heterozygous disruption of the beclin 1 autophagy gene. *J Clin Invest* **112**(12): 1809-1820.
- Quigley CA, De Bellis A, Marschke KB, el-Awady MK, Wilson EM, French FS. 1995. Androgen receptor defects: historical, clinical, and molecular perspectives. *Endocr Rev* **16**(3): 271-321.
- Radogna F, Cerella C, Gaigneaux A, Christov C, Dicato M, Diederich M. 2015. Cell type-dependent ROS and mitophagy response leads to apoptosis or necroptosis in neuroblastoma. *Oncogene*.
- Rahman KM, Banerjee S, Ali S, Ahmad A, Wang Z, Kong D, Sakr WA. 2009. 3,3'-Diindolylmethane enhances taxotere-induced apoptosis in hormone-refractory prostate cancer cells through survivin down-regulation. *Cancer Res* **69**(10): 4468-4475.
- Rahman KW, Sarkar FH. 2005. Inhibition of nuclear translocation of nuclear factor- κ B contributes to 3,3'-diindolylmethane-induced apoptosis in breast cancer cells. *Cancer Res* **65**(1): 364-371.
- Recouvreux MV, Wu B, Gao AC, Zonis S, Chesnokova V, Bhowmick N, Chung LW, Melmed S. 2017. Androgen receptor regulation of local growth hormone in prostate cancer cells. *Endocrinology*.
- Reed GA, Arneson DW, Putnam WC, Smith HJ, Gray JC, Sullivan DK, Mayo MS, Crowell JA, Hurwitz A. 2006. Single-dose and multiple-dose administration of indole-3-carbinol to women: pharmacokinetics based on 3,3'-diindolylmethane. *Cancer Epidemiol Biomarkers Prev* **15**(12): 2477-2481.
- Richmond O, Ghotbaddini M, Allen C, Walker A, Zahir S, Powell JB. 2014. The aryl hydrocarbon receptor is constitutively active in advanced prostate cancer cells. *PLoS One* **9**(4): e95058.
- Risbridger GP, Bianco JJ, Ellem SJ, McPherson SJ. 2003. Oestrogens and prostate cancer. *Endocr Relat Cancer* **10**(2): 187-191.
- Robbins AS, Whittemore AS, Van Den Eeden SK. 1998. Race, prostate cancer survival, and membership in a large health maintenance organization. *J Natl Cancer Inst* **90**(13): 986-990.
- Robinson D, Van Allen EM, Wu YM, Schultz N, Lonigro RJ, Mosquera JM, Montgomery B, Taplin ME, Pritchard CC, Attard G et al. 2015. Integrative clinical genomics of advanced prostate cancer. *Cell* **161**(5): 1215-1228.
- Rochette-Egly C. 2003. Nuclear receptors: integration of multiple signalling pathways through phosphorylation. *Cell Signal* **15**(4): 355-366.
- Rokhlin OW, Taghiyev AF, Bayer KU, Bumcrot D, Koteliansk VE, Glover RA, Cohen MB. 2007. Calcium/calmodulin-dependent kinase II plays an important role in prostate cancer cell survival. *Cancer Biol Ther* **6**(5): 732-742.
- Ron D, Walter P. 2007. Signal integration in the endoplasmic reticulum unfolded protein response. *Nat Rev Mol Cell Biol* **8**(7): 519-529.
- Roninson IB. 2003. Tumor cell senescence in cancer treatment. *Cancer Res* **63**(11): 2705-2715.

- Rosenfeldt MT, O'Prey J, Morton JP, Nixon C, MacKay G, Mrowinska A, Au A, Rai TS, Zheng L, Ridgway R et al. 2013. p53 status determines the role of autophagy in pancreatic tumour development. *Nature* **504**(7479): 296-300.
- Rove KO, Crawford ED. 2014. Traditional androgen ablation approaches to advanced prostate cancer: new insights. *Can J Urol* **21**(2 Supp 1): 14-21.
- Russell PJ, Kingsley EA. 2003. Human prostate cancer cell lines. *Methods Mol Med* **81**: 21-39.
- Ryan CJ, Smith MR, Fong L, Rosenberg JE, Kantoff P, Raynaud F, Martins V, Lee G, Kheoh T, Kim J et al. 2010. Phase I clinical trial of the CYP17 inhibitor abiraterone acetate demonstrating clinical activity in patients with castration-resistant prostate cancer who received prior ketoconazole therapy. *J Clin Oncol* **28**(9): 1481-1488.
- Safe S. 2001. Molecular biology of the Ah receptor and its role in carcinogenesis. *Toxicol Lett* **120**(1-3): 1-7.
- Sak K. 2012. Chemotherapy and dietary phytochemical agents. *Chemother Res Pract* **2012**: 282570.
- Salas TR, Kim J, Vakar-Lopez F, Sabichi AL, Troncoso P, Jenster G, Kikuchi A, Chen SY, Shemshedini L, Suraokar M et al. 2004. Glycogen synthase kinase-3 beta is involved in the phosphorylation and suppression of androgen receptor activity. *J Biol Chem* **279**(18): 19191-19200.
- Saleem A, Dvorzhinski D, Santanam U, Mathew R, Bray K, Stein M, White E, DiPaola RS. 2012. Effect of dual inhibition of apoptosis and autophagy in prostate cancer. *Prostate* **72**(12): 1374-1381.
- Santoro R, Strano S, Blandino G. 2014. Transcriptional regulation by mutant p53 and oncogenesis. *Subcell Biochem* **85**: 91-103.
- Sato A, Klaunberg B, Tolwani R. 2004. In vivo bioluminescence imaging. *Comp Med* **54**(6): 631-634.
- Sayers TJ. 2011. Targeting the extrinsic apoptosis signaling pathway for cancer therapy. *Cancer Immunol Immunother* **60**(8): 1173-1180.
- Scarlatti F, Maffei R, Beau I, Codogno P, Ghidoni R. 2008. Role of non-canonical Beclin 1-independent autophagy in cell death induced by resveratrol in human breast cancer cells. *Cell Death Differ* **15**(8): 1318-1329.
- Scher HI, Fizazi K, Saad F, Taplin ME, Sternberg CN, Miller K, de Wit R, Mulders P, Chi KN, Shore ND et al. 2012. Increased survival with enzalutamide in prostate cancer after chemotherapy. *N Engl J Med* **367**(13): 1187-1197.
- Scher HI, Graf RP, Schreiber NA, McLaughlin B, Lu D, Louw J, Danila DC, Dugan L, Johnson A, Heller G et al. 2017. Nuclear-specific AR-V7 Protein Localization is Necessary to Guide Treatment Selection in Metastatic Castration-resistant Prostate Cancer. *Eur Urol* **71**(6): 874-882.
- Schiller JT, Lowy DR. 2010. Vaccines to prevent infections by oncoviruses. *Annu Rev Microbiol* **64**: 23-41.

- Schmitt CA. 2003. Senescence, apoptosis and therapy--cutting the lifelines of cancer. *Nat Rev Cancer* **3**(4): 286-295.
- Schmitt CA, Fridman JS, Yang M, Lee S, Baranov E, Hoffman RM, Lowe SW. 2002. A senescence program controlled by p53 and p16INK4a contributes to the outcome of cancer therapy. *Cell* **109**(3): 335-346.
- Schroder M, Kaufman RJ. 2005. The mammalian unfolded protein response. *Annu Rev Biochem* **74**: 739-789.
- Schweichel JU, Merker HJ. 1973. The morphology of various types of cell death in prenatal tissues. *Teratology* **7**(3): 253-266.
- Sethi N, Kang Y. 2011. Unravelling the complexity of metastasis - molecular understanding and targeted therapies. *Nat Rev Cancer* **11**(10): 735-748.
- Shankar S, Srivastava RK. 2004. Enhancement of therapeutic potential of TRAIL by cancer chemotherapy and irradiation: mechanisms and clinical implications. *Drug Resist Updat* **7**(2): 139-156.
- Shappell SB, Thomas GV, Roberts RL, Herbert R, Ittmann MM, Rubin MA, Humphrey PA, Sundberg JP, Rozengurt N, Barrios R et al. 2004. Prostate pathology of genetically engineered mice: definitions and classification. The consensus report from the Bar Harbor meeting of the Mouse Models of Human Cancer Consortium Prostate Pathology Committee. *Cancer Res* **64**(6): 2270-2305.
- Sharifi N, Auchus RJ. 2012. Steroid biosynthesis and prostate cancer. *Steroids* **77**(7): 719-726.
- Shaw RJ, Cantley LC. 2006. Ras, PI(3)K and mTOR signalling controls tumour cell growth. *Nature* **441**(7092): 424-430.
- Shen J, Chen X, Hendershot L, Prywes R. 2002. ER stress regulation of ATF6 localization by dissociation of BiP/GRP78 binding and unmasking of Golgi localization signals. *Dev Cell* **3**(1): 99-111.
- Shi X, Wang X. 2015a. The role of MTDH/AEG-1 in the progression of cancer. *International Journal of Clinical and Experimental Medicine* **8**(4): 4795-4807.
- . 2015b. The role of MTDH/AEG-1 in the progression of cancer. *Int J Clin Exp Med* **8**(4): 4795-4807.
- Siddiqui IA, Sanna V, Ahmad N, Sechi M, Mukhtar H. 2015. Resveratrol nanoformulation for cancer prevention and therapy. *Ann N Y Acad Sci* **1348**(1): 20-31.
- Siegel RL, Miller KD, Jemal A. 2016. Cancer statistics, 2016. *CA Cancer J Clin* **66**(1): 7-30.
- . 2017. Cancer Statistics, 2017. *CA Cancer J Clin* **67**(1): 7-30.
- Singh-Gupta V, Banerjee S, Yunker CK, Rakowski JT, Joiner MC, Konski AA, Sarkar FH, Hillman GG. 2012. B-DIM impairs radiation-induced survival pathways independently of androgen receptor expression and augments radiation efficacy in prostate cancer. *Cancer Lett* **318**(1): 86-92.
- Sinicrope FA. 2010. DNA mismatch repair and adjuvant chemotherapy in sporadic colon cancer. *Nat Rev Clin Oncol* **7**(3): 174-177.

- Skulachev VP. 2006. Bioenergetic aspects of apoptosis, necrosis and mitoptosis. *Apoptosis* **11**(4): 473-485.
- Smith L, Bryan S, De P, Rahal R, Shaw A, Turner D, Weir H, Woods R, Dixon M. 2018a. Canadian Cancer Statistics 2018. In *Toronto, ON: Canadian Cancer Society. Available at: cancer.ca/Canadian-Cancer-Statistics-2018-EN.* .
- Smith MR, Saad F, Chowdhury S, Oudard S, Hadaschik BA, Graff JN, Olmos D, Mainwaring PN, Lee JY, Uemura H et al. 2018b. Apalutamide Treatment and Metastasis-free Survival in Prostate Cancer. *N Engl J Med* **378**(15): 1408-1418.
- Sobel RE, Sadar MD. 2005. Cell lines used in prostate cancer research: a compendium of old and new lines--part 1. *J Urol* **173**(2): 342-359.
- Somasundaram S, Edmund NA, Moore DT, Small GW, Shi YY, Orlowski RZ. 2002. Dietary curcumin inhibits chemotherapy-induced apoptosis in models of human breast cancer. *Cancer Res* **62**(13): 3868-3875.
- Sotelo J, Briceno E, Lopez-Gonzalez MA. 2006. Adding chloroquine to conventional treatment for glioblastoma multiforme: a randomized, double-blind, placebo-controlled trial. *Ann Intern Med* **144**(5): 337-343.
- Srivastava J, Siddiq A, Emdad L, Santhekadur PK, Chen D, Gredler R, Shen XN, Robertson CL, Dumur CI, Hylemon PB et al. 2012. Astrocyte elevated gene-1 promotes hepatocarcinogenesis: novel insights from a mouse model. *Hepatology* **56**(5): 1782-1791.
- Stanbrough M, Bubley GJ, Ross K, Golub TR, Rubin MA, Penning TM, Febbo PG, Balk SP. 2006. Increased expression of genes converting adrenal androgens to testosterone in androgen-independent prostate cancer. *Cancer Res* **66**(5): 2815-2825.
- Steiner H, Godoy-Tundidor S, Rogatsch H, Berger AP, Fuchs D, Comuzzi B, Bartsch G, Hobisch A, Culig Z. 2003. Accelerated in vivo growth of prostate tumors that up-regulate interleukin-6 is associated with reduced retinoblastoma protein expression and activation of the mitogen-activated protein kinase pathway. *Am J Pathol* **162**(2): 655-663.
- Steward WP, Brown K. 2013. Cancer chemoprevention: a rapidly evolving field. *Br J Cancer* **109**(1): 1-7.
- Su ZZ, Chen Y, Kang DC, Chao W, Simm M, Volsky DJ, Fisher PB. 2003. Customized rapid subtraction hybridization (RaSH) gene microarrays identify overlapping expression changes in human fetal astrocytes resulting from human immunodeficiency virus-1 infection or tumor necrosis factor-alpha treatment. *Gene* **306**: 67-78.
- Sun L, Wang H, Wang Z, He S, Chen S, Liao D, Wang L, Yan J, Liu W, Lei X et al. 2012a. Mixed lineage kinase domain-like protein mediates necrosis signaling downstream of RIP3 kinase. *Cell* **148**(1-2): 213-227.
- Sun S, Ke Z, Wang F, Li S, Chen W, Han A, Wang Z, Shi H, Wang LT, Chen X. 2012b. Overexpression of astrocyte-elevated gene-1 is closely correlated with poor prognosis in human non-small cell lung cancer and mediates its metastasis through up-regulation of matrix metalloproteinase-9 expression. *Hum Pathol* **43**(7): 1051-1060.
- Surh YJ. 2003. Cancer chemoprevention with dietary phytochemicals. *Nat Rev Cancer* **3**(10): 768-780.

- Svenning S, Johansen T. 2013. Selective autophagy. *Essays Biochem* **55**: 79-92.
- Tabas I, Ron D. 2011. Integrating the mechanisms of apoptosis induced by endoplasmic reticulum stress. *Nat Cell Biol* **13**(3): 184-190.
- Tanida I, Ueno T, Kominami E. 2004. LC3 conjugation system in mammalian autophagy. *Int J Biochem Cell Biol* **36**(12): 2503-2518.
- Taplin ME, Ho SM. 2001. Clinical review 134: The endocrinology of prostate cancer. *J Clin Endocrinol Metab* **86**(8): 3467-3477.
- Tato-Costa J, Casimiro S, Pacheco T, Pires R, Fernandes A, Alho I, Pereira P, Costa P, Castelo HB, Ferreira J et al. 2016. Therapy-Induced Cellular Senescence Induces Epithelial-to-Mesenchymal Transition and Increases Invasiveness in Rectal Cancer. *Clin Colorectal Cancer* **15**(2): 170-178 e173.
- Tereshchenko IV, Zhong H, Chekmareva MA, Kane-Goldsmith N, Santanam U, Petrosky W, Stein MN, Ganesan S, Singer EA, Moore D et al. 2014. ERG and CHD1 heterogeneity in prostate cancer: use of confocal microscopy in assessment of microscopic foci. *Prostate* **74**(15): 1551-1559.
- Thakur N, Sorrentino A, Heldin CH, Landstrom M. 2009. TGF-beta uses the E3-ligase TRAF6 to turn on the kinase TAK1 to kill prostate cancer cells. *Future Oncol* **5**(1): 1-3.
- Thalmann GN, Anezinis PE, Chang SM, Zhou HE, Kim EE, Hopwood VL, Pathak S, von Eschenbach AC, Chung LW. 1994. Androgen-independent cancer progression and bone metastasis in the LNCaP model of human prostate cancer. *Cancer Res* **54**(10): 2577-2581.
- Timmins JM, Ozcan L, Seimon TA, Li G, Malagelada C, Backs J, Backs T, Bassel-Duby R, Olson EN, Anderson ME et al. 2009. Calcium/calmodulin-dependent protein kinase II links ER stress with Fas and mitochondrial apoptosis pathways. *J Clin Invest* **119**(10): 2925-2941.
- Toren P, Zoubeidi A. 2014. Targeting the PI3K/Akt pathway in prostate cancer: challenges and opportunities (review). *Int J Oncol* **45**(5): 1793-1801.
- Turnbull C, Sud A, Houlston RS. 2018. Cancer genetics, precision prevention and a call to action. *Nat Genet* **50**(9): 1212-1218.
- Ukimura O, Marien A, Palmer S, Villers A, Aron M, de Castro Abreu AL, Leslie S, Shoji S, Matsugasumi T, Gross M et al. 2015. Trans-rectal ultrasound visibility of prostate lesions identified by magnetic resonance imaging increases accuracy of image-fusion targeted biopsies. *World J Urol* **33**(11): 1669-1676.
- Umar A, Dunn BK, Greenwald P. 2012. Future directions in cancer prevention. *Nat Rev Cancer* **12**(12): 835-848.
- van Bokhoven A, Varella-Garcia M, Korch C, Hessels D, Miller GJ. 2001. Widely used prostate carcinoma cell lines share common origins. *Prostate* **47**(1): 36-51.
- Vander Griend DJ, Karthaus WL, Dalrymple S, Meeker A, DeMarzo AM, Isaacs JT. 2008. The role of CD133 in normal human prostate stem cells and malignant cancer-initiating cells. *Cancer Res* **68**(23): 9703-9711.

- Vanderlaag K, Su Y, Frankel AE, Burghardt RC, Barhoumi R, Chadalapaka G, Jutooru I, Safe S. 2010. 1,1-Bis(3'-indolyl)-1-(p-substituted phenyl)methanes induce autophagic cell death in estrogen receptor negative breast cancer. *BMC Cancer* **10**: 669.
- Vaziri H, Benchimol S. 1999. Alternative pathways for the extension of cellular life span: inactivation of p53/pRb and expression of telomerase. *Oncogene* **18**(53): 7676-7680.
- Veldscholte J, Berrevoets CA, Ris-Stalpers C, Kuiper GG, Jenster G, Trapman J, Brinkmann AO, Mulder E. 1992. The androgen receptor in LNCaP cells contains a mutation in the ligand binding domain which affects steroid binding characteristics and response to antiandrogens. *J Steroid Biochem Mol Biol* **41**(3-8): 665-669.
- Veldscholte J, Ris-Stalpers C, Kuiper GG, Jenster G, Berrevoets C, Claassen E, van Rooij HC, Trapman J, Brinkmann AO, Mulder E. 1990. A mutation in the ligand binding domain of the androgen receptor of human LNCaP cells affects steroid binding characteristics and response to anti-androgens. *Biochem Biophys Res Commun* **173**(2): 534-540.
- Venturini NJ, Drake CG. 2018. Immunotherapy for Prostate Cancer. *Cold Spring Harb Perspect Med*.
- Vercammen D, Brouckaert G, Denecker G, Van de Craen M, Declercq W, Fiers W, Vandenamee P. 1998. Dual signaling of the Fas receptor: initiation of both apoptotic and necrotic cell death pathways. *J Exp Med* **188**(5): 919-930.
- Vermeulen K, Van Bockstaele DR, Berneman ZN. 2003. The cell cycle: a review of regulation, deregulation and therapeutic targets in cancer. *Cell Prolif* **36**(3): 131-149.
- Vicencio JM, Galluzzi L, Tajeddine N, Ortiz C, Criollo A, Tasmimir E, Morselli E, Ben Younes A, Maiuri MC, Lavandro S et al. 2008. Senescence, apoptosis or autophagy? When a damaged cell must decide its path--a mini-review. *Gerontology* **54**(2): 92-99.
- Vidal SJ, Rodriguez-Bravo V, Quinn SA, Rodriguez-Barrueco R, Lujambio A, Williams E, Sun X, de la Iglesia-Vicente J, Lee A, Readhead B et al. 2015. A targetable GATA2-IGF2 axis confers aggressiveness in lethal prostate cancer. *Cancer Cell* **27**(2): 223-239.
- Vivar OI, Lin CL, Firestone GL, Bjeldanes LF. 2009. 3,3'-Diindolylmethane induces a G(1) arrest in human prostate cancer cells irrespective of androgen receptor and p53 status. *Biochem Pharmacol* **78**(5): 469-476.
- Vyas AR, Hahm ER, Arlotti JA, Watkins S, Stolz DB, Desai D, Amin S, Singh SV. 2013. Chemoprevention of prostate cancer by d,l-sulforaphane is augmented by pharmacological inhibition of autophagy. *Cancer Res* **73**(19): 5985-5995.
- Vykhovanets EV, Shankar E, Vykhovanets OV, Shukla S, Gupta S. 2011. High-fat diet increases NF-kappaB signaling in the prostate of reporter mice. *Prostate* **71**(2): 147-156.
- Wade CA, Kyprianou N. 2018. Profiling Prostate Cancer Therapeutic Resistance. *Int J Mol Sci* **19**(3).
- Waitz R, Fassio M, Allison JP. 2012. CTLA-4 blockade synergizes with cryoablation to mediate tumor rejection. *Oncoimmunology* **1**(4): 544-546.
- Wallace DM, Chisholm GD, Hendry WF. 1975. T.N.M. classification for urological tumours (U.I.C.C.) - 1974. *Br J Urol* **47**(1): 1-12.

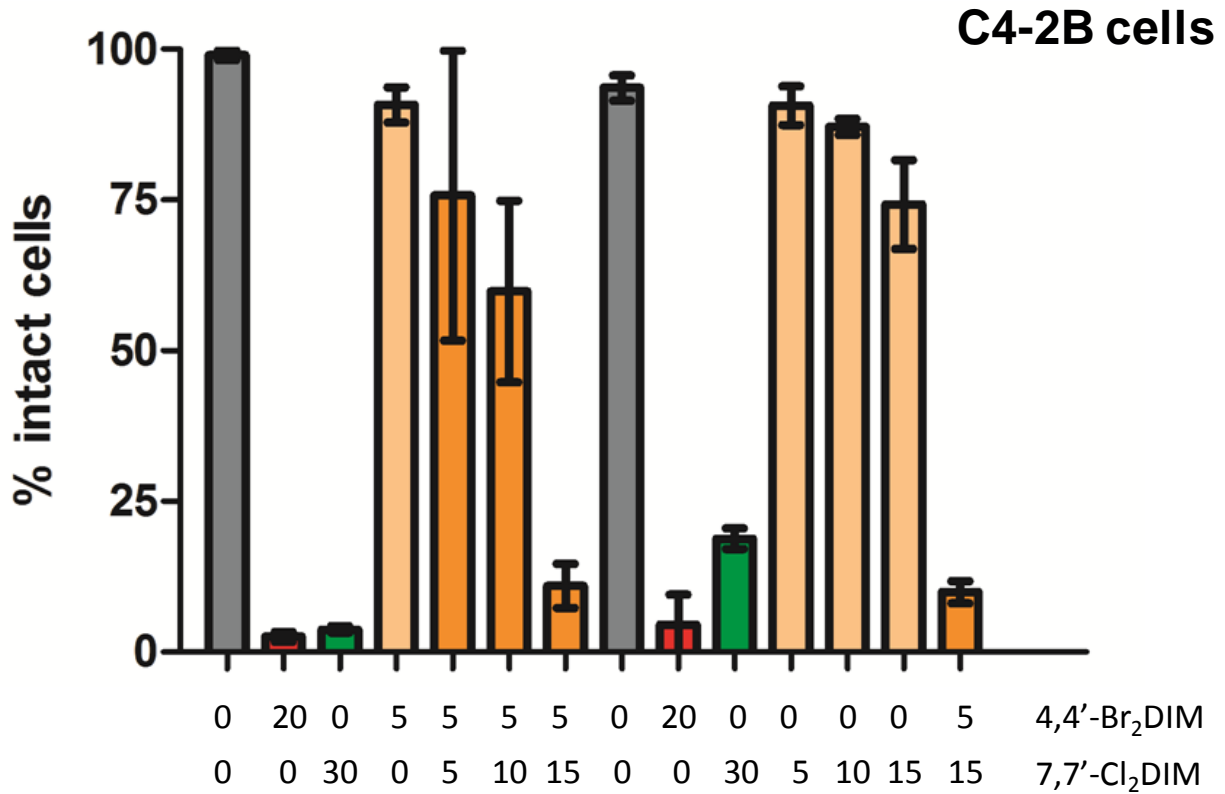
- Wang C, Yang Q. 2011. Astrocyte elevated gene-1 and breast cancer (Review). *Oncol Lett* **2**(3): 399-405.
- Wang F, Ke ZF, Sun SJ, Chen WF, Yang SC, Li SH, Mao XP, Wang LT. 2011. Oncogenic roles of astrocyte elevated gene-1 (AEG-1) in osteosarcoma progression and prognosis. *Cancer Biol Ther* **12**(6): 539-548.
- Wang Q, Wang H, Jia Y, Pan H, Ding H. 2017. Luteolin induces apoptosis by ROS/ER stress and mitochondrial dysfunction in gliomablastoma. *Cancer Chemother Pharmacol* **79**(5): 1031-1041.
- Wang TT, Schoene NW, Milner JA, Kim YS. 2012. Broccoli-derived phytochemicals indole-3-carbinol and 3,3'-diindolylmethane exerts concentration-dependent pleiotropic effects on prostate cancer cells: comparison with other cancer preventive phytochemicals. *Mol Carcinog* **51**(3): 244-256.
- Wegiel B, Bjartell A, Culig Z, Persson JL. 2008. Interleukin-6 activates PI3K/Akt pathway and regulates cyclin A1 to promote prostate cancer cell survival. *Int J Cancer* **122**(7): 1521-1529.
- White E. 2015. The role for autophagy in cancer. *J Clin Invest* **125**(1): 42-46.
- Wilson KJ, Gilmore JL, Foley J, Lemmon MA, Riese DJ, 2nd. 2009. Functional selectivity of EGF family peptide growth factors: implications for cancer. *Pharmacol Ther* **122**(1): 1-8.
- Woods A, Dickerson K, Heath R, Hong SP, Momcilovic M, Johnstone SR, Carlson M, Carling D. 2005. Ca²⁺/calmodulin-dependent protein kinase kinase-beta acts upstream of AMP-activated protein kinase in mammalian cells. *Cell Metab* **2**(1): 21-33.
- Wu HC, Hsieh JT, Gleave ME, Brown NM, Pathak S, Chung LW. 1994. Derivation of androgen-independent human LNCaP prostatic cancer cell sublines: role of bone stromal cells. *Int J Cancer* **57**(3): 406-412.
- Wu TY, Khor TO, Su ZY, Saw CL, Shu L, Cheung KL, Huang Y, Yu S, Kong AN. 2013a. Epigenetic modifications of Nrf2 by 3,3'-diindolylmethane in vitro in TRAMP C1 cell line and in vivo TRAMP prostate tumors. *AAPS J* **15**(3): 864-874.
- Wu X, Gong S, Roy-Burman P, Lee P, Culig Z. 2013b. Current mouse and cell models in prostate cancer research. *Endocr Relat Cancer* **20**(4): R155-170.
- Wu Z, Chang PC, Yang JC, Chu CY, Wang LY, Chen NT, Ma AH, Desai SJ, Lo SH, Evans CP et al. 2010. Autophagy Blockade Sensitizes Prostate Cancer Cells towards Src Family Kinase Inhibitors. *Genes Cancer* **1**(1): 40-49.
- Xu Y, Dalrymple SL, Becker RE, Denmeade SR, Isaacs JT. 2006. Pharmacologic Basis for the Enhanced Efficacy of Dutasteride against Prostatic Cancers. *Clin Cancer Res* **12**(13): 4072-4079.
- Xue W, Zender L, Miething C, Dickins RA, Hernando E, Krizhanovsky V, Cordon-Cardo C, Lowe SW. 2007. Senescence and tumour clearance is triggered by p53 restoration in murine liver carcinomas. *Nature* **445**(7128): 656-660.

- Yamaoka M, Hara T, Kusaka M. 2010. Overcoming persistent dependency on androgen signaling after progression to castration-resistant prostate cancer. *Clin Cancer Res* **16**(17): 4319-4324.
- Yang SY, Winslet MC. 2011. Dual role of autophagy in colon cancer cell survival. *Ann Surg Oncol* **18 Suppl 3**: S239.
- Yang X, Niu B, Wang L, Chen M, Kang X, Wang L, Ji Y, Zhong J. 2016. Autophagy inhibition enhances colorectal cancer apoptosis induced by dual phosphatidylinositol 3-kinase/mammalian target of rapamycin inhibitor NVP-BEZ235. *Oncol Lett* **12**(1): 102-106.
- Ye Y, Fang Y, Xu W, Wang Q, Zhou J, Lu R. 2016. 3,3'-Diindolylmethane induces anti-human gastric cancer cells by the miR-30e-ATG5 modulating autophagy. *Biochem Pharmacol* **115**: 77-84.
- Yin XF, Chen J, Mao W, Wang YH, Chen MH. 2012. A selective aryl hydrocarbon receptor modulator 3,3'-Diindolylmethane inhibits gastric cancer cell growth. *J Exp Clin Cancer Res* **31**: 46.
- Yoo BK, Chen D, Su ZZ, Gredler R, Yoo J, Shah K, Fisher PB, Sarkar D. 2010. Molecular mechanism of chemoresistance by astrocyte elevated gene-1. *Cancer Res* **70**(8): 3249-3258.
- Yoo BK, Emdad L, Su ZZ, Villanueva A, Chiang DY, Mukhopadhyay ND, Mills AS, Waxman S, Fisher RA, Llovet JM et al. 2009. Astrocyte elevated gene-1 regulates hepatocellular carcinoma development and progression. *J Clin Invest* **119**(3): 465-477.
- Yu Z, Pestell TG, Lisanti MP, Pestell RG. 2012. Cancer stem cells. *Int J Biochem Cell Biol* **44**(12): 2144-2151.
- Yun EJ, Zhou J, Lin CJ, Hernandez E, Fazli L, Gleave M, Hsieh JT. 2016. Targeting Cancer Stem Cells in Castration-Resistant Prostate Cancer. *Clin Cancer Res* **22**(3): 670-679.
- Zeegers MP, Jellema A, Ostrer H. 2003. Empiric risk of prostate carcinoma for relatives of patients with prostate carcinoma: a meta-analysis. *Cancer* **97**(8): 1894-1903.
- Zemskova M, Lilly MB, Lin YW, Song JH, Kraft AS. 2010. p53-dependent induction of prostate cancer cell senescence by the PIM1 protein kinase. *Mol Cancer Res* **8**(8): 1126-1141.
- Zhang C, Li HZ, Qian BJ, Liu CM, Guo F, Lin MC. 2015. MTDH/AEG-1-based DNA vaccine suppresses metastasis and enhances chemosensitivity to paclitaxel in pelvic lymph node metastasis. *Biomed Pharmacother* **70**: 217-226.
- Zhang D, Wang W, Sun X, Xu D, Wang C, Zhang Q, Wang H, Luo W, Chen Y, Chen H et al. 2016. AMPK regulates autophagy by phosphorylating BECN1 at threonine 388. *Autophagy* **12**(9): 1447-1459.
- Zhang X, Sukamporn P, Zhang S, Min KW, Baek SJ. 2017. 3,3'-diindolylmethane downregulates cyclin D1 through triggering endoplasmic reticulum stress in colorectal cancer cells. *Oncol Rep* **38**(1): 569-574.

- Zheng N, Zhang P, Huang H, Liu W, Hayashi T, Zang L, Zhang Y, Liu L, Xia M, Tashiro S et al. 2015. ERalpha down-regulation plays a key role in silibinin-induced autophagy and apoptosis in human breast cancer MCF-7 cells. *J Pharmacol Sci* **128**(3): 97-107.
- Zhou H, Yuan M, Yu Q, Zhou X, Min W, Gao D. 2016. Autophagy regulation and its role in gastric cancer and colorectal cancer. *Cancer Biomark* **17**(1): 1-10.
- Zhou J, Gurates B, Yang S, Sebastian S, Bulun SE. 2001. Malignant breast epithelial cells stimulate aromatase expression via promoter II in human adipose fibroblasts: an epithelial-stromal interaction in breast tumors mediated by CCAAT/enhancer binding protein beta. *Cancer Res* **61**(5): 2328-2334.
- Zhu H, Mao Q, Lin Y, Yang K, Xie L. 2011. RNA interference targeting mutant p53 inhibits growth and induces apoptosis in DU145 human prostate cancer cells. *Med Oncol* **28 Suppl 1**: S381-387.
- Ziparo E, Petrunaro S, Marini ES, Starace D, Conti S, Facchiano A, Filippini A, Giampietri C. 2013. Autophagy in prostate cancer and androgen suppression therapy. *Int J Mol Sci* **14**(6): 12090-12106.
- Zoncu R, Efeyan A, Sabatini DM. 2011. mTOR: from growth signal integration to cancer, diabetes and ageing. *Nat Rev Mol Cell Biol* **12**(1): 21-35.
- Zou M, Zhu W, Wang L, Shi L, Gao R, Ou Y, Chen X, Wang Z, Jiang A, Liu K et al. 2016. AEG-1/MTDH-activated autophagy enhances human malignant glioma susceptibility to TGF-beta1-triggered epithelial-mesenchymal transition. *Oncotarget* **7**(11): 13122-13138.

Appendix I

Effect of combination of 4,4-Br₂DIM with non-cytotoxic concentrations of 7,7'-Cl₂DIM on C4-2B prostate cancer cells



The toxicity of 4,4-Br₂DIM is potentiated in the presence of non-cytotoxic concentrations of 7,7'-Cl₂DIM. C4-2B cells were exposed to ring-DIMs for 24 h.

Appendix II

LITHOCHOLIC ACID INDUCES ENDOPLASMIC RETICULUM STRESS, AUTOPHAGY AND MITOCHONDRIAL DYSFUNCTION IN HUMAN PROSTATE CANCER CELLS

Ahmed A. Gafar^{1,2}, Hossam M. Draz^{1,3}, Alexander A. Goldberg^{1,4}, Mohamed A. Bashandy², Sayed Bakry², Mahmoud A. Khalifa², Walid AbuShair², Vladimir I. Titorenko⁵ and J. Thomas Sanderson¹

1 Institut Armand-Frappier, INRS, Laval, QC, Canada

2 Zoology Department, Faculty of Science, Al-Azhar University, Cairo, Egypt

3 Department of Biochemistry, National Research Centre, Dokki, Cairo, Egypt

4 McGill University Health Centre, Montréal, QC, Canada

5 Department of Biology, Concordia University, Montréal, QC, Canada

This article was published in PeerJ (2016), 4:e2445.

Author contributions:

Ahmed Gafar designed and performed the experiments for endoplasmic reticulum stress and mitochondrial dysfunction.

Hossam Draz designed and performed the experiments for autophagy as well as writing and revising sections of the manuscript.

Dr. Alexander Goldberg supervised the experiments for mitochondrial dysfunction.

Prof. Mohamed Bashandy, Dr. Sayed Bakry, Dr. Mahmoud Khalifa, and Dr. Walid Abushair participated in designing the experiments.

Prof. Vladimir Titorenko participated in supervising the project and revised the manuscript.

Prof. Thomas Sanderson obtained the research funding, supervised the project, analysed the results and wrote most of the manuscript.

Lithocholic acid induces endoplasmic reticulum stress, autophagy and mitochondrial dysfunction in human prostate cancer cells

Ahmed A. Gafar^{1,2}, Hossam M. Draz^{1,3}, Alexander A. Goldberg^{1,4}, Mohamed A. Bashandy², Sayed Bakry², Mahmoud A. Khalifa², Walid AbuShair², Vladimir I. Titorenko⁵ and J. Thomas Sanderson¹

¹ Institut Armand-Frappier, Institut National de la Recherche Scientifique (INRS), Laval, QC, Canada

² Zoology Department, Faculty of Science, Al-Azhar University, Cairo, Egypt

³ Department of Biochemistry, National Research Centre, Dokki, Cairo, Egypt

⁴ McGill University Health Centre, Montréal, QC, Canada

⁵ Department of Biology, Concordia University, Montréal, QC, Canada

ABSTRACT

Lithocholic acid (LCA) is a secondary bile acid that is selectively toxic to human neuroblastoma, breast and prostate cancer cells, whilst sparing normal cells. We previously reported that LCA inhibited cell viability and proliferation and induced apoptosis and necrosis of androgen-dependent LNCaP and androgen-independent PC-3 human prostate cancer cells. In the present study, we investigated the roles of endoplasmic reticulum (ER) stress, autophagy and mitochondrial dysfunction in the toxicity of LCA in PC-3 and autophagy deficient, androgen-independent DU-145 cells. LCA induced ER stress-related proteins, such as CCAAT-enhancer-binding protein homologous protein (CHOP), and the phosphorylation of eukaryotic initiation factor 2- α (p-eIF2 α) and c-Jun N-terminal kinases (p-JNK) in both cancer cell-types. The p53 upregulated modulator of apoptosis (PUMA) and B cell lymphoma-like protein 11 (BIM) levels were decreased at overtly toxic LCA concentrations, although PUMA levels increased at lower LCA concentrations in both cell lines. LCA induced autophagy-related conversion of microtubule-associated proteins 1A/1B light chain 3B (LC3BI-LC3BII), and autophagy-related protein ATG5 in PC-3 cells, but not in autophagy-deficient DU-145 cells. LCA (>10 μ M) increased levels of reactive oxygen species (ROS) concentration-dependently in PC-3 cells, whereas ROS levels were not affected in DU-145 cells. Salubrinal, an inhibitor of eIF2 α dephosphorylation and ER stress, reduced LCA-induced CHOP levels slightly in PC-3, but not DU-145 cells. Salubrinal pre-treatment increased the cytotoxicity of LCA in PC-3 and DU-145 cells and resulted in a statistically significant loss of cell viability at normally non-toxic concentrations of LCA. The late-stage autophagy inhibitor bafilomycin A1 exacerbated LCA toxicity at subtoxic LCA concentrations in PC-3 cells. The antioxidant α -tocotrienol strongly inhibited the toxicity of LCA in PC-3 cells, but not in DU-145 cells. Collectively, although LCA induces autophagy and ER stress in PC-3 cells, these processes appear to be initially of protective nature and subsequently consequential to, but not critical for the ROS-mediated mitochondrial dysfunction and cytotoxicity of LCA. The full mechanism

Submitted 21 January 2016
Accepted 13 August 2016
Published 15 November 2016

Corresponding author
J. Thomas Sanderson,
thomas.sanderson@iaf.inrs.ca

Academic editor
Jie Liu

Additional Information and
Declarations can be found on
page 20

DOI 10.7717/peerj.2445

© Copyright
2016 Gafar et al.

Distributed under
Creative Commons CC-BY 4.0

OPEN ACCESS

How to cite this article Gafar et al. (2016), Lithocholic acid induces endoplasmic reticulum stress, autophagy and mitochondrial dysfunction in human prostate cancer cells. *PeerJ* 4:e2445; DOI 10.7717/peerj.2445

of LCA-induced mitochondrial dysfunction and cytotoxicity in the similarly sensitive DU-145 cells remains to be elucidated.

Subjects Toxicology, Oncology

Keywords Lithocholic acid, Prostate cancer cells, Pc-3, Du-145, Autophagy, Endoplasmic reticulum stress, RWPE-1, Cell death, Reactive oxygen species, Tocotrienol

INTRODUCTION

Prostate cancer is the second most common cancer worldwide in males and the fourth most common cancer overall, with more than 1,112,000 new cases diagnosed in 2012, representing 15% of male cancer cases and 8% of all cancers (Ferlay et al., 2015). In Western men, prostate cancer diagnosis ranks first among male cancers and second as cause of cancer-related death (Malvezzi et al., 2015; American Cancer Society, 2015; Canadian Cancer Society's Advisory Committee on Cancer Statistics, 2016). Standard treatment of prostate cancer consists of surgery (prostatectomy), antihormonal therapy and radiotherapy. Although these treatments are successful for early-stage prostate cancer, they each have potentially serious side-effects (Martin & D'Amico, 2014; Nguyen et al., 2015), among which some that last a life-time (Sanda et al., 2008). Androgen-deprivation therapy uses drugs that blocking the action of male sex hormones either through androgen receptor antagonism (bicalutamide, hydroxyflutamide) or inhibition of androgen biosynthesis (finasteride, abiraterone). These treatments are initially effective in controlling androgen-dependent prostate tumor growth, although side-effects include increased insulin-resistance, bone density loss, hypogonadism, gynecomastia, muscle mass loss and fatigue (Conde & Aronson, 2003; Nguyen et al., 2015). In addition, a certain percentage of tumors that have undergone androgen-deprivation therapy progresses to an androgen-independent state, which is difficult to treat resulting in increased mortality. The limitations of current standard treatments of prostate cancer has encouraged the search for safer and more effective molecules based on naturally occurring compounds.

Lithocholic acid (LCA) is a secondary bile acid produced by microflora in the gut, which we found to exhibit selective toxicity to human neuroblastoma cells and prostate cancer cells at relatively low concentrations that did not affect normal cells (Goldberg et al., 2011; Goldberg et al., 2013). LCA triggered both intrinsic and extrinsic pathways of apoptotic cell death that were, at least in part, caspase-dependent. In addition, LCA selectively decreased the viability of human breast cancer and rat glioma cells (Goldberg et al., 2011). Various bile acids have been reported to have anti-neoplastic and anti-carcinogenic properties in a number of cancer cell models: chenodeoxycholic acid (CDCA) reduced growth of tamoxifen-resistant breast cancer cells by downregulation of human epidermal growth factor receptor 2 (HER2) promoter activity (Giordano et al., 2011), LCA and several of its synthetic enantiomers reduced colon cancer cell proliferation and viability (Katona et al., 2009). Deoxycholic acid (DCA), ursodeoxycholic acid (UDCA) and their taurine-derivatives delayed cell cycle progression in Jurkat human T leukemia cells and DCA induced apoptosis (Fimognari et al., 2009). These findings indicate that the bile acid

structure may form the basis for the development of potent and selective drugs for the treatment of various cancers including those of the prostate.

The mechanisms underlying the cytotoxicity of LCA are not well understood and remain a continuing topic of investigation. Studies have found that certain bile acids can induce apoptosis via a variety of mechanisms including chronic endoplasmic reticulum (ER) stress (*Perez & Briz, 2009*), autophagy (*Gao et al., 2014*) or disruption of mitochondrial function (*Goldberg et al., 2013*). The endoplasmic reticulum is cell organelle responsible for the synthesis, folding and maturation of proteins, the storage and release of intracellular calcium (Ca^{2+}) and a large number of biotransformation reactions. A variety of factors (radiation, pathogens, hypoxia, disease states and chemical agents) can disrupt healthy ER function, resulting in a so-called unfolded protein response (UPR), due to the accumulation of unfolded or misfolded proteins in the lumen of the ER. As an adaptive response to these stress factors, the UPR aims to restore normal cell function by halting protein translation, degrading misfolded proteins and increasing the production of molecular chaperones involved in protein folding. However, chronic activation of the UPR fails to promote cell survival and the cell is broken down by a proapoptotic ER stress-mediated response pathway. CCAAT-enhancer-binding protein homologous protein (CHOP) is a transcriptional regulator induced by ER stress, which is a modulator of ER stress-mediated apoptosis (*Marciniak et al., 2004*) and autophagy (*Shimodaira et al., 2014*). CHOP levels may be increased through activation of various ER stress sensor-pathways, including those initiated by activating transcription factor 6 (ATF6), inositol-requiring enzyme 1 alpha ($\text{IRE1}\alpha$) and protein kinase R-like endoplasmic reticulum kinase (PERK), the latter which phosphorylates eukaryotic initiation factor 2-alpha ($\text{eIF2}\alpha$), and the downstream transcription factor ATF4 which in turn induces the transcription of CHOP.

Autophagy is a catabolic process for the autophagosomic/lysosomal degradation of bulk cytoplasmic contents (*Reggiori & Klionsky, 2002; Codogno & Meijer, 2005*). Autophagy is generally activated by nutrient deprivation but is also important in physiological processes such as fetal development and cell differentiation, as well as diseases such as neurodegeneration, infection and cancer (*Levine & Yuan, 2005*). The molecular machinery of autophagy was largely uncovered in yeast by the discovery of autophagy-related genes (Atg). Formation of the autophagosome involves a ubiquitin-like conjugation system in which Atg12 is covalently bound to Atg5 and targeted to autophagosomal vesicles (*Mizushima et al., 1998a; Mizushima et al., 1998b*). Upon induction of autophagy, a fraction of microtubule-associated proteins 1A/1B light chain 3 (LC3-I) is conjugated to phosphotidylethanolamine (PE) to produce LC3-II proteins, which are required for autophagosome membrane expansion and fusion (*Tanida, Ueno & Kominami, 2004*). LC3-I-to-II conversion is reliable marker of autophagosome formation (*Mizushima et al., 2001*).

Bile acids have also been reported to induce apoptosis via disruption of mitochondrial function, ligand-independent activation of death receptor pathways and modulation of certain members of the Bcl2 protein family. We have previously shown that LCA induces intrinsic and extrinsic apoptosis in LNCaP and PC-3 prostate cancer cells that involved a decrease in the mitochondrial protein Bcl-2 and cleavage of Bax, concomitant

with an increase of mitochondrial outer membrane permeability. It has been suggested that the well-known solubilising properties of bile acids could explain disruption of (mitochondrial) membranes and induction of mitochondrial dysfunction leading to cell death. However, the lack of or far poorer toxicity of several enantiomers of toxic bile acids suggests physico-chemical properties alone cannot explain cell toxicity (Katona *et al.*, 2009) and that a specific three-dimensional structure is required to explain the selectivity of LCA-mediated toxicity in cancer cells.

Our present study aims to investigate to which extent the involvement of ER stress, autophagy or disruption of mitochondrial function is critical to LCA-induced prostate cancer cell death.

MATERIALS AND METHODS

Cell lines and reagents

PC3 and DU-145 cells were obtained from the American Type Culture Collection (Manassas, VA). PC-3 cells were grown in 1:1 (v/v) Dulbecco's modified Eagle medium/Ham's F-12 nutrient mix (DMEM/F12; Life Technologies, Grand Island, NY, USA) supplemented with 10% fetal bovine serum (FBS; Mediatech, Corning, Manassas, VA, USA) and 1% penicillin/streptomycin (Life Technologies). DU-145 and RWPE-1 cells were cultured in RPMI-1640 medium (Life Technologies) supplemented with 10% FBS, 1% HEPES, 1% sodium pyruvate (Sigma-Aldrich, St. Louis, MO, USA) and penicillin/streptomycin. All cells were incubated in a humidified atmosphere of 95% air and 5% CO₂ at 37 °C. LCA was purchased from Sigma-Aldrich and dissolved in DMSO as 100 mM a stock solution and 1,000-fold concentrated serial dilutions were prepared in DMSO for treatment of the cells. Bafilomycin A1, salubrinal and D- α -tocotrienol (Sigma-Aldrich) were dissolved in DMSO at 1,000-fold stock solutions of 2 μ M, 20 mM and 20 mM, respectively.

Cell viability

Each cell type was added to 96-well plates at a density of 1×10^4 cells/well in 200 μ l of complete medium. After 24 h, medium was replaced with fresh medium containing 2% dextran-coated charcoal-treated (stripped) FBS and various concentrations of LCA (0, 5, 10, 25, 50 and 75 μ M) in a final DMSO concentration in culture medium of 0.1%. Cell viability was assessed using a WST-1 Cell Proliferation Reagent kit (Roche, Laval, QC) according to the manufacturer's instructions. Absorbance was measured at 440 nm using a SpectraMax M5 multifunctional spectrophotometer (Molecular Devices, Sunnydale, CA).

Fluorescence microscopy

PC-3 and DU-145 cells were added to 24-well plates at a density of 1×10^5 cells/well in 1 ml of complete medium. After 24 h, cells were treated with several concentrations of LCA (0, 1, 3, 10 and 30 μ M) in fresh medium containing 2% stripped FBS and another 24 h later, Hoechst 33342 (Sigma-Aldrich) and propidium iodide (Invitrogen, Carlsbad, CA, USA) were each added at a concentration of 1 μ g/ml per well. After a 15 min incubation

at 37 °C, cells were observed and counted under a Nikon Eclipse (TE-2000U) inverted fluorescence microscope at 20× magnification. Hoechst- and propidium iodide-positive cells were made visible using filter cubes with excitation wavelengths of 330–380 nm and 532–587 nm, respectively. To measure autophagy, PC-3 cells were exposed to LCA (0, 3, 10, 30 and 50 μM) for 24 h and then stained with Hoechst 33342 and 2 μL of Cyto-ID® Green Detection Reagent (ENZ-51031-K200; Enzo Life Science, Farmingdale, NY, USA). After a 15 min incubation at 37 °C, cells were observed and counted under a Nikon Eclipse (TE-2000U) inverted fluorescence microscope at 20× magnification.

SDS–PAGE and immunoblot analysis

Cells were added to 6-well Cell-Bind plates (Fisher Scientific, Ottawa, ON) at a density of 7.5×10^5 cells/well in 2 ml of complete culture medium and allowed to adhere for 24 h. Cells were then exposed to LCA (0, 3, 10, 30 and 50 μM) in fresh medium with 2% stripped FBS for 1, 8 or 24 h, dependent on the experiment. Adherent cells were collected using a cell scraper, then rinsed three times in cold phosphate-buffered saline (PBS) followed by centrifugation at 700× g for 5 min. After removing the PBS, the cell pellets were lysed in RIPA buffer containing 1× protease and phosphatase inhibitor cocktail. Then, cell lysates were centrifuged at 15,000 rpm for 15 min at 4 °C and protein concentrations in the supernatant were determined using a BCA protein assay kit (Pierce Biotechnologies, Rockford, IL, USA). Proteins (40 μg) were diluted with loading buffer and boiled for 5 min, then loaded onto 10% sodium dodecyl sulfate-polyacrylamide gels. After electrophoresis, gels were transferred to polyvinylidene difluoride (PVDF) membranes using a Trans-Blot Turbo System (Bio-Rad, Mississauga, ON). Membranes were then blocked using Tris-buffered saline (TBS) containing 5% milk powder (blocking buffer) for 1 h at room temperature, after which the membranes were incubated overnight in blocking buffer with the appropriate primary antibodies (anti CHOP, eIF2α, p-eIF2α, JNK, p-JNK, PUMA, BIM, cleaved caspase 3, LC3BI/II, ATG5 and β-actin at 1:1,000 dilution; Cell Signaling, Beverly, MA) at 4 °C. The next day, membranes were washed three times with Tris-buffered saline containing 0.1% Tween (TBS-T) followed by a 1-h incubation with the appropriate secondary antibody at room temperature. Membranes were washed another three times with TBS-T and then incubated with Immobilon Western Chemiluminescent Horseradish Peroxidase Substrate (EMD Millipore, Billerica, MD, USA) for 5 min to make the bands visible; membranes were sealed in plastic wrap and photographed using a ChemiDoc gel documentation system (Bio-Rad). B-actin was used as reference protein and loading control.

Gene-silencing using small interfering RNA (siRNA)

CHOP expression was silenced by transfecting PC-3 and DU-145 cells with SMARTpool ON-TARGETplus siRNA oligonucleotides selective for CHOP (Dharmacon, Lafayette, CO) using lipofectamine RNAiMAX (Life Technologies, Burlington, ON, USA) in serum free Opti-MEM according to manufacturer's protocols. ON-TARGETplus Non-targeting Control siRNA was used as negative control. After a 24-h transfection period, cells were exposed to various concentrations of LCA (0, 10 and 30 μM) for 24 h. CHOP protein levels were evaluated by immunoblotting as described above.

Measurement of reactive oxygen species (ROS)

PC3 and DU-145 cells were added to 96-well plates at a concentration of 1×10^4 cells/well in 200 μ l of their respective culture medium containing 2% stripped FBS. After 24 h, medium was removed and the cells were incubated in prewarmed PBS at 37 °C containing 10 mM fluorescent ROS probe (CM-H2DCFDA; Life Technologies). After 30 min, the PBS mixture was removed and cells were exposed to various concentrations of LCA or 1 μ M H₂O₂ for 60 min at 37 °C temperature. In experiments with α -tocotrienol and N-acetylcysteine, cells were preincubated with the antioxidants for 4 h prior to exposure to LCA. ROS production was quantified using a SpectraMax M5 multifunctional spectrophotometer (Molecular Devices, Sunnydale, CA, USA) with an excitation wavelength of 490 and emission wavelength of 545 nm.

Statistical analysis

Statistical analyses were performed using GraphPad Prism version 5.0 (GraphPad Software, San Diego, CA, USA). Results are presented as means \pm standard deviations of at least three experiments. IC₅₀ values were determined from concentration–response curves by non-linear curve-fitting. Statistically significant differences of LCA treatments compared to vehicle control were determined by one-way analysis of variance (ANOVA) and a Dunnett post-hoc test or by two-way ANOVA and a Bonferroni post-hoc test when assessing differences between concentration–response curves. A *p*-value less than 0.05 was considered statistically significant.

RESULTS

LCA decreases the viability and induces apoptosis and necrosis of PC-3 and DU-145 human prostate cancer cells

A 24-h exposure to LCA reduced the viability of PC-3 and DU-145 cells concentration-dependently, with IC₅₀ values of 32.0 μ M and 30.4 μ M, respectively (Fig. 1). The viability of RWPE-1 immortalized normal prostate epithelial cells was not affected by concentrations of LCA between 5 and 75 μ M (Fig. 1). Hoechst 33342 and propidium iodide-staining of PC-3 and DU-145 cells exposed for 24 h to LCA showed a significant concentration-dependent increase in staining, with both necrotic (and late-apoptotic) and early-apoptotic cells starting to appear at a concentration at or above 3 μ M (Fig. 2).

LCA induces ER stress in PC-3 and DU-145 cells

To determine whether the ER stress pathway was involved in LCA-induced prostate cancer cell death, we determined the concentration- and time-dependent effects of LCA on p-JNK, JNK, p-eIF2 α , eIF2 α and CHOP protein levels, as well as on levels of BIM and PUMA in PC-3 and DU-145 cells exposed for 24 h to sub-cytotoxic (3 and 10 μ M) and overtly cytotoxic (30 and 50 μ M) concentrations of LCA. Levels of BIM and PUMA were decreased concentration-dependently by LCA in PC-3 and DU-145 cells, although in DU-145 cells PUMA levels increased at 3 and 10 μ M before decreasing strongly at overtly cytotoxic concentrations (Fig. 3). LCA concentration-dependently increased levels of p-JNK (46 and 54 kDa) and CHOP (27 kDa) in PC-3 and DU-145 cells (Fig. 3). Phosphorylation of

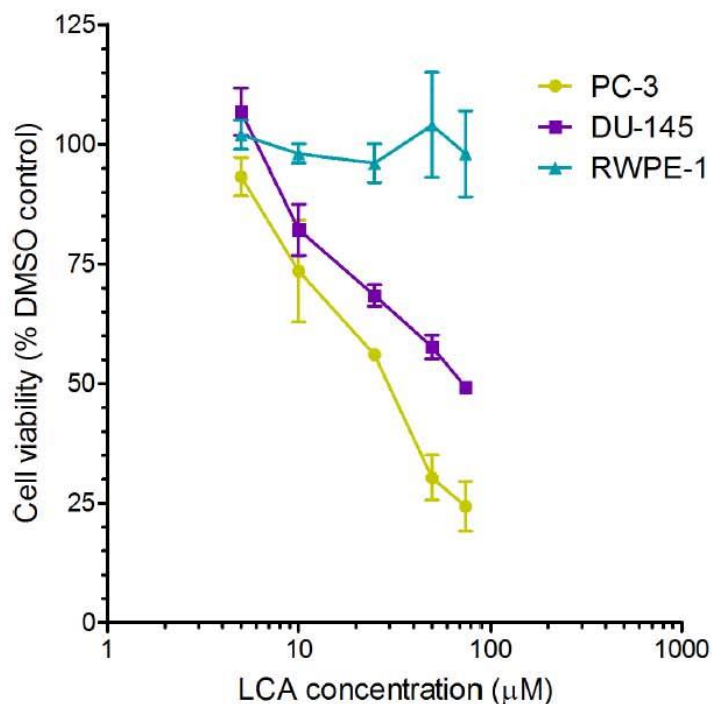


Figure 1 Lithocholic acid (LCA) decreases the viability of PC-3 and DU-145 human prostate cancer cells, but not RWPE-1 immortalized normal prostate epithelial cells. Cells were exposed to increasing concentrations of LCA (5–75 µM) for 24 h. IC₅₀ values for LCA-induced cytotoxicity in PC-3 and DU-145 cells were 32.0 µM and 30.4 µM, respectively. Experiments were performed three times; per experiment, each concentration was tested in triplicate.

eIF2 α was increased in a concentration-dependent manner in DU-145 cells, but was poorly detectable in PC-3 cells after a 24 h exposure to any of the LCA concentrations (Fig. 3).

To determine the effects of LCA on the ER stress response at earlier time-points, PC-3 and DU-145 cells were exposed to cytotoxic concentrations (30 and 50 µM) of LCA for 1 and 8 h (Fig. 4). BIM and PUMA levels were decreased concentration-dependently by LCA in both cell lines. In PC-3 cells BIM levels were somewhat higher at 8 h than 1 h (Fig. 4), which appeared to be an effect of the vehicle control, although they were, nevertheless, decreased by LCA, as was observed after 24 h exposure (Fig. 3). In DU-145 cells BIM levels were detectable at 1 h but not at 8 h. PUMA levels were decreased concentration-dependently by LCA in both cell lines, although basal levels in each cell line increased between 1 h and 8 h of culture (Fig. 4). Levels of p-JNK underwent a biphasic response in both cell lines with expression levels appearing lower after 8 h than 1 h of exposure to LCA, whereas levels were increased again after 24 h of exposure, in particular to 50 µM LCA. Levels of p-eIF2 α increased concentration-dependently after a 1 h and 8 h exposure of PC-3 and DU-145 cells to LCA (Fig. 4), but decreased time-dependently

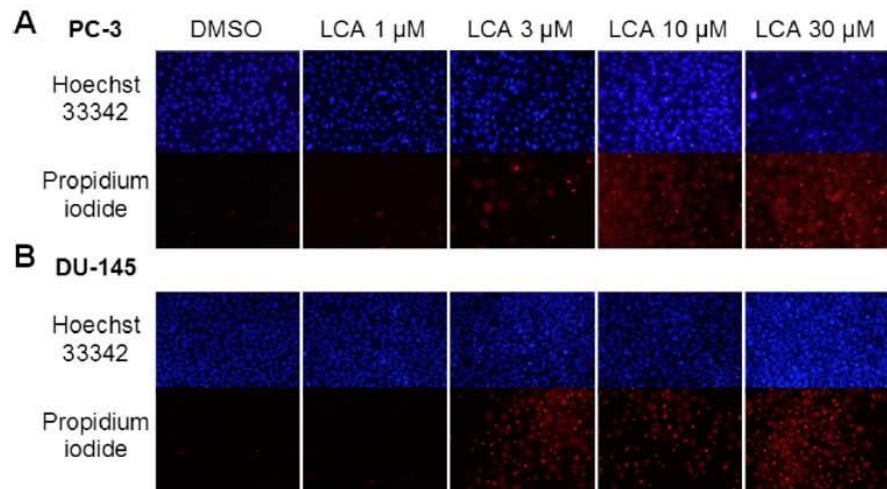


Figure 2 Lithocholic acid (LCA) induces apoptotic and necrotic death of PC-3 and DU-145 prostate cancer cells. Apoptotic nuclear morphology (chromatin condensation) was observed with Hoechst 33342 staining using fluorescence microscopy. Propidium iodide staining was used to distinguish apoptotic from necrotic (and late-apoptotic) cell death. The concentration–response experiment was performed three times using different cell passages. Per experiment, concentrations were tested in triplicate.

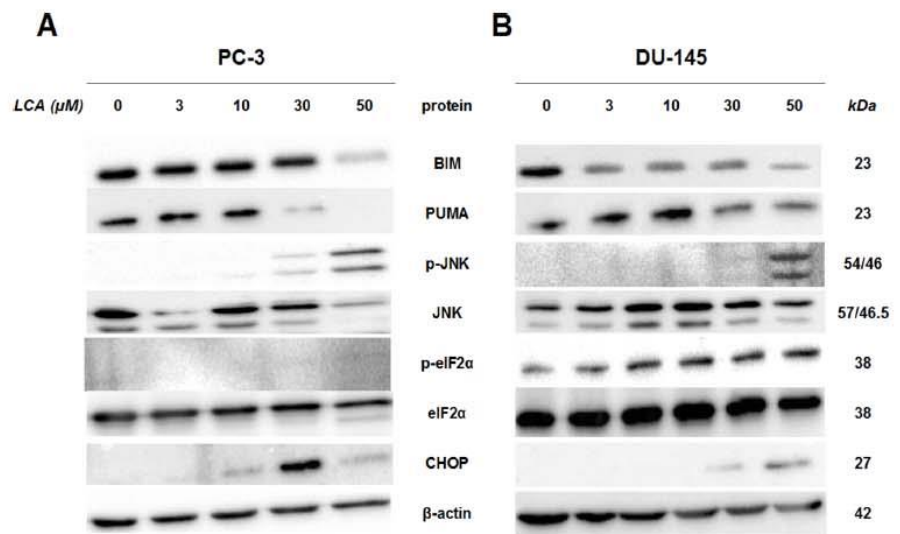


Figure 3 Lithocholic acid (LCA) induces ER stress in PC-3 and DU-145 prostate cancer cells. Cells were exposed to 3, 10, 30 or 50 μM of LCA for 24 h. BIM, PUMA, p-JNK, JNK, eIF2 α , p-eIF2 α , CHOP and β -actin were detected by immunoblotting; one representative gel of three is shown.

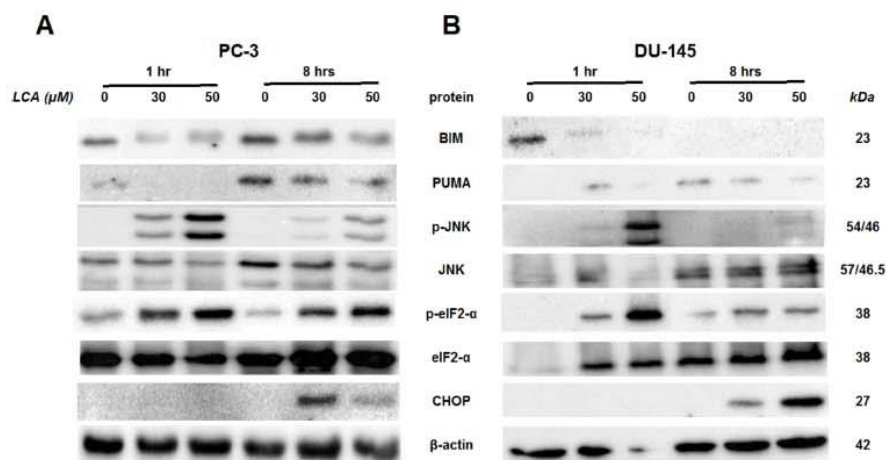


Figure 4 Time-dependent induction of ER stress by overtly cytotoxic concentrations of lithocholic acid (LCA) in PC-3 and DU-145 prostate cancer cells. Cells were exposed to 30 or 50 μM LCA for 1 and 8 h. BIM, PUMA, p-JNK, JNK, p-eIF2 α , eIF2 α , CHOP and β -actin were detected by immunoblotting; one representative gel of three is shown.

in both cell lines and, after 24 h of exposure, to non-detectable levels in PC-3 cells (Fig. 3). LCA (30 and 50 μM) visibly increased CHOP levels after 8 h in both cell lines.

ER stress-inhibitor salubrinal and CHOP gene-silencing do not abrogate LCA-induced cytotoxicity or apoptosis

To determine the role of ER stress in causing the cytotoxicity of LCA to PC-3 and DU-145 cells, each cell type was pretreated for 4 h with salubrinal, a selective inhibitor of eIF2 α dephosphorylation, before exposure to toxic concentration of 30 or 50 μM LCA. After an 8-h exposure, LCA increased levels of cleaved caspase 3, p-eIF2 α and CHOP in both cell lines (Fig. 5). Salubrinal pretreatment reduced each of these LCA-mediated increases in PC-3 cells, although in DU-145 cells salubrinal pretreatment increased CHOP levels induced by 50 μM LCA (Fig. 5). In addition, salubrinal pretreatment did not alleviate LCA-induced death of PC-3 and DU-145 cells, but exacerbated the toxicity of LCA statistically significantly at most test concentrations (Fig. 6).

Given that salubrinal-pretreatment further increased levels of LCA-induced CHOP in DU-145 cells, we assessed the effect of blocking CHOP gene expression using CHOP-selective siRNA. Gene silencing reduced LCA-induced levels of CHOP protein to undetectable levels in DU-145 cells (Fig. 7A). However, no effect of CHOP silencing on LCA-induced cytotoxicity in DU-145 cells was observed (Fig. 7B). This was confirmed using Hoechst staining to evaluate the effect of CHOP silencing on LCA-induced apoptosis in both DU-145 and PC-3 cells (Fig. 8).

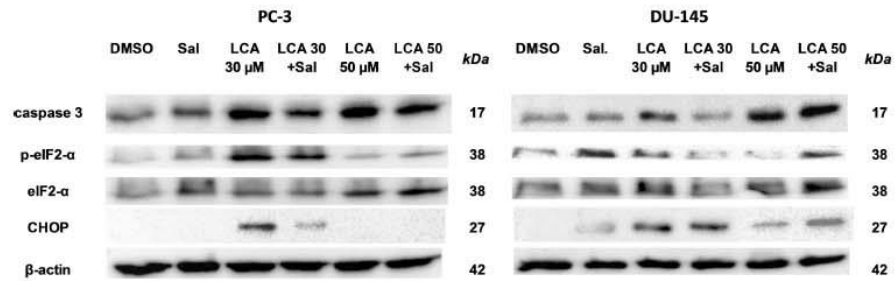


Figure 5 The effects of salubrinal-pretreatment on lithocholic acid-(LCA)-induced cleaved caspase 3, p-eIF2 α and CHOP levels in PC-3 and DU-145 prostate cancer cells. PC-3 and DU-145 were exposed to LCA (30 and 50 μ M) for 8 h in the presence or absence of 20 μ M salubrinal. The expression of caspase-3, p-eIF2 α and CHOP was determined by immunoblotting; one representative gel of three is shown.

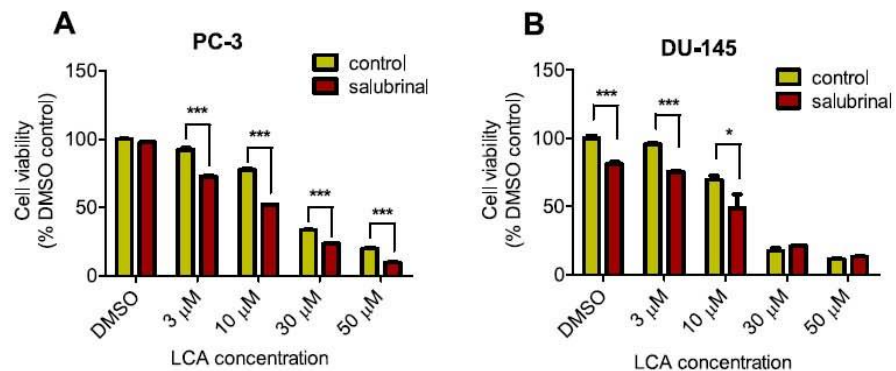


Figure 6 Salubrinal-pretreatment exacerbates the cytotoxicity of lithocholic acid (LCA) in PC-3 and DU-145 prostate cancer cells (24 h exposure). Statistically significant differences in cell viability between salubrinal-treated and vehicle control-treated cells were observed by two-way ANOVA and Bonferroni post-hoc test (* $p < 0.05$; *** $p < 0.001$). Experiments were performed in triplicate using different cell passages; per experiment each concentration was tested in triplicate.

LCA induces autophagy in PC-3 cells

PC-3 cells exposed to increasing concentrations of LCA for 24 h were stained with Cyto ID Green to detect the formation of autophagic vacuoles. A significant concentration-dependent increase of green fluorescence signal was observed starting at an LCA concentration as low as 1 μ M (Fig. 9). Further confirming the autophagic response, a concentration-dependent increase of the conversion of LC3B I to LC3B II was observed in PC-3 cells (Fig. 10). A time-course experiment indicated that noticeable conversion of LC3B was seen as early as 1 h after exposure to 30 or 50 μ M LCA (Fig. 10). When PC-3 cells were pretreated with the autophagy inhibitor bafilomycin A1, the toxicity of relatively non-toxic concentrations of LCA (3 and 10 μ M) was increased to a statistically significant degree, whereas no effects on the toxicity of LCA were observed at overtly toxic concentrations of 30 and 50 μ M (Fig. 11A). Similarly, silencing LC3B gene expression also

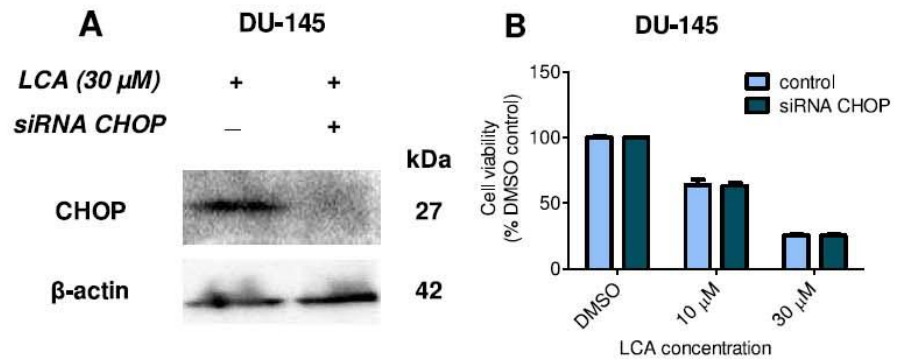


Figure 7 CHOP gene silencing does not affect lithocholic acid-(LCA)-induced cytotoxicity in DU-145 prostate cancer cells. No statistically significant effects were observed of siRNA treatment on control or LCA-decreased DU-145 cell viability by two-way ANOVA ($p = 0.9$; $n = 3$).

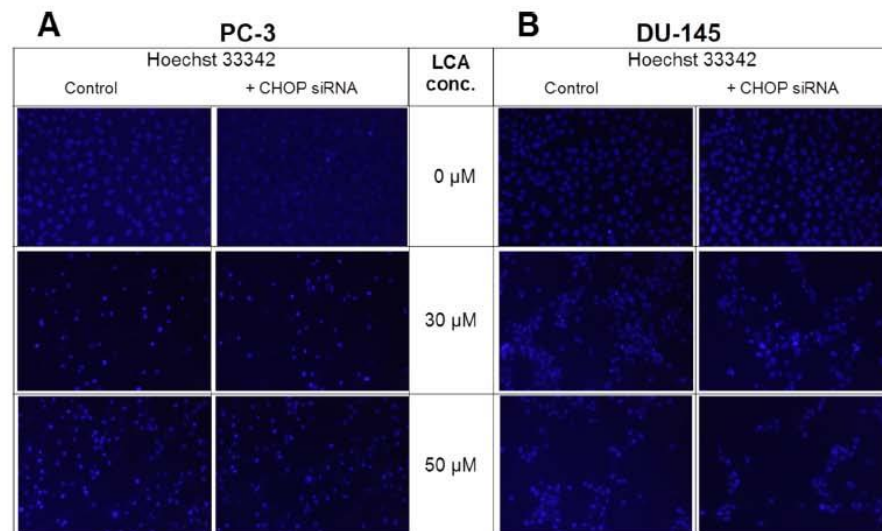


Figure 8 CHOP gene silencing does not affect lithocholic acid-(LCA)-induced apoptosis in PC-3 and DU-145 prostate cancer cells. Apoptotic nuclear morphology (chromatin condensed nuclei) was observed by Hoechst 33342 staining using fluorescence microscopy. The concentration-response experiment was performed three times using different cell passages; per experiment, concentrations were tested in triplicate.

increased the toxicity of LCA at lower concentrations (Fig. 11B). To establish if there was a link between induction of CHOP by LCA and that of autophagy, PC-3 cells were treated with siRNA to silence CHOP and then exposed to 30 or 50 μ M LCA (Fig. 12). CHOP silencing did not alter the increased conversion of LC3BI to II or alter the levels of ATG5 protein that were increased by LCA.

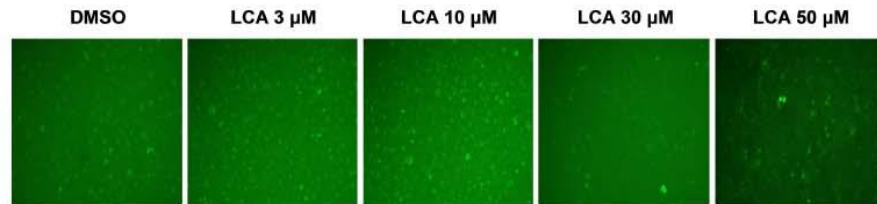


Figure 9 Lithocholic acid (LCA) induces autophagy in PC-3 prostate cancer cells. Cells were exposed to increasing concentrations of LCA for 24 h and then stained with Cyto-ID® Green dye for 10 min to detect autophagic vacuoles. LCA concentration-dependently increased the accumulation of autophagic vacuoles (bright green fluorescence) as detected by Cyto-ID® Green dye staining using fluorescence microscopy. The concentration–response experiment was performed three times using different cell passages; per experiment, concentrations were tested in triplicate.

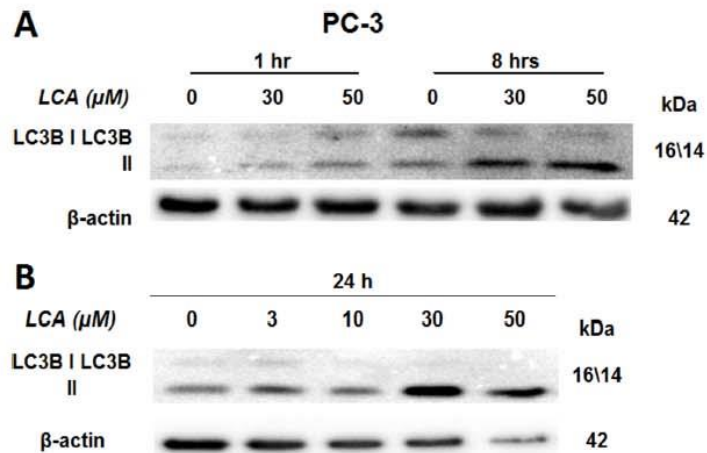


Figure 10 Lithocholic acid (LCA) induces LC3B conversion in PC-3 prostate cancer cells. Cells were exposed to increasing concentrations of LCA for 1, 8 or 24 h. Proteins were detected by immunoblotting; one representative gel of three is shown.

LCA induces mitochondrial dysfunction in PC-3 and DU-145 cells

Lithocholic acid induced mitochondrial dysfunction in PC-3 and DU-145 as measured using TMRE dye (Fig. 13), which is sequestered by active mitochondria, but fails to accumulate in mitochondria that have reduced or lost their outer membrane potential. PC-3 and DU-145 were exposed to different concentration of LCA (0, 1, 3, 10 and 30 μM) for 8 h and observed a concentration-dependent decrease in TMRE sequestration, which was most apparent at 30 μM LCA (Fig. 13). The loss of mitochondrial membrane potential coincided with an increase in nuclear staining with Hoechst 33342 (Fig. 13).

LCA induces reactive oxygen species (ROS)

LCA increased the production of ROS concentration dependently in PC-3 but not DU-145 cells at concentrations between 1 and 50 μM . (Fig. 14). To determine if the antioxidant

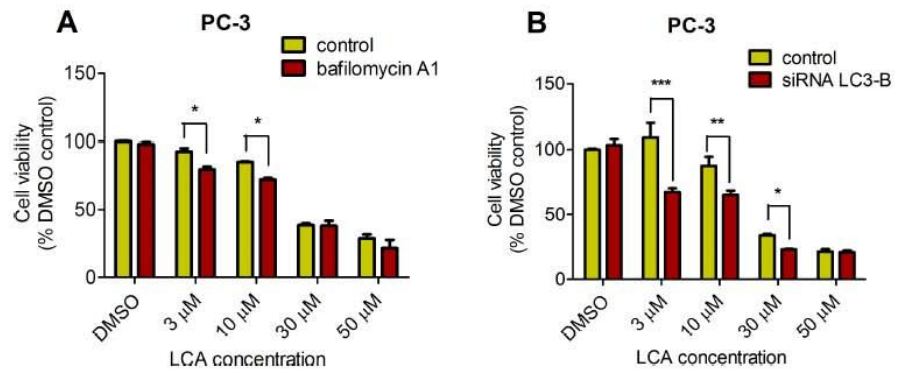


Figure 11 Bafilomycin A1-pretreatment (A) or LC3B gene silencing (B) enhanced the cytotoxicity of lithocholic acid (LCA) in PC-3 prostate cancer cells. Statistically significant differences in cell viability between bafilomycin A1- or LC3B siRNA-treated PC-3 cells and vehicle control-treated cells were determined by two-way ANOVA and Bonferroni post-hoc test (* $p < 0.05$; ** $p < 0.01$; *** $p < 0.001$). Experiments were performed in triplicate using different cell passages; per experiment, each concentration was tested in triplicate.

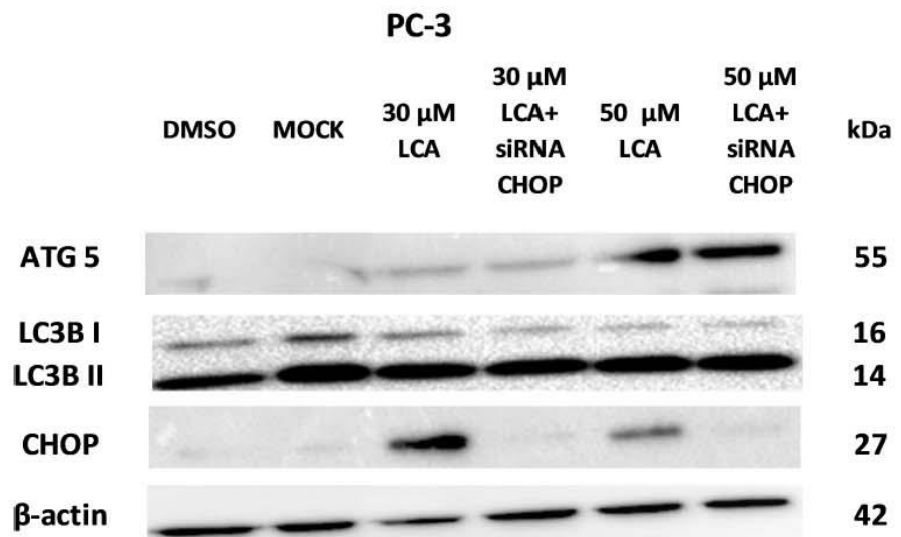


Figure 12 CHOP silencing had no effect on LCA-mediated induction of the autophagic markers LC3B conversion or ATG5 expression. Proteins were detected by immunoblotting; one representative gel of three is shown.

α -tocotrienol (T-3; 20 μ M) could reduce the cytotoxicity of LCA, PC-3 and DU-145 cells were incubated with T-3 four hours prior to a 24-h exposure to LCA. T-3 protected significantly against LCA-induced cytotoxicity in PC-3 cells whereas in DU-145 cells, T-3 had no effect (Fig. 15).

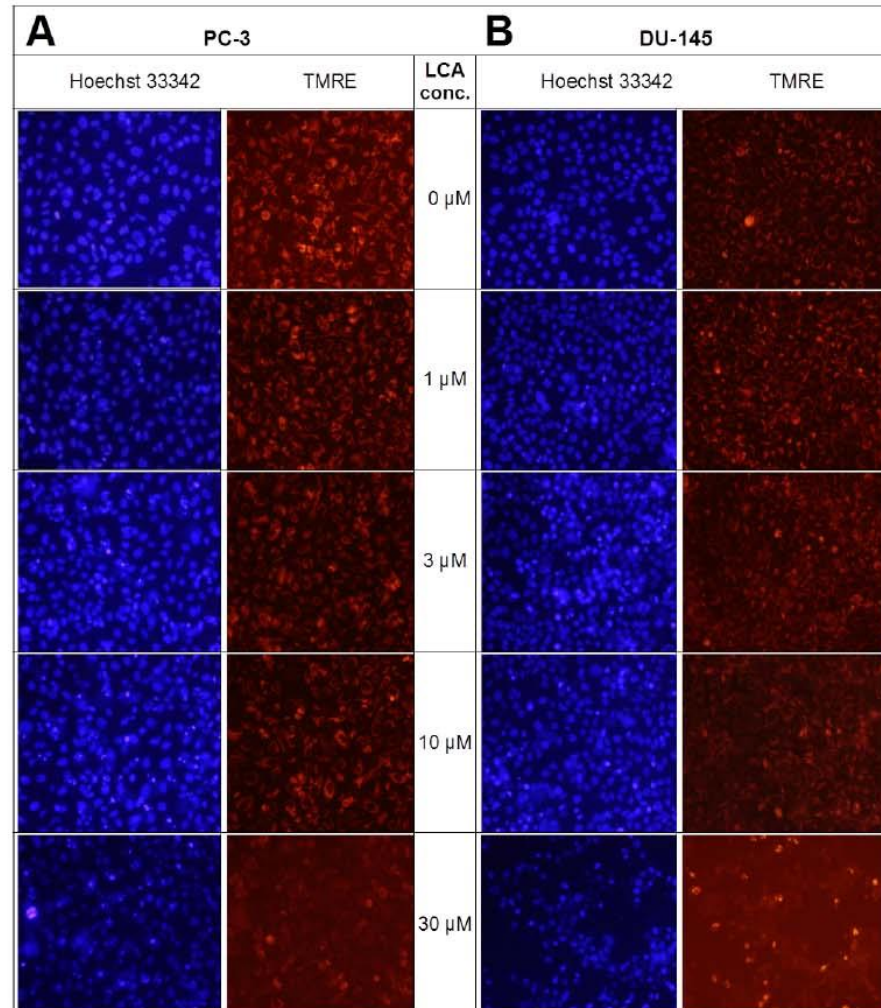


Figure 13 Lithocholic acid induces mitochondrial dysfunction in PC-3 and DU-145 cells. Cells were exposed to different concentrations of LCA for 8 h. Apoptotic nuclear morphology (chromatin condensed nuclei) was observed by Hoechst 33342 staining and mitochondrial membrane permeability was measured using TMRE fluorescent dye by fluorescence microscopy. The concentration–response experiment was performed three times using different cell passages; per experiment, each concentrations was tested in triplicate.

DISCUSSION

LCA induces selective cancer cell death

In our study, we found that LCA reduces the viability of androgen-independent DU-145 and PC-3 human prostate cancer cells, but not RWPE-1 immortalized human prostate epithelial cells (Fig. 1), confirming and expanding upon our previous observations in

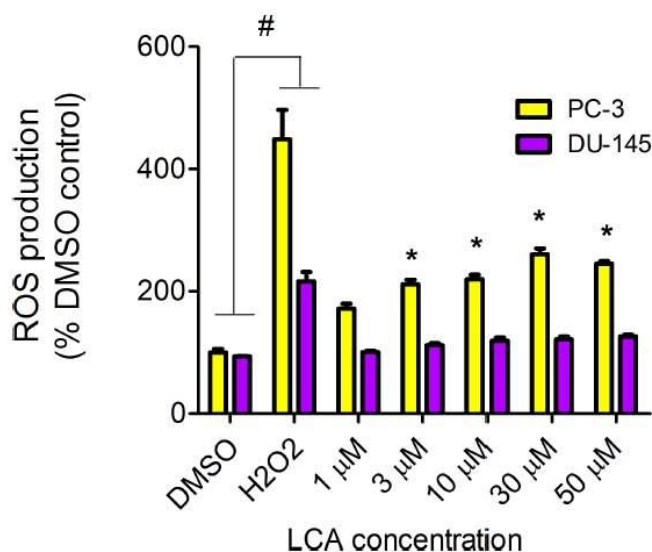


Figure 14 LCA induces reactive oxygen species (ROS) concentration dependently in PC-3 but not DU-145 cells. Cells were exposed to LCA for 60 min in culture medium containing 10 mM fluorescent probe dye (CM-H₂DCFDA). H₂O₂ (20 μM) was used as a positive control for ROS production, which was measured using a fluorescence spectrophotometer. (#) A statistically significant difference between DMSO- and H₂O₂-treated cells. (*) A statistically significant difference between DMSO- and LCA-treated cells determined by one-way ANOVA followed by a Dunnett test. One of three experiments is shown; each concentration was tested in triplicate.

prostate cancer cells that included androgen-dependent LNCaP cells (Goldberg *et al.*, 2013). LCA triggered concentration-dependent death of PC3 and DU-145 cells via apoptotic and necrotic pathways (Fig. 2). The selectiveness of LCA in killing cancer cells has recently been demonstrated in hepatocytes, where galactosylated poly(ethylene glycol)-conjugated LCA was toxic to HepG2 human hepatocarcinoma cells, but not to immortalized human LO2 liver cells (Gankhuyag *et al.*, 2015). Furthermore, we have previously shown that LCA killed neuroblastoma cells, whilst sparing normal neuronal cells (Goldberg *et al.*, 2011).

LCA induces ER stress in prostate cancer cells

We show for the first time that LCA induces ER stress in human androgen-independent prostate cancer cells in a time- and concentration-dependent manner (Figs. 3 and 4). Toxic concentrations of LCA reduced BIM and PUMA, and increased CHOP levels and the phosphorylation of eIF2 α and JNK in both cancer cell types. Increased phosphorylation of eIF2 α and JNK were early (1 h) responses to toxic concentrations of LCA, whereas concentration-dependent decreases of BIM and PUMA were sustained between 1 and 24 h of exposure (Figs. 3 and 4). The increased cleavage of caspase 3 by LCA (Fig. 5) likely explains why BIM and PUMA levels decreased at toxic concentrations of LCA, as it is known that active caspase 3 downregulates PUMA (Hadjji *et al.*, 2010) and BIM (Wakeyama *et al.*, 2007) expression in other cell types. At lower LCA concentrations

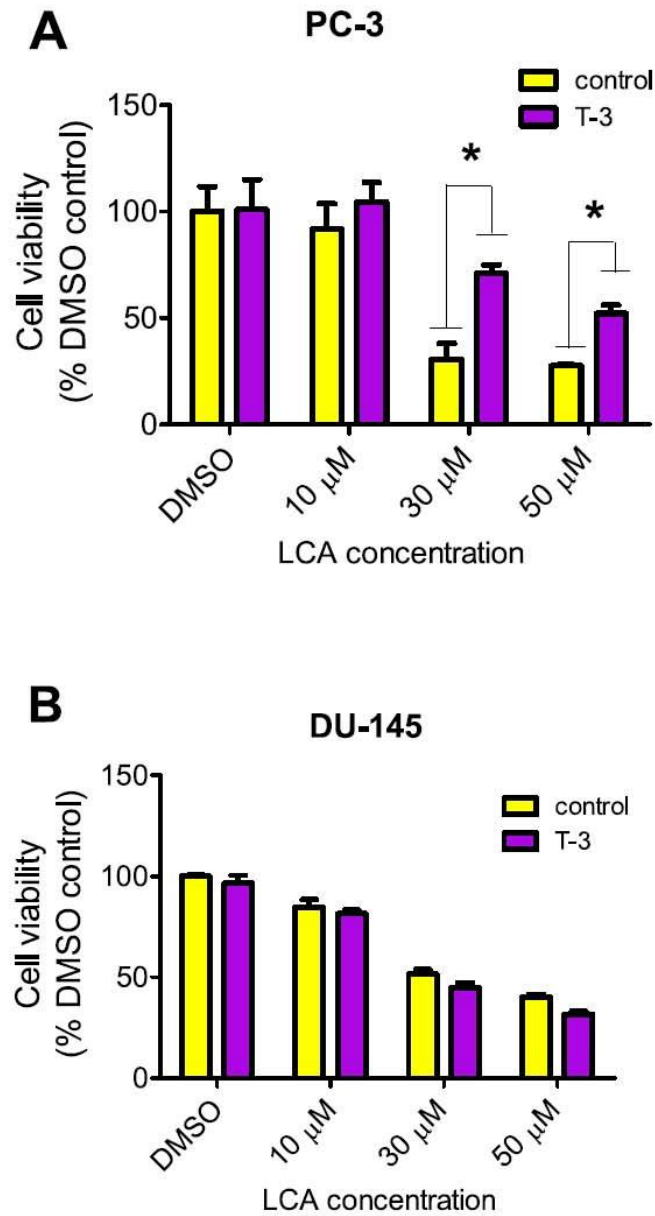


Figure 15 Effects of a 4-hour pretreatment with the antioxidant α -tocotrienol (T-3; 20 μM) on the cytotoxicity of LCA (24 h exposure) in (PC-3 cells or DU-145 cells). Statistically significant differences in cell viability between antioxidant-treated and vehicle control-treated cells were observed by two-way ANOVA and Bonferroni post-hoc test (* $p < 0.05$). One of three experiments is shown; each concentration was tested in triplicate.

and at earlier exposure durations, on the other hand, PUMA is initially increased, suggesting that PUMA is involved in triggering mitochondrial apoptosis (as discussed later) and caspase 3 activation that ultimately results in its breakdown. The up-regulation of PUMA is clearly p53-independent in PC-3 cells as these cells are p53-deficient (Rubin *et al.*, 1991).

LCA caused sustained induction of CHOP at 30 μM in PC-3 cells, although levels were sharply lower at 50 μM , possibly due to excessive cell death (Figs. 3–5). In DU-145 cells CHOP levels were increased by 30 and 50 μM LCA, but levels declined between 8 and 24 h of exposure (Figs. 3 and 4). Our observations suggest that LCA-induced ER stress involves activation of the eIF2 α phosphorylation pathway and subsequent induction of p-JNK (early response) and CHOP (later response), resulting in caspase 3-dependent apoptosis. However, an attempt to block this particular pathway with salubrinal reduced CHOP induction in PC-3 cells only, although it decreased LCA-induced caspase 3 in both cell lines (Fig. 5). Yet, salubrinal pretreatment resulted in increased toxicity of LCA in both cell lines (Fig. 6). We have previously shown that direct inhibition of the catalytic activity of caspase 3 did result in partial protection against LCA-induced cytotoxicity in LNCaP and PC-3 prostate cancer cells (Goldberg *et al.*, 2013), and in neuroblastoma cells (Goldberg *et al.*, 2011). It is possible that the observed decreases in cleaved caspase 3 protein levels do not reflect a significant change in its catalytic activity.

Furthermore, blocking CHOP expression using CHOP-selective siRNA had no effect on the reduced viability (Fig. 7) or apoptosis (as determined by measuring chromatin condensation and fragmentation using the fluorescent dye Hoechst 33342) (Fig. 8) of DU-145 and PC-3 cells after exposure to increasing concentrations of LCA. Therefore, inhibition of ER stress signaling alone does not appear to be essential for LCA-induced prostate cancer cell death.

Other studies have observed the induction of ER stress by bile acids. In HepG2 cells, the secondary bile acids LCA and DCA were the most toxic, followed by CDCA, although they induced cell death at concentrations of 100 μM and above (Adachi *et al.*, 2014), which are significantly greater than the concentrations of LCA that we have found to be toxic to prostate cancer cells. The same investigators detected increased expression of genes involved in ER stress, such as GRP78 and CHOP after 24 h exposures to 100 μM of LCA, DCA or CDCA. Using CDCA as a prototype bile acid, it was found to increase caspase 3 activity at 200 μM , but not 100 μM . Although cytotoxicity and CHOP induction, but not caspase 3 activation, appeared to occur concurrently after exposure to certain bile acids (Adachi *et al.*, 2014), a direct link between ER stress and HepG2 cell death was not established. Glycochenodeoxycholic acid (GCDCA) has been shown to induce ER stress in freshly isolated rat hepatocytes and this study interestingly showed that ER stress-mediated activation of caspase 12 occurred at a later stage than mitochondrial apoptosis mediated by cytochrome c release and caspase 3 activation (Tsuchiya *et al.*, 2006), suggesting induction of ER stress may not be critical to cell death. In a follow-up study, the investigators determined that caspase 8 activation via the extrinsic Fas pathway triggered ER stress in response to 300 μM GCDCA in HepG2 human hepatocarcinoma cells (Iizaka *et al.*, 2007). It is unclear how critical caspase activation is for bile acid-induced cell death. Glycodeoxycholate induced caspase 3-dependent apoptosis in rat hepatocytes after a 2 h

exposure and inhibition of caspase 3 activity resulted in less apoptosis, but whether this translated into less cell death was not reported (Webster, Usechak & Anwer, 2002). We point out that these previous studies were performed with remarkably high concentrations of bile acids and whether cells were dying due to excess necrosis was never reported. We have previously shown in LNCaP and PC-3 prostate cancer cells that LCA (50 and 75 μ M, respectively) activates caspases 8, 9 and 3, and that caspase 9 activation was likely secondary to caspase 8-induced truncation of Bid (Goldberg et al., 2013), a finding consistent with those of Iizaka et al. (2007). Inhibition of caspases 8 or 3 resulted in partial protection against LCA induced cytotoxicity, suggesting that the cytotoxicity of LCA is, at least in part, caspase-dependent (Goldberg et al., 2013). However, we are currently performing studies to show that necrotic signaling pathways may play a significant role in LCA-induced death of prostate cancer cells.

LCA induces autophagy in PC-3 cells

We found that LCA induces a general autophagic response in PC-3 cells based on a time- and concentration-dependent increase of LC3B conversion observed in these cells (Figs. 9 and 10). To delineate the protective or cytotoxic nature of the autophagic response to LCA, cells were exposed to LCA after pre-incubation with the autophagy inhibitor bafilomycin A1. Cells were also treated with siRNA specific for LC3B to silence the expression of this protein. Inhibiting autophagy in PC-3 cells in either of these manners enhanced the toxicity of normally sub-cytotoxic concentrations of LCA (Fig. 11A and 11B). This observation indicates that the autophagic response of PC-3 cells to LCA exposure is, at least initially, of a protective nature. Similarly, autophagy was shown to provide protection against cell death of rat hepatocytes induced by glycochenodeoxycholate, as its inhibition using the autophagy inhibitor chloroquine exacerbated toxicity whereas induction of autophagy using rapamycin provided protection against cell death (Gao et al., 2014). Our laboratory has also recently shown that blocking autophagy in LNCaP and LNCaP C4-2B prostate cancer cells, resulted in a strong sensitization of these cells to the cytotoxicity of diindolylmethane and a series of ring-substituted dihalogenated DIM derivatives again demonstrating the protective nature of the autophagic process in these cells (Goldberg et al., 2015).

To our knowledge, this is the first reported observation that LCA induces autophagy in human (prostate) cancer cells, although a link between bile acids and autophagy has been recently proposed via activation of the farnesoid X receptor (FXR) (Nie, Hu & Yan, 2015). The FXR is a cytoplasmic receptor and an important target for hydrophilic primary bile acids, but is unlikely to play a large role in the biological effects of LCA, which is very hydrophobic and remains almost entirely outside the cell (Goldberg et al., 2013). More likely targets for LCA are cell membrane surface receptors such as the death receptors or the G-protein-coupled bile acid receptor (GPBAR1), the latter for which LCA has a particularly strong affinity. Although the role of the GPBAR1 in LCA mediated signaling in healthy cells is currently under intense investigation (Tiwari & Maiti, 2009; Stepanov, Stankov & Mikov, 2013; Fiorucci & Distrutti, 2015; Li & Chiang, 2015; Perino & Schoonjans, 2015), nothing is known about its functions in prostate cancer cells. Our preliminary results

show strong expression of GPBAR1 protein in LNCaP, PC-3 and DU-145 cells and we are currently investigating the role of this receptor in triggering various cell death or survival pathways in these prostate cancer cells.

We did not establish a link between the induction of ER stress by LCA and its induction of autophagy. CHOP silencing did not alter the autophagic response of PC-3 cells to LCA at the tested concentration of 30 and 50 μ M as we observed no changes in the induction of LC3B conversion or ATG5 protein levels (Fig. 12). A recent study showed that whether triggering ER stress resulted in induction of either autophagy or apoptosis depended on the type of trigger. They found that triggering ER stress with thapsigargin only resulted in induction of apoptosis, whereas the ER stress inducer tunicamycin only caused autophagy (Matsumoto *et al.*, 2013). However, it was not made clear whether the induction of either autophagy or apoptosis was directly mediated by ER stress or could have been due to off-target effects of the typical ER stress inducers. Our results indicate that the induction of ER stress by LCA was not directly responsible for the induction of either cell death or autophagy, and that likely these effects are secondary to the disruption of mitochondrial function by LCA.

LCA induces mitochondrial dysfunction in PC-3 and DU-145 cells

We have shown that LCA impairs mitochondrial function by increasing mitochondrial outer-membrane permeability (Fig. 13). These results confirm our earlier finding that LCA impairs mitochondrial membrane potential in PC-3 and LNCaP cells as early as 1 h after exposure and was sustained for at least 8 h (Goldberg *et al.*, 2013). In the present study, we found that induction of ROS by LCA (Fig. 14) appeared to be a key trigger of cell death in PC-3 cells as the antioxidant T-3 was able to protect these cells against the cytotoxicity of LCA (Fig. 15). Interestingly LCA did not induce ROS in DU-145 cells (Fig. 14) and consistent with this, antioxidant pretreatment had no protective effect against LCA-mediated cytotoxicity in these cells (Fig. 15). These remarkable differences in (anti)oxidative responses between the two cell lines warrant further investigation.

CONCLUSIONS

In summary, we have found that LCA induces an ER stress response in PC-3 and DU-145 human prostate cancer cells via a p-eIF2 α -dependent pathway and an autophagic response in autophagy-capable PC-3 cells. These pathways appear to play a cytoprotective role against LCA-induced cell death, and are rather a response to the underlying, yet to be precisely elucidated mechanisms of LCA-induced prostate cancer cell death. These underlying mechanisms appear to involve induction of ROS and subsequent mitochondrial dysfunction in PC-3 cells, whereas in DU-145 cells LCA-induced mitochondrial dysfunction and cell death occurred at similar LCA concentrations, yet in the absence of ROS formation.

ADDITIONAL INFORMATION AND DECLARATIONS

Funding

This study was supported financially by an Egyptian government scholarship from the Administration of Cultural and General Affairs and Missions to Ahmed Gafar and by the Canadian Institutes of Health Research (CIHR) of Canada (grant no. MOP-115019) to Thomas Sanderson. Hossam Draz was funded by a scholarship from the Fondation Universitaire Armand-Frappier INRS. The funders had no role in study design, data collection and analysis, decision to publish, or preparation of the manuscript.

Grant Disclosures

The following grant information was disclosed by the authors:
Administration of Cultural and General Affairs and Missions to Ahmed Gafar.
Canadian Institutes of Health Research (CIHR) of Canada: MOP-115019.
Fondation Universitaire Armand-Frappier INRS.

Competing Interests

Thomas Sanderson is an Academic Editor for PeerJ, but was not involved in the review process of this manuscript.

Author Contributions

- Ahmed A. Gafar conceived and designed the experiments, performed the experiments, analyzed the data, wrote the paper, prepared figures and/or tables.
- Hossam M. Draz performed the experiments, analyzed the data, reviewed drafts of the paper.
- Alexander A. Goldberg analyzed the data, reviewed drafts of the paper.
- Mohamed A. Bashandy, Sayed Bakry, Mahmoud A. Khalifa and Walid AbuShair contributed reagents/materials/analysis tools, secured Egyptian funding for Ahmed Gafar's stipend and research materials.
- Vladimir I. Titorenko reviewed drafts of the paper.
- J. Thomas Sanderson conceived and designed the experiments, analyzed the data, contributed reagents/materials/analysis tools, wrote the paper, prepared figures and/or tables, reviewed drafts of the paper.

Data Availability

The following information was supplied regarding data availability:

The raw data for Figs. 1, 6, 7B, 11, 14 and 15 were supplied as a [Data S1](#).

Supplemental Information

Supplemental information for this article can be found online at <http://dx.doi.org/10.7717/peerj.2445#supplemental-information>.

ADDITIONAL INFORMATION AND DECLARATIONS

Funding

This study was supported financially by an Egyptian government scholarship from the Administration of Cultural and General Affairs and Missions to Ahmed Gafar and by the Canadian Institutes of Health Research (CIHR) of Canada (grant no. MOP-115019) to Thomas Sanderson. Hossam Draz was funded by a scholarship from the Fondation Universitaire Armand-Frappier INRS. The funders had no role in study design, data collection and analysis, decision to publish, or preparation of the manuscript.

Grant Disclosures

The following grant information was disclosed by the authors:
Administration of Cultural and General Affairs and Missions to Ahmed Gafar.
Canadian Institutes of Health Research (CIHR) of Canada: MOP-115019.
Fondation Universitaire Armand-Frappier INRS.

Competing Interests

Thomas Sanderson is an Academic Editor for PeerJ, but was not involved in the review process of this manuscript.

Author Contributions

- Ahmed A. Gafar conceived and designed the experiments, performed the experiments, analyzed the data, wrote the paper, prepared figures and/or tables.
- Hossam M. Draz performed the experiments, analyzed the data, reviewed drafts of the paper.
- Alexander A. Goldberg analyzed the data, reviewed drafts of the paper.
- Mohamed A. Bashandy, Sayed Bakry, Mahmoud A. Khalifa and Walid AbuShair contributed reagents/materials/analysis tools, secured Egyptian funding for Ahmed Gafar's stipend and research materials.
- Vladimir I. Titorenko reviewed drafts of the paper.
- J. Thomas Sanderson conceived and designed the experiments, analyzed the data, contributed reagents/materials/analysis tools, wrote the paper, prepared figures and/or tables, reviewed drafts of the paper.

Data Availability

The following information was supplied regarding data availability:

The raw data for [Figs. 1, 6, 7B, 11, 14 and 15](#) were supplied as a [Data S1](#).

Supplemental Information

Supplemental information for this article can be found online at <http://dx.doi.org/10.7717/peerj.2445#supplemental-information>.

- (ring-DIMs) induce differential mechanisms of survival and death in androgen-dependent and -independent prostate cancer cells. *Genes Cancer* 6:265–280.
- Goldberg AA, Titorenko VI, Beach A, Sanderson JT. 2013. Bile acids induce apoptosis selectively in androgen-dependent and -independent prostate cancer cells. *PeerJ* 1:e122 DOI 10.7717/peerj.122.
- Hadji A, Clybouw C, Auffredou MT, Alexia C, Poalas K, Burlion A, Feraud O, Leca G, Vazquez A. 2010. Caspase-3 triggers a TPCK-sensitive protease pathway leading to degradation of the BH3-only protein puma. *Apoptosis* 15:1529–1539 DOI 10.1007/s10495-010-0528-2.
- Iizaka T, Tsuji M, Oyamada H, Morio Y, Oguchi K. 2007. Interaction between caspase-8 activation and endoplasmic reticulum stress in glycochenodeoxycholic acid-induced apoptotic HepG2 cells. *Toxicology* 241:146–156 DOI 10.1016/j.tox.2007.08.095.
- Katona BW, Anant S, Covey DF, Stenson WF. 2009. Characterization of enantiomeric bile acid-induced apoptosis in colon cancer cell lines. *Journal of Biological Chemistry* 284:3354–3364 DOI 10.1074/jbc.M805804200.
- Levine B, Yuan J. 2005. Autophagy in cell death: an innocent convict? *The Journal of Clinical Investigation* 115:2679–2688 DOI 10.1172/JCI26390.
- Li T, Chiang JY. 2015. Bile acids as metabolic regulators. *Current Opinion in Gastroenterology* 31:159–165 DOI 10.1097/MOG.0000000000000156.
- Malvezzi M, Bertuccio P, Rosso T, Rota M, Levi F, La Vecchia C, Negri E. 2015. European cancer mortality predictions for the year 2015: does lung cancer have the highest death rate in EU women? *Annals of Oncology* 26:779–786 DOI 10.1093/annonc/mdv001.
- Marciniak SJ, Yun CY, Oyadomari S, Novoa I, Zhang Y, Jungreis R, Nagata K, Harding HP, Ron D. 2004. CHOP induces death by promoting protein synthesis and oxidation in the stressed endoplasmic reticulum. *Genes & Development* 18:3066–3077 DOI 10.1101/gad.1250704.
- Martin NE, D'Amico AV. 2014. Progress and controversies: radiation therapy for prostate cancer. *CA: A Cancer Journal for Clinicians* 64:389–407 DOI 10.3322/caac.21250.
- Matsumoto H, Miyazaki S, Matsuyama S, Takeda M, Kawano M, Nakagawa H, Nishimura K, Matsuo S. 2013. Selection of autophagy or apoptosis in cells exposed to ER-stress depends on ATF4 expression pattern with or without CHOP expression. *Biology Open* 2:1084–1090 DOI 10.1242/bio.20135033.
- Mizushima N, Noda T, Yoshimori T, Tanaka Y, Ishii T, George MD, Klionsky DJ, Ohsumi M, Ohsumi Y. 1998a. A protein conjugation system essential for autophagy. *Nature* 395:395–398 DOI 10.1038/26506.
- Mizushima N, Sugita H, Yoshimori T, Ohsumi Y. 1998b. A new protein conjugation system in human. The counterpart of the yeast Apg12p conjugation system essential for autophagy. *Journal of Biological Chemistry* 273:33889–33892 DOI 10.1074/jbc.273.51.33889.
- Mizushima N, Yamamoto A, Hatano M, Kobayashi Y, Kabeya Y, Suzuki K, Tokuhiisa T, Ohsumi Y, Yoshimori T. 2001. Dissection of autophagosome formation using

- Apg5-deficient mouse embryonic stem cells. *Journal of Cell Biology* 152(4):657–668 DOI 10.1083/jcb.152.4.657.
- Nguyen PL, Alibhai SM, Basaria S, D'amico AV, Kantoff PW, Keating NL, Penson DF, Rosario DJ, Tombal B, Smith MR. 2015. Adverse effects of androgen deprivation therapy and strategies to mitigate them. *European Urology* 67:825–836 DOI 10.1016/j.eururo.2014.07.010.
- Nie YF, Hu J, Yan XH. 2015. Cross-talk between bile acids and intestinal microbiota in host metabolism and health. *Journal of Zhejiang University Science B* 16:436–446 DOI 10.1631/jzus.B1400327.
- Perez MJ, Briz O. 2009. Bile-acid-induced cell injury and protection. *World Journal of Gastroenterology* 15:1677–1689.
- Perino A, Schoonjans K. 2015. TGR5 and immunometabolism: insights from physiology and pharmacology. *Trends in Pharmacological Sciences* 36:847–857 DOI 10.1016/j.tips.2015.08.002.
- Reggiori F, Klionsky DJ. 2002. Autophagy in the eukaryotic cell. *Eukaryotic Cell* 1:11–21 DOI 10.1128/EC.01.1.11-21.2002.
- Rubin SJ, Hallahan DE, Ashman CR, Brachman DG, Beckett MA, Virudachalam S, Yandell DW, Weichselbaum RR. 1991. Two prostate carcinoma cell lines demonstrate abnormalities in tumor suppressor genes. *Journal of Surgical Oncology* 46:31–36 DOI 10.1002/jso.2930460108.
- Sanda MG, Dunn RL, Michalski J, Sandler HM, Northouse L, Hembroff L, Lin X, Greenfield TK, Litwin MS, Saigal CS, Mahadevan A, Klein E, Kibel A, Pisters LL, Kuban D, Kaplan I, Wood D, Ciezki J, Shah N, Wei JT. 2008. Quality of life and satisfaction with outcome among prostate-cancer survivors. *The New England Journal of Medicine* 358:1250–1261 DOI 10.1056/NEJMoa074311.
- Shimodaira Y, Takahashi S, Kinouchi Y, Endo K, Shiga H, Kakuta Y, Kuroha M, Shimosegawa T. 2014. Modulation of endoplasmic reticulum (ER) stress-induced autophagy by C/EBP homologous protein (CHOP) and inositol-requiring enzyme 1alpha (IRE1alpha) in human colon cancer cells. *Biochemical and Biophysical Research Communications* 445:524–533 DOI 10.1016/j.bbrc.2014.02.054.
- Stepanov V, Stankov K, Mikov M. 2013. The bile acid membrane receptor TGR5: a novel pharmacological target in metabolic, inflammatory and neoplastic disorders. *Journal of Receptor and Signal Transduction Research* 33:213–223 DOI 10.3109/10799893.2013.802805.
- Tanida I, Ueno T, Kominami E. 2004. LC3 conjugation system in mammalian autophagy. *The International Journal of Biochemistry & Cell Biology* 36(12):2503–2518 DOI 10.1016/j.biocel.2004.05.009.
- Tiwari A, Maiti P. 2009. TGR5: an emerging bile acid G-protein-coupled receptor target for the potential treatment of metabolic disorders. *Drug Discovery Today* 14:523–530 DOI 10.1016/j.drudis.2009.02.005.
- Tsuchiya S, Tsuji M, Morio Y, Oguchi K. 2006. Involvement of endoplasmic reticulum in glycochenodeoxycholic acid-induced apoptosis in rat hepatocytes. *Toxicology Letters* 166:140–149 DOI 10.1016/j.toxlet.2006.06.006.

- Wakeyama H, Akiyama T, Takahashi K, Amano H, Kadono Y, Nakamura M, Oshima Y, Itabe H, Nakayama KI, Nakayama K, Nakamura K, Tanaka S. 2007. Negative feedback loop in the Bim-caspase-3 axis regulating apoptosis and activity of osteoclasts. *Journal of Bone and Mineral Research* 22:1631–1639 DOI [10.1359/jbmr.070619](https://doi.org/10.1359/jbmr.070619).
- Webster CR, Usechak P, Anwer MS. 2002. cAMP inhibits bile acid-induced apoptosis by blocking caspase activation and cytochrome c release. *American Journal of Physiology. Gastrointestinal and Liver Physiology* 283:G727–G738 DOI [10.1152/ajpgi.00410.2001](https://doi.org/10.1152/ajpgi.00410.2001).